UNIVERSIDADE DE SANTIAGO DE COMPOSTELA
FACULTADE DE MEDICINA
DEPARTAMENTO DE MEDICINA
LABORATORIO DE BIOQUÍMICA ESTRUTURAL DA PATOLOXÍA ENDOCRINOLÓXICA

FUNDAMENTAL STRUCTURAL AND BIOCHEMICAL FEATURES FOR THE OBESTATIN/GPR39 SYSTEM MITOGENIC ACTION

BEGOÑA OTERO ALÉN

Santiago de Compostela, 2016

USC
UNIVERSIDADE
DE SANTIAGO
DE COMPOSTELA

UNIVERSIDADE DE SANTIAGO DE COMPOSTELA
FACULTADE DE MEDICINA
DEPARTAMENTO DE MEDICINA
LABORATORIO DE BIOQUÍMICA ESTRUTURAL DA PATOLOXÍA ENDOCRINOLÓXICA

FUNDAMENTAL STRUCTURAL AND BIOCHEMICAL FEATURES FOR THE OBESTATIN/GPR39 SYSTEM MITOGENIC ACTION

Memoria para optar ao Grao de Doutora en Bioloxía
pola Universidade de Santiago de Compostela presentada por:

BEGOÑA OTERO ALÉN

Santiago de Compostela, 2016

USC
UNIVERSIDADE
DE SANTIAGO
DE COMPOSTELA

A memoria adxunta titulada “Fundamental structural and biochemical features for the obestatin/GPR39 system mitogenic action” que para optar ao Grao de Doutora en Bioloxía presenta Dna. Begoña Otero Alén, foi realizada baixo a nosa dirección na Área de Bioquímica Estrutural da Patoloxía Endocrinolóxica do Instituto de Investigación Sanitaria do Complexo Hospitalario Universitario de Santiago de Compostela.

Considerando que constitúe un traballo de Tese Doutoral, autorizamos a súa presentación na Universidade de Santiago de Compostela. E para que así conste, firmamos a presente en Santiago de Compostela a xullo de 2016.

Dra. Yolanda Pazos Randulfe

Investigadora SERGAS

Prof. Dr. Felipe Casanueva Freijo

Catedrático de Medicina

Prof. Dr. Tomás García-Caballero Parada

Catedrático de Histoloxía

Santiago de Compostela, xullo de 2016

USC
UNIVERSIDADE
DE SANTIAGO
DE COMPOSTELA

A Pablo,

por ensinarme que a vida está feita de cen

USC
UNIVERSIDADE
DE SANTIAGO
DE COMPOSTELA

INDEX

USC
UNIVERSIDADE
DE SANTIAGO
DE COMPOSTELA

ABSTRACT 15

ABBREVIATIONS 19

INTRODUCTION 25

OBESTATIN/GPR39 SYSTEM 27
Obestatin uncovering 27
Ghrelin 27
Obestatin biosynthesis 28
Obestatin expression 30
Obestatin structure and bioactivity features 33
Obestatin receptor 34
Obestatin bioactivity. Functions and signalling 42

OBESTATIN/GPR39 SYSTEM IN CANCER 49

GASTRIC CANCER 50
Aetiology 50
Epidemiology 53
Classification 55

OBJECTIVES 59

MATERIALS AND METHODS 63

MATERIALS 65
Peptides 65
Human samples 65
Cells 65
Antibodies 66
Protein arrays 67

METHODS 69
Structure analysis 69
[^{32}P]Orthophosphate labelling and GPR39 immunoprecipitation 71
GPR39 internalization 71
Immunoblot analysis 72
Cell proliferation assays 72

Small interfering RNA assays 73
Immunocytochemistry and immunohistochemistry 73
Immunofluorescence analysis 75
Plasmid cell transient transfection in HEK293 and A431 cells 75
Array protein assays 76
Migration and invasion assays 77
Pepsinogen secretion assays 78
Data analysis 78

RESULTS 81

CHAPTER 1. THE NMR STRUCTURE OF HUMAN OBESTATIN IN MEMBRANE-LIKE ENVIRONMENTS. STRUCTURE-BIOACTIVITY RELATIONSHIP OF OBESTATIN 83
Circular dichroism 83
Structure determination using NMR 84
Backbone HN amide and H-alpha ^{1}H chemical shifts 84
NOE pattern 85
3D structures 86
Proliferation 88
GPR39 siRNA depletion 88
ERK1/2 and Akt activation 90
Ki67 expression and proliferation 93

CHAPTER 2: NMR INTERACTION BETWEEN OBESTATIN AND GPR39 RECEPTOR USING LIVING CELLS 95
CSP effects and NOE pattern in obestatin truncates 95
CSP effects and NOE pattern in human obestatin 99
3D structure of human obestatin 102

CHAPTER 3: OBESTATIN/GPR39 SIGNALLING 105
Obestatin/GPR39 interaction 105
GPR39 phosphorylation induced by obestatin 105
GPR39 internalization/endocytosis 106
GPR39-RTKs cross-talk: differential RTK phosphorylation and protease expression patterns 107
Differential RTK phosphorylation pattern activated by obestatin in AGS and KATO III cells 107
Differential protease expression pattern activated by obestatin in AGS and KATO III cells 112
Differential RTK phosphorylation pattern in human adenocarcinomas 117
Differential protease expression pattern in human adenocarcinomas 120

CHAPTER 4: THE ROLE OF THE OBESTATIN/GPR39 SYSTEM IN HUMAN GASTRIC ADENOCARCINOMAS **123**
Obestatin and GPR39 are expressed in AGS cells 123
Obestatin induces proliferation in an autocrine/paracrine manner in AGS cells 124
Obestatin promotes cell mobility and invasion *via* EMT and cytoskeleton remodelling in AGS cells 125
Obestatin exerts its actions through the GPR39 receptor in AGS cells 128
GPR39 and obestatin expression in human healthy stomach tissue 131
GPR39, obestatin and Ki67 expression in human gastric adenocarcinomas 131

CHAPTER 5: PEPSINOGEN I SECRETION: THE FUNCTION OF THE OBESTATIN/GPR39 SYSTEM IN HUMAN STOMACH **137**
GPR39 is expressed in the chief cells of the oxyntic mucosa of the human stomach 137
Obestatin stimulates pepsinogen I secretion in AGS cells 141
Pepsinogen secretion is mediated by GPR39 142

CHAPTER 6: OBESTATIN/GPR39 SYSTEM IN HUMAN CANCER LINES: EFFECTS ON PROLIFERATION AND INVASIVENESS **143**
Obestatin and GPR39 are expressed in cancer cell lines 143
Obestatin causes cytoskeleton reorganization and increases proliferation in KATO III cell line 145
Obestatin stimulates proliferation of cancer cell lines *via* the GPR39 146

DISCUSSION **151**

CONCLUSIONS **169**

RESUMO **173**

ACKNOWLEDGEMENTS **183**

BIBLIOGRAPHY **187**

SUPPLEMENTARY MATERIAL **203**

USC
UNIVERSIDADE
DE SANTIAGO
DE COMPOSTELA

ABSTRACT

USC
UNIVERSIDADE
DE SANTIAGO
DE COMPOSTELA

In 2005, a new peptide derived from the ghrelin peptide precursor, named obestatin, was discovered. One of the most important functions of obestatin is its mitogenic activity. Obestatin and the GPR39 receptor were reported to be involved in the control of mitogenesis of gastric cancer cell lines; this fact prompted us to investigate obestatin/GPR39 signalling and the relationship between the system and gastric cancer progression, and explored their potential functional roles.

The main objective of this doctoral thesis is to establish the relationship between obestatin and GPR39 receptor in healthy and tumour-like surroundings, from structural to tissue level, to determinate the fundamental parameters of its mitogenic bioactivity. This issue will be accomplished with the following points:

1. To determine the structural features of obestatin required for the interaction with its receptor.

2. To elucidate the detailed activation/regulation mechanism of GPR39 receptor signalling triggered by obestatin.

3. To analyse the role of obestatin/GPR39 system in the development and malignity of tumours.

Our results demonstrated that:

At structural level, the amidation at the C-terminus is essential to adopt an α-helix structure and stabilize the GPR39 conformations necessary for the full range of receptor activities. Furthermore, human (11-23)-obestatin is able to induce selective coupling to the β-arrestin-dependent signalling, representing the first example of an endogenous biased ligand for GPR39. Meanwhile, mouse and human obestatin exhibit clear conformational differences beyond their primary structure. This evidence supports the species-specific activity of this peptide. Additionally, obestatin-GPR39 interaction might involve an *E*/*Z* isomerization of the peptide and the posibility that GPR39 could be acting as a prolyl *cis*-*trans* isomerase.

Regarding the activation/regulation mechanism of GPR39 signalling triggered by obestatin, our results show that obestatin increases GPR39 phosphorylation and induces receptor endocytosis. In this signalling network, the transactivation process induced by obestatin GPR39-EGFR is a key mechanism, regulated by MMPs. The RTKs and proteases expression profiles confirm the implication of EGFR and MMPs in the obestatin signalling pathway, and introduce other proteases and RTKs in this cross-talk.

In human tissues, we observe that the obestatin/GPR39 system regulates pepsinogen secretion. This result provide the first biological function for the obestatin/GPR39 system in healthy stomach. This system also regulates proliferation, motility, EMT, and invasion of gastric cancer cells. More importantly, the GPR39 expression levels found in human gastric adenocarcinomas provide the rationale for including GPR39 as a prognostic marker of these tumours. The ubiquitous expression of GPR39 and its cancer-associated overexpression, together with obestatin, provokes the proliferation and cell motillity of diverse human cancer cell lines. Moreover, these effects depend not only on GPR39, but also on the expression of key components of its signalling pathway, i.e. RTKs, proteases.

USC
UNIVERSIDADE
DE SANTIAGO
DE COMPOSTELA

ABBREVIATIONS

USC
UNIVERSIDADE
DE SANTIAGO
DE COMPOSTELA

ABBREVIATIONS

1D: One-dimensional
2D: Two-dimensional
3D: Three-dimensional
aa: Amino acid
AB: Antibody
ABCA1: ATP-binding cassette A1
AC: Adenylate cyclase
ACC: Acetyl-CoA-carboxylase
ADAM: A desintegrin and metalloproteinase
ADAMTS: A desintegrin and metalloproteinase with thrombospondin motifs
AIDS: Acquired immune deficiency syndrome
Akt: Serine/threonine kinase (protein kinase B)
Ala: Alanine
AMP: Adenosine monophosphate
AMPK: Adenosine monophosphate-activated protein kinase
ANOVA: Analysis of variance
AP-1: Adaptor protein 1
Arg: Arginine
AS160: Akt substrate of 160 kDa
ATP: Adenosine triphosphate
BMI: Body mass index
BrdU: Bromodeoxiuridine
BSA: Bovine serum albumin
C/EBP: CCAAT/enhancer-binding protein
CA3: Cornu Ammonis region 3
CaMKII: Calmodulin-dependent protein kinase II
cAMP: Cyclic adenosine monophosphate
CaSR: Calcium-sensing receptor
CC2: Cell conditioning solution 2
CCAAT: Cytidine-cytidine-adenosine-adenosine-thymidine
CD: Circular dichroism
cDNA: Complementary DNA
CIMP: CpG island methylator phenotype
CIN: Chromosomal instability
CM: Conditioned medium
CMAPs: Cyclohexyl-methyl aminopyrimidine chemotype compounds
CoA: Coenzyme A
CREB: cAMP response element-binding protein
CSI: Chemical shift index
CSP: Chemical shift perturbation
CTS: Cathepsin
D_2O: Deuterated water
DAB: 3-3'-Diaminobenzidine
DAG: Diacylglycerol
DDR: Discoidin domain receptor
DLBCL: Diffuse large B-cell lymphoma
DNA: Deoxyribonucleic acid
DPC: Dodecyl-phosphocholine
DTT: Dithiothreitol
EBV: Epstein-Barr virus-positive
ECL: Enterochromaffin-like
EDTA: Ethylenediaminetetraacetic acid
EGF: Epidermal growth factor
EGFP: Enhanced green fluorescent protein
EGFR: Epidermal growth factor receptor
ELISA: Enzyme-linked immunosorbent assay
EMT: Epithelial-mesenchymal transition
EphR: Ephrin receptor
ER: Endoplasmic reticulum
ERK1/2: Extracellular signal-regulated kinase-1/2
ESCC: Oesophageal squamous cell carcinoma
ET: Experimental time
Ex-4: Exendin-4
FAT: Fatty acid transport
FATP4: Fatty acid transport proteins 4
FBS: Foetal bovine serum
FFPE: Fixed in formalin and embedded in paraffin
FGFR: Fibroblast growth factor receptor
Flk-1: Foetal liver kinase 1/VEGFR2
Flt-3: Fms-like tyrosine kinase 3
G1: Gap 1 phase
GAPDH: Glyceraldehyde 3-phosphate dehydrogenase

GFP: Green fluorescent protein
GH: Growth hormone
GHSR1a: Growth hormone secretagogue receptor type 1a
GIST: Gastrointestinal stromal tumour
Gln: Glutamine
GLP-1: Glucagon-like peptide
GLP1R: Glucagon-like peptide-1 receptor
Glu: Glutamic acid
GLUT 4: Glucose transporter type 4
Gly: Glycine
GOAT: Ghrelin O-acyltransferase
GPCR: G-protein-coupled receptor
GPR39: G-protein 39-coupled receptor
GRK: G-protein-coupled receptor kinase
GS: Genomically stable
GSK3: Glycogen synthase kinase 3
GTP: Guanosine 5' triphosphate
HDGC: Hereditary diffuse gastric cancer
HEK: Human embryonic kidney cells
HEPES: Hydroxyethyl piperazineethanesulfonic acid
HFD: High-fat diet
HGFR: Hepatocyte growth factor receptor
Hh: Hedgehog
HHS: Harry´s haematoxylin solution
His: Histidine
HRP: Horseradish peroxidase
hRPEs: Human retinal pigmented epithelial cells
IC: Immunocytochemistry
IEM: Immunoelectronic microscopy
IF: Immunofluorescence
IGF: Insulin-like growth factor
IGF1R: Insulin-like growth factor-1 receptor
IgG: Immunoglobulin G
IH: Immunohistochemistry
Ile: Isoleucine
IM: Intestinal metaplasia
In1: Intron 1
IP3: Inositol trisphosphate
IR: Immunoreactive
IRS: Insulin-receptor substrate
kDa: kiloDalton
KLK: Kallikrein
Leu: Leucine
Lys: Lysine
MALT: Mucosa-associated lymphoid tissue
MAP: Mitogen-activated protein
MAPK: Mitogen-activated protein kinase
M-CSFR: Macrophage colony-stimulating factor receptor
MD: Moderately differentiated
MEK: Mitogen-activated protein kinase kinase
MHC: Myosin heavy chain
mLST8: mTOR associated-protein LST8
MMP: Metalloproteinase
mRNA: Messenger RNA
mSin1: Mammalian stress-activated protein kinase interacting protein 1
MSPR: Macrophage-stimulating protein receptor
mTOR: Mammalian target of rapamycin
mTORC1: mTOR complex 1
mTORC2: mTOR complex 2
NA: Neutralization assay
NET: Neuroendocrine tumour
NF-κβ: Nuclear factor-kappa-light-chain-enhancer of activated B cells
NMR: Nuclear magnetic resonance
NOE: Nuclear Overhauser effect
NOESY: Nuclear Overhauser effect spectroscopy
NTR: Neurotensin receptor
OB: Obestatin
O/N: Overnight
PAL: Peptidylamido-glycolate lyase
PAM: Peptidyl glycine α-amidating monooxygenase
PAR-2: Proteinase-activated receptor 2
PBS: Phosphate buffer saline
PBST: Phosphate buffer saline containing Tween-20
PC: Proprotein convertase

PD: Poorly differentiated
PDGFR: Platelet-derived growth factor receptors
PDK1: 3-Phosphoinositide-dependent kinase-1
PDT: Population doubling time
Pdx-1: Pancreatic and duodenal homeobox-1
PEDF: Pigment epithelium derived factor
PFA: Paraformaldehyde
PGI: Pepsinogen I
Phe: Phenylalanine
PHM: Peptidyl glycine α-hydroxylating monooxygenase domain
PI: Proliferative index
PI3K: Phosphatidylinositol 3-kinase
PKA: Protein kinase A
PKC: Protein kinase C
PLC: Phospholipase C
PPARγ: Peroxisome proliferator–activated receptor-γ
ppm: part per million
Pro: Proline
PT: Proliferative time
PTRN3: Proteinase 3
Raf: Rapidly accelerated fibrosarcoma kinase
RICTOR: Rapamycin-insensitive companion of mammalian target of rapamycin
RMSD: Root mean square deviation
RNA: Ribonucleic acid
ROESY: Rotating-frame nuclear Overhauser effect spectroscopy
RT: Room temperature
RTK: Receptor tyrosine kinase
RTSK: Receptor serine/threonine kinase
S: Synthesis phase
S6K: S6 kinase
***sc*:** Subcutaneous
SCE: Slow conformational exchange
SCFR: Mast/stem cell growth factor receptor
SDS: Sodium dodecyl sulphate
SDS-d_{25}: Perdeuterated sodium dodecyl sulphate
SE: Standard error
Ser: Serine
siRNA: Small interfering RNA
SPEM: Spasmolytic polypeptide expressing metaplasia
Src: Proto-oncogene tyrosine-protein kinase
SRE: Serum response element
SSC: Standard saline citrate
TBS: Tris buffer solution
TBST: Tris buffer solution containing Tween-20
TCA: Trichloroacetic acid
TFE: Trifluoroethanol
TieR: Angiopoietin receptor
TNM: Tumour, node and metastasis cancer classification
TOCSY: Total correlation spectroscopy
TrkR: Tropomyosin receptor kinase receptor
TSP: Trimethylsilylpropionic acid
Tyr: Tyrosine
UAG: Unacylated ghrelin
uPA: Urokinase-type plasminogen activator
Val: Valine
VEGF: Vascular endothelial growth factor
VEGFR: Vascular endothelial growth factor receptor
VMAT-2: Vesicular monoamine transporter-2
WAT: White adipose tissue
WB: Western blot
WD: Well differentiated
WHO: World Health Organization
WT: Wild type
ZnR: Zinc sensing receptor

USC
UNIVERSIDADE
DE SANTIAGO
DE COMPOSTELA

INTRODUCTION

USC
UNIVERSIDADE
DE SANTIAGO
DE COMPOSTELA

OBESTATIN/GPR39 SYSTEM

OBESTATIN UNCOVERING

In 2005, using a bioinformatics approach, Zhang *et al* discovered a new peptide derived from the ghrelin peptide precursor, called obestatin. The word **obestatin** is a contraction of obese, from Latin '*obedere*' meaning 'to devour', and '*statin*', denoting suppression. It was firstly isolated from stomach and was identified as a physiological opponent of ghrelin on food intake, body weight, and gastric emptying.[1] Obestatin has been a controversial peptide since its discovery, and many questions have made on it. In recent years, some issues have been clarified but many of them are still unrevealed.

GHRELIN

Several years ago, ghrelin had already been characterized as one of the most important gut peptides for their ability to regulate food intake and energy homeostasis.[2,3] It was discovered using "reverse pharmacology" in gastric extracts as the natural ligand of the orphan growth hormone secretagogue receptor type 1a (GHSR1a).[4] Ghrelin is a 28 amino acid peptide hormone with a unique post-translational modification of O-*n*-octanoylation at Ser3,[5] which is mainly produced in the stomach by the enteroendocrine X/A-like cells of the oxyntic mucosa, although it is also synthesized in other organs and tissues, as some sections of the gastrointestinal tract, pancreas, kidney, pituitary and hypothalamus.[6,7] The acylation modification is essential for the binding to the GHSR1a, for the release of growth hormone (GH) both *in vivo* and *in vitro* and for most of its other endocrine actions.[4] This octanoyl modification is catalysed by the ghrelin O-acyl transferase (GOAT) enzyme, which has been discovered by using bioinformatics predictions.[8,9] Ghrelin possess other no endocrine activities such as the control of body energy, gastric motility, acid-gastric secretion, influence on pancreatic activity and glucose metabolism, cardiovascular effects and mitogenic effects on different cell lines. Furthermore, the non-acylated peptide, commonly named des-acyl ghrelin or unacylated ghrelin (UAG), which circulates in a greater amount respect to acylated ghrelin, possess its own biological functions. UAG has different no endocrine functions like cardiovascular and antiproliferative effects[10,11] and numerous reports

[1] Zhang JV, Ren PG, Avsian-Kretchmer O, *et al*. Obestatin, a peptide encoded by the ghrelin gene, opposes ghrelin's effects on food intake. Science. 2005;310:996-9.

[2] Cummings DE, Overduin J. Gastrointestinal regulation of food intake. J Clin Invest. 2007;117:13-23.

[3] Van der Lely AJ, Tschöp M, Heiman ML, *et al*. Biological, physiological, pathophysiological, and pharmacological aspects of ghrelin. Endocr Rev. 2004;25:426-57.

[4] Kojima M, Hosoda H, Date Y, *et al*. Ghrelin is a growth-hormone-releasing peptide from stomach. Nature. 1999;402:656-60.

[5] Kojima M, Hosoda H, Matsuo H, *et al*. Ghrelin: discovery of the natural endogenous ligand for the growth hormone secretagogue receptor. Trends Endocrinol Metab. 2001;12:118-22.

[6] Horvath TL, Diano S, Sotonyi P, *et al*. Minireview: ghrelin and the regulation of energy balance: a hypothalamic perspective. Endocrinology. 2001;142:4163-9.

[7] Inui A. Ghrelin: an orexigenic and somatotrophic signal from the stomach. Nat Rev Neurosci. 2001;2:551-60.

[8] Yang J, Brown MS, Liang G, *et al*. Identification of the acyltransferase that octanoylates ghrelin, an appetite-stimulating peptide hormone. Cell. 2008;132:387-96.

[9] Gutierrez JA, Solenberg PJ, Perkins DR, *et al*. Ghrelin octanoylation mediated by an orphan lipid transferase. Proc Natl Acad Sci USA. 2008;105:6320-5.

[10] Korbonits M, Goldstone AP, Gueorguiev M, *et al*. Ghrelin: a hormone with multiple functions. Front Neuroendocrinol. 2004;25:27-68.

[11] Bowers CY. Unnatural growth hormone-releasing peptide begets natural ghrelin. J Clin Endocrinol Metab. 2001;86:1464-9.

point to the possibility that its actions were mediated by other receptor distinct from the GHSR1a.[12]

OBESTATIN BIOSYNTHESIS

Obestatin is a 23-amino acid peptide hormone derived from the post-translational cleavage of the ghrelin gene with a Leu residue on the carboxyterminal domain that can be amidated. The human ghrelin gene is located on the chromosome position 3p25-26 and comprises five exons and three introns,[13,14] being the short first exon which encodes part of the 5' untranslated region.[15,16] Mature ghrelin is encoded by exons 2 and 3 with the remaining proghrelin peptide sequence contained in exons 4 and 5.[17] Different transcriptional initiation sites have been described in the ghrelin gene originating distinct messenger ribonucleic acid (mRNA) transcripts: an alternative splicing product from exon 2 to exon 4 that is the main form of human ghrelin,[16] and some mRNA splicing variants that generate peptides with small changes in their sequences compared with native ghrelin. These are the cases of des-Gln14-ghrelin, a spliced variant without the codon for Gln in position 14;[18] the Ex3-deleted ghrelin that lacks the coding region for obestatin;[19] and a novel ghrelin variant generated by retention of intron 1 (In1), named In1-ghrelin.[20] It has also been identified multiple ghrelin-derived molecules produced by post-translational processing, on the basis of amino acid length and by type of acylation at Ser3.[18] Human ghrelin mRNA codes for a 117 amino acid long peptide called preproghrelin. Preproghrelin contains 23 amino acids conforming the signal peptide and a 94 amino acid fragment called proghrelin (1-94). Proghrelin includes the mature ghrelin (1-28) and a 66 amino acid tail (29-94)[4,17] and it is cleaved by the proprotein convertase (PC) 1/3.[21] The signal sequence is eliminated subsequently in the endoplasmic reticulum (ER) and then a proteolytic processing occurs giving the mature ghrelin and a 66 amino acids C-terminal fragment named C-ghrelin.[22] C-ghrelin is able to circulate as a full-length peptide or be processed into smaller peptides, mainly obestatin [proghrelin (53-75)]. Obestatin results from proteolysis of proghrelin at two cleavage sites of the preproghrelin molecule, between Arg75 and Phe76, and between Lys100 and Phe101 (**Figure 1**). It is proposed that Arg75 and Lys100 predict the monobasic recognition sites for an unknown protease besides the known PCs.

[12] Baldanzi G, Filigheddu N, Cutrupi S, *et al*. Ghrelin and des-acyl ghrelin inhibit cell death in cardiomyocytes and endothelial cells through ERK1/2 and PI 3-kinase/AKT. J Cell Biol. 2002;159:1029-37.

[13] Camina JP. Cell biology of the ghrelin receptor. J Neuroendocrinol. 2006;18:65-76.

[14] McKee KK, Palyha OC, Feighner SD, *et al*. Molecular analysis of rat pituitary and hypothalamic growth hormone secretagogue receptors. Mol Endocrinol. 1997;11:415-23.

[15] Kishimoto M, Okimura Y, Nakata H, *et al*. Cloning and characterization of the 50- flanking region of the human ghrelin gene. Biochem Biophys Res Commun. 2003;305:186-92.

[16] Kanamoto N, Akamizu T, Tagami T, *et al*. Genomic structure and characterization of the 50-flanking region of the human ghrelin gene. Endocrinology. 2004;145:4144-53.

[17] Jeffery PL, Duncan RP, Yeh AH, *et al*. Expression of the ghrelin axis in the mouse: an exon 4-deleted mouse proghrelin variant encodes a novel C terminal peptide. Endocrinology. 2005;146:432-40.

[18] Hosoda H, Kojima M, Mizushima T, *et al*. Structural divergence of human ghrelin. Identification of multiple ghrelin-derived molecules produced by post-translational processing. J Biol Chem. 2003;278:64-70.

[19] Yeh AH, Jeffery PL, Duncan RP, *et al*. Ghrelin and a novel preproghrelin isoform are highly expressed in prostate cancer and ghrelin activates mitogen-activated protein kinase in prostate cancer. Clinical Cancer Research. 2005;11:8295-03.

[20] Gahete MD, Cordoba-Chacon J, Hergueta-Redondo M, *et al*. a A novel human ghrelin variant (In1-ghrelin) and ghrelin-O-acyltransferase are overexpressed in breast cancer: potential pathophysiological relevance. PLoS ONE. 2011;6:e23302.

[21] Romero A, Kirchner H, Heppner K, *et al*. GOAT: the master switch for the ghrelin system? Eur J Endocrinol. 2010;163:1-8.

[22] Gualillo O, Lago F, Casanueva FF, *et al*. One ancestor, several peptides post-translational modifications of preproghrelin generate several peptides with antithetical effects. Mol Cell Endocrinol. 2006;256:1-8.

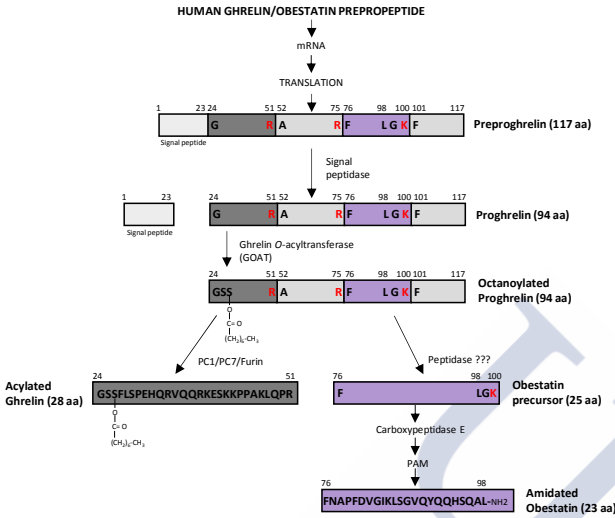

Figure 1. Proposed post-translational processing of human ghrelin/obestatin prepropetide to mature ghrelin and mature obestatin. Modified from: J Clin Endocrinol Metab. 2007;92:3396-8.

After the cleavage, the Lys residue at the carboxy terminal of the obestatin precursor is cleaved by carboxypeptidase E, and the next Gly residue donates the amide group to the carboxy-terminal Leu residue. The amidation is likely catalysed by the bifunctional enzyme peptidyl glycine α-amidating monooxygenase (PAM, **Figure 1**).[23] However, the proteolytic cleavage of preproghrelin is an intriguing feature. Studies of animals lacking diverse PCs suggest that PC1 is involved in processing of proghrelin to ghrelin as well as to obestatin, although the direct processing of proghrelin to obestatin was not evaluated.[24] Other report suggests that PC7 and furin might also be involved in ghrelin processing.[25] But what happens to obestatin? These proteases recognize di-basic residues Lys-Arg or Arg-Arg and cleave the peptide bond carboxyterminal to the dibasic pair.[26] They may also recognize monobasic residue cleavage sites, but the cleavage is not efficient. The release of ghrelin after signal peptide elimination involves a single cleavage (C-terminus), but obestatin release requires the cleavage at the amino- and carboxy-terminus. The efficiency of these two cleavages for obestatin is unclear because the proposed cleavage sites lack the more efficient dibasic residues. Furthermore, *in vitro* digestion of proghrelin using several convertases failed to yield obestatin.[25] So, does obestatin production require other proteases or even work in a different microenvironment? The answer remains unclear.

Obestatin amidation. The structure of obestatin was deduced by amino acid sequencing of a purified 20-residue peptide, combined with mass spectrometry data, to generate a 23 amino acid sequence. On the basis of a C-terminal Gly-Lys motif, amidation of obestatin was assumed and verified as a prerequisite for biological activity.[1] Amidation is a quite common post-translational modification. Hydroxylation at the methylene carbon of a C-terminal Gly residue is the first step in the conversion of Gly-extended prohormones into the physiologically active α-amidated peptide hormones. A bifunctional enzyme, the PAM enzyme, catalyses peptide α-amidation. The first step is brought about the copper-dependent N-terminal peptidyl Gly α-hydroxylating monooxygenase domain (PHM) and followed by the zinc-containing peptidylamido-glycolate lyase (PAL) domain.[27]

[23] Garg A. The ongoing saga of obestatin: is it a hormone? J Clin Endocrinol Metab. 2007;92:3396-8.

[24] Zhu X, Cao Y, Voogd K, *et al*. On the processing of proghrelin to ghrelin. J Biol Chem. 2006;281:38867-70.

[25] Ozawa A, Cai Y, Lindberg I. Production of bioactive peptides in an *in vitro* system. Anal Biochem. 2007;366:182-9.

[26] Steiner DF. The proprotein convertases. Curr Opin Chem Biol. 1998;2:31-9.

[27] Owen TC, Merkler, DJ. A new proposal for the mechanism of glycine hydroxylation as catalyzed by peptidylglycine alphahydroxylating monooxygenase (PHM). Med Hypoth. 2004;62:392-400.

Although the enzyme/s responsible for obestatin amidation has not yet been identified it is likely that PHM might be involved in this process.[22]

Other biological obestatin fragments. The mass spectrometric data of Zhang's work indicated that in addition to obestatin, this peptide may be processed in stomach extracts to a 13-amino acid residue peptide: (11-23)-obestatin.[1] It has not been determined whether (11-23)-obestatin occurs physiologically and the details of the obestatin peptide processing have yet to be elucidated, however, searching of enzyme databases reveals that trypsin, endopeptidase LysC and α-secretase might, in theory, perform the enzymatic cleavage from full obestatin to (11-23)-obestatin. Furthermore, the fact that trypsin were native to the intestine would enable the participation of this enzyme in the process, but further information is required to establish exactly how (11-23)-obestatin is formed, and if the process occurs either during biosynthesis, intracellular processing or upon secretion. Regarding the biological properties of (11-23)-obestatin, several reports indicate that this isoform is biologically active. Green *et al* reported that mouse (1-23)-obestatin and (11-23)-obestatin were both to be equally effective in reducing glucose excursions and insulin responses to feeding in normal mice, and reduced food intake by approximately 50% compared with control mice, but their results indicate no direct actions on glucose homeostasis or insulin secretion.[28] Nagaraj *et al* demonstrated, in rodents, that (11-23)-obestatin was more effective than full length obestatin in lowering plasma cholesterol and triglycerides, equally as effective in reducing perirenal fat, and less effective in decreasing epididymal fat.[29] Later, Subasinghage *et al* showed that in high-fat fed mice administration of either the full length peptide or the (11-23)-fragment led to significantly reduced food intake and post-meal glucose responses. In this study human obestatin and (11-23)-obestatin similarly affected food intake in high-fat fed mice, however, the glucose responses to feeding were smaller and insulin responses were not affected.[30]

In addition to (11-23)-obestatin, a diverse range of degradatory fragments appears to be formed when obestatin is incubated *in vitro* in mouse plasma and kidney or liver homogenate.[31] This study had reported the formation of an N-terminal fragment: (1-10)-obestatin. A later published work from Nagaraj's group indicated that this (1-10)-fragment showed improved bio-active features when some residues were modified,[32] however, several studies so far suggested that this peptide is an inactive metabolite.[29,30]

OBESTATIN EXPRESSION

The main producer of obestatin is the stomach, and most of the obestatin-producing cells are distributed in the basal end of the gastric oxyntic mucosa. Furthermore, it was found that the removal of the stomach by gastrectomy reduces obestatin-circulating levels around 50-80%.[33] Nevertheless, obestatin- and

[28] Green BD, Irwin N, Flatt PR. Direct and indirect effects of obestatin peptides on food intake and the regulation of glucose homeostasis and insulin secretion in mice. Peptides. 2007;28:981-7.

[29] Nagaraj S, Peddha MS, Manjappara UV. Fragments of obestatin as modulators of feed intake, circulating lipids, and stored fat. Biochem Biophys Res Commun. 2008;366:731-7.

[30] Subasinghage AP, Green BD, Flatt PR, *et al*. Metabolic and structural properties of human obestatin (1-23) and two fragments peptides. Peptides. 2010;31:1697-705.

[31] Vergote V, Van Dorpe S, Peremans K, *et al*. In vitro metabolic stability of obestatin: kinetics and identification of cleavage products. Peptides. 2008;29:1740-8.

[32] Nagaraj S, Peddha MS, Manjappara UV. Fragment analogs as better mimics of obestatin. Regul Pept. 2009;158:143-8.

[33] Furnes MW, Stenstrom B, Tømmerås K, *et al*. Feeding behavior in rats subjected to gastrectomy or gastric bypass surgery. Eur Surg Res. 2008;40:279-88.

ghrelin-immunoreactive (IR) cells were found throughout the entire gastrointestinal tract. [34]

Grönberg *et al* showed that obestatin and ghrelin peptides were expressed in the whole human stomach including cardia, fundus, corpus, and antrum. The IR cells were more abundant in the stomach region, less in duodenum, occasional in jejunum, and rare in ileum. The vast majority of the obestatin and ghrelin-IR cells were located in the deeper third of the glands, whereas few cells were found in the superficial mucosa regions of the cardia, fundus, duodenum, and ileum. No IR cells were detected in the colonic mucosa or caudally. A substantial number of obestatin-IR cells and ghrelin-IR cells were found in the crypts of Lieberkühn, whereas only a few scattered IR cells were seen in the Brunner's glands (**Figure 2**).

Grönberg's work also showed a limited number of both obestatin and ghrelin-IR cells in the periphery of the pancreatic islets and a few scattered cells detected in connection to the exocrine pancreatic ducts. Likewise, ghrelin and obestatin were expressed in human mammary glands with similar patterns. Cytoplasmic IR was seen in ductal epithelial cells, whereas the myoepithelial cells were non-IR. Pituitary, prostate, testis, placenta, ovaries, thyroid, and parathyroid human tissues showed a weak expression for obestatin. By double immunofluorescence microscopy, it was showed that all cells detected were IR for both peptides. Furthermore, the subcellular localization of ghrelin and obestatin was essentially identical, indicating that obestatin and ghrelin are stored in the same secretory vesicles. Interestingly, epithelial cells of the ducts of the mammary glands showed different IR for both peptides.

One year later, Volante *et al* published a work showing that obestatin is produced in the same cells that express endocrine ghrelin in the human foetal pancreas and stomach, adult stomach and small intestine tissues.[35] In foetal tissues, obestatin was detected diffusely in the endocrine cells and thyroid, and in single or small clusters of cells in the pituitary, lung, gastrointestinal tract and pancreas. Other endocrine (adrenal) and non-endocrine (spleen, thymus, liver, kidney and heart) tissues did not show obestatin expression.

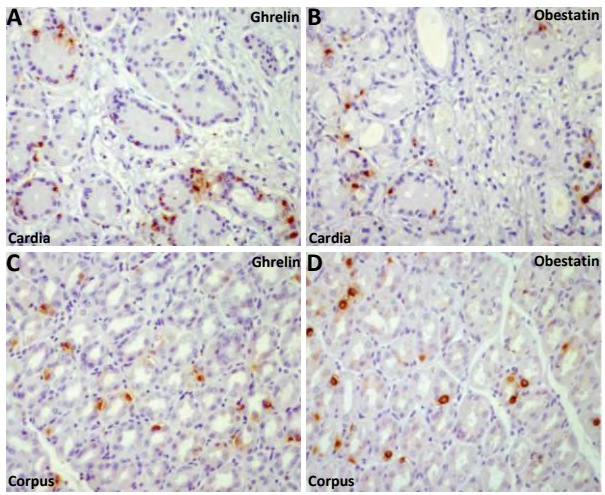

Figure 2. Ghrelin and obestatin immunohistochemical staining in human stomach tissue. The sections show the immunoreactivity for ghrelin (A, C) and obestatin (B, D). Cardia (A, B): obestatin and ghrelin IR cells are localised in the deeper regions of the mucosa including the cardiac glands. Corpus (C, D): scattered obestatin and ghrelin IR cells are seen throughout the whole mucosa. Bar=50 µm. Modified from: J Histochem Cytochem. 2008;56:793-801.

[34] Grönberg M, Tsolakis AV, Magnusson L, *et al*. Distribution of obestatin and ghrelin in human tissues: inmunoreactive cells in the gastrointestinal tract, pancreas, and mammary glands. J Histochem Cytochem. 2008;56:793-801.

[35] Volante M, Rosas R, Ceppi P, *et al*. Obestatin in human neuroendocrine tissues and tumours: expression and effect on tumour growth. J Pathol. 2009;218:458-66.

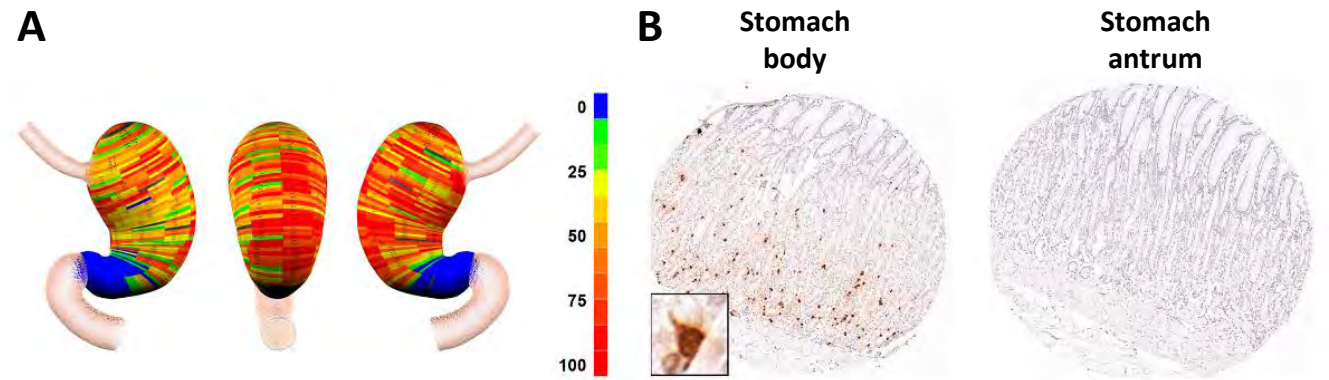

Figure 3. Geographic mapping of the ghrelin/obestatin cell lineage of the human stomach. A. On the left panel are shown the quantitated cell lineage numbers per core mapped onto three-dimensional stomach maps to demonstrate the distribution of ghrelin/obestatin IR-cells in the gastric mucosa. The scale bars represent the range of positive IR-cells in a core. B. Two representative cores from the body and antrum showing the ghrelin/obestatin cell-staining pattern are shown on the right panel. Modified from: Gut. 2014;63:1711-20.

In adult tissues, obestatin-positive cells were identified in the pituitary and in pancreatic islets and, to a lower extent, in the bronchial tree and gastrointestinal tract. Thyroid parenchyma, as well as all other tissues tested (parathyroid, adrenal, liver, thymus, lymph node, kidney, testis and ovary) did not show any IR. In both foetal and adult tissues, they showed the neuroendocrine nature of obestatin-expressing cells by double immunofluorescence with chromogranin A. Furthermore, they observed that obestatin colocalized with GH in the adenohypophysis. Tsolakis *et al* also demonstrated that in human mucosa cells obestatin/ghrelin rarely co-express with the vesicular monoamine transporter-2 (VMAT-2), a marker for enterochromaffin-like cells (ECL).[36]

In 2014, Goldenring's group published a cell lineage distribution atlas of the human stomach. They reported that enteroendocrine cells showed distinct patterns of localisation in the gastric mucosa, and that the existence of antral glands with mixed cell lineages indicated that human antral glands might be functionally chimeric with glands assembled from multiple distinct stem cell populations. Regarding ghrelin-expressing cells, they were essentially excluded from the distal stomach and were abundant in the body regions with a relatively even distribution throughout the body mucosa and a similar staining pattern was also observed for obestatin (**Figure 3**). An inverse relationship between gastrin and ghrelin expression was observed and these findings suggested that gastrin and ghrelin/obestatin cells define the anatomical division between the human stomach body and antrum, respectively.[37]

In rats, the expression of obestatin was found in gastric mucosa, pancreas, and Leydig and myenteric ganglion cells showing that the peptide is bioactive on central neurons.[38] Additionally, rat pancreas immunoreactivity correlates positively with insulin

[36] Tsolakis AV, Grimelius L, Stridsberg M, *et al*. Obestatin/ghrelin cells in normal mucosa and endocrine tumours of the stomach. Eur J Endocrinol. 2009;160-941-9.

[37] Choi E, Roland JT, Barlow BJ, *et al*. Cell lineage distribution atlas of the human stomach reveals heterogeneous gland populations in the gastric antrum. Gut. 2014;63:1711-20.

[38] Dun SL, Brailoiu E, Yang J, *et al*. Distribution and biological activity of

secretion, suggesting that obestatin could contribute to pancreatic β cell function.[39]

OBESTATIN STRUCTURE AND BIOACTIVITY FEATURES

Regarding obestatin structure, the primary structure is formed by 23 amino acids with a post-translational amide modification on the Leu of the C-terminus.[1]

Since its discovery, a few reports were published about obestatin structure and conformation. Scrima *et al* performed circular dichroism (CD) and nuclear magnetic resonance (NMR) studies to determine the possible secondary structure of mouse obestatin and its (11-23)-obestatin truncated biological isoform in the presence of dodecyl-phosphocholine (DPC)/sodium dodecy sulphate (SDS) micelles.[40]

The results showed the preference of both peptides to assume regular secondary structures at the C-terminus rather than in its N-terminal portion, and that carboxy-amidation is a prerequisite for the biological activity because it is necessary to induce and to stabilize the regular conformations. Their data showed that a regular backbone arrangement might be required to provide the conformational prerequisites of important residues for receptor binding. Furthermore, investigating the occurrence of the sequence Gln15-Tyr-Gln-Gln-His-Gly-Arg-Ala-Leu23 in protein databanks, they found that the sequence Gln-Tyr-Gln-Gln-His-Gly-Arg results exclusively present among the different obestatin species. Moreover, Gln15-Tyr16, Gln18-His19, and Ala22-Leu23 pairs were completely conserved, indicating a possible participation of these residues to the biological specificity of obestatin (**Table 1**).

Human obestatin	FNAPFDVGIKLSGVQYQQHSQAL-NH_2
Human (11-23)-obestatin	LSGVQYQQHSQAL-NH_2
Mouse obestatin	FNAPFDVGIKLSGAQYQQHGRAL-NH_2
Mouse (11-23)-obestatin	LSGAQYQQHGRAL-NH_2

Table 1. Amino acid sequence comparison between human and mouse obestatin and its active biological fragments

In 2008, Nagaraj *et al* published a work about the relationship between the primary structure and the bioactivity of mouse obestatin. They synthesized mouse obestatin and the three overlapping fragments on the C-terminus: N-terminal, (11-23)-obestatin; middle (6-18)-obestatin, and the C- terminal (11-23)-obestatin fragment. Their results showed that the N-terminal peptide harboured the ability to reduce the feed intake and gain in body weight and was as effective as obestatin in reducing the epididymal and perirenal fat; whereas the middle fragment, less effective in altering the feed intake and gain in body weight, did very effectively reduce the amount of stored fat. They concluded that residues 1-18 in obestatin with a C-terminal amidation seem to be vital for appetite suppression, body weight loss, and reduction in total fat.[29]

Later, Subasinghage *et al* performed a structure-bioactivity study in rodents using human obestatin.[30] They evaluated the acute metabolic effects of human obestatin and the fragments (1-10) and (11-23)-obestatin in high-fat fed mice, and investigated their solution structure by NMR spectroscopy. Structure results showed that in aqueous solution none of the obestatin peptides possessed secondary structural features. However, in a 2,2,2-trifluoroethanol (TFE)-d_3:H_2O solvent mixture, the structure of human

obestatin in the rat. J Endocrinol. 2006;191:481-9.

[39] Chanoine JP, Wong AC, Barrios V. Obestatin, acylated and total ghrelin concentrations in the perinatal rat pancreas. Horm Res. 2006;66:81-8.

[40] Scrima M, Campiglia P, Esposito C, *et al*. Obestatin conformational features: a strategy to unveil obestatin´s biological role? Biochem Biophys Res Commun. 2007;363:500-5.

obestatin was characterized by an alpha-helix followed by a single turn helix conformation between residues Pro4 and Gln15 and His19 and Ala22 respectively. (1-10)-obestatin showed no structural components whereas (11-23) fragment contained an alpha-helix between residues Val14 and Ser20 in a mixed solvent (**Figure 4**). Regarding bioactivity study, they observed that full lenght and (11-23)-obestatin significantly reduced food intake (86% and 90%, respectively) and lowered glucose responses to feeding, whilst leaving insulin responses unchanged. They did not find metabolic changes following the administration of (1-10)-obestatin, correlating the presence of secondary conformations with biological actions.

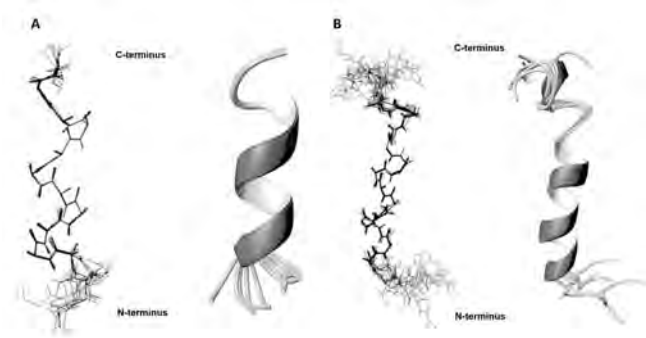

Figure 4. Three-dimensional structure of human (11-23)-obestatin (A) and full-length human obestatin (B) in TFE solution showing the ribbon representation and backbone conformations. Helical segments showing best-fit residues are represented for both peptides. (11-23)-obestatin shows an helical conformation between residues 14 and 20 (A). Full-length obestatin suggests an α-helical arrangement between residues 4 and 15 and 19 and 22 (B). Modified from: Peptides. 2010;31:1697-705.

More recently, Raghothama's group published a NMR analysis on synthetic mice obestatin and six analogue peptides: three overlapping 13 residue fragments (1-13), (6-18) and (11-23)-obestatin; and three mutant analogues Nt8U, NtCha and MF38dU incorporating helix-inducing residues. They demonstrated the formation of helical secondary structure in all the peptide analogues and found that these unusual amino acids could provide protection from immediate degradation and aid structure stabilization, enhancing efficacy of obestatin for better drug development.[41]

Taken together, obestatin structure have been already established; however, the fact that all published reports have been performed in mice using even human obestatin,[30] and the use of solutions that favours helical conformations like TFE or methanol puts these results into question. A proper study of the structure-activity should be based on knowledge of the bioactive conformation when obestatin binds to its receptor. NMR techniques using living cells enriched with receptor could be suitable for this purpose. Since the system has adequate kinetic facts, these experiments with living cells, would avoid the need to isolate the receptor and work in *quasi*-physiological conditions.[42]

OBESTATIN RECEPTOR

GPR39 RECEPTOR

When it was discovered, obestatin was characterized to bind selectively to the orphan G-protein 39-coupled receptor (GPR39), a G-protein-coupled receptor (GPCR) that was first characterized in 1997 from a foetal brain cDNA library by hybridization.[43] GPR39

[41] Krishnarjuna B, Ganjiwale AD, Manjappara UV, *et al*. NMR Structure implications of enhanced efficacy of obestatin fragment analogs. Int J Pept Res Ther. 2011;17:259-70.

[42] Martín-Pastor M, De Capua A, Álvarez CJ, *et al*. Interaction between ghrelin and the ghrelin receptor (GHS-R1a), a NMR study using living cells. Bioorg Med Chem. 2010;18:1583-90.

[43] McKee KK , Tan CP, Palyha OC, *et al*. Cloning and characterization of two human G protein-coupled receptor genes (GPR38 and GPR39) related to the growth hormone secretagogue and neurotensin receptors. Genomics. 1997;46:426-34.

belongs to the same family as ghrelin (GHSR1a), motilin (GPR38) and neurotensin receptor (NTR)1 (**Figure 5, upper panel**), and it was speculated to have a gut peptide ligand, since all the other receptors homologous to GHSR have such ligands.[44] In this context, GPR39 was considered an orphan GPCR until 2005, when Zhang *et al* based on the data of radiolabelled ligand binding assays proposed obestatin as its selective ligand.[1]

GPR39 structure. The human GPR39 is a 435-amino acid seven transmembrane GPCR (**Figure 5, bottom panel**). It is encoded by a single copy gene located in chromosome 2, band q21–q2243 and spans about 200 kb. Two different transcripts called sbGPR39-1a and sbGPR39-1b were identified derived through a process of alternative splicing.[45] The gene has two exons, the first one encodes residues 1 to 285, corresponding to the N-terminal region and the first five transmembrane helices; and the second exon encodes residues 286 to 435, corresponding to the last two transmembrane helices and the C-terminal region. Between the two exons there is an intron of 200 kb, whose analogue appears in the genes of the ghrelin receptor and the motilin receptor. The second exon also shares a segment of DNA with LYPD1 gene; GPR39 is encoded by the forward strand of DNA, while *LYPD1* is transcribed from the reverse strand. The two-exon structure and *LYPD1* gene-overlapping pattern are conserved among several species.[46] GPR39-1a is considered the canonical form. The splice variant, GPR39-1b, is encoded by the first exon and it is truncated after the fifth transmembrane helix. GPR39-1b was believed to have no functionality until very recently.[47] Novel reports found that GPR39-1b could be implied in anxiety-related behaviours and appetite disorders[48] and in a novel regulatory mechanism in NTR1 signalling.[49] GPR39 has a relatively high constitutive activity independent from its ligand like GHSR1a and the neurotensin receptor.[50] But, whereas GHSR1a and NTR2 have more efficiency than GPR39 in signalling through the inositol triphosphate and cAMP element pathways, GPR39 is mainly constitutively active through the serum response element (SRE)-dependent pathway. The structural basis for the unusually high degree of constitutive activity is determined in the three ghrelin-like receptors (GHSR1a, NTR2, GPR39) by an aromatic cluster on the inner face of the extracellular ends of transmembrane domains VI and VII; nevertheless, receptors also display major differences in their internalization properties. Holliday *et al* found that GHSR1a internalization was regulated by its C-terminus, and that constitutive activity is required but not enough for receptor endocytosis. They observed that β-arrestin-independent mechanisms contributed to GHSR internalization. Furthermore, GPR39 displayed constitutive signalling, but only ghrelin receptor undergo basal internalization, and GPR39

[44] Kojima, M. Kangawa K. Ghrelin: structure and function. Physiol. Rev. 2005;85:495-522.

[45] Zhang Y, Zhao H, Peng H, *et al*. Two alternatively spliced GPR39 transcripts in seabream: molecular cloning, genomic organization, and regulation of gene expression by metabolic signals. J Endocrinol. 2008;199:457-70.

[46] Egerold KL, Holst B, Petersen PS, *et al*. GPR39 splice variants versus antisense gene LYPD1: expression and regulation in gastrointestinal tract, endocrine pancreas, liver, and white adipose tissue. Mol Endocrinol. 2007;21:1685-98.

[47] Zhang JV, Li L, Huang Q, *et al*. Obestatin receptor in energy homeostasis and obesity pathogenesis. Prog Mol Biol Transl Sci. 2013;114:89-107.

[48] Ishitobi Y, Akiyoshi J, Honda S, *et al*. Administration of antisense DNA for GPR39-1b causes anxiolytic-like responses and appetite loss in rats. Neurosci Res. 2012;72:257-62.

[49] Yasuda S, Ishida J. GPR39-1b, the 5-transmembrane isoform of GPR39 interacts with neurotensin receptor NTSR1 and modifies its function. J Recept Signal Transduct Res. 2014;34:307-12.

[50] Holst B, Holliday ND, Bach A, *et al*. Common structural basis for constitutive activity of the ghrelin receptor family. J Biol Chem. 2004;279:53806-17.

phosphorylation were not sufficient for β-arrestin 2 recruitment.[51]

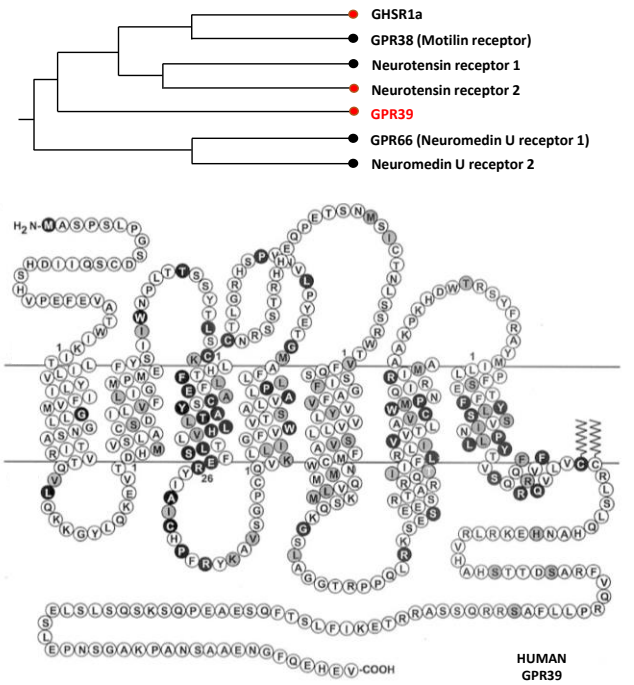

Figure 5. The GPR39 receptor family. Upper panel. Schematic phylogenic tree of the GPR39 receptor family. Red dots indicate the three receptors that display a high degree of constitutive signalling activity. Bottom panel. Serpentine model of GPR39 receptor. Residues that are identical among GPR39, GHSR1a, and NTR2 are highlighted in white on black circles. Modified from: J Biol Chem. 2004;279:53806-17.

GPR39 expression. GPR39 is widely expressed throughout the body, both human and rat, but the highest expression levels are localized in the gastrointestinal mucosa (stomach, duodenum, jejunum, ileum…), white adipose tissue, kidney,[43] pancreas (β-cells, duct epithelium), liver, spleen, lung, heart, and reproductive tissues.[52] In the brain, high expression levels are observed in the septum and in discrete cells in the amygdala and hippocampus.[43,53,54] In contrast to the original study of Zhang *et al*, several groups failed to detect GPR39 expression in the hypothalamus.[53,54,55,56.]

GPR39 relevant physiological functions

Digestive system. The GPR39 receptor family is involved in the regulation of gastrointestinal motility.[57,58,59] In addition, GPR39 is expressed mostly in stomach and intestine. Therefore it is reasonable to think that GPR39 receptor exerts functions in the gastrointestinal tract. Moechars *et al* published a work showing that in GPR39 null mice gastric emptying was accelerated and that transit and expulsion of faecal pellets was more effective.[53] Furthermore, gastric secretion was increased. These studies suggest that GPR39 agonists may inhibit gastric and colonic motility and could have an important role in energetic homeostasis.

[51] Holliday ND, Holst B, Rodionova EA, *et al*. Importance of constitutive activity and arrestin-independent mechanisms for intracellular trafficking of the ghrelin receptor. Mol Endocrinol. 2007;21:3100-12.
[52] Depoortere I. GI functions of GPR39: novel biology. Curr Opin Pharmacol. 2012;12:647-52.
[53] Moechars D, Depoortere I, Moreaux B, *et al*. Altered gastrointestinal and metabolic function in the GPR39-obestatin receptor-knockout mouse. Gastroenterology. 2006;131:1131-41.
[54] Jackson VR, Nothacker HP, Civelli O. GPR39 receptor expression in the mouse brain. Neuroreport. 2006;17:813-6.
[55] Holst B, Egerod KL, Schild E, *et al*. GPR39 signaling is stimulated by zinc ions but not by obestatin. Endocrinology. 2007;148:13-20.
[56] Nogueiras R , Pfluger P, Tovar S, *et al*. Effects of obestatin on energy balance and growth hormone secretion in rodents. Endocrinology. 2007;148:21-6.
[57] Zhao D, Pothoulakis C. Effects of NT on gastrointestinal motility and secretion, and role in intestinal inflammation. Peptides. 2006;27:2434-44.
[58] Brighton PJ, Szekeres PG, Willars GB. Neuromedin U and its receptors: structure, function, and physiological roles. Pharmacol Rev. 2004;56:231-48.
[59] De Smet B, Mitselos A, Depoortere I. Motilin and ghrelin as prokinetic drug targets. Pharmacol Ther. 2009;123:207-23.

Metabolic functions. Published reports showing a GPR39 role on metabolism exhibited conflicting results. Gastric emptying acceleration observed in GPR39 null mice in Moechars' work were expected to enhance appetite signalling and contributed to body weight gain. GPR39 null mice, really showed higher mature body weights and body fat compositions, reduced hyperphagia after fasting, and increased cholesterol levels.[53] Tremblay *et al* reported similar observations with respect to food intake but the increase in body weight was not observed, probably because mice were a few weeks age.[60]

Contradictory results related to body weight were also reported when GPR39 null mice were put on a high-fat diet (HFD) after weaning. Authors found no difference[61] or an increase[62] in body weight between both genotypes. Verthulst *et al* also suggested that GPR39, through intracellular crosstalk with the β-adrenergic receptors signalling pathways, could modulate lipolysis. Furthermore, they observed an increase in octanoyl ghrelin levels in GPR39 null mice with HFD.[61] Petersen's work reported that whereas food intake was normal, energy storage was increased with an almost complete elimination of diet-induced thermogenesis. This increase in fat accumulation was due to impaired lipolysis since expression levels and activity of lipolytic enzymes was downregulated in adipocytes.[62] Others reports in GPR39 null mice fed either with a low-fat/high-sucrose or a high-fat/high-sucrose diet, showed no changes in energy intake and body weight.[63] But the age of initial exposure to the diet and the type of diet can be essential to reveal differences in body weight. In obese patients with type 2 diabetes and in mice fed a HFD, expression of GPR39 in white adipose tissue was decreased and did not correlate with changes in body mass index (BMI) or body weight but correlated negatively to fasting glucose levels.[64] All these studies suggest a more important role of GPR39 in the regulation of glucose homeostasis than in changes of body weight.

Role of GPR39 in glucose homeostasis. GPR39 is expressed in pancreatic beta cells.[53,55] In a pancreatic islets model, glucose-induced insulin secretion was impaired in female but not male GPR39 null mice. Islet architecture was normal but the expression of the master regulator of islet development, pancreatic and duodenal homeobox-1 (Pdx-1), was down-regulated.[55] In the Verhults' study mentioned above, mice on a HFD after weaning displayed a less overt diabetic phenotype, with lower glucose levels in the fed state despite reduced insulin levels suggesting changes in insulin sensitivity.[61] Mice preferentially used carbohydrates as an energy source instead of fat which could reduced blood glucose levels. However, glucose tolerance tests revealed an impaired insulin response, which did not result in changes in glucose levels. Similar results were observed in mice fed a low-fat/high-sucrose or a high-fat/high-sucrose diet.[63] These studies suggested a direct effect of GPR39 on insulin secretion and that GPR39 null mice are less

[60] Tremblay F, Perreault M, Klaman LD, *et al*. Normal food intake and body weight in mice lacking the G protein-coupled receptor GPR39. Endocrinology. 2007;148:501-6.

[61] Verhulst PJ, Lintermans A, Janssen S, *et al*. GPR39, a receptor of the ghrelin receptor family, plays a role in the regulation of glucose homeostasis in a mouse model of early onset diet-induced obesity. J Neuroendocrinol. 2011;23:490-500.

[62] Petersen PS, Jin C, Madsen AN, *et al*. Deficiency of the GPR39 receptor is associated with obesity and altered adipocyte metabolism. FASEB J. 2011;25:3803-14.

[63] Tremblay F, Richard AM, Will S, *et al*. Disruption of G protein-coupled receptor 39 impairs insulin secretion in vivo. Endocrinology. 2009;150:2586-95.

[64] Catalán V, Gómez-Ambrosi J, Rotellar F, *et al*. The obestatin receptor (GPR39) is expressed in human adipose tissue and is down-regulated in obesity-associated type 2 diabetes mellitus. Clin Endocrinol. 2007;66:598-601.

prone to develop diabetes. In contrast, in the same model of HFD-induced obese GPR39 null mice in Petersen's work, increased blood glucose levels and impaired insulin sensitivity did not implied effects on insulin secretion.[62] GPR39 could also have a role on type 1 diabetes. GPR39 overexpression in a β-cell model, affected cell mass and slightly impaired the glucose tolerance, but nevertheless totally protected against the gradual hyperglycaemia in a model of type 1 streptozotocin-induced diabetes.[65]

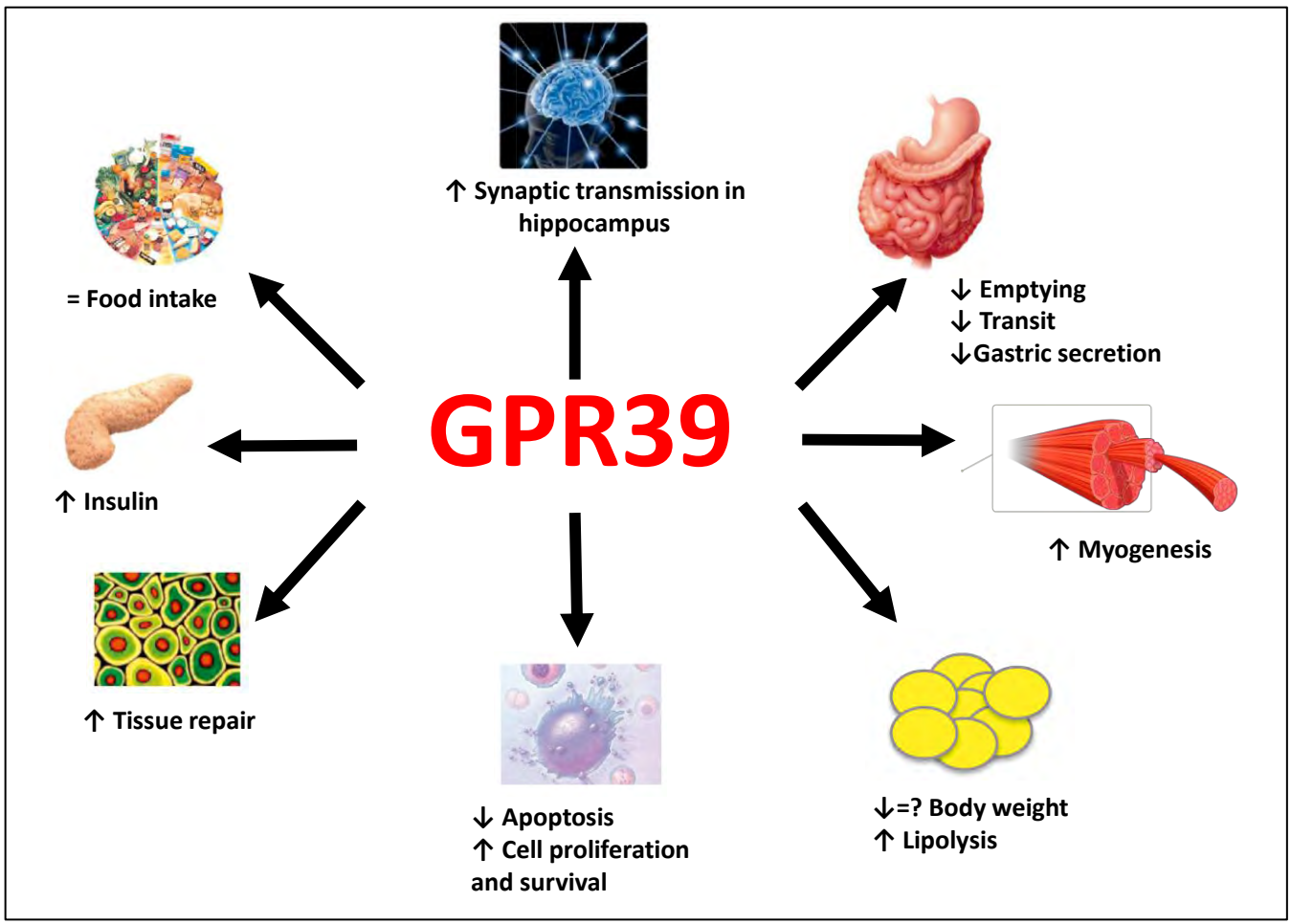

Figure 6. Relevant physiological actions of GPR39. The data are provided by studies with Zn^{+2} and obestatin agonists, mice overexpressing GPR39, GPR39 knockout mice and *in vitro* assays. Modified from: Curr Opin Pharmacol. 2012;12:647-52.

[65] Egerold KL, Jin C, Petersen PS, *et al*. Beta-cell specific overexpression of GPR39 protects against streptozotocin-induced hyperglycemia. Int J Endocrinol. 2011;2011:401258.

Taken together, the type and treatment period of diet, and the age and gender of the mice seem to influence the role of GPR39 in the regulation of glucose homeostasis. However the overall finding of these studies is that GPR39 has an important role on insulin secretion.

Other functions. In these years, other physiological functions were reported for GPR39. GPR39 protects to oxidative stress, endoplasmic reticulum stress and apoptosis in a hippocampal cell line overexpressing GPR39.[66] In this way, GPR39 was proposed to be a novel inhibitor of cell death through its constitutive activity. In human keratinocytes, GPR39 also mediates the epithelial injury repairing wound effects.[67] In brain, Cornu Ammonis 3 (CA3) hippocampal region showed neurons and dendrites immunoreactive for GPR39.[68] Small interfering RNA (siRNA) GPR39 in a neuronal cell line and hippocampal slices studies of GPR39 null mice showed that endogenous GPR39 mediates Zn^{+2}-dependent signalling in neurons.[68,69] These studies suggest that GPR39 has a role in memory formation. Very recently, GPR39 was involved with adipocite metabolism[70] and insulin action on adipogenesis,[71] as well as myogenesis[72] and skeletal muscle repair.[73]

Is GPR39 the obestatin receptor?

Obestatin was described as the selective ligand of GPR39,1 however, there are several studies that indicate that obestatin is not its natural ligand, since there is not specific binding on GPR39-transfected cells, display any effect such as cAMP production or activation of signal transduction pathways.[60,74,75] The authors of the discovery of obestatin, unable to reproduce their original trials of binding and activation of GPR39, observed that the absence of binding could be due to loss of obestatin bioactivity after its poly-iodization. Moreover, De Spiegeleer's group found that the quality of the peptides was insufficient for *in vitro* and *in vivo* experiments.[76] In this way, Zhang *et al* found that mono-iodinated obestatin was able to bind human embrionyc kidney (HEK)293T cells transfected with plasmids encoding the GPR39.[77] The same authors also found that treating stomach cells with obestatin induced the expression of c-fos (a

[66] Dittmer S, Sahin M, Pantlen A, *et al*. The constitutively active orphan G-protein-coupled receptor GPR39 protects from cell death by increasing secretion of pigment epithelium-derived growth factor. J Biol Chem. 2008;283:7074-81.

[67] Sharir H, Zinger A, Nevo A, *et al*. Zinc released from injured cells is acting via the Zn2+-sensing receptor, ZnR, to trigger signaling leading to epithelial repair. J Biol Chem. 2010;285:26097-106.

[68] Besser L, Chorin E, Sekler I, *et al*. Synaptically released zinc triggers metabotropic signaling via a zinc-sensing receptor in the hippocampus. J Neurosci. 2009;29:2890-901.

[69] Chorin E, Vinograd O, Fleidervish I, *et al*. Upregulation of KCC2 activity by zinc-mediated neurotransmission via the mZnR/GPR39 receptor. J Neurosci. 2011;31:12916-26.

[70] Gurriarán-Rodríguez U, Al-Massaddi O, Roca-Rivada A, *et al*. Obestatin as a regulator of adipocyte metabolism and adipogenesis. J Cell Mol Med. 2011;15:1927-40.

[71] Gurriarán-Rodríguez U, Al-Massadi O, Crujeiras AB, *et al*. Preproghrelin expression is a key target for insulin action on adipogenesis. J Endocrinol. 2011;210:R1-7.

[72] Gurriarán-Rodríguez U, Santos-Zas I, Al-Massadi O, *et al*. The obestatin/GPR39 system is up-regulated by muscle injury and functions as an autocrine regenerative system. J Biol Chem. 2012;287:38379-89.

[73] Gurriarán-Rodríguez U, Santos-Zas I, González-Sánchez J, *et al*. Action of obestatin in skeletal muscle repair: stem cell expansion, muscle growth, and microenvironment remodeling. Mol Ther. 2015;23:1003-21.

[74] Chartrel N, Alvear-Pérez R, Leprince J, *et al*. Comment on Obestatin, a peptide encoded by the ghrelin gene, opposes ghrelin's effects on food intake. Science. 2007;315:766.

[75] Lauwers E, Landuyt B, Arckens L, *et al*. Obestatin does not activate orphan G protein-coupled receptor GPR39. Biochem Biophys Res Commun. 2006;351:21-5.

[76] De Spiegeleer B, Vergote V, Pezeshki A, *et al.* Impurity profiling quality control testing of synthetic peptides using liquid chromatography-photodiode array-fluorescence and liquid chromatography-electrospray ionization-mass spectrometry: the obestatin case. Anal Biochem. 2008;376:229-34.

[77] Zhang JV, Jahr H, Luo CW, *et al*. Obestatin induction of early-response gene expression in gastrointestinal and adipose tissues and the mediatory role of G protein-coupled receptor, GPR39. Mol endocrinol. 2008;22:1464-75

transcription factor marker of gastrointestinal activity) in wyld type (WT) mice, but not in GPR39 null mice; and, in cultured 3T3-L1 cells, treatment with obestatin, but not motilin, induced c-*fos* expression and also stimulated ERK1/2 phosphorylation. Immunohistochemistry analysis using antibodies against the third extracellular loop of GPR39 also indicated a colocalization for GPR39 and c-fos in different obestatin-targeted cells.[77] Previously, other group had constructed a GPR39-knockout mice model, and partially confirmed the *in vivo* effects of obestatin depending on GPR39.[53] GPR39 null mice showed accelerated gastric emptying; increased gastric secretion, higher mature body weights and body fat compositions; reduced hyperphagia after fasting; and increased cholesterol levels. Furthermore, studies on bone metabolism[78] and term pregnancy[79] have shown the correlation of expression levels of both receptor and ligand. Other studies tested the influence of the acute GPR39 deficiency by siRNA showing that the observed obestatin effects were mediated by the GPR39 receptor in several cell lines (healthy and pathological).[71,72] Very recently, Camiña's group demonstrated that obestatin coimmunoprecipitated specifically with GPR39, validating the binding of obestatin to this receptor in cultured C2C12 myoblast cells.[73] All these data points clearly in the direction that obestatin is able to bind GPR39 receptor to perform their functions.

GPR39 as the Zn^{+2}-Sensing Receptor

After the first published works on the inability of obestatin to activate the GPR39,[75] some groups started to work about the possibility that Zn^{+2} were an effective activator of this receptor, which could indicate its validity as an agonist or physiological modulator of GPR39.[55] Specially, Hershfinkel's group considered GPR39 as Zn^{+2}-sensing receptor (ZnR), [68] and not as the obestatin receptor. Their results found that GPR39 is implied in neuronal function[68] and synapsis,[69] is activated in injury and promoted signalling leading to epithelial repair.[67] In addition, ZnR/GPR39 was tuned to sense physiologically relevant changes in extracellular pH that thus regulate ZnR-dependent signalling and ion transport activity.[80] They also showed that the receptor, activated by Zn^{+2}, had a dual role in promoting proliferation of colonocytes and in controlling their differentiation and might be a therapeutic target for promoting epithelial function and tight junction barrier integrity during ulcerative colon diseases.[81] In cancer cell lines, they found that GPR39 enhanced survival of HT-29 colonocytes.[82] In addition, in human prostate cancer PC3 cells, they found that endogenous ZnR/GPR39 activity was regulated by the expression and activity of another cation sensing GPCR, the Ca^{+2}-sensing receptor (CaSR). ZnR/GPR39 was required for mediating the Zn^{+2}-dependent activation of mitogen-activated protein kinase (MAPK) and phosphatidlyinositol 3-kinase (PI3K) pathways leading to enhanced cell growth; and also enhanced the

[78] Pacheco-Pantoja EL, Ranganath LR, Gallagher JA, *et al*. Receptors and effects of gut hormones in three osteoblastic cell lines. BMC Physiol. 2011;11:12-52.

[79] Fontenot E, DeVente JE, Seidel ER. Obestatin and ghrelin in obese and in pregnant women. Peptides. 2007;28:1937-44.

[80] Cohen L, Asraf H, Sekler I, *et al*. Extracellular pH regulates zinc signaling via an Asp residue of the zinc-sensing receptor (ZnR/GPR39). J Biol Chem. 2008;287:33339-50.

[81] Cohen L, Sekler I, Hershfinkel M. The zinc sensing receptor, ZnR/GPR39, controls proliferation and differentiation of colonocytes and thereby tight junction formation in the colon. Cell Death Dis. 2014;5:e1307.

[82] Cohen L, Azriel-Tamir H, Arotsker N, *et al*. Zinc sensing receptor signaling, mediated by GPR39, reduces butyrate-induced cell death in HT29 colonocytes via upregulation of clusterin. PLoS One. 2012;7:e35482.

expression of the Ca^{+2}-binding protein S100A4 that is linked to invasion of prostate cancer cells.[83]

Nowak *et al*, also support the possibility that GPR39 were the ZnR. Their results showed that the receptor is an important target for zinc "transmission" (its activation modulates/induces diverse biochemical pathways involved in neuroprotection) and plays a pivotal role in antidepressant action being a new target for depression drug development. [84,85,86,87,88]

Other authors reported other actions for GPR39 activated by Zn^{+2} like an important transducer of autocrine and paracrine Zn^{+2} signals, impacting upon cellular processes such as insulin secretion, gastric emptying, neurotransmission and epithelial repair;[89] or a role in signalling pathways in sperm capacitation and acrosome reaction.[90]

COULD OBESTATIN EXERT ITS ACTION THROUGH GLP1R?

Granata *et al* published in 2008 that obestatin action might be mediated partially by the glucagon-like peptide-1 (GLP-1) receptor (GLP1R) in pancreatic β-cells, which would explain its insulinotropic and survival effects.[91,92] They observed that obestatin bound to GLP1R and promoted β-cells and islet cell survival. The interaction among them was proposed based on binding displacement assays of radiolabelled GLP-1 by obestatin. Obestatin inhibited dose-dependently binding of GLP-1 to cell membrane, thus, obestatin and GLP-1 recognized the same binding sites. In addition, obestatin did not influence GLP1 secretion so that promotion of cell survival was independent of GLP-1. However, these results were questioned based on results obtained from INS-1β and HEK cells overexpressing GLP1R in which obestatin was not able to displace radiolabelled GLP-1 binding[93] and the fact that this work is prior to the report about quality of obestatin peptides.[76] Furthermore, there is no report showing a specific binding between obestatin and GLP1R. In this sense, although it might be possible for obestatin to activate GLP1R by transactivation, the role of GLP1R in obestatin signalling still needs to be unravelled.

[83] Asraf H, Salomon S, Nevo A, *et al*. The ZnR/GPR39 interacts with the CaSR to enhance signaling in prostate and salivary epithelia. J Cell Physiol. 2014;229:868-77.

[84] Młyniec K, Budziszewska B, Reczyński W, *et al*. The role of the GPR39 receptor in zinc deficient-animal model of depression. Behav Brain Res. 2013;238:30-5.

[85] Młyniec K, Budziszewska B, Holst B, *et al*. GPR39 (zinc receptor) knockout mice exhibit depression-like behavior and CREB/BDNF down-regulation in the hippocampus. Int J Neuropsychopharmacol. 2014;18:pii:pyu002.

[86] Młyniec K, Doboszewska U, Szewczyk B, *et al*. The involvement of the GPR39-Zn(2+)-sensing receptor in the pathophysiology of depression. Studies in rodent models and suicide victims. Neuropharmacology. 2014;79:290-7.

[87] Młyniec K, Singewald N, Holst B, *et al*. GPR39 Zn(2+)-sensing receptor: a new target in antidepressant development? J Affect Disord. 2015;174:89-100.

[88] Nowak G. Zinc, future mono/adjunctive therapy for depression: Mechanisms of antidepressant action. Pharmacol Rep. 2015;67:659-62.

[89] Popovics P, Stewart AJ. GPR39: a Zn(2+)-activated G protein-coupled receptor that regulates pancreatic, gastrointestinal and neuronal functions. Cell Mol Life Sci. 2011;68:85-95.

[90] Michailov Y, Ickowicz D, Breitbart H. Zn2+-stimulation of sperm capacitation and of the acrosome reaction is mediated by EGFR activation. Dev Biol. 2014;396:246-55.

[91] Granata R, Settanni F, Gallo D, *et al*. Obestatin promotes survival of pancreatic β-cells and human islets and induces expression of genes involved in the regulation of β-cell mass and function. Diabetes. 2008;57:967-79.

[92] Favaro E, Granata R, Miceli I, *et al*. The ghrelin gene products and exendin-4 promote survival of human pancreatic islet endothelial cells in hyperglycaemic conditions, through phosphoinositide 3-kinase/Akt, extracellular signal-related kinase (ERK)1/2 and cAMP/protein kinase A (PKA) signalling pathways. Diabetologia. 2012;55:1058-70.

[93] Unniappan S, Speck M, Kieffer TJ. Metabolic effects of chronic obestatin infusion in rats. Peptides. 2008;29:1354-61.

OBESTATIN BIOACTIVITY. FUNTIONS AND SIGNALLING

Ruling out the role of obestatin in food intake, numerous biological functions have been described for it in both central and peripheral tissues (**Figure 7**).

Role of obestatin in adipose tissue

Regarding the abilities of obestatin in adipose tissue, several works by different groups go in the same direction and showed that this peptide regulates two key enzymes of cell metabolism: Akt and AMP-activated protein kinase (AMPK) in preadipocytes and adipocytes.[70,71,94,95] Obestatin inhibits AMPK and activates Akt and their targets, glycogen synthase kinase 3 (GSK3) (regulator of the synthesis of glycogen), AS160 (regulator of glucose transporters), mammalian target of rapamycin (mTOR) and S6K (regulator of protein synthesis), in preadipocytes and adipocytes 3T3-L1. This fact was confirmed *in vivo* in white adipose tissue obtained from rats under chronic sc administration of obestatin. The relevance of the role of obestatin on the metabolism of preadipocytes and adipocytes is supported by glucose transporter type 4 (GLUT4) translocation to the plasma membrane with the consequent increase in glucose uptake. On the contrary, obestatin did not modify the translocation of fatty acid carriers fatty acid transport (FAT) protein 4 (FATP4) and FAT/CD36 to the plasma membrane. Surprisingly, obestatin regulated the expression of transcription factors involved in adipogenesis: CCAAT/enhancer binding protein (C/EBP)α, C/EBPβ, C/EBPδ and peroxisome proliferator-activated receptor γ (PPARγ) promoting the differentiation.

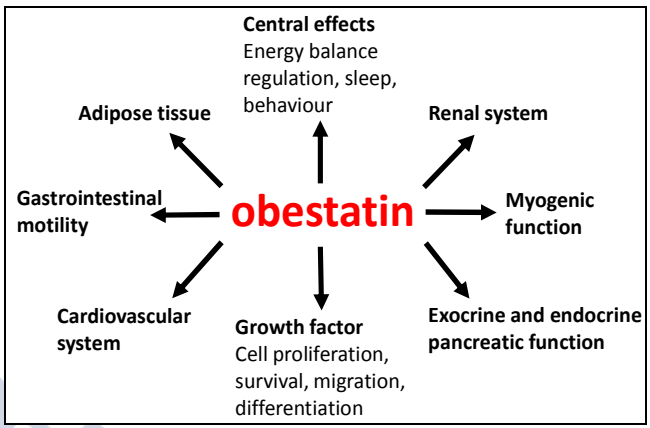

Figure 7. Functions of obestatin. Obestatin may act by endocrine, paracrine, or autocrine mechanisms. These biological effects have been described in central and peripheral tissues, and might be direct or indirect. Modified from: Mol Cell Endocrinol. 2011;340:111-7.

Remarkably, preproghrelin expression, and therefore obestatin expression, showed an increase during adipogenesis being sustained in late differentiation.[71] Furthermore, the neutralization of endogenous obestatin secreted during differentiation of 3T3-L1 preadipocytes decreased significantly in adipogenesis, and GPR39 siRNA studies reduced obestatin action involving this receptor as an extracellular target for obestatin.[55] From these results, it might be concluded that obestatin promotes adipogenesis as an autocrine/paracrine factor. Interestingly, obestatin also regulates lipid metabolism by inhibiting lipolysis, as observed in 3T3-L1 and human subcutaneous (*sc*) and omental adipocytes isolated from both lean and

[94] Granata R, Gallo D, Luque RM, *et al*. Obestatin regulates adipocyte function and protects against diet-induced insulin resistance and inflammation. FASEB J. 2012;26:3393-411.

[95] Gargantini E, Grande C, Trovato L, *et al*. The role of obestatin in glucose and lipid metabolism. Horm Metab Res. 2013;45:1002-8.

obese individuals, and from HFD-treated mice.[94,96] Moreover, AMPK phosphorylation, whose increase has been associated with inhibition of lipolysis, was found enhanced by obestatin in both 3T3-L1 and human adipocytes.[94] *In vivo* studies also showed that in rat, plasma triglyceride levels were significantly reduced by a chronic treatment with a stable obestatin analogue,[97] suggesting a possible role for obestatin in lipid homeostasis. Furthermore, in cow white adipose tissue (WAT), obestatin infusion decreased the expression levels of ATP-binding cassette A1 (ABCA1), a key cholesterol transporter.[98] In addition, and in agreement with the results obtained in cultured adipocytes, mice treated with obestatin showed increased plasma adiponectin and reduced leptin levels, in both epididymal and sc adipose tissue of HFD mice. In these mice, obestatin even reduced inflammation, a hallmark of insulin resistance and diabetes, by inhibiting proinflammatory cytokine release in fat, muscle and liver, through activation of signalling pathways involved in glucose metabolism and insulin signalling.[28]

Obestatin bioactivity in pancreas

Obestatin expression has been demonstrated in the endocrine pancreas, suggesting that may act together as local regulator of β-cell fate and function.[34,35,91,99,100,101] Obestatin was also secreted by pancreatic β-cell lines and human pancreatic islets, and has been shown to reduce apoptosis and to promote proliferation of β-cells and human pancreatic islets upregulating the expression of genes which play a key role in insulin signalling, glucose homeostasis and β-cell survival and differentiation, such as insulin receptor substrate 2 (IRS-2), cAMP response element-binding protein (CREB), Pdx-1 and glucokinase. These obestatin effects in β-cells involve multiple molecular mechanisms, suggesting an intercom with ghrelin and GLP1R.[102,92] It have also been investigated the ability of obestatin to promote *in vitro* β-cell generation from mouse pancreatic islet derived precursors. Obestatin induced the generation of islet-like cell clusters and showed increased levels of insuline gene expression and C-peptide secretion.[103] However, the role of obestatin in glucose metabolism in humans is in contradiction with the results demonstrated in mice

[96] Miegueu P, St Pierre D, Broglio F, *et al*. Effect of desacyl ghrelin, obestatin and related peptides on triglyceride storage, metabolism and GHSR signalling in 3T3-L1 adipocytes. J Cell Biochem. 2011;112:704-14.

[97] Agnew A, Calderwood D, Chevallier OP, *et al*. Chronic treatment with a stable obestatin analog significantly alters plasma triglyceride levels but fails to influence food intake; fluid intake; body weight; or body composition in rats. Peptides. 2011;32:755-62.

[98] Grala TM, Kay JK, Walker CG, *et al*. Expression analysis of key somatotropic axis and liporegulatory genes in ghrelin- and obestatin-infused dairy cows. Domest Anim Endocrinol. 2010;39:76-83.

[99] Zhao CM, Furnes MW, Stenstrom B, *et al*. Characterization of obestatin- and ghrelinproducing cells in the gastrointestinal tract and pancreas of rats: an immunohistochemical and electron- microscopic study. Cell Tissue Res. 2008;331:575-87.

[100] Walia P, Asadi A, Kieffer TJ, *et al*. Ontogeny of ghrelin, obestatin, preproghrelin, and prohormone convertases in rat pancreas and stomach. Pediatr Res. 2009;65:39-44.

[101] Turk N, Dagistanli FK, Sacan O *et al*. Obestatin and insulin in pancreas of newborn diabetic rats treated with exogenous ghrelin. Acta Histochem. 2012;114:349-57.

[102] Granata R, Volante M, Settanni F, *et al*. Unacylated ghrelin and obestatin increase islet cell mass and prevent diabetes in streptozotocin-treated newborn rats. J Mol Endocrinol. 2010;45:9-17.

[103] Baragli A, Grande C, Gesmundo I, *et al*. Obestatin enhances in vitro generation of pancreatic islets through regulation of developmental pathways. PLoS One. 2013;8:e64374.

regarding insulin levels[104,105,106] and insulin release.[107,108] Another study indicated that obestatin may have dual effects on insulin release in response to glucose high levels in perfused rodent islets.[109] Taken together, all these findings suggest an important role of obestatin in pancreas formation and regeneration and its potential application for treating metabolic disorders such as insulin resistance, diabetes mellitus and in the pathogenesis of the metabolic syndrome.

Myogenic effect of obestatin

Recent publications of Camiña's group revealed the role of obestatin in muscle. Results showed that this peptide activated Akt and its downstream targets, GSK3α/β, and S6K1, in L6E9 myotube cells. Simultaneously, obestatin inactivated AMPK in this cell model. In keeping with this, acetyl-CoA-carboxilase (ACC) phosphorylation was also decreased. This fact was confirmed *in vivo* in rat skeletal muscle, gastrocnemius and soleus, obtained from male rats under continuous *sc* infusion of obestatin.[72] In differentiating L6E9 cells, preproghrelin expression and correspondingly obestatin, increased during myogenesis being sustained throughout terminal differentiation. Autocrine action was demonstrated by neutralization and knock-down experiments confirming the contribution of obestatin to the myogenic program. Furthermore, the overexpression of the obestatin/GPR39 system in skeletal muscle enhanced muscle regeneration after muscle injury by stimulating satellite stem cell expansion as well as myofiber hypertrophy through a kinase hierarchy. The effective action was due to the specific regulation of this peptide on different stages affecting myogenesis: proliferation, fusion and myofiber growth. Added to the myogenic action, obestatin administration resulted in increased expression of vascular endothelial growt factor (VEGF)/VEGF receptor 2 (VEGFR2) and the consequent microvascularization, with no significant effect on collagen deposition in developing skeletal muscle.[73]

Obestatin in the cardiovascular system

Different groups have investigated the cardiovascular effects of obestatin. Changes in obestatin levels have been reported in patients with heart failure[110] or ischaemic heart disease.[111] Moreover, binding sites for obestatin have been identified in the heart; and obestatin might be playing a role in protecting myocardial function following reperfusion injury of cardiac muscle cells, reducing infarct size and contractile dysfunction in a concentration-dependent manner. Obestatin also reduced cardiomyocyte apoptosis and reduced caspase-3 activation.[112]

[104] Gao XY, Kuang HY, Liu XM, *et al*. Decreased obestatin in plasma in metabolically obese, normal-weight men with normal glucose tolerance. Diab Res Clin Pract. 2008;79:e5-6.

[105] Lippl F, Erdmann J, Lichter N, *et al*. Relation of plasma obestatin levels to BMI, gender, age and insulin. Horm Metab Res. 2008;40:806-12.

[106] Li ZF, Guo ZF, Cao J, *et al*. Plasma ghrelin and obestatin levels are increased in spontaneously hypertensive rats. Peptides.2010;31:297-300.

[107] Qader SS, Hakanson R, Rehfeld JF, *et al*. Proghrelin derived peptides influence the secretion of insulin, glucagon, pancreatic polypeptide and somatostatin: a study on isolated islets from mouse and rat pancreas. Regul Pept. 2008;146:230-7.

[108] Ren AJ, Guo ZF, Wang YK, *et al*. Inhibitory effect of obestatin on glucose-induced insulin secretion in rats. Biochem Biophys Res Commun. 2008;369:969-72.

[109] Egido EM, Hernandez R, Marco J, *et al*. Effect of obestatin on insulin, glucagon and somatostatin secretion in the perfused rat pancreas. Regul Pept. 2009;152:61-6.

[110] Xin X, Ren AJ, Zheng X, *et al*. Disturbance of circulating ghrelin and obestatin in chronic heart failure patients especially in those with cachexia. Peptides. 2009;30:2281-5.

[111] Ozbay Y, Aydin S, Dagli AF, *et al*. Obestatin is present in saliva: alterations in obestatin and ghrelin levels of saliva and serum in ischemic heart disease. BMB Rep. 2008;41:55-61.

[112] Alloatti G, Arnoletti E, Bassino E, *et al*. Obestatin affords cardioprotection to the ischemic-reperfused isolated rat heart and inhibits apoptosis in cultures of similarly stressed cardiomyocytes. Am J Physiol Heart Circ Physiol. 2010;299:H470-81.

However, obestatin was also found unable to prevent apoptosis or to have effect on cell cycle or viability of HL-1 cardiomyocytes.[113]

Other work showed that an increase in the contraction force of *ex vivo* frog hearts stimulated by obestatin was blocked by β-blockers and a protein kinase A (PKA) inhibitor, indicating that obestatin influenced beta-adrenergic receptors of cardiac muscle cells.[114] Obestatin also preserved papillary muscle contractility, β-adrenergic response, as well as β1-adrenoreceptors and α-myosin heavy chain (α-MHC) levels in rat diabetic myocardial tissue.[115]

Furthermore, obestatin may also have a role in regulating blood pressure. The ghrelin:obestatin ratio and obestatin levels were reduced in patients with high blood pressure,[116] and fasting plasma obestatin levels had also been shown to have a negative correlation with systolic blood pressure in humans.[117] In pregnant women with pregnancy-induced hypertension, obestatin levels were elevated compared to normotensive pregnant women.[118] In contrast, in hipertensive rats, obestatin levels were increased,[106] or did not alter blood pressure.[119]

Mitogenic capabilities

Camiña's group were the first to show the proliferative capabilities of obestatin in human retinal pigment epithelium (RPE) cells. They evaluated the effect of obestatin in primary cultures of RPE cells. The results showed that this peptide induces cell proliferation in a dose-dependent manner with the phosphorylation of MEK/ERK1/2. The signalling pathway towards ERK1/2 activation involves consecutive Gi, PI3K, Src and protein kinase C (PKC)ε novel.[120] Peripheral administration of obestatin also induced an early response gene that undergoes rapid transcriptional activation by growth factors and mitogens, in white adipose tissue and cultured mouse adipocytes.[77] Nevertheless, obestatin did not modify the cell cycle or viability in HL-1 murine cardiomyocytes[113] and inhibited proliferation in a human chondrocyte cell line.[121] Other group showed the role of this peptide in proliferation, apoptosis and secretion in pig ovarian granulosa cells. In these cells, obestatin increased proliferation, apoptosis and secretion of progesterone and might regulate turnover and remodelling of ovarian follicles.[122] It was also described that obestatin promoted cell growth and cell survival in β cells and human pancreatic islets.[91,102] The same mitogenic

[113] Iglesias MJ, Salgado A, Pineiro R, *et al*. Lack of effect of the ghrelin gene-derived peptide obestatin on cardiomyocyte viability and metabolism. J Endocrinol Invest. 2007;30:470-6.

[114] Sazdova I, Ilieva B, Minkov I, *et al*. Obestatin as contractile mediator of excised frog heart. Cent. Eur J Biol. 2009;4:327-34.

[115] Aragno M, Mastrocola R, Ghe C, *et al*. Obestatin-induced recovery of myocardial dysfunction in type 1 diabetic rats: underlying mechanisms. Cardiovasc Diabetol. 2012;11:129.

[116] Li ZF, Guo ZF, Yang SG, *et al*. Circulating ghrelin and ghrelin to obestatin ratio are low in patients with untreated mild-to-moderate hypertension. Regul Pept. 2010;65:206-9.

[117] Anderwald-Stadler M, Krebs M, Promintzer M, *et al*. Plasma obestatin is lower at fasting and not suppressed by insulin in insulin-resistant humans. Am J Physiol Endocrinol Metab. 2007;293:E1393-8.

[118] Ren AJ, He Q, Shi JS, *et al*. Association of obestatin with blood pressure in the third trimesters of pregnancy. Peptides. 2009;30:1742-5.

[119] Li ZF, Song SW, Qin,YW, *et al*. Bolus intravenous injection of obestatin does not change blood pressure level of spontaneously hypertensive rat. Peptides. 2009;30:1928-30.

[120] Camiña JP, Campos JF, Caminos JE, *et al*. Obestatin-mediated proliferation of human retinal pigment epithelial cells: regulatory mechanisms. J Cell Phsiol. 2007;211:1-9.

[121] Lago R, Gomez R, Dieguez C, *et al*. Unlike ghrelin, obestatin does not exert any relevant activity in chondrocytes. Ann Rheum Dis. 2007;66:1399-400.

[122] Mészárosová M, Sitotkin AV, Grossmann R, *et al*. The effect of obestatin on porcine ovarian granulosa cells. Anim Reprod Sci. 2008;108:196-207.

result through ERK signalling pathway was discovered in the human gastric carcinoma cell line KATO III.[123]

Other functions

In addition to all the capabilities mentioned above, obestatin has a role in many other physiological functions. Obestatin suppresses thirst,[124] decreases anxiety and improves memory,[125,126] decreases the secretion of GH *in vivo*[127] but stimulates GH release in GC cells,[128] regulates sleep,[129] increases vasopressin secretion,[130] and actives cortical neurons.[38] In chronic obstructive pulmonary disease obestatin levels are elevated.[131] In addition, obestatin might play a role in kidney diseases. Obestatin levels are elevated in plasma of patients with chronic kidney disease[132,133] and kidney failure (end stage renal of disease),[134] and patients undergoing haemodialysis resulted in lower plasma levels.[135] Other works showed antagonic results about the physiological significance of plasma obestatin levels[136] but seems to be that this peptide could be an useful biomarker for some disease states like inflammatory bowel disease,[137] atrophic gastritis[138] or anorexia nervosa.[139,140,141]

Obestatin signalling

Pazos' group dilucidated the transmembrane signalling pathway responsible for obestatin induced-Akt activation in human gastric carcinoma cells, KATO III and AGS.[142] They carried out an analysis of the sequential transmembrane signalling pathway of obestatin to characterize the intracellular mechanisms responsible for the activation of Akt, a serine/threonine kinase that acts as a key molecule of apoptosis, transcription and cell cycle, in addition to

[123] Pazos Y, Álvarez CJ, Camiña JP, *et al*. Stimulation of extracellular signal-regulated kinases and proliferation in the human gastric cancer cells KATO-III by obestatin. Growth Factors. 2007;25:373-81.

[124] Samson WK, White MM, Price C, *et al*. Obestatin acts in brain to inhibit thirst. Am J Physiol-Regul Integr Comp Physiol. 2007;292:R637-43.

[125] Carlini VP, Schiöth HB, de Barioglio SR. Obestatin improves memory performance and causes anxiolytic effects in rats. Biochem Biophys Res Commun. 2007;352:907-12.

[126] Szakács J, Csabafi K, Lipták N, *et al*. The effect of obestatin on anxiety-like behaviour in mice. Behav Brain Res. 2015;293:41-5.

[127] Zizzari P, Longchamps R, Epelbaum J, *et al*. Obestatin partially affects ghrelin stimulation of food intake and growth hormone secretion in rodents. Endocrinology. 2007;148:1648-53.

[128] Pazos Y, Alvarez CJ, Camiña JP, *et al*. Role of obestatin on growth hormone secretion: An in vitro approach. Biochem Biophys Res Commun. 2009;390:1377-81.

[129] Szentirmai E, Krueger JM. Obestatin alters sleep in rats. Neurosci Lett. 2006;404:222-6.

[130] Samson WK, Yosten GL, Chan JK, *et al*. Obestatin inhibits vasopressin secretion: evidence for a physiological role in the control of fluid homeostasis. J Endocrinol. 2008;196:559-64.

[131] Lei Y, Liang Y, Chen Y, *et al*. Increased circulating obestatin in patients with chronic obstructive pulmonary disease. Multidiscip Respir Med. 2014;9:5.

[132] Buscher AK, Buscher R, Hauffa BP, *et al*. Alterations in appetite regulating hormones influence protein-energy wasting in pediatric patients with chronic kidney disease. Pediatr Nephrol. 2010;25:2295-301.

[133] Borges N, Moraes C, Barros AF, *et al*. Acyl-ghrelin and obestatin plasma levels in different stages of chronic kidney disease. J Ren Nutr. 2014;24:100-4.

[134] Aygen B, Dogukan A, Dursun FE, *et al*. Ghrelin and obestatin levels in end-stage renal disease. J. Int. Med. Res. 2009;37:757-65.

[135] Mafra D, Guebre-Egziabher F, Cleaud C, *et al*. Obestatin and ghrelin interplay in hemodialysis patients. Nutrition. 2010;26:1100-4.

[136] Gao XY, Kuang HY, Liu XM, *et al*. Plasma obestatin levels in men with chronic atrophic gastritis. Peptides. 2008;29:1749-54.

[137] Alexandridis E, Zisimopoulos A, Liratzopoulos N, *et al*. Obestatin/ghrelin ratio: a new activity index in inflammatory bowel diseases. Inflamm Bowel Dis. 2009;15:1557-61.

[138] Gao XY, Kuang HY, Liu XM, *et al*. Circulating ghrelin/ obestatin ratio in subjects with Helicobacter pylori infection. Nutrition. 2009;25:506-11.

[139] Monteleone P, Serritella C, Martiadis V, *et al*. Plasma obestatin, ghrelin, and ghrelin/obestatin ratio are increased in underweight patients with anorexia nervosa but not in symptomatic patients with bulimia nervosa. J Clin Endocrinol Metab. 2008;93:4418-21.

[140] Germain N, Galusca B, Grouselle D, *et al*. Ghrelin and obestatin circadian levels differentiate bingeing-purging from restrictive anorexia nervosa. J Clin Endocrinol Metab. 2010;95:3057-62.

[141] Sedlackova D, Kopeckova J, Papezova H, *et al*. Changes of plasma obestatin, ghrelin and NPY in anorexia and bulimia nervosa patients before and after a high-carbohydrate breakfast. Physiol Res. 2011;60:165-73.

[142] Álvarez CJ, Lodeiro M, Theodoropoulou M, *et al*. Obestatin stimulates Akt signalling in gastric cancer cells through b-arrestin-mediated epidermal growth factor receptor transactivation. Endocr-Relat Cancer. 2009;16:599-611.

his role on the regulation of metabolism.[143] Results showed that Akt activation requires the phosphorylation of T308 in the A-loop by the phosphoinositide-dependent kinase 1 (PDK1) and S473 within the HM by the mTOR kinase complex 2 (mTORC2: RICTOR, mLST8, mSin1, mTOR kinase) with participation neither of Gi/o-protein nor Gβ dimers. Obestatin induces the association of the GPR39/β-arrestin1/Src signalling complex leading to the transactivation of the epidermal growth factor (EGF) receptor (EGFR) and subsequently to the activation of Akt (**Scheme 1**). After administration of obestatin, phosphorylation of both mTOR (S2448) as p70S6K1 (T389) increases with a time course in parallel to the activation of Akt. Apart from the obvious complexity and specificity of cellular signalling pathways of EGFR transactivation, in KATO III cells they found that the signalling routes of ERK1/2 and Akt act in parallel. It is clear that the specificity of signalling routes not only depends on the presence of an ErbB specific receptor of EGFR family, but also on the biochemical characteristics of every EGF-like ligands.[144] These ligands are bivalent, a property that determines which combinations homo- or heterodimeric are formed and the active signalling cascade.[144] In addition, β-arrestin-scaffolding complex presumably located different members for ensuring the substrate specificity and metalloproteinases (MMPs) activity. Such complexity reflects the importance of this process in obestatin transactivation signalling. Some studies show that Zn^{+2} induces phosphorylation of EGFR through the release of EGF-like ligands, process mediated by MMPs.[145,146] Treatment with Zn^{+2} triggers the activation of MAPK and PI3K/Akt signalling pathways through EGFR activation in several cell types.[147,148,149] These findings also suggest that there are specific marked differences to each cell type in the EGFR activation mechanism induced by Zn^{+2}. All these data could imply that the stimulatory effects of Zn^{+2} in GPR39 signalling might be due to the activation of MMP-EGFR pathways, since obestatin needs EGFR transactivation and MMPs activity.

It would be necessary to determine the exact function of Zn^{+2} on the GPR39 signalling in the absence of MMP and/or EGFR to clearly define its function as a ligand or ago-allosteric modulator of this receptor.[150] This signalling pathway adds a new component to the intracellular signalling targets regulated by obestatin. In this sense, obestatin is added to the group of MMPs regulator factors, which have been implicated in diverse human diseases, such as inflammatory diseases and cancer.[151,152] It would be possible that EGFR transactivation induced by obestatin implied a key mechanism by which MMPs regulate these

[143] Manning BD, Cantley LC. Akt/PKB signalling: navigating downstream. Cell. 2007;129:1261-74.

[144] Olayioye MA, Neve RM, Lane HA, *et al*. The ErbB signalling network: receptor heterodimerization in development and cancer. EMBO J. 2000;19:3159-67.

[145] Wu W, Samet JM, Silbajoris R, *et al*. Heparin-binding epidermal growth factor cleavage mediates zinc-induced epidermal growth factor receptor phosphorylation. Am J Respir Cell Mol Biol. 2004;30:540-7.

[146] Hwang JJ, Park MH, Choi SY, *et al*. Activation of the Trk signaling pathway by extracellular zinc. Role of metalloproteinases. J Biol Chem. 2005;280:11995-2001.

[147] Wu W, Graves LM, Gill GN, *et al*. Src-dependent phosphorylation of the epidermal growth factor receptor on tyrosine 845 is required for zinc-induced Ras activation. J Biol Chem. 2002;277:24252-7.

[148] Samet JM, Dewar BJ, Wu W, *et al*. Mechanisms of Zn(2+)-induced signal initiation through the epidermal growth factor receptor. Toxicol Appl Pharmacol. 2003;191:86-93.

[149] Wu W, Silbajoris RA, Whang YE, *et al*. p38 and EGF receptor kinase-mediated activation of the phosphatidylinositol 3-kinase/Akt pathway is required for Zn2+-induced cyclooxygenase-2 expression. Am J Physiol Lung Cell Mol Physiol. 2005;289:L883-9.

[150] Storjohann L, Holst B, Schwartz TW. Molecular mechanism of Zn2+ agonism in the extracellular domain of GPR39. FEBS Lett. 2008;582:2583-8.

[151] Huovila AP, Turner AJ, Pelto-Huikko M, *et al*. Shedding light on ADAM metalloproteinases. Trends Biochem Sci. 2005;30:413-22.

[152] Seals DF, Courtneidge SA. The ADAMs family of metalloproteases: multidomain proteins with multiple functions. Genes Dev. 2003;17:7-30.

diseases. Supporting this hypothesis, numerous studies have shown that the alteration in the expression and/or mutations in genes of members of the EGFR/ErbB receptor family are present in tumours and cell lines derived, and these changes may contribute to cancer progression.[153,154,155] However, it seems to be necessary a detailed elucidation of the mechanism of activation/regulation of EGFR transactivation stimulated by obestatin and the pathophysiological significance of these signalling processes.

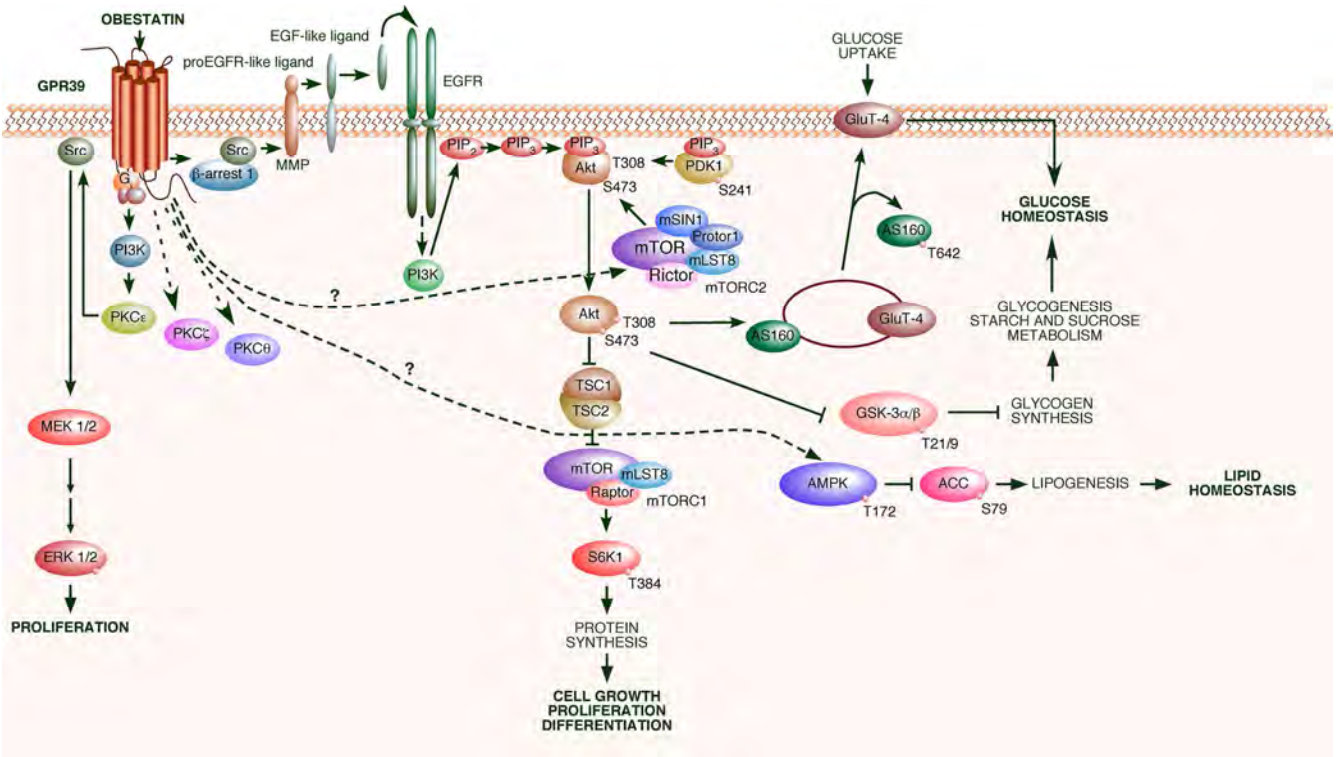

Scheme 1. Proposed model of signalling pathway for Akt and ERK1/2 activation in response to obestatin. Traslocation of β-arrestins 1 to obestatin receptor (GPR39) allows its association with Src. β-arrestin 1 activates Src (phosphorylation at Y416) triggering the transactivation of EGFR and the subsequent downstream Akt signalling. Modified from: Endocr-Relat Cancer. 2009;16:599-611.

[153] Bhola NE, Grandis JR . Crosstalk between G-protein-coupled receptors and epidermal growth factor receptor in cancer. Front Biosci. 2008;13:1857-65.

[154] Normanno N, De Luca A, Bianco C, *et al*. Epidermal growth factor receptor (EGFR) signalling in cancer. Gene. 2006;366:2-16.

[155] Ohtsu H, Dempsey PJ, Eguchi S. ADAMs as mediators of EGF receptor transactivation by G-protein-coupled receptors. Am J Phys Cell Physiol. 2006;291:C1-10.

OBESTATIN/GPR39 SYSTEM IN CANCER

Since 2009, several papers were published about the obestatin role in various types of cancer. It has been reported that low EGFR expression in a rat pituitary adenoma cell line (GC) blocked obestatin induced cell proliferation, showing that EGFR expression is the key to its proliferative activity.[128] In humans, Volante[35] and Tsolakis'[36] groups reported that obestatin was expressed in gastric well-differentiated (WD) neuroendocrine tumours (NETs). Interestingly, immunohistochemical studies suggested that obestatin expression is reduced in thyroid and pancreatic tumour tissue and obestatin may be specifically downregulated by these tumours types in order to circumvent the inhibition of the proliferation demonstrated *in vitro*.[35] Immunoassay-based studies have reported that obestatin levels are higher in the blood of patients with ovarian cancer than in normal controls,[156] but there was no correlation between plasma levels of obestatin and the disease status, however, in prostate cancer[157] and uterine leiomyoma patients.[158] In serous ovarian tumours, severe expression of ghrelin and obestatin correlated with an increase in malignancy, suggesting that ghrelin and obestatin may be effective in the malignant transformation.[159] Furthermore, obestatin immunoreactivity was observed in benign nodular goiter, as well as in cancer thyroid cells. The differences between ghrelin and obestatin immunoreactivity in benign and malignant thyroid tumours could support the theory of alternative transcription of the pre-proghrelin gene and thus of the independent production of ghrelin and obestatin.[160] However, the possible usefulness of the modulation of the ghrelin/obestatin axis in neoplastic conditions using either synthetic agonists or antagonists, though interesting in perspective, is still far from clinical applicability, and probably more related to the regulation of specific metabolic pathways in tumour cells, including lipid and carbohydrate use, than to the specific modulation of cell proliferation.[161] Taken together, the available evidence shows that obestatin is an autocrine/paracrine growth factor in peripheral tissues and may play a role in cancer progression.[162]

On the other hand, it has been reported that GPR39 was an inhibitor of cell death in hippocampal cells and GPR39 overexpression led to increased secretion of the cytoprotective pigment epithelium-derived factor (PEDF), which might represent a therapeutic target with implications for processes involving apoptosis and endoplasmic reticulum stress like cancer, ischemia/reperfusion injury, and neurodegenerative disease.[66] Additionally, GPR39 reduced butyrate-induced cell death in HT-29 colonocytes;[82] and in human prostate cancer PC3 cells, GPR39 signalling enhanced cell growth and might be linked to invasion of these cells.[83] Furthermore, GPR39 receptor was found to be frequently overexpressed in primary

[156] Markowska A, Ziolkowska A, Jaszczynska-Nowinka K, *et al*. Elevated blood plasma concentrations of active ghrelin and obestatin in benign ovarian neoplasms and ovarian cancers. Eur J Gynaecol Oncol. 2009;30:518-22.

[157] Malendowicz W, Ziolkowska A, Szyszka M, *et al*. Elevated blood active ghrelin and unaltered total ghrelin and obestatin concentrations in prostate carcinoma. Urol Int. 2009;83,471-5.

[158] Markowska A, Ziolkowska A, Nowinka K, *et al*. Elevated blood active ghrelin and normal total ghrelin and obestatin concentrations in uterine leiomyoma. Eur J Gynaecol Oncol. 2009;30:281-4.

[159] Nurkalem C, Celik H, Dagli F, *et al*. Ghrelin and obestatin expression in serous ovarian tumours. Gynecol Endocrinol. 2012;28:941-4.

[160] Gurgul E, Kasprzak A, Blaszczyk A, *et al*. Ghrelin and obestatin in thyroid gland - immunohistochemical expression in nodular goiter, papillary and medullary cancer. Folia Histochem Cytobiol. 2015;53:19-25.

[161] Papotti M, Duregon E, Volante M. Ghrelin and tumors. Endocr Dev. 2013;25:122-34.

[162] Seim I, Walpole C, Amorim L, *et al*. The expanding roles of the ghrelin-gene derived peptide obestatin in health and disease. Mol Cell Endocrinol. 2011;340:111-7.

oesophageal squamous cell carcinomas (ESCCs) in both mRNA level and protein level, which was significantly associated with the lymph node metastasis and advanced TNM stage suggesting that GPR39 played an important tumorigenic role in the development and progression of ESCC.[163] Introduction of GPR39 gene into ESCC cell line KYSE30 promotes cell proliferation, increases foci formation, colony formation in soft agar, and tumour formation in nude mice. The mechanism by which amplified GPR39 induces tumorigenesis was associated with its role in promoting G1/S transition via up-regulation of cyclin D1 and CDK6. GPR39 also enhanced cell motility and invasiveness by inducing epithelial-mesenchymal transition (EMT) and remodelling cytoskeleton. Moreover, depletion of endogenous GPR39 by siRNA could effectively decrease the oncogenicity of ESCC cells. Finally, a recent published article, using a phenotypic screening approach, postulates GPR39 as the unknown GPCR able to inhibit Hedgehog (Hh) signalling, which determinates cell fate during development and can drive tumorigenesis.[164] The GPR39 is necessary for compound activity and the proposed model of activation involved the cyclohexyl-methyl aminopyrimidine chemotype compounds (CMAPs), driving the signalling to the Gli transcription factors in crosstalk with MAPK pathway. This mechanism may involve Gi pathway activation, Gβγ signalling or β-arrestin recruitment blocking the Hh signalling.

GASTRIC CANCER

Gastric cancer is a cancer disease emerging from the stomach epithelium. It is often diagnosed at an advanced stage because there are no clear early signs or symptoms. The cancer may spread from the stomach to other parts of the body, particularly the liver, lungs, bones, lining of the abdomen and lymph nodes.[165]

AETIOLOGY

Signs and Symptoms. Gastric cancer is often either asymptomatic or it may cause nonspecific symptoms in early stages like indigestion, a bloated sensation after eating, and heartburn. As it progresses, symptoms may include dyspepsia, nausea, diarrhoea or constipation, bloody stools, vomiting blood, loss of appetite, weight loss, anaemia, and sensations of full-ness or pressure in the stomach. By the time symptoms occur, the cancer has often reached an advanced stage and may have also metastasized, which is one of the main reasons for its relatively poor prognosis.[166]

Risk factors and causes. Chronic infection with *Helicobacter pylori* is the strongest identified risk factor for stomach cancer, with more than 60% of new stomach cancer cases worldwide attributed to this bacterium.[167] It is not known with certainty how *H. pylori* is spread, but the most likely route of transmission is from person to person through faecal-oral or oral-oral routes. Possible environmental sources include water contaminated with human

[163] Xie F, Liu H, Zhu YH, *et al*. Overexpression of GPR39 contributes to malignant development of human esophageal squamous cell carcinoma. BMC Cancer. 2011;11:86.

[164] Bassilana F, Carlson A, DaSilva JA, *et al*. Target identification for a Hedgehog pathway inhibitor reveals the receptor GPR39. Nat Chem Biol. 2014;10:343-9.

[165] Ruddon RW. Cancer biology. 4th ed. Oxford: Oxford University Press. 2007.

[166] Statistics and outlook for stomach cancer. Cancer Research UK. 2014.

[167] González CA, Sala N, Rokkas T. Gastric cancer: epidemiologic aspects. Helicobacter. 2013;18:34-8.

waste. Prevalence of *H. pylori* infection is higher in developing countries (74%) than in developed countries (58%). Notably, less than 5% of the chronically infected individuals will develop stomach cancer.[167] The mechanism by which *H. pylori* induces stomach cancer potentially involves chronic inflammation, or the action of *H. pylori* virulence factors such as CagA.[168] It was estimated that Epstein–Barr virus is also responsible for 84,000 cases per year.[167]

Dietary risk factors for stomach cancer include a diet rich in smoked foods, salted meat or fish, and pickled vegetables;[169] fresh fruits and vegetables appear to lower risk.[170] Smoking also increases risk of stomach cancer.[171] Smokers have a 50% to 60% increased risk for stomach cancer compared with non-smokers. Some studies show increased risk with alcohol consumption as well.[172] Obesity is associated with increased risk of adenocarcinoma of the gastric cardia, possibly due to gastroesophageal reflux disease or chronic inflammation.[173]

Gastric cancer shows a male predominance in its incidence as up to two males are affected for every female. Oestrogen may protect women against the development of this cancer type.[174]

Approximately 10% of cases show a genetic component.[175] A genetic risk factor for gastric cancer is a genetic defect of the *CDH1* gene known as hereditary diffuse gastric cancer (HDGC). The *CDH1* gene, which codes for E-cadherin, lies on the 16th chromosome. When the gene experiences a particular mutation, gastric cancer develops through a mechanism that is not fully understood. [176]

Other factors associated with increased risk are diabetes,[177] pernicious anaemia, acquired immune deficiency syndrome (AIDS), Menetrier's disease,[178] chronic atrophic gastritis and intestinal metaplasia.[179]

Treatment. The main treatments for stomach cancer are surgery, chemotherapy, targeted therapy, and radiation therapy. Often the best approach uses two or more of these treatment methods. Treatment for advanced stage cancer is often aimed at relieving symptoms.

Biology of gastric cancer. *H. pylori* infection is considered as the single most important risk factor leading to gastric cancer,[180] through chronic inflammatory changes in the gastric mucosa, followed by pre-neoplastic changes such as atrophy and metaplasia, as in the Correa cascade (**Figure 8**).[181] Over 20 years ago, Correa delineated the association

[168] Keyama M, Higashi H. Helicobacter pylori CagA: a new paradigm for bacterial carcinogenesis. Cancer Sci. 2005;96:835-43.
[169] Jakszyn P, González CA. Nitrosamine and related food intake and gastric and oesophageal cancer risk: A systematic review of the epidemiological evidence. World J Gastroenterol. 2006;12:4296-303.
[170] Buckland G, Agudo A, Lujan L, *et al*. Adherence to a Mediterranean diet and risk of gastric adenocarcinoma within the European Prospective Investigation into Cancer and Nutrition (EPIC) cohort study. Am J Clin Nutr. 2009;91:381-90.
[171] Trédaniel J, Boffetta P, Buiatti E, *et al*. Tobacco smoking and gastric cancer: Review and meta-analysis. Int J Cancer. 1997;72:565-73.
[172] What Are The Risk Factors For Stomach Cancer? American Cancer Society. 2010.
[173] Crew K, Neugut A. Epidemiology of gastric cancer. World Journal of Gastroenterol. 2006;12 354-62.
[174] World Cancer Report 2014. World Health Organization. 2014.
[175] Hereditary Diffuse Cancer. No Stomach for Cancer. 2014.
[176] Gastric Cancer: Intestinal- and diffuse-type. International Cancer Genome Consortium. 2014.
[177] Tseng CH, Tseng FH, Tseng T. Diabetes and gastric cancer: The potential links. World J Gastroenterol. 2014;20:1701-11.
[178] Kim J, Cheong JH, Chen J, *et al*. Menetrier's Disease in Korea: Report of Two Cases and Review of Cases in a Gastric Cancer Prevalent Region. Yonsei Med J. 2004;45:555-60.
[179] Tsukamoto T, Mizoshita T, Tatematsu M, *et al*. Gastric-and-intestinal mixed-type intestinal metaplasia: aberrant expression of transcription factors and stem cell intestinalization. Gastric Cancer. 2006;9:156-66.
[180] IARC monographs on the evaluation of carcinogenic risks to humans. IARC. 2012:385-435.
[181] Correa P. A human model of gastric carcinogenesis. Cancer Res. 1988;48:3554-60.

of intestinal metaplasia with the development of intestinal-type gastric cancer. In Correa's model of gastric carcinogenesis, *H. pylori* infection triggers the progressive sequence of gastric lesions from chronic gastritis, gastric atrophy, intestinal metaplasia, dysplasia, and finally, gastric adenocarcinoma. However, the details of how metaplasia is initiated and how it can progress towards cancer have remained elusive until recently.

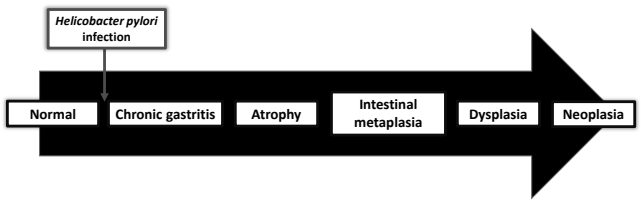

Figure 8. Correa's gastric carcinogenesis model. Carcinogenesis model for the Laurén intestinal type gastric carcinomas, according to the proposed by Pelayo Correa in 1992. Modified from: Gastritis and Gastric Cancer. New Insights in Gastroprotection, Diagnosis and Treatments. 2011.

This initiating event in gastric pre-neoplasia in humans with chronic infection with *H. pylori*,[182] initiates both parietal cell loss (and oxyntic atrophy) and prominent inflammation. Loss of parietal cells appears to represent a key fulcrum in the process of pre-neoplasia due to the role of the acid secreting cells as the coordinate source of a number of critical growth factors.[183] Loss of parietal cell-derived signalling molecules disrupts the proper differentiation of other lineages most notably the zymogen-secreting chief cells.[184,185] The chronic *Helicobacter* infection also elicits prominent inflammation throughout the mucosa. Thus, the combination of oxyntic atrophy along with prominent inflammation is a prerequisite for progression of metaplasia to gastric adenocarcinoma.[186] Oxyntic atrophy triggers a series of changes in the cells lining the gastric mucosa. In humans, two types of metaplasia arise in the milieu of oxyntic atrophy and inflammation: intestinal metaplasia (IM) and spasmolytic polypeptide expressing metaplasia (SPEM). Both IM and SPEM have been associated with the progression to intestinal type gastric cancer.[187,188,189,190,191] Mouse models of both chronic *Helicobacter* infection and acute pharmacological oxyntic atrophy have led to the recognition that SPEM arises from transdifferentiation of mature chief cells. The presence of inflammation promotes the expansion of SPEM in mice. Furthermore, human studies indicates that SPEM likely represents a precursor for development of IM (**Figure 9**).

These findings indicate that the loss of parietal cells, augmented by chronic inflammation, leads to a

[182] Blaser M, Parsonnet J. Parasitism by the 'slow' bacterium Helicobacter pylori leads to altered gastric homeostasis and neoplasia. J Clin Invest. 1994;94:4-8.

[183] Jain RN, Brunkan CS, Chew CS, *et al*. Gene expression profiling of gastrin target genes in parietal cells. Physiol Genomics. 2006;24:124-32.

[184] Li Q, Karam SM, Gordon JI. Diphtheria toxin-mediated ablation of parietal cells in the stomach of transgenic mice. J Biol Chem. 1996;271:3671-6.

[185] Bredemeyer AJ, Geahlen JH, Weis VG, *et al*. The gastric epithelial progenitor cell niche and differentiation of the zymogenic (chief) cell lineage. Dev Biol. 2009;325:211-24.

[186] El-Zimaity HMT, Ota H, Graham DY, *et al*. Patterns of gastric atrophy in intestinal type gastric carcinoma. Cancer. 2002;94:1428-36.

[187] Filipe MI, Munoz N, Matko I, *et al*. Intestinal metaplasia types and the risk of gastric cancer: a cohort study in Slovenia. Int J Cancer. 1994;57:324-9.

[188] Hattori T, Fujita S. Tritiated thymidine autotradiographic study on histogenesis and spreading of intestinal metaplasia in human stomach. Pathol Res Practice. 1979;164:224-37.

[189] Schmidt PH, Lee JR, Joshi V, *et al*. Identification of a metaplastic cell lineage associated with human gastric adenocarcinoma. Lab Invest. 1999;79:639-46.

[190] Yamaguchi H, Goldenring JR, Kaminishi M, *et al*. Association of spasmolytic polypeptide expressing metaplasia (SPEM) with carcinogen administration and oxyntic atrophy in rats. Lab Invest. 2002;82:1045-52.

[191] Halldorsdottir AM, Sigurdardottir M, Jonasson JG, *et al*. Spasmolytic polypeptide expressing metaplasia (SPEM) associated with gastric cancer in Iceland. Dig Dis Sci. 2003;48:431-41.

cascade of metaplastic events. Thus, oxyntic atrophy in association with prominent inflammation incites the induction of gastric lineages that predispose to the development of gastric cancer.[192] Nevertheless, the factors mediating progression from oxyntic atrophy to gastric cancer remain unclear.

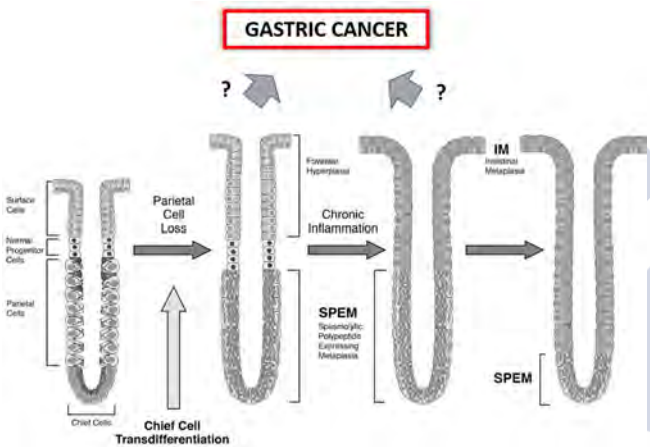

Figure 9. Proposed model for the origin and progression of different gastric metaplasias in humans by Goldenring and Nam. The oxyntic atrophy and subsequent loss of parietal cells would lead to chief cell transdifferentiation and the SPEM-type metaplasia emergence. In the presence of chronic inflammation from *H. pylori* infection, SPEM would progress into intestinal metaplasia and gastric neoplasia. Modified from: Prog Mol Biol Transl Sci. 2010;96:117-31.

EPIDEMIOLOGY

Gastric cancer was the fourth most common malignancy in the world in 2012, with an estimated 951,600 new cases; and is the third and fifth leading cause of cancer death in men and women, respectively.[193] About 723,100 people worldwide died from gastric cancer in 2012.[194] Its incidence rates vary widely across countries, but, in general, the highest incidence rates are in Asia (particularly in Korea, Mongolia, Japan, and China) and many parts of South America and the lowest rates are in Northern America and most parts of Africa. Generally, gastric cancer rates are about twice as high in men as in women. These data suggest that environmental and lifestyle factors are strongly implicated in the carcinogenesis of this tumour.

Gastric cancer is a disease with a poor prognosis. A low rate of cases is diagnosed at an early stage, with a wide variation between countries and, in developing countries, survival rates are generally below 20%.[195] However, a steady decline in gastric cancer incidence and mortality rates has been observed in most developed countries of Northern America and Europe since the mid-20th century.[196,197] Similar decreasing trends have been noted in more recent years in areas with historically high rates, including several countries in Asia, Latin America and Europe.[198] The factors to have contributed to these declines include a trend to a healthier diet, and a reduction in chronic *H. pylori* infection due to improvements in sanitation and

[192] Goldenring JR, Taek Nam K. Oxyntic atrophy, metaplasia and gastric cancer. Prog Mol Biol Transl Sci. 2010;96:117-31.

[193] Ferlay J, Soerjomataram I, Dikshit R, *et al*. Cancer incidence and mortality worldwide: sources, methods and major patterns in GLOBOCAN 2012. Int J Cancer. 2015;136:E359-86.

[194] Global battle against cancer won't be won with treatment alone. Effective prevention measures urgently needed to prevent cancer crisis. World Health Organization. 2014.

[195] Orditura M, Galizia G, Sforza V, *et al*. Treatment of gastric cancer. World J Gastroenterol. 2014;20:1635-49.

[196] Howson CP, Hiyama T, Wynder EL. The decline in gastric cancer: epidemiology of an unplanned triumph. Epidemiol Rev. 1986;8:1-27.

[197] Malvezzi M, Bonifazi M, Bertuccio P, *et al*. An age-period-cohort analysis of gastric cancer mortality from 1950 to 2007 in Europe. Ann Epidemiol. 2010;20:898-905.

[198] Bertuccio P, Chatenoud L, Levi F, *et al*. Recent patterns in gastric cancer: a global overview. Int J Cancer. 2009;125:666-73.

antibiotics.[199] In developed countries, decreases in smoking prevalence may also account.[200] Although gastric cancer is declining overall, adenocarcinoma of the gastric cardia is increasing in Northern America and Europe and is thought to be due to increased obesity and metabolic diseases.

In Spain, gastric cancer average rate is 31/100,000 and is the third cause of death, only lung and colon cancer have higher rates. The areas that still retain a high risk of death from gastric cancer are large areas of Castilla and León, and the Atlantic coast of Galicia, specially Pontevedra.[201,202] Over an 8,000 new cancers and 6,000 cancers deaths were predicted in Spain in 2020.

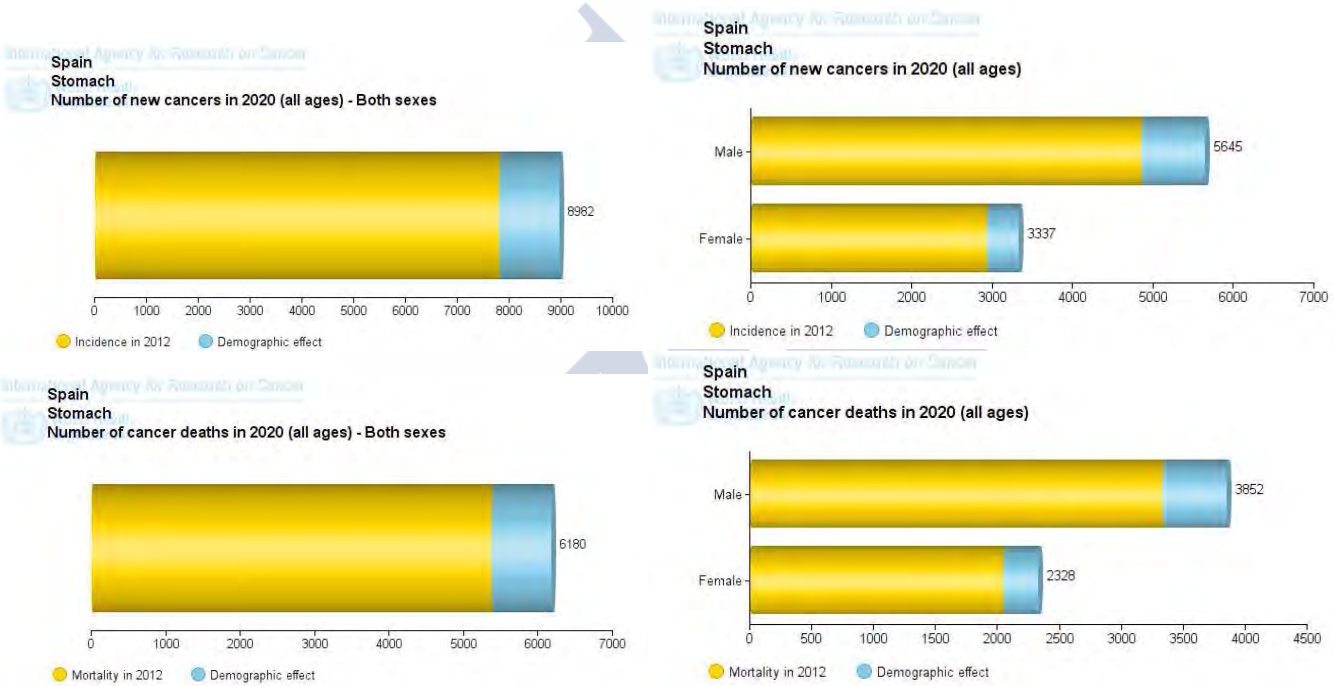

Figure 10. Prediction of number of new gastric cancers and cancer deaths in Spain in 2020. Population forecasts were extracted from the United Nations, World Population prospects, the 2012 revision. Numbers are computed using age-specific rates and corresponding populations for 10 age-groups. Source: GLOBOCAN. Over an 8,000 new cancers and 6,000 cancers deaths were predicted in Spain in 2020. However, a steady decline in gastric cancer incidence and mortality rates were observed.

[199] Parkin DM. The global health burden of infection-associated cancers in the year 2002. Int J Cancer. 2006;118:3030-44.

[200] Jemal A, Center MM, DeSantis C, *et al*. Global patterns of cancer incidence and mortality rates and trends. Cancer Epidemiol Biomarkers Prev. 2010;19:1893-907.

[201] Aragonés N, Goicoa T, Pollán M, *et al*. Spatio-temporal trends in gastric cancer mortality in Spain: 1975-2008. Cancer Epidemiol. 2013;37:360-9.

[202] Seoane-Mato D, Aragonés N, Ferreras E, *et al*. Trends in oral cavity, pharyngeal, oesophageal and gastric cancer mortality rates in Spain, 1952-2006: an age-period-cohort analysis. BMC Cancer. 2014;14:254.

CLASSIFICATION

Gastric cancer classification has necessitated the use of histological features of tumour cells together with information about their respective tissues-of-origin, differentiation states, and biological behaviours; together these characteristics make possible to develop a taxonomy of tumours that has proven useful for the diagnosis and clinical management of most of them. Numerous pathohistological and clinical classification systems have been established for gastric cancer thus far, but there is still controversy as to which classifications unify a prognostic correlation with a high validity and practicability in diagnosis and clinical routine.

Almost all gastric cancers are adenocarcinomas. Other types are gastrointestinal carcinoid tumours, gastrointestinal stromal tumours, and lymphomas.[203] Gastric adenocarcinoma is a malignant epithelial tumour, originating from glandular epithelium of the gastric mucosa. 90% of gastric carcinomas are adenocarcinomas and tend to invade gastric wall, infiltrating the muscularis mucosae, submucosa and muscularis propia. Lymphomas [mucosa-associated lymphoid tissue (MALT) lymphomas or MALTomas] are around 5% of gastric malignancies.

Grades of gastric cancer. The grade of stomach cancer is based on the degree of differentiation of the cells and their rate of growth.

G1. Well differentiated (WD) or low grade. Slow growing, less likely to spread.
G2. Moderately differentiated (MD) or moderate grade.
G3. Poorly differentiated (PD) or high grade.
G4. Undifferentiated. Tend to grow quickly and are more likely to spread.

HISTOPATHOLOGICAL CLASSIFICATIONS

Laurén classification. Since its establishment in 1965, the Laurén classification of gastric cancer has been the most commonly used and the most studied classification for gastric adenocarcinoma among all of the classification systems. Laurén divided the histology of gastric cancer into two groups the intestinal type and the diffuse type. Later, the indeterminate type was included to describe an uncommon histology.[204,205]

Intestinal type adenocarcinoma. Characterized by tumour cells that describe irregular tubular structures, harbouring pluristratification, multiple lumen and reduced stroma. Often, it associates intestinal metaplasia in neighbouring mucosa and with the presence of *H. pylori*. Depending on glandular architecture, cellular pleomorphism and mucosecretion, the adenocarcinoma may present 3 degrees of differentiation: well, moderate and poorly differentiated.
Diffuse type adenocarcinoma. Characterized by tumour cells that are discohesive and secrete mucus, which is delivered in the interstitium, producing large pools of mucus/colloid. It is poorly differentiated. If the mucus remains inside the tumour cell, it pushes the nucleus to the periphery and forms the type *signet-ring cell*. It metastasizes much quicker than intestinal type tumours.
Mixed type adenocarcinomas. They have both intestinal and diffuse type growth patterns.

[203] Kumar V, Abbas AK, Aster JC. Pathologic Basis of Disease. 8th ed. Saunders Elsevier. 2010.
[204] Laurén P. The two histological main types of gastric carcinoma: Diffuse and so-called intestinal-type carcinoma an attempt at a histo-clinical classification. Acta Pathol Microbiol Scand. 1965;64:31-49.
[205] Leocata P, Ventura L, Giunta M, *et al*. Gastric carcinoma: a histopathological study of 705 cases. Ann Ital Chir. 1998;69:331-7.

WHO classification. The World Health Organization (WHO) classification issued in 2010 appears to be the most detailed among all pathohistological classification systems. This classification includes not only adenocarcinoma of the stomach but also all other types of gastric tumours of lower frequency.

Epithelial tumours
Premalignant lesions
8140/0. Adenoma, NOS
8148/0. Glandular intraepithelial neoplasia, low grade
8148/2. Glandular intraepithelial neoplasia, high grade
Carcinoma
8140/3. Adenocarcinoma, NOS
8260/3. Papillary adenocarcinoma, NOS
8211/3. Tubular adenocarcinoma
8480/3. Mucinous adenocarcinoma
8490/3. Poorly cohesive carcinoma, including signet ring cell carcinoma and other variants
8255/3. Adenocarcinoma with mixed subtypes
8560/3. Adenosquamous carcinoma
8512/3. Medullary carcinoma with lymphoid stroma
8576/3. Hepatic carcinoma
8070/3. Squamous cell carcinoma, NOS
8020/3. Undifferentiated carcinoma
Neuroendocrine neoplasms
8240/3. NET G1 /Carcinoid
8249/3. NET G2
8246/3. Neuroendocrine carcinoma, NOS
8013/3. Large cell neuroendocrine carcinoma
8041/3. Small cell neuroendocrine carcinoma
8244/3. Mixed adenoneuroendocrine carcinoma
8241/3. Enterochromaffin cell (EC), serotonin-producing NET
8153/3. Gastrinoma, malignant

Lymphomas
9680/3. Diffuse large B-cell lymphoma (DLBCL), NOS
9699/3. Extranodal marginal zone MALT lymphoma
9673/3. Mantle cell lymphoma
9687/3. Burkitt lymphoma
9827/3. Adult T-cell leukaemia/lymphoma
9650/3. Classical Hodgkin lymphoma
Mesenchymal tumours
8711/0. Glomus tumour, NOS
9580/0. Granular cell tumour, NOS
8890/0. Leiomyoma, NOS
8811/0. Plexiform fibromyxoma
9560/0. Schwannoma, NOS
8825/1. Inflammatory myofibroblastic tumour
8936/0. Gastrointestinal stromal tumour, benign
8936/1. Gastrointestinal stromal tumour, NOS
8936/3. Gastrointestinal stromal tumour, malignant
9140/3. Kaposi sarcoma
8890/3. Leiomyosarcoma, NOS
9040/3. Synovial sarcoma, NOS
Secondary tumours

MOLECULAR CLASSIFICATION

Gastric cancer is a multifaceted disease with different aetiologies, genetic changes and phenotypes. Recent data based on genetic alterations suggested that it could be classified into four subclasses (**Figure 11**).[206] This schematic lists some of the salient features associated with each of the four molecular subtypes of gastric cancer.

[206] The Cancer Genome Atlas Research Network. Comprehensive molecular characterization of gastric adenocarcinoma. Nature. 2014;513:202-9.

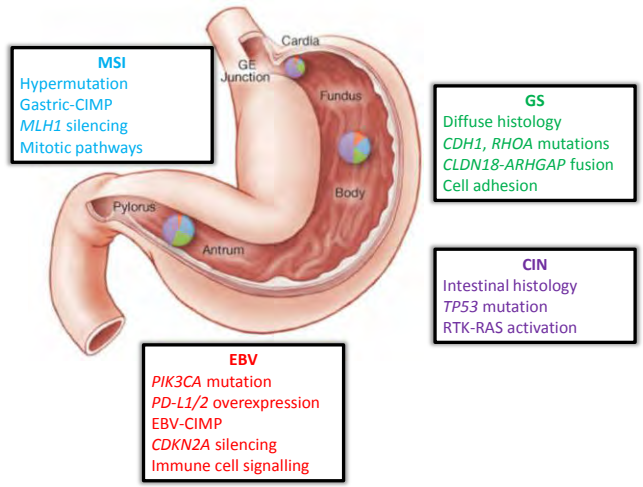

Figure 11. Molecular subtypes of gastric cancer. Insert charts represent the distribution of molecular subtypes in tumours obtained from distinct regions of the stomach. CIN: chromosomal instability. EBV: Epstein-Barr virus-positive. GS: genomically stable. MSI: microsatellite instability. CIMP: CpG island methylator phenotype. Modified from: Nature. 2014;513:202-9.

MOST RELEVANT CLINICAL CLASSIFICATIONS

Borrmann classification

The Borrmann classification describes the macroscopic appearance and growth patterns of advanced gastric cancer:

Type I: polypoid. Tumours grow outward from the stomach wall and stick out into the stomach. The tumours have no ulcers or areas of erosion.
Type II: fungating. Tumours grow outward from the stomach wall in irregular patterns. The tumours may have ulcers or areas of erosion.
Type III: ulcerated. Tumours have ulcers with irregular, hard, stiff margins of raised tissue. There are areas of dead or dying tissue (necrosis) within the ulcer.
Type IV: infiltrated. Tumours spread along the mucosa or submucosa of the stomach wall, producing flat tumours. These tumours may eventually cause the stomach wall to become hard and rigid.
Type V: unclassifiable. Tumours do not fit into any of the other 4 categories.

TNM classification

TNM stands for Tumour, Node and Metastasis. The system describes the size and spread of the stomach tumour (T), whether cancer cells have spread to lymph nodes (N); and whether the cancer has spread to a different part of the body (M).[207]

Primary tumour (T)
Tx. Primary tumour cannot be assessed
T0. No evidence of primary tumour
Tis. Carcinoma in situ: intraepithelial tumour without invasion of the lamina propria
T1a. Tumour invades lamina propria or muscularis mucosae
T1b. Tumour invades submucosa
T2. Tumour invades muscularis propria
T3. Tumour penetrates subserosal connective tissue without invasion of visceral peritoneum or adjacent structures*,**,***
T4. Tumour invades serosa (visceral peritoneum) or adjacent structures**,**
T4a. Tumour invades serosa (visceral peritoneum)
T4b. Tumour invades adjacent structures

* A tumour may penetrate the muscularis propria with extension into the gastrocolic or gastrohepatic ligaments, or into the greater or lesser omentum, without perforation of the visceral peritoneum covering the gastric ligaments or the omentum, the tumour should be classified T4.
** The adjacent structures of the stomach include the spleen, transverse colon, liver, diaphragm, pancreas, abdominal wall, adrenal gland, kidney, small intestine, and retroperitoneum.

[207] Edge SB, Byrd DR, Compton CC, *et al*. AJCC cancer staging manual. 7th ed. New York: Springer-Verlag. 2009.

[***] Intramural extension to the duodenum or oesophagus is classified by the depth of the greatest invasion in any of these sites, including the stomach.

Regional lymph nodes (N)

Nx. Regional lymph nodes cannot be assessed
N0. No regional lymph nodes metastasis
N1. Metastasis in 1 to 2 regional lymph nodes
N2. Metastasis in 3 to 6 regional lymph nodes
N3. Metastasis in 7 or more regional lymph nodes
N3a. Metastasis in 7 to 15 regional lymph nodes
N3b. Metastasis in 16 or more regional lymph nodes

[*] A designation of pN0 should be used is all examined lymph nodes are negative, regardless of the total number removed and examined.

Distant metastasis (M)

M0. No distant metastasis (no pathologic M0; use clinical M to complete stage group)
M1. Distant metastasis

OBJECTIVES

USC
UNIVERSIDADE
DE SANTIAGO
DE COMPOSTELA

OBJECTIVES

The main objective of this doctoral thesis is to establish the relationship between obestatin and the GPR39 receptor in healthy and tumour-like surroundings, from structural to tissue level, to determinate the fundamental parameters of its mitogenic bioactivity.

This issue will be accomplished with the following points:

1. To determine the structural features of obestatin required for the interaction with its receptor.

2. To elucidate the detailed activation/regulation mechanism of GPR39 receptor signalling triggered by obestatin.

3. To analyse the role of obestatin/GPR39 system in the development and malignity of tumours.

USC
UNIVERSIDADE
DE SANTIAGO
DE COMPOSTELA

MATERIALS AND METHODS

USC
UNIVERSIDADE
DE SANTIAGO
DE COMPOSTELA

MATERIALS

PEPTIDES

Materials	Code	Manufacturer
Human obestatin (1)	471-97	California Peptide Research Inc (Napa, CA, US)
Human non-amidated obestatin (2)	SE-4764	Biomedal (Sevilla, ES)
Human 6-23 obestatin (3)	SE-4764	Biomedal (Sevilla, ES)
Human 11-23 obestatin (4)	SE-4764	Biomedal (Sevilla, ES)
Human 16-23 obestatin (5)	SE-4764	Biomedal (Sevilla, ES)
Human 1-10 obestatin (7)	SE-4764	Biomedal (Sevilla, ES)
Mouse obestatin (6)	475-97	California Peptide Research Inc (Napa, CA, US)

Table 1. Peptides. Relation of the peptides used in the different analyses performed in this work.

HUMAN SAMPLES

The study protocol of human samples was approved by the local ethical committee (CAEI Galicia, 2009/118) and carried according to the Declaration of Helsinki. One human healthy sample and 28 gastric adenocarcinomas were used. Histological classification of the gastric adenocarcinomas was performed according to the Laurén system:[204] 22 were intestinal type adenocarcinomas (with signet ring cells, n=1), 3 diffuse type adenocarcinomas (with signet ring cells, n=2), and 3 mixed (with signet ring cells, n=2). Three levels of differentiation were used to classify grading as: well in 9, moderately in 10 and poorly differentiated in 9 patients. Pathological tumour staging was assessed according to the 7th edition of American Joint Committee on Cancer TNM classification.[207] The pathological tissue samples were from gastric adenocarcinomas located in antrum and corpus. The surgical control specimens were located at least 3 cm from the adenocarcinoma. All the examined control tissues originated from macro- and microscopically normal gastric mucosa.

CELLS

Cell culture

All of the cell lines used in this work were cultured as described by the supplier (ATCC, Manassas, VA, US) with 100 U/mL penicillin G, 100 mg/mL streptomycin sulphate and 2.5 mM L-glutamine with 5% CO_2 at 37 °C. Cells have been used always with passages lower than 15 in all the experiments.

Cell line	Growth medium (v/v)
ARPE-19. Retinal pigment epithelium cells	DMEM:F12 + 10% FBS
HEK293. Embryonic kidney cells	EMEM + 10% FBS
AGS. Gastric adenocarcinoma	HAM´s F12 + 10% FBS
KATO III. Gastric carcinoma	RPMI-1640 + 10% FBS
PANC-1. Pancreatic carcinoma	DMEM + 10% FBS FBS
MCF7. Breast adenocarcinoma	EMEM + 10% FBS
HT-29. Colorectal adenocarcinoma	McCoy´s 5A + 10% FBS
PC3. Prostate adenocarcinoma	HAM´S F12K + 10% FBS
A549 . Lung carcinoma	HAM´S F12K + 10% FBS
SW872. Liposarcoma	Leivobitz L15 + 10% FBS
BeWo. Choriocarcinoma	HAM´S F12K + 10% FBS
A431. Epidermoid carcinoma	DMEM + 10% FBS

Table 2. Cells. Relation of human cell lines and its growth medium used in this work. FBS: foetal bovine serum.

ANTIBODIES

Antibodies	Use	Dilution	Code	Manufacturer
Anti-Human GPR39 Peptide Antibody	IC IEM	1:500 1:50	GPR392-A	Alpha Diagnostic International
Anti-Human GPR39 (C-terminal region) Antibody	IH	1:500	SAB4200185	Sigma Chemical
Anti-GPCR GPR39 Antibody	WB	1:1000	ab39227	Abcam
Anti-Mouse/Rat/Human Obestatin Peptide Antibody	IC, IH IEM	1:500 1:50	OBSN11-A	Alpha Diagnostic International
Obestatin (Human, Monkey) Antibody	NA	10 µg/mL	G-031-92	Phoenix Pharmaceuticals
Anti-Human Ki67 Antigen Clone MIB-1	IC, IH	Ready to use	M724001	Dako Agilent
Anti-Ki67 Antibody	WB	1:1000	ab15580	Abcam
Phospho-p44/42 MAPK (Erk1/2) (Thr202/Tyr204) Antibody	WB	1:2000	9101S	Cell Signaling Technology
P44/42MAPK Antibody	WB	1:2000	9102S	Cell Signaling Technology
Phospho-Akt (Ser473) Antibody	WB	1:2000	9271S	Cell Signaling Technology
Akt Antibody	WB	1:1000	9272S	Cell Signaling Technology
Anti-Actin Antibody - Loading Control	WB	1:4000	ab1801	Abcam
Anti-Active beta-Catenin Antibody	WB	1:1000	05-665	Millipore
Anti-E-Cadherin Antibody	WB	1:1000	ab76055	Abcam
Anti-N-Cadherin Antibody	WB	1:1000	ab76011	Abcam
Anti-Vimentin Antibody	WB	1:1000	ab92547	Abcam
Anti-Flk1 (C-1158) Antibody	WB	1:500	sc-504	Santa Cruz
Anti-VEGF (A-20) Antibody	WB	1:500	sc-152	Santa Cruz
Anti-PEDF (H-25) Antibody	WB	1:500	sc-25594	Santa Cruz
Anti-EGFR Antibody	WB	1:1000	2232	Cell Signaling Technology
Anti-Pepsinogen I Antibody	WB	1:1000	ab135403	Abcam
Anti-Pepsinogen I Antibody	IH	1:2000	ab50123	Abcam
Anti-GAPDH Antibody	WB	1:1000	ab9485	Abcam
Anti-GFP Antibody	WB	1:1000	ab111258	Abcam
Anti-Phospho-Tyrosine-HRP Detection Antibody	PA	1:5000	ARY100B	R&D Systems
Phalloidin CruzFluor™-594	IF	1:1000	sc-363795	Santa Cruz Biotechnology
Peroxidase-AffiniPure Goat Anti-Rabbit IgG (H+L)	WB	1:10000	111-035-003	Jackson ImmunoResearch Europe
Peroxidase-AffiniPure Goat Anti-Mouse IgG (H+L)	WB	1:10000	115-035-003	Jackson ImmunoResearch Europe
Peroxidase-AffiniPure Rabbit Anti-Goat IgG (H+L)	WB	1:10000	305-035-003	Jackson ImmunoResearch Europe
Alexa Fluor 594 Antibody	IF	1:1000	A-11012	ThermoFisher
Alexa Fluor 488 Antibody	IF	1:1000	ab150089	Abcam
DAPI	IF			Invitrogen
Human GPR39 Control Antigen Peptide	IC	1:5*	GPR392-P	Alpha Diagnostic International
Human GPR39 Control Antigen Peptide	WB	1:5	ab39283	Abcam
Mouse/Rat/Human Obestatin Control Peptide	IC	1:5*	OBSN11-P	Alpha Diagnostic International

Table 3. Antibodies. Relation of the antibodies used in the different analyses performed in this work. Abbreviations: IC: immunocytochemistry; IEM: immunoelectron microscopy; IH: immunohistochemistry; WB: western blot; NA: neutralization assay; IF: immunofluorescence; PA: protein array. *10 nmol/mL.

PROTEIN ARRAYS

Human phospho-Receptor Tyrosine Kinase Array

Coordinate	Receptor family	RTK/Control	Coordinate	Receptor family	RTK/Control
A1, A2	Reference Spots		D1, D2	Tie	**Tie2**
A23, A24	Reference Spots		D3, D4	NGFR	**TrkA**
B1, B2	EGFR	**EGFR**	D5, D6	NGFR	**TrkB**
B3, B4	EGFR	**ErbB2**	D7, D8	NGFR	**TrkC**
B5, B6	EGFR	**ErbB3**	D9, D10	VEGFR	**VEGFR1**
B7, B8	EGFR	**ErbB4**	D11, D12	VEGFR	**VEGFR2**
B9, B10	FGFR	**FGFR1**	D13, D14	VEGFR	**VEGFR3**
B11, B12	FGFR	**FGFR2α**	D15, D16	MuSK	**MuSK**
B13, B14	FGFR	**FGFR3**	D17, D18	EphR	**EphA1**
B15, B16	FGFR	**FGFR4**	D19, D20	EphR	**EphA2**
B17, B18	Insulin R	**Insulin R**	D21, D22	EphR	**EphA3**
B19, B20	Insulin R	**IGF1R**	D23, D24	EphR	**EphA4**
B21, B22	Axl	**Axl**	E1, E2	EphR	**EphA6**
B23, B24	Axl	**Dtk**	E3, E4	EphR	**EphA7**
C1, C2	Axl	**Mer**	E5, E6	EphR	**EphB1**
C3, C4	HGFR	**HGFR**	E7, E8	EphR	**EphB2**
C5, C6	HGFR	**MSPR**	E9, D10	EphR	**EphB4**
C7, C8	PDGFR	**PDGFRα**	E11, E12	EphR	**EphB6**
C9, C10	PDGFR	**PDGFRβ**	E13, E14	Insulin R	**ALK**
C11, C12	PDGFR	**SCFR**	E15, E16		**DDR1**
C13, C14	PDGFR	**Flt-3**	E17, E18		**DDR2**
C15, C16	PDGFR	**M-CSFR**	E19, E20	EphR	**EphA5**
C17, C18	RET	**c-Ret**	E21, E22	EphR	**EphA10**
C19, C20	ROR	**ROR1**	F1, F2	Reference Spots	
C21, C22	ROR	**ROR2**	F5, F6	EphR	**EphB3**
C23, C24	Tie	**Tie1**	F7, F8		**RYK**
			F23, F24	Control (-)	PBS

Table 4. RTKs. Human phospho-receptor tyrosine kinase (RTKs) included in the array and the correspondent coordinates. R&D Systems (Minneapolis, MN, US).

Human Protease Array

Coordinate	Analyte/Control	Isoform Specificity	Alternate nomenclature	Coordinate	Analyte/Control	Isoform Specificity	Alternate nomenclature
A1,A2	**Reference spots**		RS	C5, C6	**Kallikrein 7**	Proform & Active	KLK7, SCCE, PRSS6, hK7
A3,A4	**ADAM8**	Ectodomain	MS2, CD156a	C7, C8	**Kallikrein 10**	Proform & Active	KLK10, NES1, PRSSL1
A5,A6	**ADAM9**	Ectodomain	MDC9, meltrin g	C9,C10	**Kallikrein 11**	Proform & Active	KLK11, TLSP, PRSS20
A7, A8	**ADAMTS1**	Proform	METH1	C11,C12	**Kallikrein 13**	Proform & Active	KLK13, KLKL4
A9, A10	**ADAMTS13**	Active	von Willebrand factor-cleaving protease	C13,C14	**MMP1**	Proform & Active	Collagenase 1, Interstitial Collagenase
A11, A12	**Cathepsin A**	Proform & Active	CTSA, Lysosomal Carboxypeptidase A	C15,C16	**MMP2**	Proform & Active	Gelatinase A
A13, A14	**Cathepsin B**	Proform	CTSB, APPS, CPSB	C17,C18	**MMP3**	Proform & Active	Stromelysin-1
A15, A16	**Cathepsin C**	Proform & Active	CTSC	D3,D4	**MMP7**	Proform & Active	Matrilysin, PUMP1
A17, A18	**Cathepsin D**	Proform & Active	CTSD, CPSD	D5,D6	**MMP8**	Proform & Active	Collagenase 2, Neutrophil Collagenase
A19, A20	**Reference Spots**		RS	D7, D8	**MMP9**	Proform & Active	Gelatinase B, CLG4B, GELB
B3, B4	**Cathepsin E**	Proform & Active	CTSE, CATE	D9, D10	**MMP12**	Proform & Active	Macrophague Elastase
B5, B6	**Cathepsin L**	Proform & Active	CTSL, CATL, MEP, Cathepsin L1	D11, D12	**MMP13**	Proform	Collagenase 3
B7, B8	**Cathepsin S**	Proform & Active	CTSS	D13, D14	**Neprilysin/CD10**	Ectodomain	MME, NEP, CALLA
B9, B10	**Cathepsin V**	Proform & Active	CTSV, CTSL2, CTSU, Cathepsin L2	D15,D16	**Presenilin-1**	N-terminal fragment	PSEN1, AD3, PS-1
B11, B12	**Cathepsin X/Z/P**	Proform & Active	CTSX, CTSZ	D17,D18	**Proprotein Convertase 9**	Active	PC9, NARC1
B13, B14	**DPPIV/CD26**	Ectodomain	ADABP, ADCP2	E1, E2	**Reference spots**		RS
B15, B16	**Kallikrein 3/PSA**	Proform & Active	KLK3, hK3, KLK2A1	E3, E4	**Proteinase 3**	Active	PRTN3, Myeloblastin
B17, B18	**Kallikrein 5**	Proform & Active	KLK4, SCTE, KLKL2	E5, E6	**uPA/Urokinase**	Proform & Active	Urokinase-type Plasminogen Activator, PLAU
C3, C4	**Kallikrein 6**	Proform & Active	KLK6	E7,E8	Negative Control		Control (-)

Table 5. Proteases. Human proteases included in the array and the correspondent coordinates. R&D Systems (Minneapolis, MN, US).

METHODS

STRUCTURE ANALYSIS

NMR spectroscopy in SDS micelles. Samples for the NMR experiments were prepared by dissolving peptides in 500 µL of a perdeuterated SDS (SDS-d_{25}) aqueous solution [9:1 H_2O:deuterated water (D_2O), phosphate buffer saline (PBS) at pH 6.5] to make a final concentration of approximately 0.8-1.0 mM and a peptide/SDS ratio of approximately 1/70. The NMR spectra were recorded at 298 K using Bruker 600 and 700 MHz spectrometers equipped with a triple-resonance Z gradient probe and processed using XWIN-NMR software (Bruker Inc.; Billerica, MA, US). The resonance of 2,2,3,3-tetradeutero-3-trimethylsilylpropionic acid (TSP) was used as a chemical shift reference in the ^{1}H NMR experiments (δ TSP=0 ppm). The one-dimensional (1D) ^{1}H homonuclear spectra were recorded in the Fourier mode using quadrature detection. The two-dimensional (2D) ^{1}H homonuclear total correlation spectroscopy (TOCSY) and nuclear Overhauser effect (NOE) spectroscopy (NOESY) spectra were collected in the phase-sensitive mode using time-proportional phase increments in t1. For each of these experiments, 512 t1 increments were used. The free induction decay in t2 consisted of 2048 data points over a spectral width of 6009.615 Hz. In general, 4096x1024 data points were collected for each block, and 96 transients were collected for the 2D experiments. The TOCSY spectra were recorded using the MLEV-17 pulse sequence with mixing times (spin-lock) of 60-80 ms. The NOESY experiments were acquired with mixing times of 250-400 ms. The experimental data were acquired and processed using the TopSpin™ (Bruker Inc; Billerica, MA, US) program on a PC station. The data matrices were multiplied by a qsine function in both dimensions and then zero-filled to 1024 data points in F1 prior to the Fourier transformation. The peptide resonance assignments were obtained using standard strategies based on the 2D NMR experiments.

NMR spectroscopy in living cells. NMR samples of the pure peptides were prepared by dissolving 400 µg of each peptide in 0.5 mL of water or of a mixture PBS buffer (pH 7.2):D_2O (95:5, v/v). To perform the NMR experiments with living cells, 4×10^6 cells were counted, washed, and dissolved in PBS, pH 7.2. Samples were prepared by placing 400 µg of each peptide in 0.5 mL of a suspension of the cells in a mixture PBS (pH 7.2):D_2O (95:5, v/v). Different samples of peptides were prepared as a suspension with the following cell lines: HEK293 and HEK293-GPR39. The exact amount of receptors on the cell surface is unknown. NMR spectra were acquired on a Varian INOVA spectrometer operating at 750 MHz and processed with NMRPipe software using a standard inverse detection triple-resonance and triple-axis gradient probe. A soft-watergate solvent suppression scheme was used to suppress the H_2O solvent signal in all the experiments. All the spectra were acquired with an external reference of TSP (0.0 ppm). 2D ^{1}H TOCSY was acquired for each NMR sample. NMR samples were prepared as previously described for each peptide using 4×10^6 cells. For each sample, three 2D ^{1}H TOCSY experiments were acquired at different times after preparation to check sample stability. The ^{1}H NOESY and rotating-frame nuclear Overhauser effect spectroscopy (ROESY) experiments were acquired with mixing times of 250-400 ms. The experiments were acquired at time 0, 7 and 24 h after sample preparation. Each spectrum was acquired in ca. 2.5 h with 24 scans and 128 complex points in the t1 dimension using the states phase sensitive mode. The spectra were processed with a 90° shifted sinebell apodization function and Fourier transformed to 2048

× 512 real points in dimensions F2 and F1, respectively. The peptide resonance assignments were obtained using standard strategies based on the 2D NMR experiments.

Structure calculation. The peak lists for the NOESY and ROESY spectra recorded with a 0.25 s mixing time were generated by interactive peak picking using the CARA software.[208] The NOESY cross-peak volumes were determined using the automated peak integration routine implemented in CARA. The three-dimensional (3D) structures of human obestatin (**1**) and its derivatives were determined using the standard protocol of combined automated NOE assignment and the structure calculation implemented in the CYANA 2.1 program.[209] Seven cycles of combined automated NOESY assignment and structure calculations were followed by a final structure calculation. The structure calculation started in each cycle from 100 randomized conformers, and the standard simulated annealing schedule was used. The 20 conformers with the lowest final CYANA target function values were retained for analysis and passed to the next cycle. Weak restraints on the ϕ/ψ torsion-angle pairs and on the side-chain torsion angles between tetrahedral carbon atoms were applied temporarily during the high-temperature and cooling phases of the simulated annealing schedule to favour the permitted regions of the Ramachandran plot and the staggered rotamer positions, respectively. The list of upper-distance bonds for the final structural calculation consists of unambiguously assigned upper-distance bonds and does not require the possible swapping of diastereotopic pairs. The 20 conformers with the lowest final CYANA target function values were subjected to restrained energy-minimization in a water shell using the AMBER 8.0 program.[210] The resulting 20 energy-minimized CYANA conformers represent the solution structures of human obestatin (**1**) and its derivatives. The MOLMOL program was used to visualize the 3D structures.[211] CYANA was used to obtain statistics on the target function values, restraint violations and Ramachandran plots according to the PROCHECK-NMR conventions.[212] The root mean square deviation (RMSD) values were calculated using CYANA for the superpositions of the backbone N, Cα and C' atoms and the heavy atoms throughout the protein. To obtain the RMSD value of a structure represented by a bundle of conformers, all of the conformers were superimposed on the average structure, and the average of the RMSD values between the individual conformers and their average coordinates was calculated.

CD spectroscopy. CD experiments of the peptides were performed using a 720-Jasco spectropolarimeter (Tokyo, JP) and a 1-mm-path-length quartz cuvette. The CD spectra of the peptides in the SDS micellar solution were recorded using a H_2O solution containing 40 μM peptide and SDS micelle at a concentration of 2.8 mM (25 °C). In all cases, 25 mM NaH_2PO_4/Na_2HPO_4 buffer was used to maintain the pH at 6.5. The CD spectra presented are the average of 5 accumulations from 190 to 250 nm, which were recorded with a bandwidth of 1 nm and a scanning speed of 20 nm/min. During all of the measurements, the trace of the high-tension voltage remained less than 700 V, which should ensure the reliability of the

[208] Keller RLJ. The Computer Aided Resonance Assignment tutorial.2004. Goldau: CANTINA Verlag. Available: http://cara.nmr-software.org/portal/

[209] Güntert P. Automated NMR structure calculation with CYANA. Methods Mol Biol. 2004;278:353-78.

[210] Case DA, Cheatham TE 3rd, Darden T, *et al*. The Amber biomolecular simulation programs. J Comput Chem. 2005;26:1668-88.

[211] Koradi R, Billeter M, Wüthrich K. MOLMOL: a program for display and analysis of macromolecular structures. J Mol Graph. 1996;14:51-4.

[212] Laskowski RA, Rullmannn JA, MacArthur MW, *et al*. AQUA and PROCHECK-NMR: programs for checking the quality of protein structures solved by NMR. J Biomol NMR. 1996;8:477-86.

obtained data.[213] Baselines of either solvent or micellar solutions without peptide were subtracted from each respective sample to yield the contribution of the sample. The secondary structure composition was estimated using the DICHROWEB web server,[214,215] with the following algorithms: CONTINLL, involving 2 different reference data sets, and K2d.[216]

[^{32}P]ORTOPHOSPHATE LABELLING AND GPR39 IMMUNOPRECIPITATION

HEK293 cells were transfected with the green fluorescent protein (GFP)-tagged human GPR39 and plated in 6-well plates at 200,000 cells/well 24 h before experimentation and serum starved overnight (O/N). For phosphorylation experiments, cells were washed three times with Krebs/hydroxyethyl piperazineethanesulfonic acid (HEPES) buffer without phosphate [containing in mM: 10 HEPES (pH 7.4), 118 NaCl, 1.3 $CaCl_2$, 4.3 KCl, 1.17 $MgSO_4$, 4.17 $NaHCO_3$, 11.7 glucose] and incubated in this buffer containing 100 µCi/mL [^{32}P]orthophosphate for 1 h at 37 °C and 5% CO_2. Cells were then stimulated with obestatin (200 nM, 5 min) and immediately lysed by addition of lysis buffer [containing in mM: 20 Tris/HCl (pH 7.4), 150 NaCl, and 3 ethylenediaminetetraacetic acid (EDTA); and supplemented with 1% (v/v) NP-40, and 0.5% (w/v) sodium deoxycholate]. GPR39 was immunoprecipitated from the cleared lysates using GFP-trap (Chromotek, DE) following manufacturer's instructions. The washed immunoprecipitates were separated on two 10% SDS/polyacrylamide gels. The first gel was dried, and radioactive bands were revealed using autoradiography film. The second gel was transferred to nitrocellulose membrane (Bio-Rad, Hercules, CA, US) as loading control. The blots were incubated with 5% non-fat milk in a Tris buffer solution (TBS) containing Tween-20 (TBST) [20 mM Tris-HCl (pH 8.0), 150 mM NaCl, 0.1% (v/v) Tween-20, solution used for all incubation and washing steps] for 1 h. The blots were then incubated with GFP and GPR39 antibodies, according to the manufacturer's instructions, and were subsequently incubated with the corresponding peroxidase-conjugated IgG antibody. After washing, the signals were visualized using an ECL plus Western Blotting Detection System (Pierce ECL Western Blotting Substrate; Thermo Fisher Scientific, Pierce, Rockford, IL). Blots shown are representative of three experiments. The image processing was performed using the NIH Image Sofware ImageJ 1.49 (National Institutes of Health, Bethesda, MD, US).

GPR39 INTERNALIZATION

For analysis of the endocytosis time course, HEK293 cells on poly-D-lysine-coated coverslips were transfected with the GFP-tagged human GPR39. The cells were grown O/N in a humidified atmosphere of 95% air and 5% CO_2 at 37 °C. The cells were preincubated for 120 min at 37 °C with 90 µM cycloheximide in all experiments to prevent *de novo* protein synthesis. The cells were preincubated for 30 min at 4 °C in ice-cold Earle's buffer [containing in mM: 140 NaCl, 5 KCl, 1.8 $CaCl_2$, and 3.6 $MgCl_2$ (pH 7.4); and, complemented with 0.2% bovine serum albumin (BSA), 0.01% glucose, 90 µM cycloheximide, and 0.8 mM 1-10 phenanthrolene] in the presence/absence of obestatin (200 nM). Internalization was promoted by placing the cells at 37 °C for the indicated times. The

[213] Kelly SM, Jess TJ, Price NC. How to study proteins by circular dichroism. Biochim Biophys Acta. 2005;1751:119-39.

[214] Whitmore L, Wallace BA. DICHROWEB: an online server for protein secondary structure analyses from circular dichroism spectroscopic data. Nucleic Acids Res. 2004;32:W668-73.

[215] Whitmore L, Wallace BA. Protein secondary structure analyses from circular dichroism spectroscopy: methods and reference databases. Biopolymers. 2008;89:392-400.

[216] Greenfield NJ. Using circular dichroism spectra to estimate protein secondary structure. Nat Protoc. 2006;1:2876-90.

cells were then rinsed three times with ice-cold Earle's buffer and subsequently fixed for 10 min with 4% paraformaldehyde (PFA) dissolved in 0.1 mM PBS (pH 7.4). The cells were rinsed again in cold Earle's buffer, mounted using Vectashield (Vector Laboratories, Compiègne, France). DAPI was used to counterstain the cell nuclei. Digital images of cell cultures were acquired with a Leica TCS-SP5 spectral confocal microscope (Leica Microsystems; Heidelberg, DE).

IMMUNOBLOT ANALYSIS

Immunoblot analysis in cells. Serum-starved cells were stimulated with obestatin and/or truncates for the indicated time period and doses at 37 °C. The medium was then aspirated, and cells were lysed in ice-cold lysis buffer [RIPA buffer: 50 mM Tris-HCl pH 7.2, 150 mM NaCl, 1 mM EDTA, 1% (v/v) NP-40, 0.25% (w/v) Na-deoxycholate, protease inhibitor cocktail (1:100, Sigma Chemical Co., St. Luis, MO, US), phosphatase inhibitor cocktail (1:100, Sigma Chemical Co., St. Luis, MO, US)]. The soluble cell lysates were pre-cleared by centrifuging at 14,000 rpm for 15 min. The protein concentration was evaluated with the QuantiPro™ BCA Assay kit (Sigma Chemical Co., St. Luis, MO, US). The same amount of protein for each sample was separated on 10% SDS/polyacrylamide gels and transferred to nitrocellulose membranes (Bio-Rad, Hercules, CA, US). The blots were then incubated with the corresponding antibodies and processed as described above. The blots shown are representative of six experiments. The image processing was performed using the NIH Image Sofware ImageJ 1.49 (National Institutes of Health, Bethesda, MD, US).

Inmunoblot analysis in human tissue samples. For each extraction, six series of 15 µm sections from fixed in formalin and embedded in paraffin (FFPE) samples, with an area of approximately 150 mm^2, were collected in an Eppendorf tube. Samples were deparaffinised using 600 µL of mineral oil (Sigma-Aldrich, US). After vortexing, samples were incubated to dissolve the wax (95 ˚C, 2 min), and finally the supernatants were removed after pelleting at 14,000 xg [room temperature, (RT); 3 min]. These incubation and centrifugation steps were repeated again by adding 350 µL of mineral oil. The pellets were resuspended in 200 µL of lysis buffer (200 mM TrisHCl pH 7.5, 200 mM NaCl, 5% SDS, and 100 mM sodium citrate) and were incubated with this buffer for 20 minutes at 100°C and then for 2 h at 80°C, both with shaking.[217] After centrifugation at 14,000 xg for 5 min at RT, supernatants were recovered and the protein was quantified with the QuantiProTM BCA Assay kit (Sigma Chemical Co., St. Luis, MO, USA). The same amount of protein for each sample was separated on 10% SDS/polyacrylamide gels and transferred to nitrocellulose membranes (Bio-Rad, Hercules, CA, US). The blots were then incubated with the corresponding antibodies and processed as described above. The image processing was performed using the NIH Image Sofware ImageJ 1.49 (National Institutes of Health, Bethesda, MD, US).

CELL PROLIFERATION ASSAYS

For the adherent cell lines the cell proliferation was measured using a bromodeoxiuridine (BrdU) cell proliferation enzyme-linked immunosorbent assay (ELISA) kit (Roche Diagnostics, Mannheim, DE). The BrdU assay was performed according to the manufacturer's protocol. Cells were cultured in a 96-

[217] Rodríguez-Rigueiro T, Valladares-Ayerbes M, Haz-Conde M, *et al*. A novel procedure for protein extraction from formalin-fixed paraffin-embedded tissues. Proteomics. 2011;11:2555-9.

well multiplate at a density of 2-5 x 10^3 cells per well in the culture medium described above for 24 h. The procedure comprised the following steps: 1) 0% FBS for 24 h; 2) stimulation with obestatin and/or truncates for the indicated time period and doses; 3) incubation with BrdU-labeling solution (10 µL, 3 h, 37 °C); 4) removal of labeling solution and fixing with FixDenat solution (200 µL, 30 min, 25 °C); 5) incubation with anti-BrdU-peroxidase (POD) antibody solution (100 µL, 90 min, 25 °C); and, 6) washing followed by the addition of substrate solution (100 µL, 30 min). The BrdU incorporation was quantified using the spectrophotometric absorbance (370 nm) measured with a VersaMaxPLUS Reader (Molecular Devices, Sunnyvale, CA, US). The mean absorbance of the control cells represented 100% cell proliferation, and the mean absorbance of the treated cells was related to the control values to determine sensitivity. In all cases, each experiment point was replicated eight times. For the non-adherent cell line KATO III, a Trypan Blue protocol was used for viable cell counting. To ensure the reliability of the experimental procedure, the adherent HT-29 cell line was also subjected to the same protocol. In brief, the cells were cultured in a 96-well multiplate at a density of 5 x 10^3 cells per well in the serum-free medium described in Table 2 for 24 h. The cells were then treated with 100 nM human obestatin, 10% FBS (positive control), 40 µM $ZnCl_2$, and 100 nM obestatin plus 40 µM $ZnCl_2$ for 48 h. For cell counting, a cell suspension in PBS was prepared. Sequentially, 0.5 mL of 0.4% Trypan Blue solution (w/v), 0.3 mL PBS and 0.2 mL of the cell suspension were added to a test tube, mixed thoroughly, and allowed to stand for 5-15 min. A hemacytometer was used to count viable cells as non-viable cells stained blue. Total cells were calculated using the following equations: Cells per mL = the average count per square × dilution factor × 10^4 (count 10 squares). Total Cells = cells per ml × the original volume of fluid from which cell sample was removed. Cell Viability (%) = total viable cells (unstained) ÷ total cells (stained and unstained) × 100. In all cases, each experiment point was replicated eight times.

SMALL INTERFERING RNA ASSAYS

siRNA silencing of gene expression in ARPE-19, AGS and PANC-1 cells. The following double-stranded siRNA duplexes of GPR39 were used (Thermo Fisher Scientific, Dharmacon, Lafayette, CO, US; ON-TARGETplus SMART pool L-005569-00-0005, Human GPR39, NM_001508): 3'-UCCAAUAUGUCCAUCUGUA-5', 3'-GCGCGAAACCAGCCAAUUC-5', 3'-GAGGCUGAUUGUUGUGACA-5', and 3'-AACCAGAUUCGGAGGAUCA-5'. A non-silencing RNA duplex was used as a control for all siRNA experiments. The cells were transfected using Lipofectamine 2000 (Invitrogen; CA, US). Silencing was quantified by immunoblotting. Only experiments with verified silencing were used.

IMMUNOCYTOCHEMISTRY AND IMMUNOHISTOCHEMISTRY

Immunocytochemistry detection of GPR39, obestatin and Ki67 in cells. Cells were cultured at a density of 4-8 x 10^3 cells per well in the culture medium described above on 8-well Lab-Tek II chamber slides covered with cell conditioning solution 2 (CC2) glass slide coverslips. After 2 days, the medium was renewed, and the cells were cultured in a serum-free medium (300 µL) for 24 h. The cells were then treated with obestatin and/or its truncates for the indicated time period and doses. After indicated time, the intact cells were fixed in 96% ethanol for 1 h. The immunocytochemical technique was automatically performed using an AutostainerLink 48 instrument (Dako Agilent Technologies, Glostrup, DK). Correspondent primary antibodies was used. EnVision™ peroxidase FLEX/HRP (Dako Agilent

Technologies, Glostrup, DK) was employed as a detection system. Briefly, the procedure comprised the following steps: 1) epitope retrieval in 10 mM citrate buffer (pH 6.0) using a microwave (750 W, 10 min); 2) incubation with peroxidase-blocking agent (5 min); 3) incubation with primary antibody (30 min); 4) incubation with labeled polymer-horseradish peroxidase (HRP, dextran polymer conjugated with HRP and affinity-isolated immunoglobulins); 30 min); 5) incubation with 3,3'-diaminobenzidine (DAB)-tetrahydrochloride (Dako Liquid DAB + Substrate-chromogen system) (10 min); and 6) counterstaining with Harris hematoxylin solution (HHS) (9 min). In all cases, triplicate dishes were used for each experimental point. The preadsorption control for obestatin and GPR39 was performed applying the primary antibody plus obestatin or the GPR39 control peptide to positive samples.

Immunocytochemistry detection of Ki67 in GPR39-siRNA depleted AGS cells. The AGS cells were cultured at a density of 8 x 10^3 cells per well in the culture medium described above on 8-well Nunc® Lab-Tek® II chamber slides covered with CC2 glass slide coverslips. After 2 days, the medium was renewed, and the cells were cultured in a serum-free medium (300 µL) for 24 h. The AGS cells were transfected using Lipofectamine 2000 (Invitrogen; CA, US). Serum-starved cells were stimulated or not with obestatin (100 nM, 24 h) at 37 °C. After 24 h, the intact cells were fixed in 96% ethanol for 1h. The immunocytochemical technique was performed as described above. In all cases, triplicate dishes were used for each experimental point.

Immunoelectron microscopy of GPR39 and obestatin in AGS cells. For the immunoelectron microscopic techniques, AGS cells were fixed (2-4 h) in a solution of 2% PFA and 0.2% glutaraldehyde in 0.1 M PBS (pH 7.4). After washing with PBS, the specimens were dehydrated in graded ethanol series and embedded in LR White (The London Resin Co, Basingstoke, UK). Polymerization was done at 60°C for 18 h, avoiding contact between resin and oxygen. Ultrathin sections (60 nm thick) were collected on uncoated 700-mesh nickel grids. Labeling procedures were performed at RT. The procedure comprised the following steps: 1) 0.5% ovalbumin (v/v) and 0.05% Tween 20 (v/v) in PBS (Solution A; 2x5 min); 2) anti-GPR39 or anti-obestatin antibody in the same buffer as used in step 1 (O/N, RT); 3) solution A (1x10 min); 4) 0.5% ovalbumin (v/v) and 0.05% Tween 20 (v/v) in TBS (0.02 M Tris-HCl, 0.65 M NaCl) (Solution B; 2 x 10 min); 5) goat anti-rabbit labeled with 10 nm (GPR39) or 20 nm (obestatin) colloidal gold (BBInternational, Cardiff, UK), both diluted at 1:20 in solution B (1x1 h); 6) standard saline citrate (SSC; SSC: 0.15 M NaCl, 0.015 M sodium citrate, pH 7.0; 1x5 min); 7) distilled water (1x5 min); 8) 2% neutral uranyl acetate (1x2 min); and 9) distilled water (2x5 min). Controls were performed by replacing the primary antibody by either normal rabbit serum or PBS, or by omitting any essential step of the reaction.[218] All ultrathin sections were observed and photographed using a JEM-1011 electron microscope (JEOL, JAPAN) equipped with a slow-scan digital camera at an accelerating voltage of 80 kV.

Immunohistochemistry detection of GPR39, obestatin, Ki67 and pepsinogen I in human gastric mucosa samples. Immunohistochemistry was performed according to the protocol used by Raghay *et al*.[219] In brief, the samples were immersion-fixed in 10% buffered formalin for 24 h, dehydrated and

[218] García-Caballero A, Gallego R, García-Caballero T, *et al*. Cellular and subcellular distribution of 7B2 in porcine Merkel cells. Anat Rec. 1997;248,:159-63.

[219] Raghay K, Garcia-Caballero T, Bravo S, *et al.* Ghrelin localization in the medulla of rat and human adrenal gland and in pheochromocytomas. Histol Histopathol. 2008;23:57-65.

embedded in paraffin by a standard procedure. The 5 µm-thick sections were mounted on Histobond adhesion microslides (Marienfeld, Lauda-Königshofen, DE), dewaxed and rehydrated. Antigen retrieval was carried out by heating in a microwave oven for 20 min at 750 W in 10 mM sodium citrate buffer (pH 6.0). For detection of obestatin, GPR39 and pepsinogen I (PGI) the corresponding antibodies were used. Detection of Ki67 was performed using the same technique as described for immunocytochemistry. All sections were counterstained with HHS for 1 min. Pre-adsorption controls of the obestatin and GPR39 immunohistochemical technique were performed in gastric tissue. Negative controls (n=3) were performed by substituting the primary antibody with PBS or pre-adsorption of the antibody with the homologous antigen. Ten different fields for each section were analyzed twice. A scale from 0 to 3+ was used to express the incidence of positive immunoreaction in a semi-quantitative assay. Photographs were taken using a Zeiss Observer Z1 microscope and the Axiovision software (Carl Zeiss, Göttingen, GE). Two different observers performed evaluation independently.

IMMUNOFLUORESCENCE ANALYSIS

Immunofluorescence detection of F-actin in AGS, PANC-1, A431 and KATO III cells. Cells were cultured at a density of 8-10 x 10^3 cells per well in the culture mediums described above on 8-well Nunc® Lab-Tek® II chamber slides covered with CC2 glass slide coverslips. After 2 days, the medium was renewed, and the cells were cultured in a serum-free medium (300 µL) for 24 h. Serum-starved cells were stimulated or not with obestatin (200 nM, 24 h) at 37 °C. After 24 h, intact cells were fixed with 4% buffered PFA-PBS for 30 min, washed, permeabilized with 0,25% Triton X-100 in PBS for 45 min, and blocked with PBS containing Tween-20 (PBST, 1% Triton X-100, 1% Tween 20, 5% heat-inactivated normal goat serum, 1% BSA in PBS) for 30 min. After three washes with PBS, cells were incubated with Phalloidin CruzFluor 594 in 1% BSA in PBST (1:1000) for 1 hour at RT. DAPI was used to counterstain the cell nuclei. Digital images of cells were acquired with a Zeiss Axio Vert.A1 fluoresecence microscope (Carl Zeiss AG, Oberkochen, Germany).

Immunofluorescence detection of F-actin in GPR39-siRNA depleted AGS and PANC-1 cells. Cells were cultured at a density of 10 x 10^3 cells per well in the culture medium described above on 8-well Nunc® Lab-Tek® II chamber slides covered with CC2 glass slide coverslips. After 2 days, the medium was renewed, and the cells were cultured in a serum-free medium (300 µL) for 24 h. Cells were transfected using Lipofectamine 2000 (Invitrogen; CA, US). Serum-starved cells were stimulated or not with obestatin (200 nM, 24 h) at 37 °C. After 24 h, intact cells were fixed with 4% buffered PFA-PBS for 30 min, washed, permeabilized with 0,25% Triton X-100 in PBS for 45 min, and blocked with PBST for 30 min and then incubated with anti-GPR39 rabbit antibody diluted in 1% BSA in PBST (1:500) for 1 hour at RT. After three washes with PBS, cells were incubated with the secondary antibody (Alexa 488 anti-rabbit antibody) and Phalloidin CruzFluor 594 in 1% BSA in PBST (1:1000) for 1 hour at RT. DAPI was used to counterstain the cell nuclei. Digital images of cells were acquired with a Zeiss Axio Vert.A1 fluorescence microscope (Carl Zeiss AG, Oberkochen, Germany).

PLASMID CELL TRANSIENT TRANSFECTION IN HEK293 AND A431 CELLS

The cDNA encoding GPR39 fused at its C terminus to GFP in p-CMV6-AC plasmid (Origene, Rockville, MD, US) was transfected into subconfluent HEK293 and A431 cells using Lipofectamine 2000 (Life Technologies, Invitrogen; Gran Island, NY, US),

according to the manufacturer's instructions. Cells were transiently transfected. Cell lines expressing the GPR39-GFP were cultured as described above. The GPR39 incorporation was confirmed by GFP visualization in transfected cells before and after treatment with a Zeiss Axio Vert.A1 fluorescence microscope (Carl Zeiss AG, Oberkochen, Germany).

ARRAY PROTEIN ASSAYS

Human Phospho-RTK Array and analysis

To analyze the activation profiles of RTKs the Proteome Profiler™ Human Phospho-RTK Array Kit (R&D Systems, Minneapolis, MN, USA) was used according to the manufacturer's instructions. This method allows simultaneous detection of the relative tyrosine phosphorylation levels of 49 different phospho-RTKs. Each array contained duplicate validated control and capture antibodies for specific RTKs. Serum-starved cells were stimulated with obestatin 200 nM for the indicated time period at 37 °C. The medium was then aspirated, and cells were lysed in ice-cold array lysis buffer with protease inhibitor cocktail and phosphatase inhibitor cocktail (1:100, Sigma Chemical Co., St. Louis, MO, US). After 30 min in ice-cold, samples were centrifuged at 14,000 xg for 5 min at 4 °C and the supernatant was transferred into a clean tube. FFPE samples, were deparaffinised using 600 µL of mineral oil (Sigma-Aldrich, US). After vortexing, samples were incubated to dissolve the wax (95 ˚C, 2 min), and finally the supernatants were removed after pelleting at 14,000 xg (RT; 3 min). These incubation and centrifugation steps were repeated again by adding 350 µL of mineral oil. The pellets were resuspended in 200 µL of lysis buffer (200 mM TrisHCl pH 7.5, 200 mM NaCl, 5% SDS, and 100 mM sodium citrate) and were incubated with this buffer for 20 minutes at 100 °C and then for 2 h at 80 °C, both with shaking. After centrifugation at 14,000 xg for 5 min at RT, supernatants were recovered. Total protein concentration was quantified using the QuantiPro™ BCA Assay kit (Sigma Chemical Co., St. Luis, MO, US). The membranes were incubated with 200 or 300 µg of protein. Briefly, phospho-RTK array membranes were blocked with Block Buffer (1 h) and incubated O/N with 1.5 mL of cell and tissue lysate after normalization for equal amounts of protein. After extensive washing with Wash Buffer the membranes were incubated with Anti–Phospho-Tyrosine-HRP detection antibody (RT, 2h). The unbound HRP antibody was washed with Wash Buffer. Each array was then incubated with Chemi Reagent Mix, and exposed to X-ray film (1-10 min). Dot blot densitometric analysis of the immunoblots was performed in duplicate, using NIH ImageJ software 1.49 (National Institutes of Health, Bethesda, MD, US). The relative phosphorylation profiles in 2 groups were normalized by using mean of positive control spots that are located in all 4 corners of the array. Fold changes were calculated by dividing untreated phosphorylation profile to treated profile accordingly.[220]

Human Protease Array and analysis

To analyze the expression profiles of protease proteins we used the Proteome Profiler™ Human Antibody Array Kit (R&D Systems, Minneapolis, MN, USA), according to the manufacturer's instructions. This method allows for simultaneous detection of the relative expression levels of 34 different proteases. Each array contained duplicate validated control and capture antibodies for specific proteases. Serum-starved cells were stimulated with obestatin 200 nM

[220] Gur S, Sikka SC, Abdel-Mageed AB, *et al*. Imatinib mesylate (Gleevec) induces human corpus cavernosum relaxation by inhibiting receptor tyrosine kinases (RTKs): identification of new RTK targets. Urology. 2013;82:745.

for the indicated time period at 37 °C. For the metalloproteases experiments, it was necessary to obtain the cellular secretome. The stimulation medium was recollected and filtered with a 3 kDa filter (Merck Millipore, Billerica, MA, US). Cells were lysed in ice-cold array lysis buffer with protease inhibitor cocktail and phosphatase inhibitor cocktail (1:100, Sigma Chemical Co., St. Louis, MO, US). After 30 min in ice-cold, samples were centrifuged at 14,000 xg for 5 min at 4 °C and the supernatant was transferred into a clean tube. FFPE samples were processed as described above. Total protein concentration was quantified using the QuantiPro™ BCA Assay kit (Sigma Chemical Co., St. Luis, MO, US). The membranes were incubated with 200 or 300 µg of protein. Briefly, protease array membranes were blocked with Block Buffer for 1 hour. Supernatants and lysates of treated and untreated cells were centrifuged and mixed with 15 µl of Detection Antibody Cocktail for 1 h at RT. Then, the membranes were incubated with the sample/antibody mixtures O/N at 4 °C on a rocking platform. Following a washing step to remove unbound material, membranes were incubated with Streptavidin-HRP reagent for 30 minutes. The unbound Streptavidin-HRP reagent was washed with Wash Buffer. Each array was then incubated with Chemi Reagent Mix, and exposed to X-ray film for 1-10 minutes. Dot blot densitometric analysis of the immunoblots was performed in duplicate, using NIH ImageJ software 1.49 (National Institutes of Health, Bethesda, MD, US). The relative expression profiles in 2 groups were normalized by using mean of positive control spots that are located in all 4 corners of the array. Fold changes were calculated by dividing untreated expression profile to treated profile accordingly.[221]

MIGRATION AND INVASION ASSAYS

Wound healing assay (migration assay). AGS cells were seeded on 6-well plates, grown to 100% confluence and then wounded with a sterile pipette tip to remove cells by linear scratches. The cells were washed and maintained in culture medium or culture medium with 200 nM obestatin. The progress of migration was photographed immediately after injury and at 24 h after wounding, near the crossing point. The wound was calculated by tracing along the border of the scratch using the ImageJ64 analysis software and using the following equation: %wound closure=[[wound area (0 h)-wound area (x h)]/ wound area (0 h)] x 100.[72]

Cell-inverted invasion assay. Gastric adenocarcinoma AGS cells were cultured as described above. The invasion assay was conducted as previously described.[222] Obestatin (200 nM) was used as chemoattractant. Cells were allowed to migrate and invade into growth factor-reduced Matrigel for 24 h, pretreated with 50 µM cytarabine (to avoid proliferation), stained with 4 µmol/L calcein-acetoxymethyl ester (Invitrogen), and visualized by confocal microscopy (Leica TCS SP2 confocal microscope) using a ×10 objective. Optical sections were scanned at 5 µm intervals moving up from the underside of the membrane into the Matrigel. The fluorescence from each optical section was quantified with LCS Lite software (Leica Microsystems, Heidelberg, DE).

[221] Kumar D, Moore R, Nash A, *et al*. Decidual GM-CSF is a critical common intermediate necessary for thrombin and TNF induced in-vitro fetal membrane weakening. Placenta. 2014;35:1049-56.

[222] Muinelo-Romay L, Colas E, Barbazan J, *et al*. High-risk endometrial carcinoma profiling identifies TGF-β1 as a key factor in the initiation of tumor invasion. Mol Cancer Ther. 2011;10:1357-66.

PEPSINOGEN SECRETION ASSAYS

Haemoglobin-substrate pepsinogen secretion. Pepsinogen secretion was measured by the conversion of pepsinogen to pepsin using haemoglobin as a substrate as was described by Hersey *et al*.[223] In brief, serum-starved cells were stimulated with obestatin 200 nM for 30, 40, 50 and 60 minutes at 37 °C. The stimulated secreted medium was recollected, filtered with a 30 kDa filter (Merck Millipore, Billerica, MA, US) and concentrated by centrifugation. This concentrated solution was then mixed with haemoglobin solution and incubated for 50 min at 37°C. 10% trichloroacetic acid (TCA) was added to stop the reaction. After spinning to pellet proteins, the resulting supernatant was incubated with 0.5 M NaOH and quantified using the QuantiPro™ BCA Assay kit (Sigma Chemical Co., St. Luis, MO, US). The absorbance was measured at 280 nm by use of DU730 Life Science UV/Vis spectrophotometer (Beckman Coulter, Indianapolis, IN, US) and the concentration of pepsinogen in each sample was calculated from a pepsin standard curve.

Pepsinogen secretion by immunoblot analysis. Serum-starved cells were stimulated with obestatin (200nM) for 40 minutes at 37 °C. The secreted medium was collected and incubated with 20% TCA for 2 hours at 4 °C. Medium was then centrifuged (14,000 rpm, 10 min) and washed twice with ice-cold acetone (14,000 rpm, 5 min).[224] Once the pellet is collected, precipitated secretome protein was diluted in blue loading sample buffer [62.5 mM Tris-HCl, 2% SDS, 25% glycerol, 50 mM dithiothreitol (DTT) and 0,01% bromophenol blue]. Each sample was separated on 10% SDS/polyacrylamide gels and transferred to nitrocellulose membranes (Bio-Rad, Hercules, CA, US). Before blocking, blots were stained with Ponceau S [1% (v/v) acetic acid] for 5 min and scanned as loading control. Blots were then incubated with 5% non-fat milk in TBST (solution used for all incubation and washing steps) for 1 h. After blocking, blots were incubated with pepsinogen I antibody, according to the manufacturer's instructions, and were subsequently incubated with the corresponding peroxidase-conjugated IgG antibody. After washing, the signals were visualized using an ECL plus Western Blotting Detection System (Pierce ECL Western Blotting Substrate; Thermo Fisher Scientific, Pierce, Rockford, IL). The blots shown are representative of three experiments. The image processing was performed using the NIH Image Sofware ImageJ 1.49. Cell lysates were treated as described above in immunoblot analysis in cells.

DATA ANALYSIS

Data analysis. All of the data are reported as the mean±SEM. A Shapiro-Wilk normality test was performed for each data set. T-tests were carried out for comparisons between two samples. Unpaired t-test was used to assess the statistical significance of one-way or two-way analysis when the test statistic followed a normal distribution. Mann-Whitney test was employed to assess the statistical significance of one-way or two-way analysis when the test statistic did not follow a normal distribution. For multiple comparisons, a statistical ANOVA analysis was performed using an analysis of variance with the Bonferroni post hoc test. Values of $P<0.05$ were considered to be statistically significant and are marked with an asterisk (*) or a dagger (#). Asterisk

[223] Hersey SJ, Tang L, Pohl J, *et al*. Pepsinogen secretion in vitro. Methods Enzymol. 1990;192:124-39.

[224] Méchin V, Damerval C, Zivy M. Total Protein Extraction with TCA-Acetone. Methods Mol Biol. 2007;355:1-8.

(**, ***) denotes P<0.01 and P<0.001, respectively. The strength of the relationship between the different parameters for GPR39 expression quantization was estimated by a Pearson correlation coefficient after a Shapiro-Wilk normallity test.

Scoring systems of gastric adenocarcinomas. For assessment of the patterns of expression of GPR39 in gastric adenocarcinomas, staining intensity was scored as 0 (absent), 1 (weak), 2 (moderate), or 3 (strong) by three independent observers. For assessment of cell proliferation in tumour tissue, percentage of Ki67 positivity was obtained by ACIS® Assisted Quantitative Image Analysis (Dako Agilent Technologies, Glostrup, DK).

USC
UNIVERSIDADE
DE SANTIAGO
DE COMPOSTELA

RESULTS

USC
UNIVERSIDADE
DE SANTIAGO
DE COMPOSTELA

CHAPTER 1: THE NMR STRUCTURE OF HUMAN OBESTATIN IN MEMBRANE-LIKE ENVIRONMENTS. STRUCTURE-BIOACTIVITY RELATIONSHIP OF OBESTATIN

The quest for therapeutic applications of obestatin involves, as a first step, the determination of its 3D solution structure and the relationship between this structure and the biological activity of obestatin. On this basis, we have employed a combination of circular dichroism, nuclear magnetic resonance spectroscopy, and modelling techniques to determine the solution structure of human obestatin (**1**). Other analogues, including human non-amidated obestatin (**2**), the fragment peptides (6-23)-obestatin (**3**), (11-23)-obestatin (**4**), and (16-23)-obestatin (**5**); and mouse obestatin (**6**) have also been scrutinized. These studies have been performed in a micellar environment to mimic the cell membrane (SDS micelles). Furthermore, structural-activity relationship studies have been performed by assessing the *in vitro* proliferative capabilities of these peptides in the human retinal pigmented epithelial cell line ARPE-19 (ERK1/2 and Akt phosphorylation, Ki67 expression, and cellular proliferation).[225]

CIRCULAR DICHROISM

Circular dichroism is a suitable and rapid approach to provide information about the secondary structural features of peptides such as obestatin in solution.[216] First, the influence of SDS micelles on the secondary structure of the different peptides was studied. A preliminary scanning of the conformational preferences of the peptides was performed in 25 mM PBS and in an SDS micelle solution. SDS was adopted based on the works of Schwyzer, who hypothesized that previous contact with the membrane is essential for the peptide to adopt the proper conformation to further interact with its receptor.[226]

As shown in **Figure S1.1**, the CD spectra of the peptides (40 μM) suggested that random coil conformations were prevalent in PBS, whereas the spectra recorded in the micelle solution indicated the presence of a certain amount of α-helical structure (**Figure S1.2**). Both human (**1**) and mouse obestatin (**6**) exhibited similar tendencies (**Figure S1.3**).

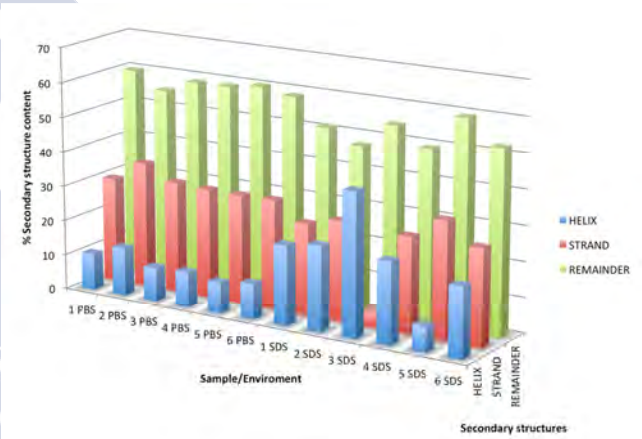

Figure 1.1. Secondary structure analyses performed using the DICHROWEB web server with the CONTINLL algorithm and reference data set 4. The relative amounts of α-helix and β-sheet were determined by adding together the contributions from helix 1 plus helix 2 and strand 1 plus strand 2, respectively, whereas the amounts of β-turn and random structure were read directly from the output. The peptides clearly showed greater helicity in SDS than in PBS.

[225] Alén BO, Nieto L, Gurriarán-Rodríguez U, *et al*. The NMR structure of human obestatin in membrane-like environments: insights into the structure-bioactivity relationship of obestatin. PLoS One. 2012;7:e45434.

[226] Schwyzer R. In search of the "bio-active conformation" – is it induced by the target cell membrane? J Mol Recognit. 1995;8:3-8.

The secondary structure analyses were performed using the DICHROWEB web server,[214,215] with the following algorithms: CONTINLL, which incorporated 2 different reference data sets, and K2d.[215] The conformational weights of the secondary structures obtained with CONTINLL were paired with 2 different data sets for the data ranging between 190 and 240 nm. Although an important caveat of this method is that the reference data sets are primarily appropriated for aqueous environments, it is nonetheless evident that the peptides in SDS have the greatest helicity (**Table S1.1**). An example of the obtained results is represented in **Figure 1.1**.

STRUCTURE DETERMINATION USING NMR

The NMR spectra of the peptides were collected in the presence of the SDS micelles. Peptides **1-6** provided well-dispersed 2D spectra. A small number of cross-peaks were observed for peptides **2** and **3**. **Figures S1.4** and **S1.5** exemplify the quality of the spectra, of which the amide region of the 2D NOESY spectra of human obestatin (**1**) and its truncated analogue (**4**) are shown. The assignment process was straightforward because most of the proton resonances of these peptides at 298 K and pH 6.5 were well resolved and narrow. The chemical shift assignment and collection of the NOE data were performed following standard procedures.[208] The proton chemical shifts of the peptides in SDS micelles are summarized in the Supplementary Material (**Tables S1.2** to **S1.7**). The experimental NMR data were used to generate 3D models of peptides **1-6**. The 3D structures were calculated using the CYANA software based on the inter-proton distance restraints (sequential and medium-range NOE-derived restraints). The best 20 structures, out of 50 calculated, were chosen according to the lowest values of the penalty (f) for the target function. A subsequent energy refinement was performed in explicit solvent using the AMBER program. The corresponding results, including the further analysis of the resulting structures performed using MOLMOL and PROCHECK-NMR, are shown below.

Backbone HN amide and H-alpha ^{1}H chemical shifts

First, the variation of the backbone amide HN and Hα chemical shift values was monitored for significant changes that might have structural relevance. These chemical shifts in peptides **1-6** were, on average, shifted up field in relation to the typical values observed for random coils, as might be expected for helical structures (**Figure 1.2**).

Human obestatin (**1**)	FNAPFDVGIKLSGV**QYQQ**H**SQA**L-NH_2
Human NA-obestatin (**2**)	FNAPFDVGIKLSGVQ**YQQ**HSQAL
Human (6-23)-obestatin (**3**)	DVGIKLSGV**QYQQHSQA**L-NH_2
Human (11-23)-obestatin (**4**)	LSG**VQYQQ**H**SQA**L-NH_2
Human (16-23)-obestatin (**5**)	**YQQ**H**SQA**L-NH_2
Mouse obestatin (**6**)	FNAPFDVGIKLSG**AQYQQ**H**GRA**L-NH_2

Table 1.1. The underlined residues were predicted to have secondary helical structure based on the HN and Hα chemical shifts indices that were determined using the RCI server (http://wishart.biology.ualberta.ca/rci). The residues within helical structures that extended over more than two residues are represented in bold; these residues are located primarily at the C-terminus

Furthermore, the chemical shift analysis performed using the RCI server[227] predicted helical conformations for the residues located mainly at the C-termini of the peptides (**Table 1.1**).

[227] Berjanskii VM, Wishart DS. A simple method to predict protein flexibility using secondary chemical shifts. J Am Chem Soc. 2005;127:14970-1.

Figure 1.2 shows the chemical shift indices (CSI) for the NH and Hα protons of the residues at the C-termini of some of these peptides. The CSIs for the NH and Hα protons of human obestatin (**1**) between residues Tyr16 and Leu23 are generally (with a few exceptions) negative and much stronger than those of the non-amidated obestatin (**2**), indicating that the latter has a smaller percentage of helical structure at the C-terminus. The CSIs for the HN and Hα protons of human (6-23)-obestatin (**3**) generally indicate a higher percentage of helical structure relative to (**1**), suggesting that the lack of the first 5 amino acids does not have an important conformational impact on the structure.

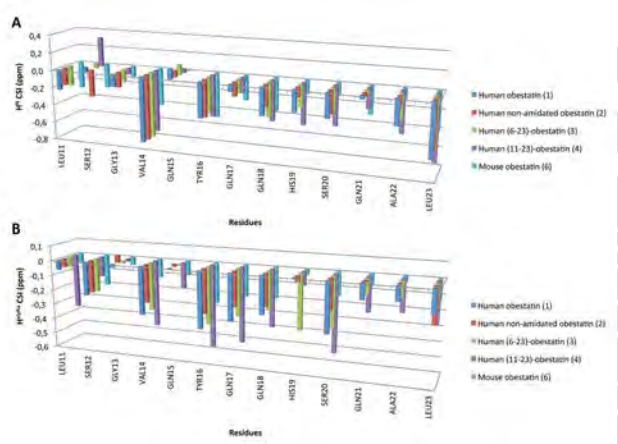

Figure 1.2. Plot of the CSIs for residues at the C-termini of the studied peptides. (A) CSIs of the backbone amide protons (HN) and (B) CSIs of the alpha protons (Hα). The peptide sequence (**6**) is aligned with that of the other peptides. The CSI is defined as $\delta^{obs} - \delta^{random\text{-}coil}$.

The truncated peptide **4**, which lacks the first 10 residues, has the strongest negative CSIs for both HN and Hα protons, thus providing further support for the formation of an α-helix at the C-terminus of this peptide. In the case of mouse obestatin (**6**), the negative CSIs for HN and Hα are indicative of an α-helix, although the comparison with the human obestatin (**1**) shows considerable variations along the sequence without a clear trend.

NOE pattern

Figure 1.3 contains a summary of all (short, medium and long range) connectivities deduced from an analysis of the NOESY spectra of the peptides. It has been previously reported that poorly ordered structures of obestatin were observed in water solutions. These peptides generally exhibited bend structures in the central Lys10-Ala14 fragment.[30,40] For peptides **1-6** in buffered SDS micelles, the backbone and side-chain proton NMR resonances could be completely assigned in a sequential manner with the aid of the TOCSY and NOESY spectra. A significant population of conformations containing an "ordered" α-helix is present, with characteristic short-range dNN(i, i+1) and medium-range dαN(i, i+3) and dαβ(i, i+3) NOE connectivities.[208] Fairly strong dNN(i, i+1) and dαN(i, i+1) NOEs were observed for most of the residues, although some gaps resulted from resonance overlap.

The data that were obtained clearly suggest the presence of a significant population of ordered α-helical structures for these peptides in SDS micelle solutions. In fact, for human obestatin (**1**), clear medium- and long-range connectivities were observed including 1) medium-range Hαi/HNi+3 (Gly8/Leu11, Lys10/Gly13, Leu11/Val14) and Hαi/Hβi+3 (Val7/Lys10, Gly8/Leu11, Gly13/Tyr16, Ser20/Leu23) connectivities and 2) a long-range Hαi/HNi+4 (Lys10/Val14) connectivity. For the non-amidated peptide **2**, fewer medium-range connectivities were observed relative to the amidated peptide **1**, including 1) medium-range Hαi/HNi+3 (Leu11/Val14, Gly13/Tyr16) connectivities but no Hαi/Hβi+3 connectivities and 2) a long-range Hαi/HNi+4 (Lys10/Val14) connectivity.

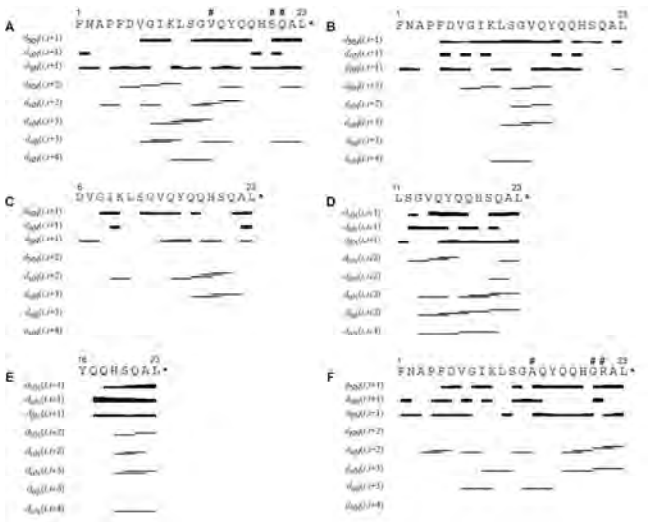

Figure 1.3. **Summary of sequential and medium-range NOE connectivities involving the HN, Hα and Hβ protons of the peptides in SDS micelles, as derived from CYANA calculation.** The thickness of the bar indicates the intensities of the NOEs for the following peptides: (A) human obestatin (**1**), (B) human non-amidated obestatin (**2**), (C) human (6-23)-obestatin (**3**), (D) human (11-23)-obestatin (**4**), (E) human (16-23)-obestatin (**5**) and (F) mouse obestatin (**6**). The asterisk (*) represents the C-terminal amidation of the molecule. The dagger (#) represents the differences between human obestatin (**1**) and mouse obestatin (**6**).

For the truncated human (6-23)-obestatin (**3**), fewer medium-range connectivities were observed: 1) medium-range Hαi/HNi+3 (Gln17/Ser20, His19/Ala22) connectivities but no Hαi/Hβi+3 connectivities were observed, and 2) no long-range Hαi/HNi+4 connectivities were observed. The presence of medium-range connectivities (Hαi/HNi+3, Hαi/Hβi+3) and long-range connectivities (Hαi/HNi+4) from Gly13 to Leu23 confirmed the presence of a fairly well defined α-helical structure at the C-terminus of human (11-23)-obestatin (**4**): 1) medium-range Hαi/HNi+3 (Gly13/Tyr16, Gln17/Ser20, Gln18/Gln21, Ser20/Leu23) and Hαi/Hβi+3 (Gly13/Tyr16, Gln15/Gln18, Gln17/Ser20, Ser20/Leu23) connectivities were observed, and 2) long-range Hαi/HNi+4 (Gly13/Gln17, Glu17/Gln21) connectivities were observed. The observed structure of the human (16-23)-obestatin (**5**) is not as well defined as that of **4**. Only residues His19/Leu23 are involved in α-helix formation: 1) medium-range Hαi/HNi+3 (His19/Ala22, Ser20/Leu23) connectivities and no Hαi/Hβi+3 connectivities were observed; 2) a long-range Hαi/HNi+4 (His19/Leu23) connectivity was also observed. A fairly similar pattern of NOEs, especially at the C-terminal region of the peptide, was found in the SDS micelles compared with the structure previously reported in DPC/SDS micelles[40] for mouse obestatin (**6**): 1) medium-range Hαi/HNi+3 (Ile9, Ser12, Gln17/**Gly20**, **Gly20**/Leu23; Hαi/Hβi+3 Val7/Lys10, Gly13/Tyr16) connectivities were observed; 2) no long-range Hαi/HNi+4 connectivities, however, were observed (bold residues are different from those of **1**).

3D structures

The best 20 structures, which possessed the lowest total energies, were considered as representatives of human obestatin (**1**) and its analogues. None of these structures had NOE violations greater than 0.2 Å or dihedral angle violations greater than 2°. A summary of the structural characteristics of the different peptide ensembles is given in **Table 1.2**.

The PROCHECK analysis of the 20 structures showed that almost all of the residues are in the most favored and 'additionally allowed' regions of the Ramachandran plot. For instance, for **1**, less than 3% of the residues were found outside the sterically allowed region of the Ramachandran plot. This fact is mostly due to Ala3, which is situated in the less-defined region of the structure (**Table 1.3**). A view of the structures obtained for **1**-**6** superimposed along their backbones is shown in **Figure 1.4**. These representations show that these peptides primarily

adopt an α-helical conformation at the C-terminus (**Table 1.3**). The analysis of the bundle of 20 structures obtained for human obestatin (**1**) demonstrated that in most of the structures, residues Gly8-Leu11 were involved in an α-helix, whereas residues Val14-Gln17 were involved in a 3_{10} helix. In a few structures, residues Ser20-Leu23 were further involved in an α-helix. This helical pattern induced under our SDS micelles conditions appears to be fairly similar to that previously reported in 33% TFE-water for the same peptide.[30]

	1	**2**	**3**	**4**	**5**	**6**
Experimental restraints [a]						
Sequential distances	267	145	145	184	123	284
Medium-range distances (i-j) < 5	99	28	31	63	38	68
Long-range distances (i-j) ≥ 5	2	0	0	0	2	7
Total	368	173	176	247	163	359
Final CYANA target function value (Å^2) [b]	0.18	0.22	0.02	0.11	0.27	0.04
RMS deviations from ideal geometry [c]						
Bond lengths (Å)	0.005	0.005	0.004	0.004	0.004	0.005
Bond angles (º)	0.7	0.7	0.6	0.5	0.5	0.6
RMSD to mean coordinates (Å) [d]	(14-20)	(14-20)	(14-20)	(14-20)	(16-23)	(14-20)
Backbone N, C^{α}, C'	0.42±0.21	1.49±0.56	0.55±0.23	0.09±0.04	0.49±0.24	0.46±0.39
All heavy atoms	1.19±0.38	2.69±0.78	1.24±0.27	0.49±0.22	1.50±0.40	0.93±0.52
Ramachandran plot statistics [c]						
Most favorable regions (%)	71.4	72.3	69.6	70.5	60.0	77.4
Additional allowed regions (%)	26.4	27.2	30.4	29.5	38.7	22.6
Generously allowed regions (%)	0.0	0.1	0.0	0.0	1.3	0.0
Disallowed regions (%)	2.2	0.3	0.0	0.0	0.0	0.0

Table 1.2. Structural statistics for the ensemble of the best 20 structures of human obestatin (1), its fragments and mouse obestatin (6). The final CYANA target function value was computed for the structures calculated using CYANA. [b] Average values of the 20 final energy-minimized CYANA conformers. [c] Calculated using PROCHECK-NMR. [d] Atomic differences are given as the average RMS difference of the mean coordinate structure (mean). Peptides: human obestatin (**1**), human non-amidated obestatin (**2**), human (6-23)-obestatin (**3**), human (11-23)-obestatin (**4**), human (16-23)-obestatin (**5**) and mouse obestatin (**6**).

Human obestatin (**1**)	FNAPFDVGIKLSGVQYQQHSQAL-NH_2
Human NA-obestatin (**2**)	FNAPFDVGIKLSGVQYQQHSQAL
Human (6-23)-obestatin (**3**)	DVGIKLSGVQYQQHSQAL-NH_2
Human (11-23)-obestatin (**4**)	LSGVQYQQHSQAL-NH_2
Human (16-23)-obestatin (**5**)	YQQHSQAL-NH_2
Mouse obestatin (**6**)	FNAPFDVGIKLSGAQYQQHGRAL-NH_2

Table 1.3. The underlined residues were predicted to have secondary helical structure based on the H^N and H^{alpha} chemical shifts indices obtained using the RCI server (http://wishart.biology.ualberta.ca/rci). The residues within helical structures that extended over more than two residues are represented in bold; these residues are located primarily at the C-terminus. The secondary helical structure obtained in our structures, as calculated by CYANA, included α-helix formation (green labels) and 3_{10}-helix formation (blue labels).

Mean atomic RMSD values for the backbone atoms (5-15) of 0.52±0.25 Å and for the heavy atoms (5-15) of 1.09±0.32 Å were calculated for the best 20 conformers of **1**, and these values are fairly similar to those reported by Subasinghage under those experimental conditions.[30] For the human non-amidated obestatin (**2**), the formation of a 3_{10} helix between residues Gly8-Ser12 and Val14-Gln17 was observed. Regarding peptide **3**, a 3_{10} helix between residues Gly8-Ser12, Val14-Gln17 and His19-Gln21 was found. For the human (11-23)-obestatin (**4**), the α-helix structure extended from Tyr16 to Leu23. The small peptide **5** displays a short α-helix from Ser20 to Leu23. Finally, our data suggest that the mouse obestatin (**6**) contained a 3_{10} helix between residues Gly8-Ser12 and Ala14-Gln17 and an α-helix between His19-Ala22. The calculated 3D structures also corroborate some details that were previously obtained from the qualitative ^{1}H chemical shift analysis described above. As can be observed from these data, the amide moiety in **1** appears to be important for stabilizing the α-helix conformation between residues Ser20 and Leu23, and this moiety is absent in the non-amidated peptide (**Figures 1.4.A** and **1.4.B**).

PROLIFERATION

GPR39 siRNA depletion

GPR39 simultaneously signals via two parallel pathways, using either heterotrimeric G proteins or multifunctional adapters such as β-arrestin 1. Although recent work has identified this receptor as a target for obestatin action,[70,71] no data are available for the proposed cell model of ARPE-19 cells, a human retinal pigment epithelial cell line.

Therefore, the endogenous expression of GPR39 was first analyzed using immunocytochemistry (**Figure 1.5.A)**. Next, the effect of acute GPR39 deficiency was determined using siRNA. Under these conditions, the constructs exhibited a decrease in GPR39 expression by 55±1% (Figure 5B). In the presence of a non-targeting control siRNA, the phosphorylation of human obestatin-activated Akt(S473) and ERK1/2(T202/Y204) were similar to that observed without any transfection. The silencing of GPR39 subsequently decreased the levels of pAkt(S473) and pERK1/2(T202/Y204) with respect to the siRNA control (to 94±3% and 60±5%, respectively) following treatment with human obestatin (**1**, 100 nM) for 10 min (**Figure 1.5.B**).

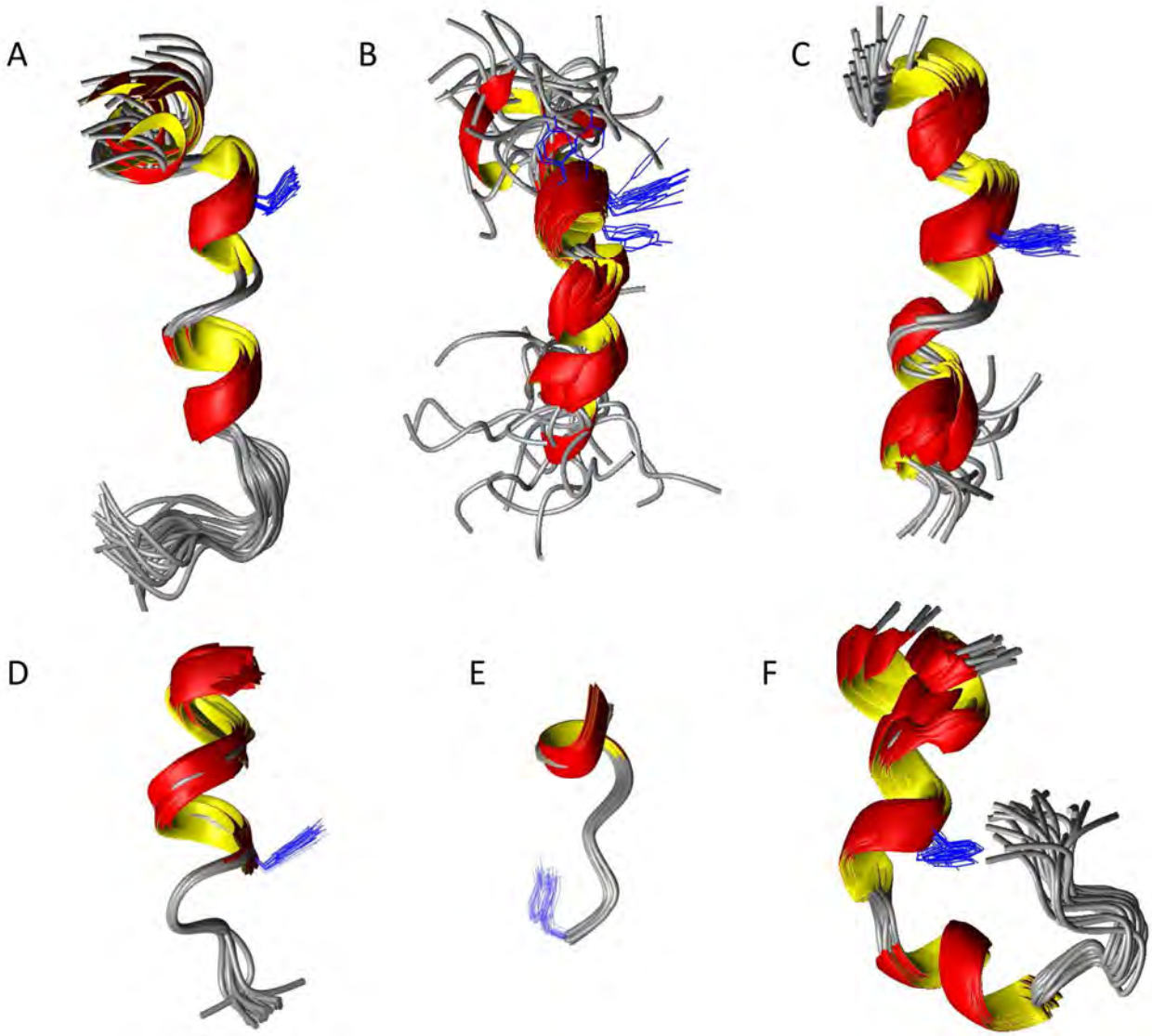

Figure 1.4. Superimposition of the 20 best representative structures of peptides 1 to 6, as calculated from the NMR data for the peptides in SDS micelles. (A) Human obestatin (**1**), (B) human non-amidated obestatin (**2**), (C) human (6-23)-obestatin (**3**), (D) human (11-23)-obestatin (**4**), (E) human (16-23)-obestatin (**5**) and (F) mouse obestatin (**6**). The Tyr16 side chain is shown in blue.

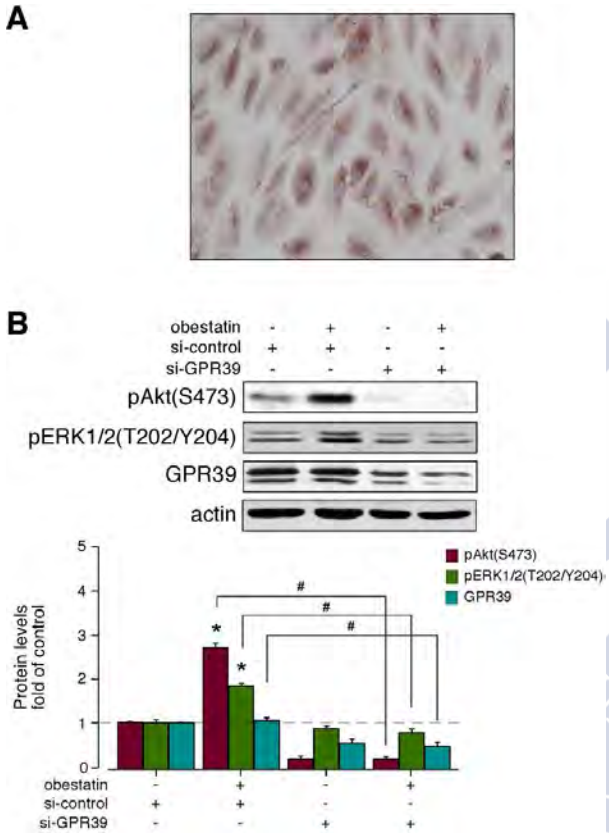

Figure 1.5. A. Immunocytochemical detection of GPR39 in ARPE-19 cells. Objective magnification x20. **B. The effect of siRNA depletion of GPR39 on pAkt(S473) and pERK1/2(T202/Y204) in ARPE-19 cells after human obestatin treatment** (**1**, 100 nM, 10 min). The ARPE-19 cells were transfected with GPR39 siRNA prior to obestatin **1** treatment. Equal amounts of protein in each sample were used to assess the expression of GPR39 by western blotting. The GPR39 level was expressed as the fold change relative to the control siRNA-transfected cells (mean±SEM). The protein expression was normalized relative to actin. The data are expressed as the mean±SEM. The asterisk (*) denotes $P<0.05$ when comparing the treated control siRNA group with the control siRNA group; the dagger (#) denotes $P<0.05$ when comparing the GPR39 siRNA group with the control siRNA group.

ERK1/2 and Akt activation

We examined the proliferative capabilities of the peptides by investigating ERK1/2 and Akt activation [pERK1/2(T202/Y204) and pAkt(S473)]. The curves obtained after the treatment of ARPE-19 cells with the peptides (100, 200 and 500 nM) exhibited a dose-dependent pattern with a maximum at 200 nM (data not shown). This maximum is the concentration reflected in **Figure 1.6**. The pattern of ERK1/2 phosphorylation (**Figure 1.6.A**) reached maximal levels within 10 min of human obestatin stimulation (**1**, 200 nM) and decreased to basal levels after 60 min. Conversely, the pAkt(S473) maximal levels were reached after 10 min of stimulation with human obestatin (**1**, 200 nM), and the activation was maintained for at least 60 min (**Figure 1.6.B**). In contrast, the human non-amidated obestatin (**2**) did not influence pAkt(S473), and exhibit even a slight inhibitory effect on pERK1/2(T202/Y204). From these data, it can be deduced that amidation is a prerequisite for maintaining the bioactivity of obestatin. Obestatins **3** and **5** had no effect on either pAkt(S473) or pERK1/2(T202/Y204). Intriguingly, the obestatin analogue **4** induced selective coupling to the Akt signalling pathway and exhibited no effect on the ERK1/2 route over the time course of the assay.

This particular ligand is processed from full length obestatin and is present in the stomach.[1] In this sense, this peptide appears to selectively enhance a restricted subset of active GPR39 conformations that are capable of promoting specific aspects of the signalling pathway within the GPR39-induced network, particularly β-arrestin-mediated signalling mechanisms. This result suggests that this molecule may act as a potential β-arrestin-biased agonist.[228]

[228] Whalen EJ, Rajagopal S, Lefkowitz RJ. Therapeutic potential of β-arrestin- and G-protein-biased agonists. Trends Mol Med. 2011;17:126-39.

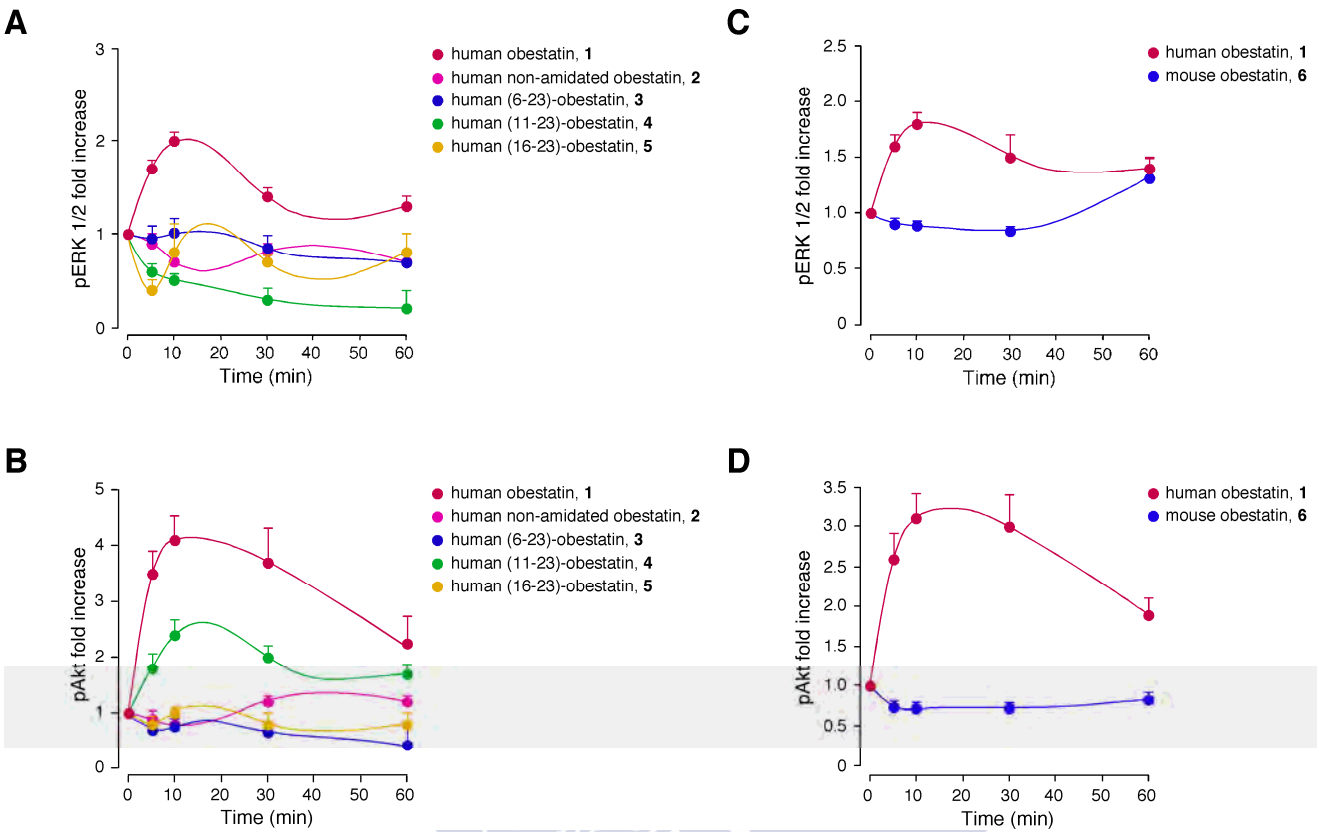

Figure 1.6. Time-course of the effect of the different peptides on ERK1/2 [pERK 1/2 (T202/Y204)] and Akt [pAkt HM (S473)] phosphorylation in ARPE-19 cells. The serum-starved cells were treated with the peptides (200 nM) at 37 °C for the indicated times. The cells were lysed and analyzed using SDS-PAGE with specific antibodies. ERK1/2 and Akt phosphorylation were quantified using densitometry and expressed as the fold change relative to the phosphorylation obtained for unstimulated cells (mean±SEM of five independent experiments).

To date, biased ligands have been identified for different G protein-coupled receptors, denoting a new class of pharmacological ligands capable of selective modulation.[229] Regarding the species-specific role of obestatin, the effect of human (**1**) and mouse (**6**) obestatin on pERK1/2(T202/Y204) and pAkt(S473) was compared under the same experimental conditions described previously. Mouse obestatin (**6**) treatment did not induce any significant change in either pERK1/2(T202/Y204) or pAkt(S473) during the tested period (**Figure 1.6.C** and **D**). This result demonstrates that, in this system, the changes in primary (Val14Ala, Ser20Gly and Gln21Arg) and secondary structure between species are critical for the activity. Thus, a species-specific behaviour occurs.

[229] Reiter E, Ahn S, Shukla AK, *et al.* Molecular mechanism of β-arrestin-biased agonism at seven-transmembrane receptors. Annu Rev Pharmacol Toxicol. 2012;52:179-97.

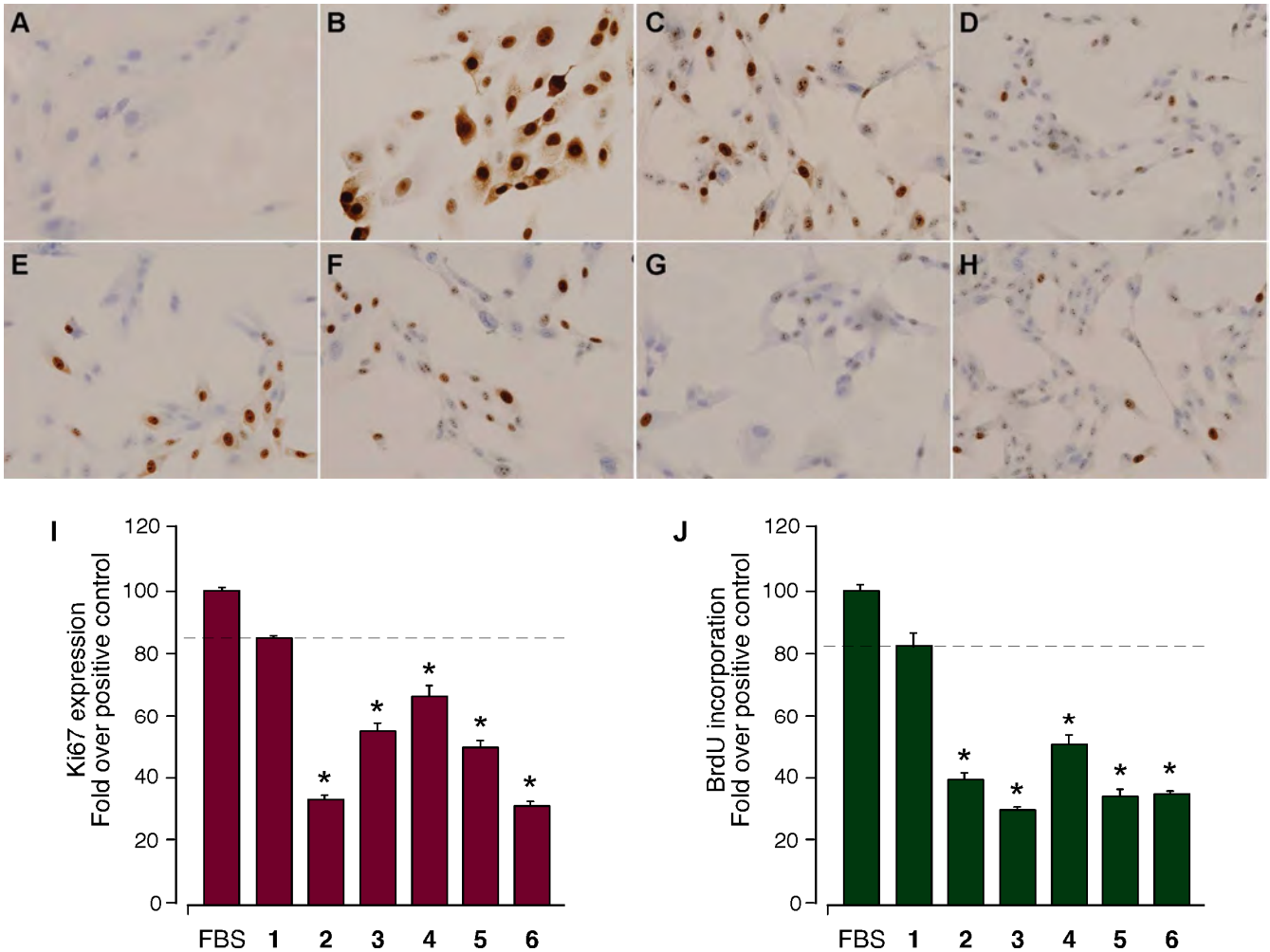

Figure 1.7. Immunocytochemical analysis of the Ki67 expression in ARPE-19 cells after 24 h of proliferation. A) Control. B) 10% FBS (v/v). C) 100 nM human obestatin (**1**). D) 100 nM human non-amidated obestatin (**2**). E) 100 nM human (6-23)-obestatin (**3**). F) 100 nM human (11-23)-obestatin (**4**). G) 100 nM human (16-23)-obestatin (**5**). H) 100 nM mouse obestatin (**6**). The magnification was 20x. I) Quantification of the immunocytochemical expression of Ki67 in ARPE-19 cells after treatment with 10% FBS (v/v; 100±2), 100 nM human obestatin (**1**; 84±1%), 100 nM human non-amidated obestatin (**2**; 33±2%), 100 nM human (6-23)-obestatin (**3**; 56±3%), 100 nM human (11-23)-obestatin (**4**; 67±3%), 100 nM human (16-23)-obestatin (**5**; 50±2%) and 100 nM mouse obestatin (**6**; 32±2%). The expression of Ki67 was expressed as the fold change relative to the expression level in FBS-treated cells in the positive control (mean±SEM). J) BrdU incorporation in ARPE-19 cells after treatment with 10% FBS (v/v; 100±1), 100 nM human obestatin (**1**; 84±4%), 100 nM human non-amidated obestatin (**2**; 39±2%), 100 nM human (6-23)-obestatin (**3**; 30±1%), 100 nM human (11-23)-obestatin (**4**; 52±3%), 100 nM human (16-23)-obestatin (**5**; 34±3%) and 100 nM mouse obestatin (**6**; 35±1%). The BrdU incorporation was expressed as the fold change relative to the level in FBS-treated cells in the positive control (mean±SEM). The data are expressed as the mean±SEM. The asterisk (*) denotes $P<0.05$ when comparing the peptide-treated ARPE-19 cells groups with the human obestatin (**1**)-treated group.

Ki67 expression and proliferation

The activation of the ERK1/2 and Akt signalling network results in the activation of a series of transcription factors that induce alterations in the expression of a variety of genes involved in the stimulation of cell proliferation. Among these factors, Ki67 is a labile non-histone nuclear protein that is intimately involved in the cell cycle.[230] The expression of Ki67 exhibits a good relationship with the growing fraction in several system models, and this factor is not expressed during the repair processes of DNA.[231] Thus, Ki67 is considered to be a marker of cell proliferation.

Consequently, the mitogenic effect of the peptides was tested by analyzing the expression of Ki67 in ARPE-19 cells using an immunocytochemical analysis. The experiments were performed at 24 h post-stimulation with the different peptides (100 nM). **Figure 1.7** shows a representative experiment of the six independent assays. Human obestatin (**1**) exhibited a clear increase in immunostaining for Ki67 (**Figure 1.7.C**), which was comparable to the positive control [10% FBS (v/v)]; **Figure 1.7.B**). The negative control (without stimuli) is shown in **Figure 1.7.A**. In accordance with the results from the immunoblots, the expression of Ki67 was marginally detected for non-amidated obestatin (**2**) and mouse obestatin (**6**) (**Figure 1.7.D**). Alternatively, human (6-23)-obestatin (**3**) and human (16-23)-obestatin (**5**) exhibited weak Ki67 expression (**Figures 1.7.E** to **1.7.G**, respectively), and the expression was higher for human (11-23)-obestatin (**4**) (**Figure 1.7.F**). These results resemble the proliferative capabilities of human obestatin (**1**; 84±4%) and the different peptides measured in terms of BrdU incorporation, in which only peptide **4** (52±3%) exhibited a slight effect (**Figure 1.7.J**).

[230] Yerushalmi R, Woods R, Ravdin PM, *et al*. Ki67 in breast cancer: prognostic and predictive potential. Lancet Oncol. 2010;11:174-83.

[231] Gerdes J, Schwab U, Lemke H, *et al*. Production of a mouse monoclonal antibody reactive with a human nuclear antigen associated with cell proliferation. Int J Cancer. 1983;31:13-20.

USC
UNIVERSIDADE
DE SANTIAGO
DE COMPOSTELA

CHAPTER 2: NMR INTERACTION BETWEEN OBESTATIN AND GPR39 RECEPTOR USING LIVING CELLS

Since the discovery of obestatin, there have been several studies aimed at determining which are the minimal structural requirements that permit to detect obestatin receptor biological activity.[225] At the present moment, no data are available regarding the bioactive conformation of obestatin and its mode of interaction of GPR39 at the key-binding site. In any case, the proper structure-activity relationship study should be based on the knowledge of the bioactive conformation of obestatin when bound to the receptor. NMR techniques are suitable to this end when working with isolated protein receptors or receptor-rich living cells. Provided that the system holds the right kinetic features, these experiments, with living cells, could avoid the requirement for isolating the protein receptor. On this basis, the approach presented herein aims at the determination of the bioactive conformation of obestatin when interacting with its receptor, GPR39, in quasy-physiological conditions. Thus, the NMR analysis of the interaction of human obestatin (**1**) and several fragment peptides with the obestatin receptor (GPR39) was performed in the HEK293 cell line bearing the GPR39 receptor.

CSP EFFECTS AND NOE PATTERN IN OBESTATIN TRUNCATES

The NMR spectra of the human obestatin peptides, (6-23)-obestatin (**3**), (11-23)-obestatin (**4**), (16-23)-obestatin (**5**), and the fragment peptide (1-10)-obestatin (**7**) were collected in the presence of H_2O, PBS, and HEK293 cells, both wild type (WT) and transiently GPR39-transfected cells (GPR39). As non-amidated obestatin (**2**) and mouse obestatin (**6**) had no biological effects on proliferation or stimulation of intracellular signalling targets triggered by **1**,[225] they were excluded from the analysis. However, the fragment peptide (1-10)-obestatin (**7**) was incorporated due to the importance acquired by its counterpart **4**, as it discovered itself as a possible endogenous biased ligand for GPR39.

The NMR spectra of the peptides were collected in the presence of H_2O, PBS, WT cells and GPR39 cells. All the peptides provided well-dispersed 2D spectra. The assignment process was straightforward because most of the proton resonances of these peptides at 298 K and pH 6.5 were well resolved and narrow. The chemical shift assignment and collection of the NOE data were performed following standard procedures[208] and obtained from the analysis of the ^{1}H-2D TOCSY and NOESY/ROESY spectra of the peptides. The proton chemical shifts of all of the peptides in H_2O, PBS, WT cells, and GPR39 cells, are summarized in the Supplementary Material section (**Tables S2.1** to **S2.30**).

Exclusive chemical shift perturbation (CSP) effects occurring in the samples were identified by comparison among spectra: the two obtained for transfected and WT cells, the spectrum of the peptide in PBS, and the spectrum in H_2O. CSPs of all peptides were calculated taking into account the differences in the chemical shifts (δ) between PBS:H_2O, WT:PBS and GPR39:WT spectra. **Figures 2.1** to **2.5** show a representation of the CSPs for the different molecules analysed in this chapter. During analysis, the numbering of the residues of each peptide is initiated in the equivalent corresponding position of the full-length obestatin **1**.

The evaluation of the spectra (using the following comparisons: PBS:H_2O, WT:PBS, and GPR39:WT)

revealed the subsequent changes, which are described below. For human (16-23)-obestatin (**5**), the comparison PBS:H_2O, showed very weak negative CSPs for Gln18, Ser20, Gln21, Ala22 and Leu23 (**Table S2.5**) for the amide protons. This smooth effect for NHs contrasted with the large positive CSPs observed for the side chain protons of the peptide residues, with the exception of His19, for which no data was available. For instance, for Gln18 there are positive CSP effects of +0.23, +0.36, +0.35, and 0.32 ppm for Hα, Hβ1, Hβ2, and Hγ, respectively (**Table S2.5**). The comparison WT:PBS, showed no information for the amide protons as the WT sample lacks the data for these protons (maybe due to fast exchange of these protons with the solvent). However, CSP changes for the side chains protons are in the range of -0.01 to +0.06 ppm. When comparing the GPR39:WT samples, only effects for the side chain protons were observed, and in the same range than for the WT:PBS comparison.

Regarding human (11-23)-obestatin (**4**), similar results were obtained for the amide protons, with the drawback of losing the amide protons in the WT sample. However, the CSP effects observed for the side chain protons in the PBS:H_2O comparison were not significant (range in the order of -0.03 to 0.01 ppm, **Table S2.11**).

The analysis of the (1-10)-peptide **7** data, afforded similar results (**Table S2.17**). The CSPs observed for the PBS:H2O comparison were very intense and varying from the negative CSPs observed for the amide protons (-0.41 ppm for Asn2 or -0.34 for Lys10) to the positive CSPs observed for all of the side chain protons with values ranging from +0.1 for Hα of Asn2 to +0.45 ppm for the Hγ of Val7. The negative values observed for the amide protons might indicate a tendency to an α-helix organisation. The data for the WT:PBS provided not less surprising results. All of the amide protons presented significant positive CSP effects, but opposite to those for PBS:H_2O, ranging from +0.11 ppm observed for Asp6 or Gly8, to the value of +0.18 observed for Ala3. This feature could indicate a tendency to reorganization to a β-strand-like structure, although it could have the meaning of a loss of the α-helix pattern. Regarding to the GPR39:WT comparison, no significant CSP values were observed.

Human (6-23)-obestatin (**3**) is the longest truncate but lacking the first five residues of the obestatin moiety, which include the only Pro. The same pattern than in **7** was observed for the PBS:H_2O comparison: mostly negative and intense CSPs (-0.36 and -0.46 ppm for His19 and Ser12, respectively). In the WT:PBS comparison, all of the amide visible protons presented positive and large CSPs. It is important to highlight the values for Ser12 and His19 (Ser12: +0.63, +0.2, and +0.03 ppm for NH, Hα, and Hβ1/β2, respectively; and His19: +0.39, +0.2, +0.06, and -0.03 ppm for NH, Hα, Hβ1, and Hβ2, respectively), however, no SCE effects were observed for this system. The GPR39 sample compared to WT presented very small negative CSPs for all of the amide protons except for His19 (0.00 ppm). These changes in the CSP signs could indicate that some conformations were more stabilised depending on the surrounding environment (**Table S2.23**).

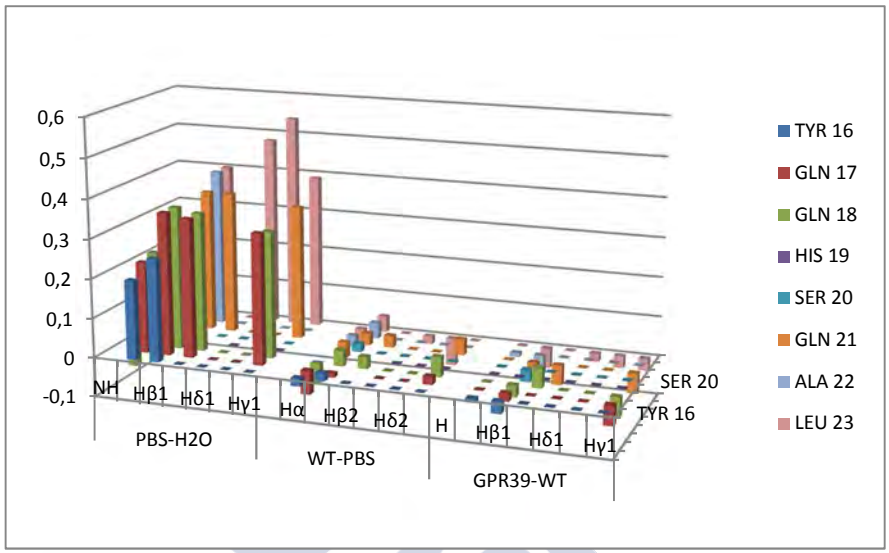

Figure 2.1. Plot of the ^{1}H CSPs for (16-23)-obestatin (5) residues between spectra. CSPs were calculated by (δ^{PBS}–δ^{H2O}), ($\delta^{HEK\text{-}WT}$–δ^{PBS}) and ($\delta^{HEK\text{-}GPR39}$–$\delta^{HEK\text{-}WT}$) for all detected protons. Only significant differences between PBS and H_2O spectra in all residues were found.

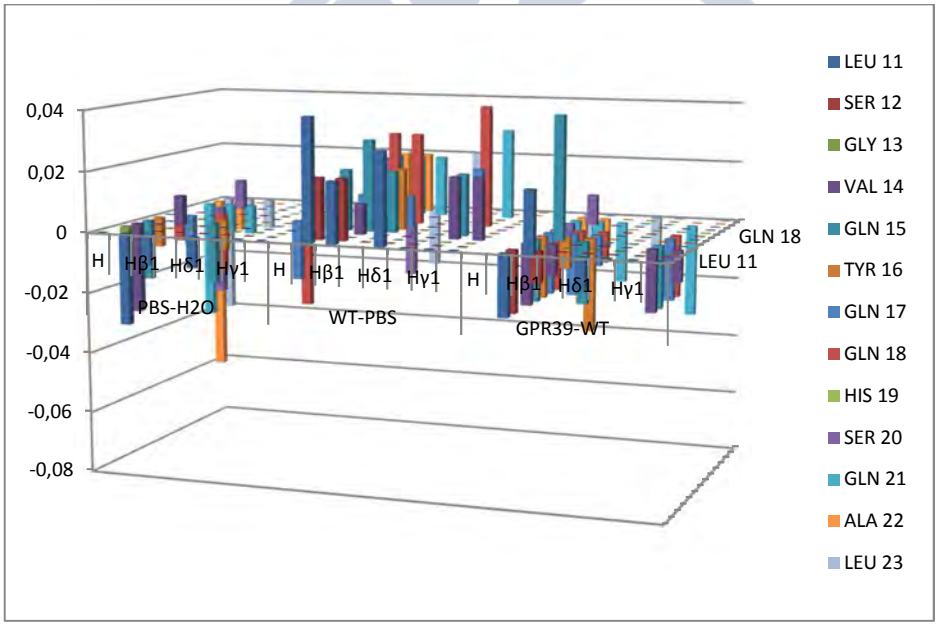

Figure 2.2. Plot of the ^{1}H CSPs for (11-23)-obestatin (4) residues between spectra. CSPs were calculated by (δ^{PBS}–δ^{H2O}), ($\delta^{HEK\text{-}WT}$–δ^{PBS}) and ($\delta^{HEK\text{-}GPR39}$–$\delta^{HEK\text{-}WT}$) for all detected protons. No significant differences between spectra were found.

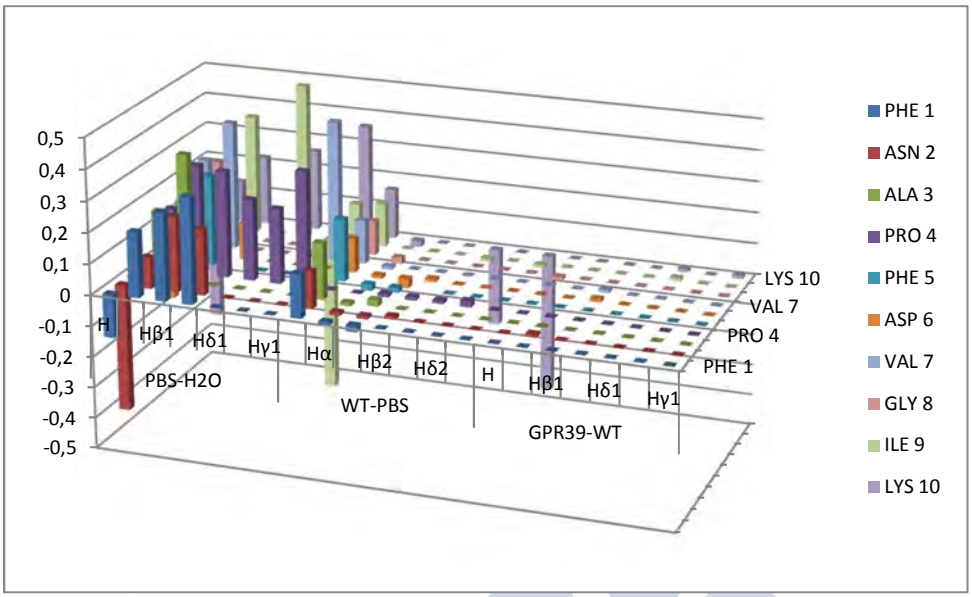

Figure 2.3. Plot of the ^{1}H CSPs for residues of (1-10)-obestatin (7) between spectra. CSPs were calculated by (δ^{PBS}–δ^{H2O}), ($\delta^{HEK\text{-}WT}$–δ^{PBS}) and ($\delta^{HEK\text{-}GPR39}$–$\delta^{HEK\text{-}WT}$) for all detected protons. Only significant differences between PBS and H2O spectra in all residues were found.

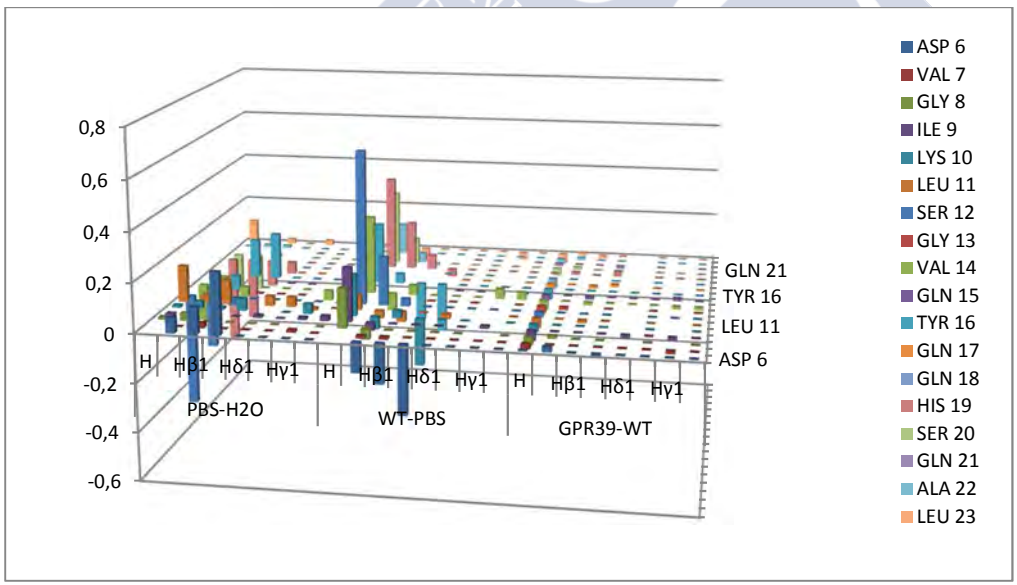

Figure 2.4. Plot of the 1H CSPs for residues of (6-23)-obestatin (2) betwee spectra. CSPs were calculated by (δ^{PBS}–δ^{H2O}), ($\delta^{HEK\text{-}WT}$–δ^{PBS}) and ($\delta^{HEK\text{-}GPR39}$–$\delta^{HEK\text{-}WT}$) for all detected protons. Only significant differences between PBS and HEK-WT spectra in amide protons were found.

Concerning peptide secondary structures, the NOESY spectra showed mainly short-range connectivities. Almost invariably, only sequential NOEs were found in all of the spectra. For human (16-23)-obestatin (**5**), (11-23)-obestatin (**4**) and (6-23)-obestatin (**3**) only fairly strong δNN(i, i+1) and δαN(i, i+1) NOEs were observed for most of the residues, although some gaps resulted from resonance overlap, which would indicate no secondary structure. In addition to the sequential NOEs, truncate **7** also showed a medium-range NOE connectivity δαN(i, i+2) between Phe1 and Ala3 in GPR39 enriched-cells, which could imply a conformational change in the presence of the receptor. However, the NOE pattern suggested a random coil conformation for all obestatin truncates samples.

In the absence of medium- and long-range connectivities, we decided to apply the analysis of the CSI. The CSI is a semi empirical protocol to determine the secondary structure of a peptide.[232] This approach compares the Hα chemical shifts of every residue within the peptide of interest with those described for the corresponding amino acid in an average of random coil structures. Although the method has its drawbacks, especially if chemical shift assignments are mis-referenced or incomplete, it accurately matches the 75-80% of the data determined by X-ray crystallography, even for small proteins. Thus, we employed the CSI protocol to verify the results suggested by the truncate NOE pattern. The CSI values for all samples in H_2O, except for the (6-23)-truncate **5** and the (1-10)-truncate **7,** showed the characteristics of unstructured peptides (**Tables S2.6**, **S2.12**, **S2.16**, and **S2.24**) in line with NOESY data. The analysis of the CSI of **5** (**Table S2.6**) and **7** (**Table S2.16**) showed an α-helix preference, with the exception of His19 and Leu23 (CSI = 0) in **5**; and Ala3, Val7 and Ile9 (CSI=0) in **7**. This helical-trend structure is consistent with the large positive CSPs effects observed for the side chain protons of the peptide residues in the PBS:H_2O comparison for both peptides.

CSP EFFECTS AND NOE PATTERN IN HUMAN OBESTATIN

Regarding full-length human obestatin (**1**), NMR data showed intriguing results. In the PBS:H_2O comparison, significant CSPs changes were found (range in the order of -0.05 to +0.05 ppm; **Table S2.29**), mainly for the amide region. In contrast, the data from the WT:PBS showed significant positive CSPs effects in all of the observed amide protons (ranging from +0.11 to +0.21 ppm) and weak differences for the side chain protons, with the exception of Gly13 (-0.10 ppm in Hα) and Pro4 (-0.18 ppm in Hβ). These positive CSPs could imply a β-strand reorganization or a loss of helical structures in WT living cells. But, the most interesting results were found between the GPR39:WT spectra (**Figures 2.6** and **2.7**; **Table S2.29**). Very strong CSPs were found for Pro4 (-0.31, -0.41 and -0.31 ppm in Hβ1, Hβ2 and Hγ, respectively) and His19 (+0.10 and +0.18 ppm in Hα and Hβ, respectively) in the presence of GPR39 cells. This difference in Pro4 between the spectra of both cell systems (WT and GPR39) could be a considerable difference for obestatin. It is important to mention that human obestatin (**1**), together with (1-10)-obestatin (***7***) are the only peptides that keep Pro4 in the structure, and the CSPs observed for Pro4 in **1** could involve an *E*/*Z* isomerization of this residue (**Figure 2.7**). However, the absence of slow conformational exchange (SCEs) effects and/or double sets of signals for obestatin in presence of the GPR39-enriched cells in the TOCSY spectrum leaves this

[232] Wishart DS, Sykes BD. Chemical shifts as a tool for structure determination. Methods Enzymol. 1994;239:363-92.

possibility without confirmation. The data obtained from NOESY spectra pointed to an obestatin random coil conformation in H_2O. Only sequential δNN(i, i+1) and δαN(i, i+1) NOEs were found. In PBS, the presence of an osmolyte such as phosphate ion could induce changes in the chemical shifts in amide proton, indicative of some type of structural reorganization,[233] but the absence of well resolved and narrow NOEs and the analysis of the CSI data (**Table S2.30**) led us to postulate that the most of the peptide was in random coil.

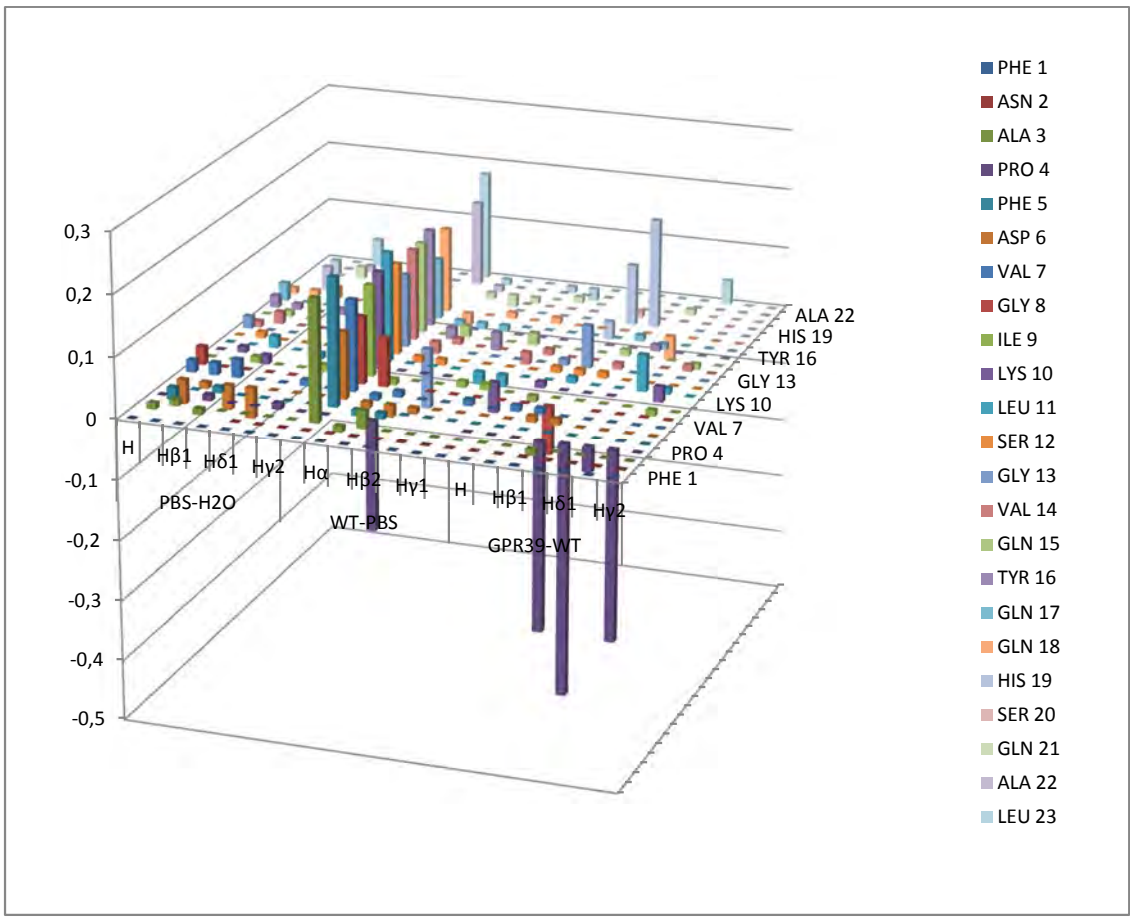

Figure 2.5. Plot of the ^{1}H CSPs for residues of human obestatin (1) between spectra. CSPs were calculated by (δ^{PBS}–δ^{H2O}), ($\delta^{HEK\text{-}WT}$–δ^{PBS}) and ($\delta^{HEK\text{-}GPR39}$–$\delta^{HEK\text{-}WT}$) for all detected protons. Only significant differences in amide protons between PBS and HEK-WT spectra were found. Furthermore, Pro4 and His19 residues showed significant CSPs in the presence of receptor, in comparison with WT cells.

[233] Celinski SA, Scholtz JM. Osmolyte effects on helix formation in peptides and the stability of coiled-coils. Protein Sci. 2002;11:2048-51.

In the presence of an SDS micellar environment that mimics the cell membrane, there is a rearrangement of the peptide that entails the formation of small areas of helix 3_{10} and alpha helix as was explained in chapter 1. In the presence of WT living cells, the ROESY spectra could not be assigned and analysis of CSI showed unstructured conformations. In addition, CSI data and NOE pattern for human obestatin (**1**) in the presence of receptor, showed strong δNN(i, i+1) and δαN(i, i+1) NOEs, and a weak medium-range δαN(i, i+2) NOE between Leu11 and Gly13, suggesting that equilibrium tended to be shifted to a random coil conformations as well as happened with obestatin truncates.

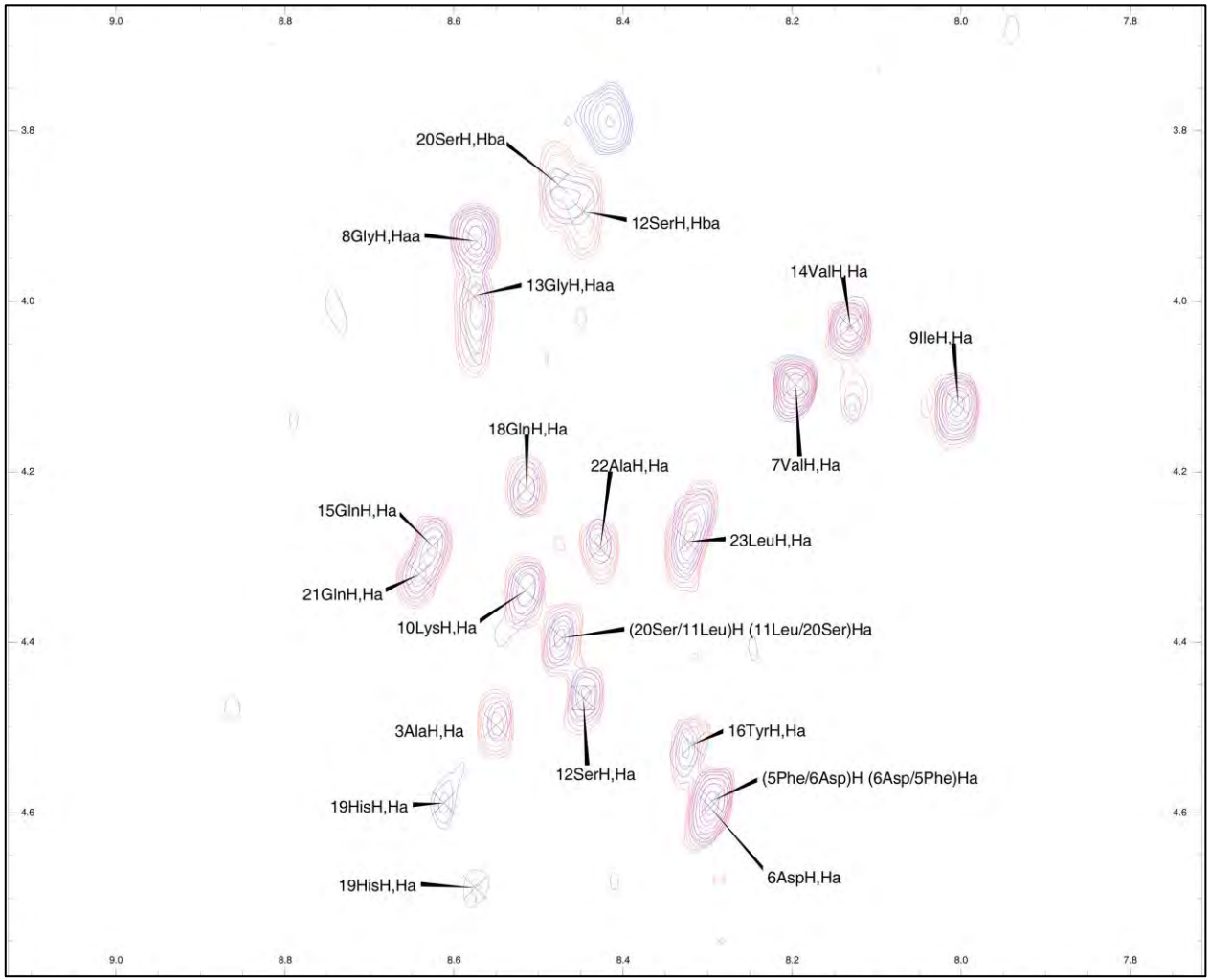

Figure 2.6. Superposition of amide region of 2D TOCSY spectra for human obestatin in HEK-WT (blue) and HEK-GPR39 (red) cells. His19 showed a strong CSP in the presence of living receptor-enriched cells.

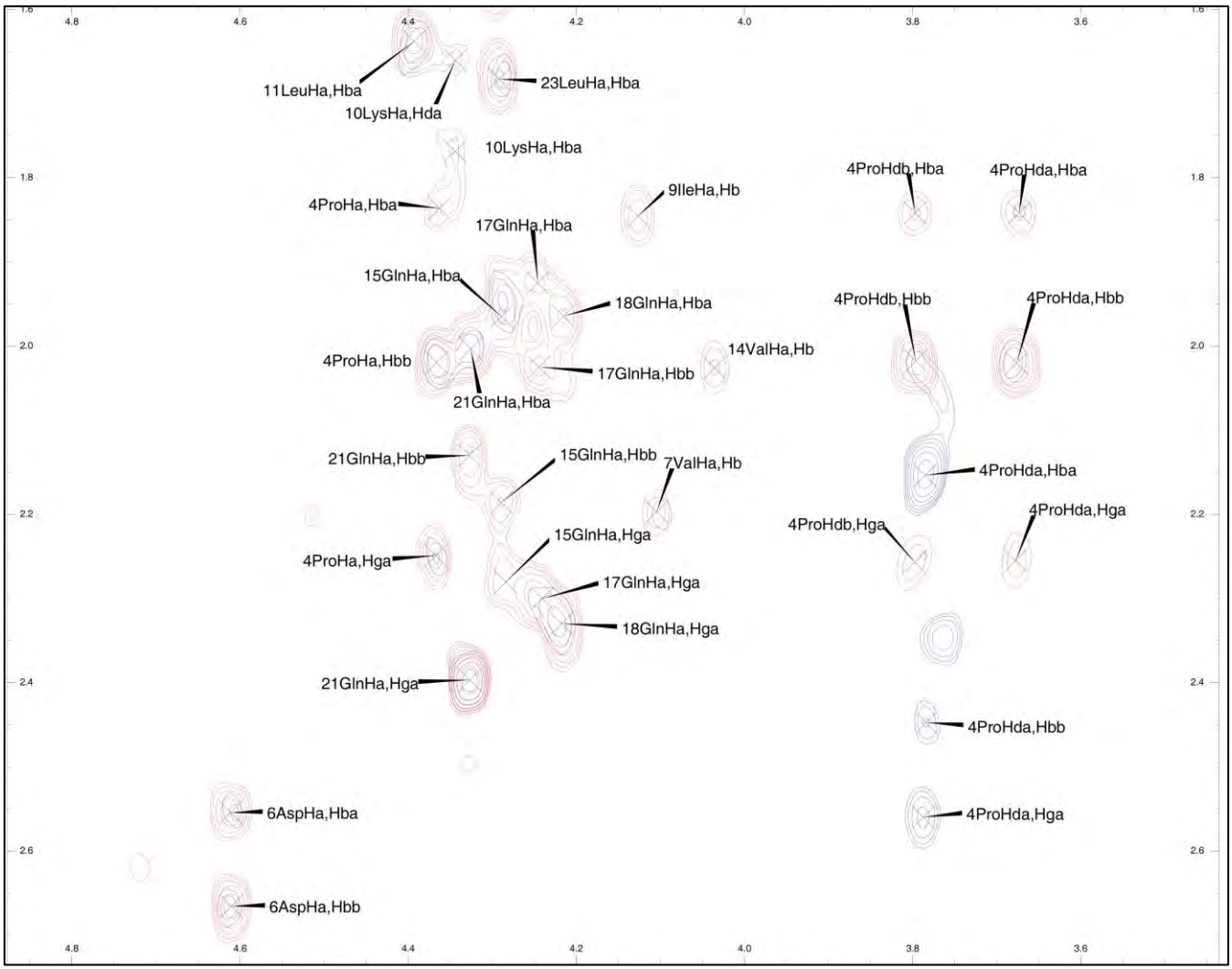

Figure 2.7. Superposition of alpha region of 2D TOCSY spectra for human obestatin in HEK-WT (blue) and HEK-GPR39 (red) cells. Pro4 showed large CSPs in different protons in the presence of living receptor-enriched cells.

3D STRUCTURE OF HUMAN OBESTATIN

The NMR assays performed might indicate that full-length obestatin (**1**) is unstructured in the presence of H_2O, PBS and WT cells. In GPR39-transfected cells, NOE pattern and CSPs data may suggest that receptor could induce a further stabilized secondary structure. Taking into account NOE restrictions, the possibility of a conformational change in His19 and Pro4, and the fact that GPR39 could be acting as a prolyl *cis-trans* isomerase, we calculated the three-dimensional structures of human obestatin using the protocols of refinement CYANA (**Figures 2.8** and **2.9**). Prolines could adopt two possible conformations *E* ($\omega = 180^o$)

and *Z* ($\omega = 0^o$), therefore, the best 6 structures for each conformation with a ω torsion restriction in Pro4, which possessed the lowest total energies, were considered as representatives of human obestatin in GPR39-enriched cells. None of these structures had NOE violations greater than 0.2 Å or dihedral angle violations greater than 2°. The analysis of the bundle of 6 structures obtained for human obestatin for *E* configuration showed a possible helix structure between residues Ala3 and Phe5, which are overlapped. In the *Z* configuration, the 6 calculated structures presented an overlying between Phe1 and Lys10 which could being part of and helical configuration, however, according to described above, the largest part of the peptide appeared to be unstructured both in the *E* and *Z* conformations.

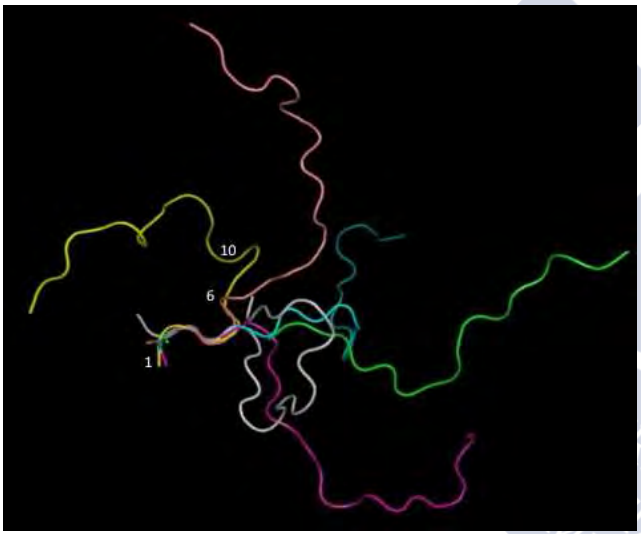

Figure 2.8. Possible conformations of human obestatin in presence of GPR39 receptor. Six structures of human obestatin were calculated using CYANA, with a ω torsion restriction in Pro4 in *E* configuration. Residues between 3-5 are overlapped.

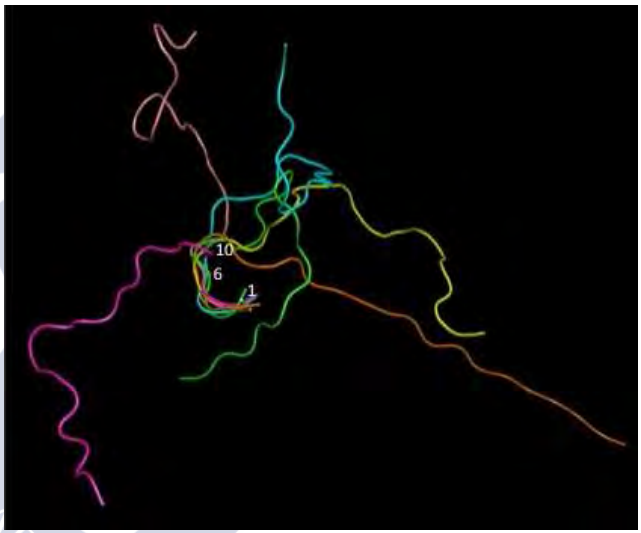

Figure 2.9. Possible conformations of human obestatin in presence of GPR39 receptor. Six structures of human obestatin were calculated using CYANA, with a ω torsion restriction in Pro4 in *Z* configuration. Residues between 1-10 are overlapped.

USC
UNIVERSIDADE
DE SANTIAGO
DE COMPOSTELA

CHAPTER 3: OBESTATIN/GPR39 SIGNALLING

OBESTATIN/GPR39 INTERACTION

Obestatin was initially discovered as the cognate ligand for GPR39[1] in 2005. However, several groups published their results challenging these data. Chartrel *et al*, one year later, published that human obestatin was not able to drive GPR39 internalization.[74] In the same year, some groups proposed Zn^{+2} as the endogenous agonist of GPR39 due to its ability to activate inositol phosphate accumulation.[55,60,74,75] Nevertheless, the same group published that Zn^{+2} treatment diminished GPR39 basal phosphorylation, even at concentrations of 1 µM. In 2015, Camiña's group using co-immunoprecipitation experiments demonstrated the binding of obestatin to GPR39 in cultured C2C12 myoblast cells.[73] Our results concerning the obestatin/GPR39 system also supported this piece of information.

The controversy generated by the obestatin/GPR39 system regarding its mode of interaction, or more importantly, whether there was any kind of interaction, prompted us to investigate the first steps in obestatin signalling, which means GPR39 phosphorylation and internalization.

GPR39 phosphorylation induced by obestatin

We measured receptor phosphorylation to assess obestatin effects *via* the GPR39 receptor. GFP-GPR39 receptor was immunoprecipitated from transiently transfected HEK293 cells loaded with ^{32}Pi, and, using the GPR39 or GFP antibodies, radiolabelled proteins were detected by gel autoradiography or Western blotting. Several bands were observed for GPR39, the main at 60 kDa (**Figure 3.1**). These bands could represent the increasing glycosylation state of receptor proteins as they reach maturity and potentially the presence of receptor dimers. A basal phosphorylation for GPR39 was observed, similar to those previously described for this receptor.[51] This basal phosphorylation could represent a high constitutive activity for GPR39. In the example presented in **Figure 3.1**, $^{32}P_i$ incorporation was augmented by obestatin treatment (200nM, 5min). The radioactive labelling of the immunoprecipitated receptor showed that obestatin increased a ~109% GPR39 phosphorylation compared to untreated cells.

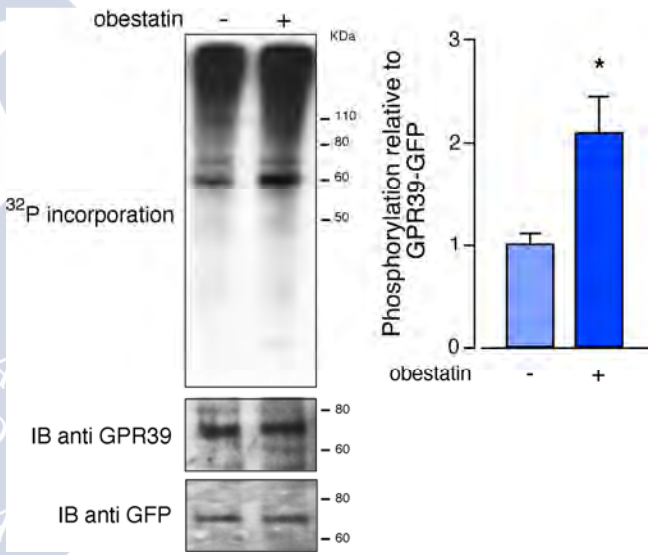

Figure 3.1. GPR39 phosphorylation activated by obestatin. HEK293 cells expressing GPR39 cells were loaded with 50 µC $^{32}P_i$ for 1h before treatment with human obestatin (200nM, 5 min; left panel). Levels of $^{32}P_i$ incorporation were quantified by densitometry, normalized to GPR39-GFP, and expressed as fold increase relative to the untreated control cells. Immunoblots are representative of three independent experiments. The data are expressed as the mean ± SEM (* $p < 0.05$; right panel).

GPR39 internalization/endocytosis

Next, we tested the effect of obestatin on receptor endocytosis by confocal microscopy in HEK293 cells transiently expressing the human GPR9 receptor. Internalization of GPR39 tagged with GFP was analysed 20, 40, 60 and 120 min after obestatin treatment (500 nM).

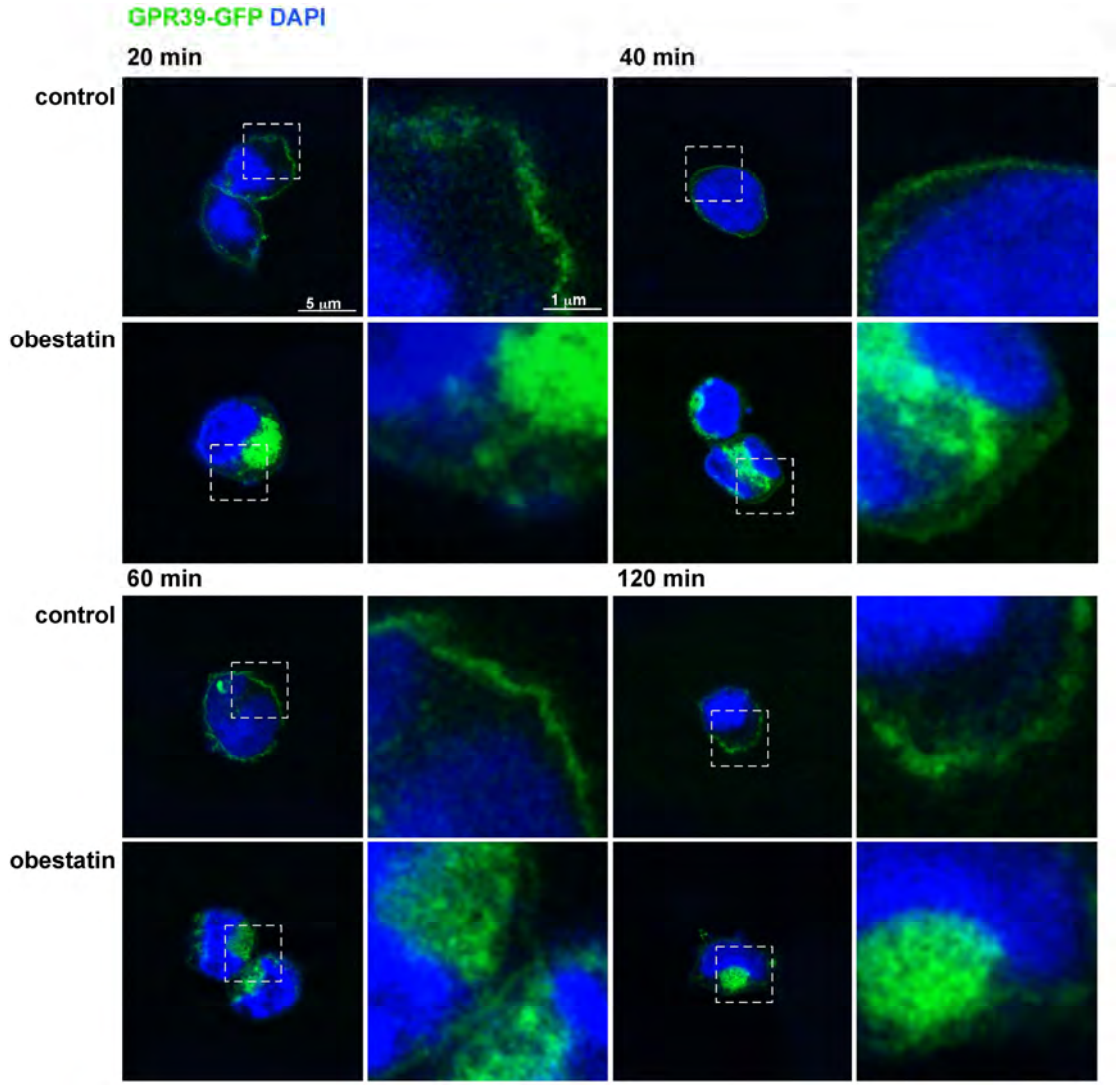

Figure 3.2. Time course of GPR39-GFP internalization in HEK293-GPR39-GFP cells after stimulation with obestatin. The localization of the GPR39 expressed in transiently transfected HEK293 cells was visualized by confocal microscopy in cells incubated for different times at 37 ^{o}C in the absence or presence of 500 nm obestatin.

In the resting cells, fluorescence associated with the receptor was predominantly confined to plasma membrane for all the time tested (**Figure 3.2**). Obestatin was rapidly bound to the GPR39 and caused clustering of the receptor on the plasma membrane within a few minutes. During the subsequent internalization of the obestatin-GPR39 complex, the receptor was detectable in punctate intracellular structures, which were evident for up to 20 min. At this time, even the GPR39 began to appear in deeper compartments adjacent to the nucleus (**Figure 3.2**). However, after 120 min incubation, the fluorescent vesicles were concentrated near the membrane, and a moderate labelling appeared at the cell surface again, suggesting that receptor could have being recycled (**Figure 3.2**).

GPR39-RTKs CROSS-TALK: DIFFERENTIAL RTK PHOSPHORYLATION AND PROTEASES EXPRESSION PATTERNS

In gastric cancer cells, once obestatin activates GPR39, two routes are triggered in parallel:[142] i) sequential activation of Gi, PI3K, PKCε novel and Src and the subsequent ERK1/2 activation; and ii) a β-arrestin 1-mediated signalling pathway that implies the recruitment of Src to the β-arrestin 1 scaffolding complex causing Akt phosphorylation. In this way, Src acts as a switch that activates MMPs to initiate the proteolytic release of the EGF-like ligands onto the cell surface, which later bind to EGFR.

This signalling network adds a new component to the intracellular signalling targets regulated by obestatin. The transactivation of EGFR-induced by obestatin could imply a key mechanism by which MMPs regulate these diseases. Supporting this hypothesis, numerous studies have shown that alterations in the expression and/or mutations in members of the family of receptors EGFR/ErbB are present in tumours and cell lines derived from these tumours, and these changes may contribute to the progression of cancer.[153,154,155]

In this sense, obestatin is added to the group of MMPs regulator factors, which have been implicated in diverse human diseases, such as inflammatory diseases and cancer.[151,152]

Summarizing, MMPs and RTKs are key pieces in the pathology of cancer. Assuming that the obestatin/GPR39 system might play a role in the development, maintenance and malignancy of cancer, especially of gastric cancer, the aim of the present study is to elucidate the detailed activation/regulation mechanism of GPR39 and receptor tyrosine kinases cross-talk triggered by obestatin; to identify MMPs activated by obestatin; and to study the possible implications in gastric tumour development. As a model, the human gastric cancer cell lines KATO III and AGS were used to describe the differential RTKs phosphorylation pattern and the proteases implicated in the intracellular signalling pathway of obestatin.

Differential RTK phosphorylation pattern activated by obestatin in AGS and KATO III cells

We performed phospho-RTK arrays to determine the phosphorylation profile of growth factor RTKs in AGS and KATO III cells in response to obestatin. The degree of the differential activation of growth factor RTK proteins between human obestatin treated or untreated cells (200 nM, 10 min) was quantitated by dot blot (49 phosphorylated growth factor RTK antibodies evaluated on the membrane). Obestatin treated or untreated cells protein samples were incubated on separate RTK membranes followed by densitometric measurements of dot blots.

The diverse RTKs were differentially activated in obestatin treated or untreated AGS cells (**Figure 3.3**). Of the 49 RTKs evaluated on the array membrane for

this study, significantly greater expression levels were observed with 18 of the phosphorylated RTKs in the obestatin treated compared with untreated samples.

The significant mean (n=4 dots) fold changes of activation of RTKs in obestatin treated over that of untreated AGS cells were: EGFR (126.7±1.1%), ErbB2 (152.2±0.1%), ErbB3 (125.7±2.6%), ErbB4 (139.9±7.9%), fibroblast growth factor receptor 4 (FGFR4, 132±6.4%), insulin R (128.6±1,3%), insulin-like growth factor (IGF) 1 receptor (IGF1R, 125.9±0.7%), tropomyosin receptor kinase C (TrkC, 170.9±4.6%), ephrin type A receptor (EphA1, 121.1±1.3%), EphB2 (137.2±1.8%), fms-like tyrosine kinase 3 (Flt3, 156.4±4.1%), c-Ret (136.4±7.1%), macrophage colony-stimulating factor receptor (M-CSFR, 131.3±1.8%), Mer (129±2.2%), receptor tyrosine kinase-like orphan receptor 2 (ROR2, 128.6±0.1%), RYK (126.9±0.5%), discoidin domain receptor 1 (DDR1, 115.6±2.2%), DDR2 (119.6±2.2%), mast/stem cell growth factor receptor (SCFR, 86.7±0.7%) and FGFR1 (94.6±0.0%) . These receptors basically belong to the EGF, insulin, FGF, ephrin and DDR growth factor gene families.

All the members of the EGFR family in array were significant activated by obestatin. Among them, ErbB2 was the most activated receptor, followed by ErbB4, EGFR and ErbB3. The ErbB receptor family comprises four receptors: EGFR (ErbB1/HER1), ErbB2 (neu, HER2), ErbB3 (HER3) and ErbB4 (HER4). There is a wealth of clinical data demonstrating the importance of ErbB receptors in the development and malignancy of human cancer. In gastric cancer, the EGF receptor/ligand system seems to be involved in the regulation of gastric mucosal proliferation and progression of gastric carcinoma. Increased EGFR binding has been observed in gastric carcinomas in comparison to adjacent normal gastric mucosa. Moreover, elevated EGFR levels have been found in gastric carcinoma with worse prognostic factors and it is considered like an indicator of poor prognosis.[234,235] The overexpression of ErbB2 in gastric carcinomas was first described by Yonemura *et al* in 1991. These findings were confirmed by many other studies, which provided further evidence that the highest rate of overexpression was found in patients with advanced disease, and that ErbB2 altered expression can be considered as an independent predictor of outcome.[236] In fact, in gastric cancer, two of the most frequently amplified RTKs were EGFR (7.7%) and ErbB2 (7.2%).[237] More recently, several studies reported evidences that considered HER3 overexpression as a predictor of poor prognosis and survival. However, this prognostic role has not yet reached a consensus.[238]

Insulin receptor and IGF1R were significantly activated too. IGF1R is overexpressed in gastric cancer tissues as compared with normal mucosa. Moreover, IGF receptors are almost universally expressed in gastric carcinomas.[239] IGF1R is associated with a poor response to chemotherapy and poor outcomes in Stage I–IV of gastric cancer. Furthermore, high levels of receptor are associated with tumour size, quantity

[234] Kopp R, Ruge M, Rothbauer E, *et al*. Impact of epidermal growth factor (EGF) radioreceptor analysis on long-term survival of gastric cancer patients. Anticancer Res. 2002;22:1161-7.

[235] García I, Vizoso F, Martín A, *et al*. Clinical significance of the epidermal growth factor receptor and HER2 receptor in resectable gastric cancer. Ann Surg Oncol. 2003;10:234-41.

[236] Yonemura Y, Ohoyama S, Kimura H, *et al*. The expression of proliferative-associated nuclear antigen p105 in gastric carcinoma. Cancer. 1991;67:2523-8.

[237] Morishita A, Gong J, Masaki T. Targeting receptor tyrosine kinases in gastric cancer. World J Gastroenterol. 2014;20:4536-45.

[238] Wang L, Yuan H, Li Y, *et al*. The role of HER3 in gastric cancer. Biomed Pharmacother. 2014;68:809-12.

[239] Kashyap MK. Role of insulin-like growth factor-binding proteins in the pathophysiology and tumorigenesis of gastroesophageal cancers. Tumour Biol. 2015;36:8247-57.

of stroma, depth of wall invasion, lymph node metastasis, TNM stage, and differentiation status.[240] IGF1R expression was related to venous invasion too. It was reported that the IGF1R axis influences MMP7 and promotes tumour progression and invasion in gastrointestinal cancer protecting tumour cells against apoptosis induced by cytotoxic drugs[241] and promoting EMT.[242]

The most activated receptor was TrkC. Some years ago, it was reported that Trk receptors family probably played a unique role in gastric cancer cell apoptosis by a novel Ras or Raf signal transduction pathway,[243] however, recent reviews showed that high expression of TrkA or TrkC may play significant roles in tumour progression, metastasis, and outcomes in gastric cancer. TrkC expression was correlated with clinical stage, lymph node metastasis, microvessel density, lymph vessel density, and poor prognosis, as well as regulated the secretion of MMP2 and MMP9.[244]

EphA1 and EphB2 were the significant obestatin-activated members of EphR family in AGS cells. There have been some reports showing that Eph families are associated with proliferation and invasion of gastrointestinal cancers. High expression of EphA1 may play a critical role in tumour progression, metastasis, and survival in gastric cancer. It is believed that EphA subgroup generally enhances tumour progression by activating Jak/Stat and Akt/PI3K signals. Furthermore, EphA1 has the possibility of being a target of molecular targeted therapy by inhibiting angiogenesis like the mechanism of VEGF inhibitor, associating EphA1 with cell proliferation, motility, and invasiveness in gastric carcinomas.[245,246] Controversially, literature shows EphB2 as a negative biomarker for gastric carcinogenesis and suggests that EphB2 may have tumour suppressor activities in gastric cancer.[247,248,249]

Flt3,[250] and c-Ret are receptors involved in proliferation, differentiation and cell migration, and c-Ret is a mediator in gastric cancer[251] and neuroendocrine tumours.[252] RYK and ROR are implicated in Wnt signalling in tumour invasion during carcinogenesis;[253] and DDR receptors regulate the cell adhesion to the extracellular matrix, and are involved

[240] Numata K, Oshima T, Sakamaki K, *et al*. Clinical significance of IGF1R gene expression in patients with Stage II/III gastric cancer who receive curative surgery and adjuvant chemotherapy with S-1. J Cancer Res Clin Oncol. 2016;142:415-22.

[241] Ichikawa W, Terashima M, Ochiai A, *et al*. Impact of insulin-like growth factor-1 receptor and amphiregulin expression on survival in patients with stage II/III gastric cancer enrolled in the adjuvant chemotherapy trial of S-1 for Gastric Cancer. Gastric Cancer. 2016. [Epub ahead of print]

[242] Li H, Xu L, Zhao L, *et al*. Insulin-like growth factor-I induces epithelial to mesenchymal transition via GSK-3β and ZEB2 in the BGC-823 gastric cancer cell line. Oncol Lett. 2015;9:143-148.

[243] Du JJ, Dou KF, Peng SY, *et al*. Expression of NGF family and their receptors in gastric carcinoma: a cDNA microarray study. World J Gastroenterol. 2003;9:1431-4.

[244] Kamiya A, Inokuchi M, Otsuki S, *et al*. Prognostic value of tropomyosin-related kinases A, B, and C in gastric cancer. Clin Transl Oncol. 2016;18:599-607.

[245] Nakagawa M, Inokuchi M, Takagi Y, *et al*. Erythropoietin-producing hepatocellular A1 is an independent prognostic factor for gastric cancer. Ann Surg Oncol. 2015;22:2329-35.

[246] Wang J, Dong Y, Wang X, *et al*. Expression of EphA1 in gastric carcinomas is associated with metastasis and survival. Oncol Rep. 2010;24:1577-84.

[247] Song JH, Kim CJ, Cho YG, *et al*. Genetic and epigenetic analysis of the EPHB2 gene in gastric cancers. APMIS. 2007;115:164-8.

[248] Davalos V, Dopeso H, Velho S, *et al*. High EPHB2 mutation rate in gastric but not endometrial tumors with microsatellite instability. Oncogene. 2007;26:308-11.

[249] Yu G, Gao Y, Ni C, *et al*. Reduced expression of EphB2 is significantly associated with nodal metastasis in chinese patients with gastric cancer. J Cancer Res Clin Oncol. 2011;137:73-80.

[250] Radomaska HS, Alberich-Jordá M, Will B, *et al*. Targeting CDK1 promotes FLT-3 activated acute myeloid leukemia differentiation through C/EBPα. J Clin Invest. 2012:122:2955-66.

[251] Zhang F, Tang JM, Wang L, *et al*. Immunohistochemical detection of RET proto-oncogene product in tumoral and nontumoral mucosae of gastric cancer. Anal Quant Cytopathol Histpathol. 2014;36:128-36.

[252] Murakumo Y, Jijiwa M, Asai N, *et al*. RET and neuroendocrine tumors. Pituitary. 2006;9:179-92.

[253] Katoh M, Katoh M. Integrative genomic analyses of WNT11: transcriptional mechanisms based on canonical WNT signals and GATA transcription factors signaling. Int J Mol Med. 2009;24:247-51.

in migration, playing an important role in tumour cell invasion and up-regulating the expression of MMP2, 7 and 9.[254]

In addition, the only two down-regulated receptors by obestatin were SCFR (c-Kit) and FGFR1. Surprisingly, mutations in c-Kit are associated with gastrointestinal stromal tumours (GISTs), the most common mesenchymal neoplasms in gastrointestinal tract. Furthermore, c-Kit–positive status may be a significant indicator of good prognosis in gastric cancer patients.[255] The fact that obestatin diminished the activation of this receptor could involve obestatin in malignancy of gastric cancer.

On the other hand, the activation of RTKs in KATO III cells after obestatin treatment (200nM, 10 min) showed a different pattern of phosphorylation (**Figure 3.3**). We found differences in EGF, insulin, VEGF, ephrin and Tie receptor families. The significant mean (n=4 dots) fold changes of activation in obestatin-treated KATO III cells were: EGFR (138.6±0.3%), IGF1R (144.8±2.3%) and EphA1 (135.8±5.2%) as well as in AGS cells; macrophage-stimulating protein receptor (MSPR, 144±0.6%), angiopoietin receptor 1 (Tie1, 120.1±0.5%), VEGFR3 (114.9±3.1%), EphA3 (120.2±3.1%) and EphA5 (132.8±3.4%). Otherwise, Mer (76.1±3.1%), Tie2 (62±3.0%), TrkA (65,6±2.1%) , EphA6 (71.8±0.3%) and EphA7 (96.5±0.6%) showed a relevant decrease in phosphorylation levels under obestatin treatment.

Overexpression of MSPR has been significantly associated with tumour size, depth of invasion, lymph node metastasis, tumour stage and poor survival in human gastric cancer indicating that this receptor is associated with tumour progression *via* the inhibition of apoptosis and cell cycle arrest.[256,257] VEGFR3 is reported implicated in cell migration/invasion of human gastric cancer cells.[258] Furthermore, VEGF /VEGFR3 system regulates lymphangiogenesis.[259]

Regarding EphR family in KATO III cells, we found that obestatin increased activation of EphA3 and EphA5. EphA3 mRNA and protein expression was significantly higher in gastric cancer than in normal mucosa and correlated with TNM stage, poor prognosis and VEGF expression, playing important roles in the angiogenesis and the prognosis of gastric carcinoma.[260] A recent report showed that EphA5 gene is expressed at very low levels in gastric cancer and gastric mucosa and did not show any significant differences.[261]

[254] Fu HL, Valiathan RR, Arkwright R, *et al*. Discoidin domain receptors: unique teceptor tyrosine kinases in collagen-mediated signaling. J Biol Chem. 2013;288:7430-74.

[255] Kurokawa Y, Matsuura N, Kawabata R, *et al*. Prognostic impact of major receptor tyrosine kinase expression in gastric cancer. Ann Surg Oncol. 2014;21:S584-90.

[256] Moser C, Lang SA, Hackl C, *et al*. Oncogenic MST1R activity in pancreatic and gastric cancer represents a valid target of HSP90 inhibitors. Anticancer Res. 2012;32:427-37.

[257] Song YA, Park YL, Kim KY, *et al*. RON is associated with tumor progression via the inhibition of apoptosis and cell cycle arrest in human gastric cancer. Pathol Int. 2012;62:127-36.

[258] Lim J, Ryu JH, Kim EJ, *et al*. Inhibition of vascular endothelial growth factor receptor 3 reduces migration of gastric cancer cells. Cancer Invest. 2015;33:398-404.

[259] Zhang X, Zheng Z, Shin YK, *et al*. Angiogenic factor thymidine phosphorylase associates with angiogenesis and lymphangiogenesis in the intestinal-type gastric cancer. Pathology. 2014;46:316-24.

[260] Xi HQ, Wu XS, Wei B, *et al*. Aberrant expression of EphA3 in gastric carcinoma: correlation with tumor angiogenesis and survival. J Gastroenterol. 2012;47:785-94.

[261] Sepulveda JL, Gutierrez-Pajares JL, Luna A, *et al*. High-definition CpG methylation of novel genes in gastric carcinogenesis identified by next-generation sequencing. Mod Pathol. 2016;29:182-93.

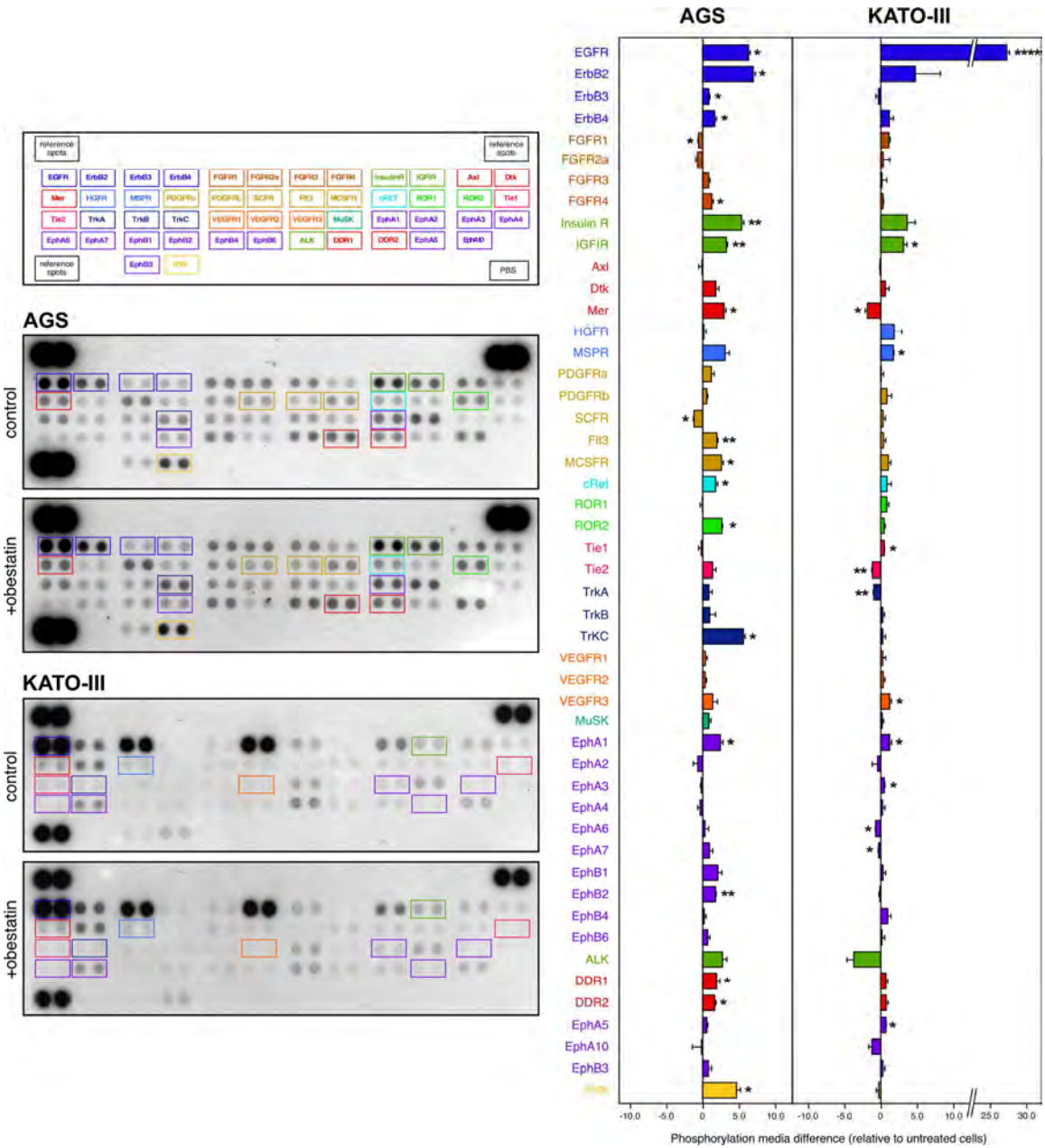

Figure 3.3. Differential expression of phosphorylated growth factor RTKs in obestatin treated compared to untreated AGS and KATO III cells. Out of the 49 RTKs analysed in the Phosphorylation of Receptor Tyrosine Kinases Array, 18 and 8 growth factor RTKs were highly activated ($P < 0.02–0.03$) in obestatin-treated (200 nM, 10 min) compared to untreated AGS and KATO III cells, respectively. These RTKs belong to the EGF, insulin, DDR, Trk, Tie and ephrin growth factor receptor gene families. 200 µg of cell lysate were run on each array.

However, EphA5 receptor is a protein that mediates the communication between pancreatic islets to regulate the pancreatic insulin secretion stimulated by glucose,[262] thus, the increased activation caused by obestatin in EphA5 phosphorylation enhanced the activity of obestatin in pancreas and insulin metabolism.[91,101,103] On the other hand, EphA6 and EphA7 are down-regulated by obestatin. Both RTKs are implicated in cell adhesion and migration.[245] Moreover, EphA7 expression was significantly lower in gastric cancer as compared with either intestinal metaplasia or non-metaplastic mucosa.[261]

By last, we found that exogenous obestatin administration in KATO III cells produced antagonistic effects in the two members of Tie receptor family; Tie1 receptor was activated whereas Tie2 was down-regulated. The Tie receptors are receptors that bind angiopoietins, protein growth factors required for the angiogenesis. Both receptors seem to be implicated in gastric carcinogenesis. Ties were highly expressed in human gastric adenocarcinoma cells and the results suggest that the Ang-Tie complex is one of the factors involved in the cellular differentiation and progression of human gastric adenocarcinoma,[263] correlating with higher TNM stage, lymph node metastasis as well as distance metastasis.[264,265] However, several reports showed that in the presence of Tie1, the ligand independence and basal Tie2 activity are attenuated, concluding that Tie1, in its normal role, antagonizes Tie2 function.[266] This piece of information corroborates the data observed in KATO III cells, which supports the inhibitory effects of Tie1 on Tie2 activation.[267,268]

These results showed that the obestatin/GPR39 system signalling pathways are more complex than might have been expected, supporting the role of the different RTKs in obestatin signalling *via* the GPR39 receptor.

Differential protease expression pattern activated by obestatin in AGS and KATO III cells

As mentioned above, MMPs are involved in the signalling pathway of obestatin[142] and play an important role in critical processes in the pathology of cancer.[269] Therefore, we have also studied the differential expression of several proteases, both in AGS and KATO III cell lines after exogenous administration of obestatin.

In this case, cells were stimulated with obestatin for 24 hours, lysate and secretome were collected to detect both intracellular and secreted proteases. This time-window was selected in order to allow synthesis and secretion of the proteases.

[262] Konstantinova I, Nikolova G, Ohara-Imaizumi M, *et al*. EphA-ephrin-A-mediated beta cell communication regulates insulin secretion from pancreatic islets. Cell. 2007;129:359-70.

[263] Nakayama T, Yoshizaki A, Kawahara N, *et al*. Expression of Tie-1 and 2 receptors, and angiopoietin-1, 2 and 4 in gastric carcinoma; immunohistochemical analyses and correlation with clinicopathological factors. Histopathology. 2004;44:232-9.

[264] Lin WC, Li AF, Chi CW, *et al*. Tie-1 protein tyrosine kinase: a novel independent prognostic marker for gastric cancer. Clin Cancer Res. 1999;5:1745-51.

[265] Wang J, Wu K, Zhang D, *et al*. Expressions and clinical significances of angiopoietin-1, -2 and Tie2 in human gastric cancer. Biochem Biophys Res Commun. 2005;337:386-93.

[266] Seegar TC, Eller B, Tzvetkova-Robev D, *et al*. Tie1-Tie2 interactions mediate functional differences between angiopoietin ligands. Mol Cell. 2010;37:643-55.

[267] Patan S. TIE1 and TIE2 receptor tyrosine kinases inversely regulate embryonic angiogenesis by the mechanism of intussusceptive microvascular growth. Microvasc Res. 1998;56:1-21.

[268] Yuan HT, Venkatesha S, Chan B, *et al*. Activation of the orphan endothelial receptor Tie1 modifies Tie2-mediated intracellular signaling and cell survival. FASEB J. 2007;21:3171-83.

[269] Gialeli C, Theocharis AD, Karamanos NK. Roles of matrix metalloproteinases in cancer progression and their pharmacological targeting. FEBS Journal. 2011;278:16-27.

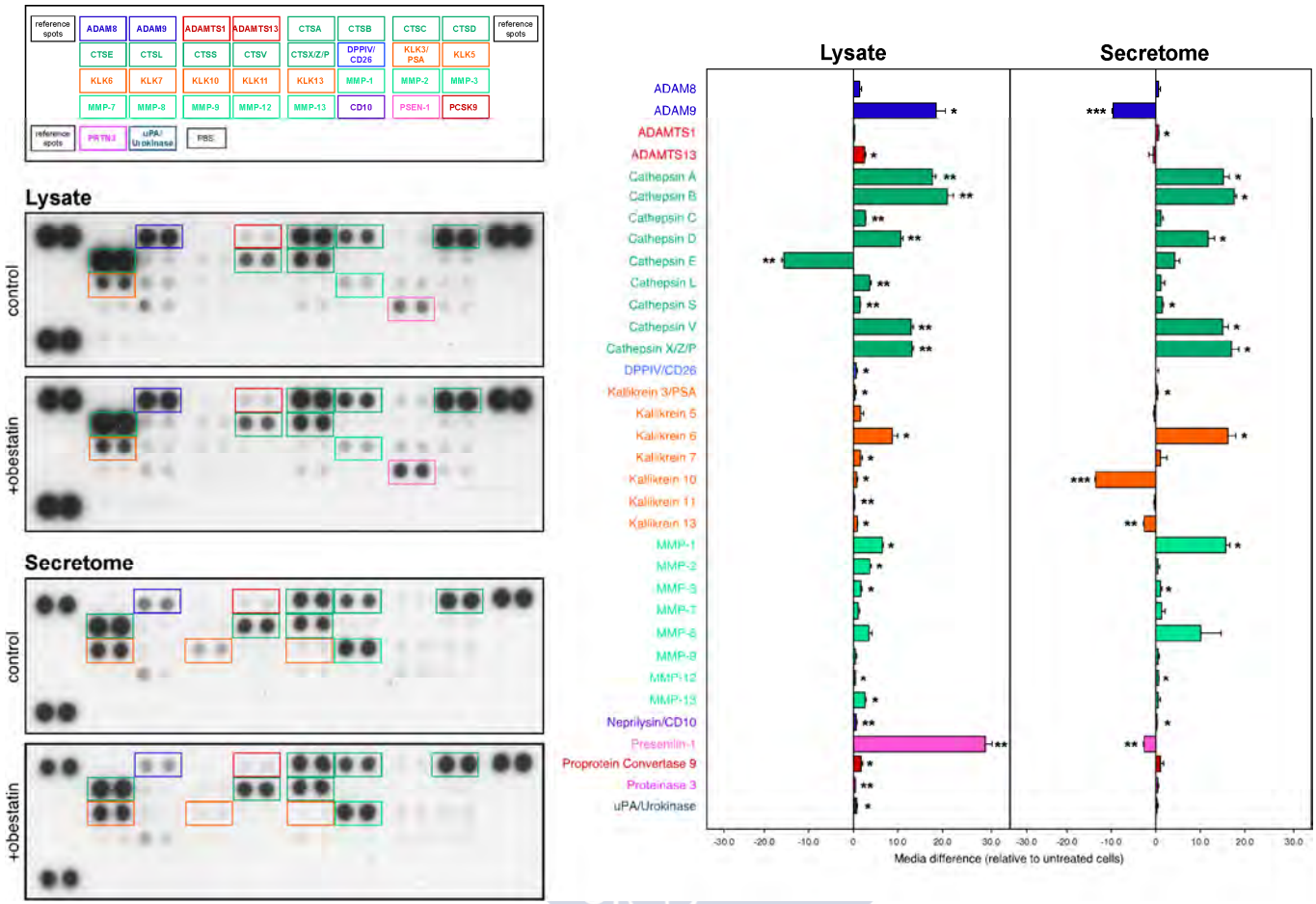

Figure 3.4. Differential expression of proteases in obestatin treated compared to untreated AGS cells. Out of the 34 proteases analysed in the array, 27 proteases in cell lysates and 13 in secretome were highly expressed ($P < 0.05$) in obestatin-treated (200 nM, 24 h) compared to untreated AGS cells. These proteases belong to the ADAM, CTS, KLK and MMP families. Only CTSE in lysates; and secreted ADAM9, KLK10, KLK13 and PSEN1 were down-regulated by obestatin. 200 µg of cell lysate and secretome were run on each array.

We performed protease arrays to determine the expression profiles. The degree of differential expression between human obestatin treated or untreated cells (200 nM, 24 h) was quantitated by dot blot (34 proteases antibodies evaluated on the membrane). Obestatin treated or untreated cells protein samples were incubated on separate proteases membranes followed by densitometric measurements of dot blots.

The diverse proteases were differentially expressed in obestatin treated or untreated AGS cells (**Figure 3.4**). The significant mean (n=4 dots) fold changes of expression in obestatin treated over that of untreated AGS cell lysates and secretomes were described below. Of the 34 proteases evaluated on the array membrane for this study, we have observed that the expression of 27 proteases in cells lysates and 13 in secretome were increased after obestatin treatment.

Otherwise, only cathepsin E (CTSE) in lysates; and secreted ADAM9, kallikrein 10 (KLK10), KLK13 and presenilin-1 (PSEN1) were down-regulated by obestatin (**Figure 3.4**). The most outstanding increases are proteases of the ADAM, CTS, KLK and MMP families.

Obestatin increased in 133.9±0.1% and 489.8±25.0% the expression of ADAM9 and ADAMTS13 respectively. ADAM9 is a cell-surface membrane glycoprotein with oncogenic properties that is overexpressed in several cancers, playing an important role in gastric cancer proliferation and invasion.[270] However, ADAMTS13 is negatively correlated with the VEGF-VEGFR2 system and signalling pathway in gastric cancer.[271]

Almost all CTSs altered its expression after obestatin treatment, but CTSB (193.4±3.9%) and CTSV (189.2±4.9%) experimented one of the greatest increment. It was reported that CTSB and CTSL were significantly higher in gastric cancer as compared to paired normal mucosa. CTSB levels were also significantly associated with TNM stage, nodal status, histological grade, and DNA ploidy in stomach carcinomas.[272,273,274] Tumours with overexpression of CTSs have powerful potential for invasiveness in the early stage of gastric carcinoma. Moreover, CTSs may be one of the determinants of the metastatic route.[275] CTSV and X/Z/P have different roles in tumour processes too.[276] In all cases, it was shown a greater increase in the fraction of secretome, because not only these proteases carry out their function within the lysosome, but also are known for their ability to degrade extracellular matrix components, such as proteoglycans, collagen and elastin. Surprisingly, CTSE (87.2±0.1%) was the only protease down-regulated in AGS cell lysates. It is a gastric aspartyl protease found in highest concentration in the surface of epithelial mucus-producing cells of the stomach. It is the first aspartic proteinase expressed in the foetal stomach and is found in more than half of gastric cancers.[277,278] Furthermore it is considered as a marker of both gastric differentiation and signet-ring cell carcinoma.[279]

In the case of the KLKs, all of them were overexpressed after obestatin treatment, especially KLK6 (139.8±4.4%) both in lysates and secretomes. KLK6 is a trypsin-like serine protease, and it has been shown to be upregulated in several cancers. KLK6 is significantly upregulated and secreted in gastric

[270] Kim JM, Jeung HC, Rha SY, *et al*. The effect of disintegrin-metalloproteinase ADAM9 in gastric cancer progression. Mol Cancer Ther. 2014;13:3074-85.

[271] Yang X, Sun HJ, Li ZR, *et al*. Gastric cancer-associated enhancement of von Willebrand factor is regulated by vascular endothelial growth factor and related to disease severity. BMC Cancer. 2015;15:80.

[272] Russo A, Bazan V, Migliavacca M, *et al*. Prognostic significance of DNA ploidy, S-phase fraction, and tissue levels of aspartic, cysteine, and serine proteases in operable gastric carcinoma. Clin Cancer Res. 2000;6:178-84.

[273] Liu Y, Xiao S, Shi Y, *et al*. Cathepsin B on invasion and metastasis of gastric carcinoma. Chin Med J. 1998;111:784-8.

[274] Czyzewska J, Guzińska-Ustymowicz K, Kemona A, *et al*. The expression of matrix metalloproteinase 9 and cathepsin B in gastric carcinoma is associated with lymph node metastasis, but not with postoperative survival. Folia Histochem Cytobiol. 2008;46:57-64.

[275] Dohchin A, Suzuki JI, Seki H, *et al*. Immunostained cathepsins B and L correlate with depth of invasion and different metastatic pathways in early stage gastric carcinoma. Cancer. 2000;89:482-7.

[276] Santamaría I, Velasco G, Cazorla M, *et al*. Cathepsin L2, a novel human cysteine proteinase produced by breast and colorectal carcinomas. Cancer Res. 1998;58:1624-30.

[277] Couvreur JM, Azuma T, Miller DA, *et al*. Assignment of cathepsin E (CTSE) to human chromosome region 1q31 by in situ hybridization and analysis of somatic cell hybrids. Cytogenet Cell Genet. 1990;53:137-9.

[278] Azuma T, Pals G, Mohandas TK, *et al*. Human gastric cathepsin E. Predicted sequence, localization to chromosome 1, and sequence homology with other aspartic proteinases. J Biol Chem. 1989;264:16748-53.

[279] Konno-Shimizu M, Yamamichi N, Inada K, *et al*. Cathepsin E is a marker of gastric differentiation and signet-ring cell carcinoma of stomach: a novel suggestion on gastric tumorigenesis. PLoS One. 2013;8:e56766.

cancer tissues and sera.[280] Furthermore, its expression was positively correlated with nodal involvement, advanced-stage disease and survival, suggesting that KLK6 might be used as a potential biomarker and therapeutic target for gastric cancer.[281] In cells secretomes, we found lower levels of KLK10 (30.2±0.1%) and mainly KLK13 (47.7±2.3%) in obestatin-treated samples. It could be due to the role of KLK13 as a favourable prognostic biomarker for gastric cancer patients' survival. A decreased in KLK13 expression was demonstrated in poorly differentiated gastric tumours[282] and its expression is implicated in the molecular pathways that are triggered after administration of anticancer agents on gastric cancer cells.[283]

All the MMPs, with the exception of MMP7, MMP8 and MMP9, showed higher expression levels triggered by obestatin; in fact, the most overexpressed protease was MMP1 (690.6±10.0%). Increased production and activation of MMP1, 2, and 3 may contribute to the remodelling of the cancer cell microenvironment.[284] Moreover, MMP1 plays a critical role in the invasion of gastric cancer,[285,286] and related to MMP10, this pro-metastatic function may be related with *H. pylori* infection.[287]

Finally, it has to be pointed out the controversial data about one protease. PSEN1 levels were significant increased (447.0±9.9%) in stimulated cell lysates, but lower than controls in secretome (58.3±1.5%). PSEN1 is a protease involved in the processes of apoptosis, cell adhesion to the matrix, as well as in the Notch signalling pathway.[288] In addition, it is involved in the pathology of Alzheimer´s disease and cancer.[289]

Concerning KATO III cells, regarding the significant mean (n=4 dots) fold changes of expression in cell lysates and secretomes, we have also found a pronounced overexpression for 23 proteases in the lysates after obestatin treatment (200nM, 24 h; **Figure 3.5**). However, obestatin only had effect on the secretion of 10 of them, increasing CTSA (131.2±0,5%), CTSB (114.6±1.1%), CTSD (107.0±0.3%), CTSX/Z/P (124.4±0.5%), DPPIV/CD26 (109.8±1.7%) and PC9 (125.3±1.5%) levels; and decreasing ADAMTS13 (87.5±0.2%), KLK3 (78.3±2.6%), MMP2 (83.4±0.6%) and PSEN1 (87.0±2.9%) releasing.

[280] Kim JJ, Kim JT, Yoon HR, *et al*. Upregulation and secretion of kallikrein-related peptidase 6 (KLK6) in gastric cancer.Tumor Biol. 2012;33:731-8.

[281] Kolin DL, Sy K, Rotondo F, *et al*. Prognostic significance of human tissue kallikrein-related peptidases 6 and 10 in gastric cancer. Biol Chem. 2014;395:1087-93.

[282] Konstantoudakis G, Florou D, Mavridis K, *et al*. Kallikrein-related peptidase 13 (KLK13) gene expressional status contributes significantly in the prognosis of primary gastric carcinomas. Clin Biochem. 2010;43:1205-11.

[283] Florou D, Mavridis K, Scorilas A. The kallikrein-related peptidase 13 (KLK13) gene is substantially up-regulated after exposure of gastric cancer cells to antineoplastic agents. Tumour Biol. 2012;33:2069-78.

[284] Holmberg C, Ghesquière B, Impens F, *et al*. Mapping proteolytic processing in the secretome of gastric cancer-associated myofibroblasts reveals activation of MMP-1, MMP-2, and MMP-3. J Proteome Res. 2013;12:3413-22.

[285] Dedong H, Bin Z, Peisheng S, *et al*. The contribution of the genetic variations of the matrix metalloproteinase-1 gene to the genetic susceptibility of gastric cancer. Genet Test Mol Biomarkers. 2014;18:675-82.

[286] Kim SJ, Shin JY, Lee KD, *et al*. Galectin-3 facilitates cell motility in gastric cancer by up-regulating protease-activated receptor-1 (PAR-1) and matrix metalloproteinase-1 (MMP-1). PLoS One. 2011;6:e25103.

[287] Jiang H, Zhou Y, Liao Q, *et al*. Helicobacter pylori infection promotes the invasion and metastasis of gastric cancer through increasing the expression of matrix metalloproteinase-1 and matrix metalloproteinase-10. Exp Ther Med. 2014;8:769-74.

[288] Chan YM, Jan YN. Roles for proteolysis and trafficking in notch maturation and signal transduction. Cell. 1998;94:423-6.

[289] Zhang S, Zhang M, Cai F, *et al*. Biological function of presenilin and its role in AD pathogenesis. Transl Neurodegener. 2013;2:15.

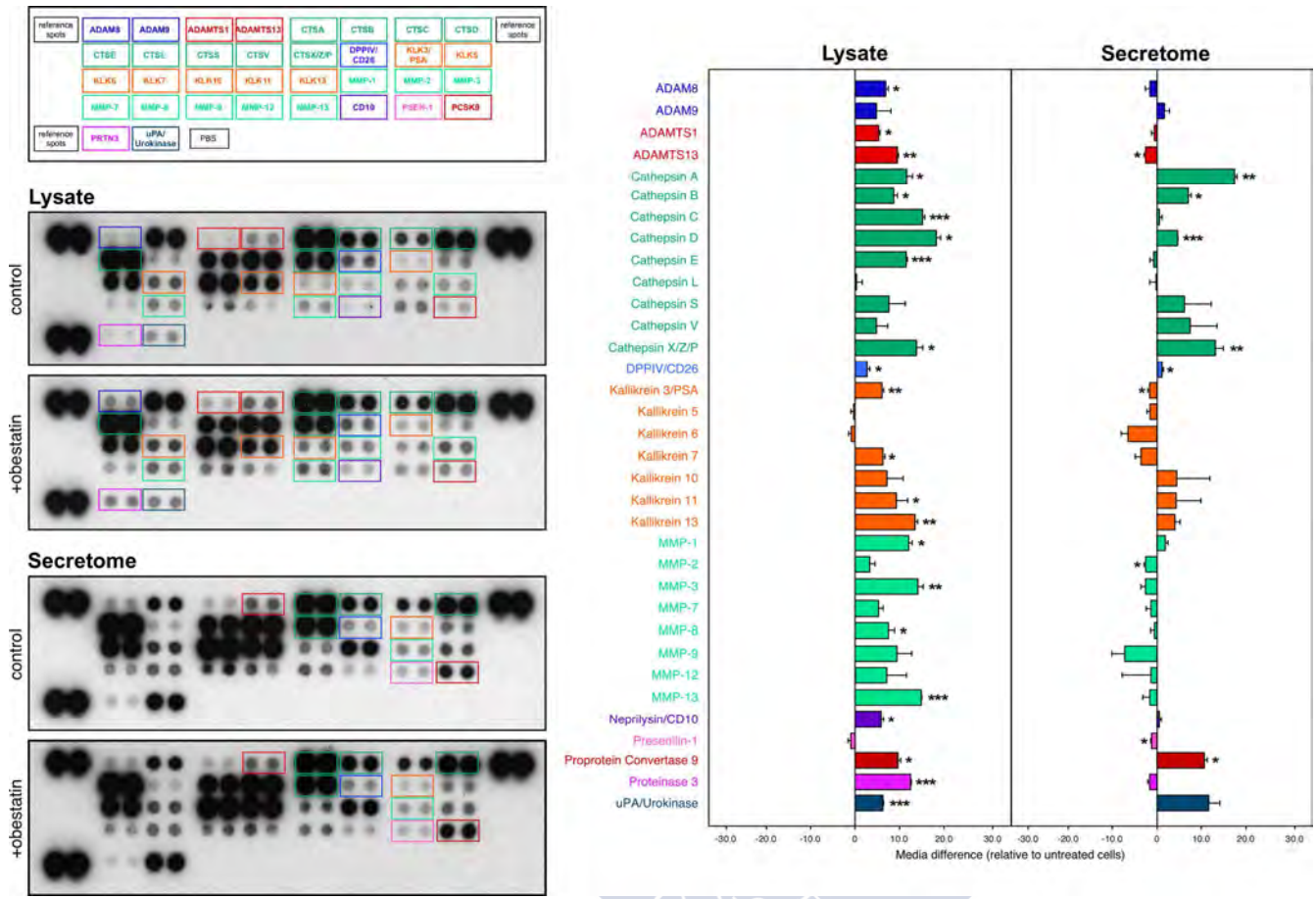

Figure 3.5. Differential expression of proteases in obestatin treated compared to untreated KATO III cells. Out of the 34 proteases analysed in the array, 23 proteases in cell lysates and 6 in secretome were highly expressed ($P < 0.05$) in obestatin-treated (200 nM, 24 h) compared to untreated KATO III cells. These proteases belong to the ADAM, CTS, KLK and MMP families. Only secreted ADAMTS13, KLK3 MMP2 and PSEN1 were down-regulated by obestatin. 200 µg of cell lysate and secretome were run on each array.

The most acute increment of the proteases in cells lysates was observed for ADAM8 (406.9±19.6%), ADAMTS1 (398.7±15.5%), CTSC (162.8±1.1%), KLK3 (358.4±12.6%), KLK13 (365.1±7.1%); MMP3 (261.9±14.2%), MMP13 (273.1±0.2%), neprilysin (CD10; 384.9±1.4%), PC9 (293.0±14.3%), proteinase 3 (PTRN3; 861.0±7.5%) and urokinase-type plasminogen activator (uPA; 172.1±1.3%). All of them are proteases implied in degradation of extracellular matrix. Besides, CTSC,[290] KLK3,[291] KLK13[292] and MMPs[269] encourage

[290] Gocheva V, Joyce JA. Cysteine Cathepsins and the cutting edge of cancer invasión. Cell Cycle. 2007;6:60-4.

[291] Balk SP, Ko YJ, Bubley GJ. Biology of prostate-specific antigen. J Clin Oncol. 2003;21:383-91.

[292] Borgoño CA, Diamandis EP. The emerging roles of human tissue kallikreins in cancer. Nat Rev Cancer. 2004;4:876-90.

invasion of tumour cells. ADAM8 is related to the degree of histological differentiation, the size, recurrence, metastasis and tumour stage,[293] and ADAMTS1 has an anti-angiogenic role blocking VEGF-routes, but it is also associated with inflammatory processes and is responsible for the plasticity and aggressiveness of tumour cells.[294]

The expression levels of CD10, PC9 and especially PRTN3 were highly augmented. All of them are proteases involved in peptide[295] and matrix degradation and in cell invasion in several oncogenic processes.[296] PC9 was discovered as an excellent marker in gastric cancer.[297] uPA expression is related to poor prognosis in stomach carcinomas and human gastric cancer cells invasiveness *via* the ERK1/2, nuclear factor-kappa-light-chain-enhancer of activated B cells (NF-κB), and adaptor protein 1 (AP-1) signalling pathways.[298,299] PRTN3 degrades extracellular matrix proteins and active MMP2 promoting cell invasion.[300]

As well as in AGS cells, ADAMTS13 (197.2±1.9%) and MMP1 (392.7±18.0%) expression was highly increased after obestatin administration.

This protease expression profile for both cell lines supports the implication of these proteases in the signalling pathway triggered by obestatin *via* the GPR39 receptor.

Differential RTK phosphorylation pattern in human adenocarcinomas

In order to validate the results obtained in the human cancer cell lines (AGS and KATO III), samples of human stomach were investigated. In this way, four human samples were selected for the study: one sample of healthy stomach (as control), and three of human gastric adenocarcinomas, represented by a WD, a MD and a PD adenocarcinoma.

First, we tested GPR39 expression by immunoblot (**Figure 3.6**). GPR39 was expressed in all of the samples with an intensity that varies among them, with the highest expression in the MD adenocarcinoma (1.59 a.u.).

Therefore, we performed phospho-RTK arrays to determine the phosphorylation profiles of RTKs in human stomach samples. The differential activation of RTK proteins between healthy gastric mucosa and gastric adenocarcinomas was quantitated by dot blot as well as in cells. The significant mean (n=2 dots) fold changes of activation of RTKs in adenocarcinomas over that of healthy mucosa sample were described below (**Figure 3.7**).

[293] Mochizuki S, Okada Y. ADAMs in cancer cell proliferation and progression. Cancer Sci. 2007;98:621-8.
[294] Tan Ide A, Ricciardelli C, Russell DL. The metalloproteinase ADAMTS1: a comprehensive review of its role in tumorigenic and metastatic pathways. Int J Cancer. 2013;133:2263-76.
[295] Marr RA, Hafez DM. Amyloid-beta and Alzheimer's disease: the role of neprilysin-2 in amyloid-beta clearance. Front Aging Neurosci. 2014;6:187.
[296] Maguer-Satta V, Besançon R, Bachelard-Cascales E. Concise review: neutral endopeptidase (CD10): a multifaceted environment actor in stem cells, physiological mechanisms, and cancer. Stem Cells. 2011;29:389-96.
[297] Marimuthu A, Subbannayya Y, Sahasrabuddhe NA, *et al*. SILAC-based quantitative proteomic analysis of gastric cancer secretome. Proteomics Clin Appl. 2013;7:355-66.
[298] Tang Z, Sheng H, Zheng X, *et al*. Upregulation of circulating cytokeratin 20, urokinase plasminogen activator and C-reactive protein is associated with poor prognosis in gastric cancer. Mol Clin Oncol. 2015;3:1213-20.
[299] Khoi PN, Xia Y, Lian S, *et al*. Cadmium induces urokinase-type plasminogen activator receptor expression and the cell invasiveness of human gastric cancer cells via the ERK-1/2, NF-κB, and AP-1 signaling pathways. Int J Oncol. 2014;45:1760-8.
[300] Pezzato E, Donà M, Sartor L, *et al*. Proteinase-3 directly activates MMP-2 and degrades gelatin and Matrigel; differential inhibition by (-) epigallocatechin-3-gallate. J Leukoc Biol. 2003;74:88-94.

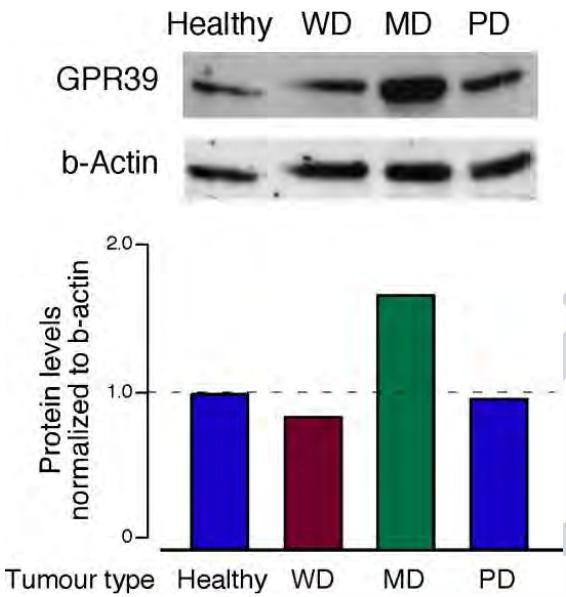

Figure 3.6. GPR39 expression in paraffin-embedded tissue samples of human stomach. GPR39 was observed in the four samples: human healthy stomach (healthy), a well differentiated (WD), a moderately differentiated (MD) and a poorly differentiated (PD) adenocarcinoma. Equal amounts of protein in each sample were used to assess the expression of GPR39 by Western blotting. Protein expression was normalized for actin.

In the WD adenocarcinoma compared with healthy mucosa sample FGFR2 (188.4±2.9%), IR (193.1±11.0%), VEGFR2 (155.7±2.9%), EphA1 (257.9±11.4%) and RYK (581.2±19.3%) were more activated in tumour tissue. Conversely, decreased phosphorylation levels in Erb2 (44.5±23.0%), Axl (42.5±8.0%), ROR2 (16.6±22.5%), and Tie1 (36.9±5.3%) were shown.

On the 49 RTKs evaluated on the array, significant phosphorylation changes were observed in 27 receptors in the MD adenocarcinoma. Erb4 (404.1±7.9%), FGFR2 (222.3±2.7%), FGFR3 (305.6±6.3%), FGFR4 (514.1±22.3%), IR (351.9±1.1%), IGF1R (207.6±7.0%), Mer (289.0±11.1%), hepatocyte growth factor receptor (HGFR, 236.7±8.4%), MSPR (162.7±1.9%), platelet derived growth factor receptor a (PDGFRa, 322.7±7.7%), PDGFRb (278.1±5.0%), Flt3 (399.0±4.5%), MCSFR (438.2±8.2%), c-Ret (420.2±3.4%), TrkA (321.1±18.7%), TrkC (238.6±3.3%), VEGFR1 (210.9±5.3%), VEGFR2 (167.5±2.9%), VEGFR3 (253.4±5.7%), MusK (333.6±1.3%), EphA1 (428.9±4.1%), ALK (466.5±8.6%), DDR1 (589.2±17.0%), EphA5 (425.5±9.4%) and EphA10 (259.3±2.0%), were highly activated. However, Axl (72.3±7.1%), and Tie1 (56.8±1.9%) levels were reduced.

In PD adenocarcinoma, 9 RTKs were differentially expressed compared to the healthy sample. Increased levels of IR (182.6±0.1%), Flt3 (206.4±10.1%), c-Ret (184.2±2.2%), MusK (168.2±0.8%), EphA1 (342.2±6.8%), EphA5 (263.5±8.1%), EphA10 (368.6±7.3) and EphB3 (231.9±13.8%) were detected. On the other hand, Axl (74.6±5.8%) activation were reduced.

Significant phosphorylation differences in ErbB3, FGFR1, Dtk, SCFR, ROR1, Tie2, DDR2 and the vast majority of EphR were not found.

EphA1 and insulin receptor were more activated in adenocarcinomas than in the mucosa healthy controls. Otherwise, Axl activation were down-regulated in tumour tissues.

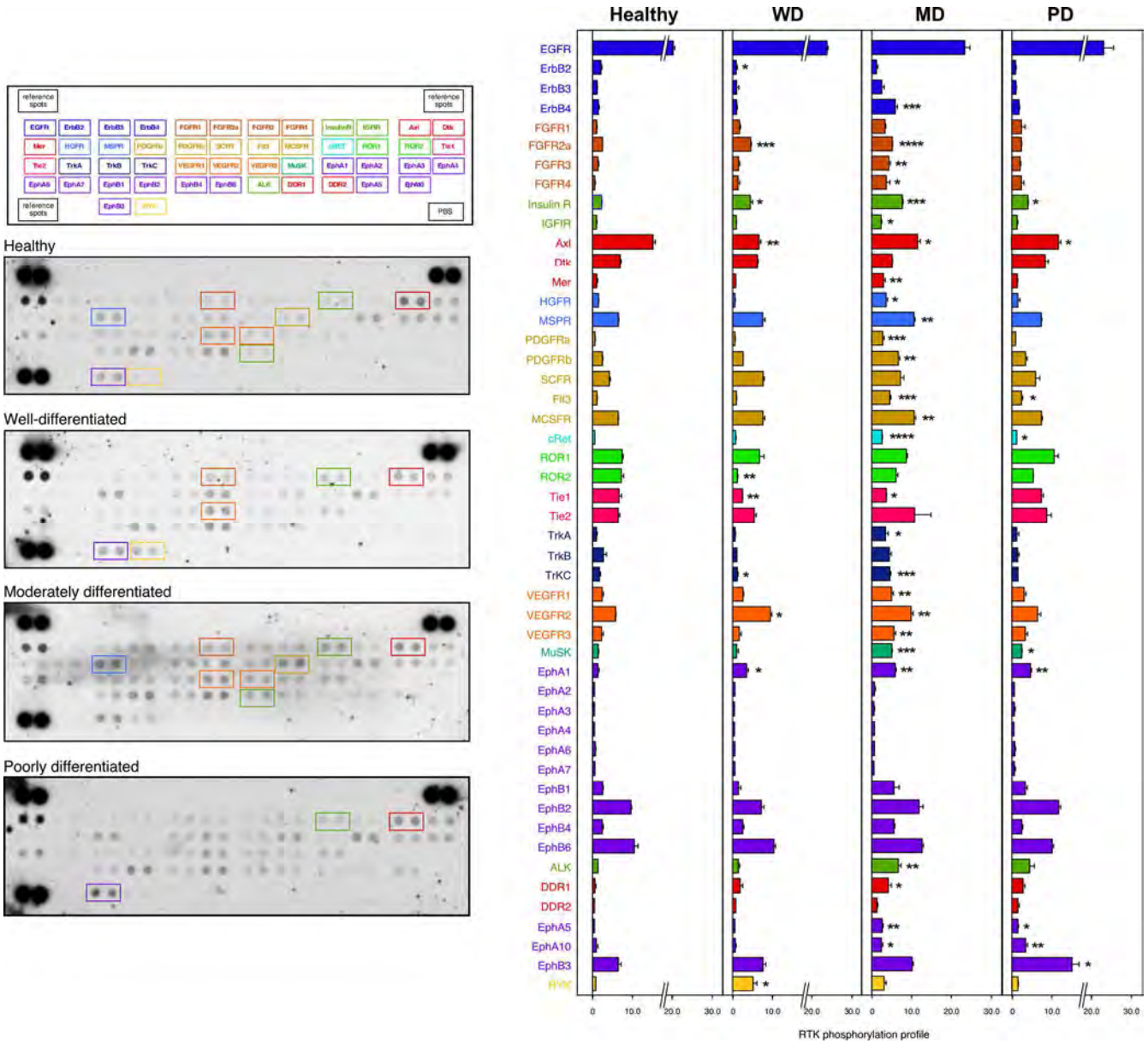

Figure 3.7. Differential expression of phosphorylated growth factor RTKs in human healthy mucosa and gastric adenocarcinomas. Out of the 49 RTKs analysed in the Phosphorylation of Receptor Tyrosine Kinases Array, 9 in WD, 27 in MD and 9 RTKs in PD adenocarcinomas were differentially activated ($P < 0.05$) compared to healthy mucosa. EphA1 and insulin receptor were more activated in all adenocarcinomas than in the mucosa healthy controls. Axl activation were down-regulated in tumour tissues. 200 µg of tissue lysate was run on each array.

Differential protease expression pattern in human adenocarcinomas

With regard to proteases, we performed protease expression arrays to determine their profiles in the same human stomach samples used in RTK arrays. The significant mean (n=2 dots) fold changes of expression were described below. The diverse proteases were differentially expressed in human healthy mucosa or gastric adenocarcinomas (**Figure 3.8**).

On the 34 proteases evaluated on the array, significantly expression changes were observed in 11 proteases in the WD adenocarcinoma compared with healthy mucosa sample. ADAM9 (116.9±3.0%), CTSX/Z/P (179.6±2.4%), KLK3 (128.8±2.0%) and KLK6 (150.1±4.5%) were more expressed in tumour tissue. Conversely, decreased levels in ADAMTS13 (53.6±6.6%), CTSB (74.6±3.3%), CTSS (68.7±1.6%), CTSV (54.1±4.6%), CTSD (39.7±7.1%), KLK7 (61.5±4.2%) and PSEN1 (79.7±7.8%) were observed.

In the MD adenocarcinoma, increased levels of CTSA (126.4±0.6%), CTSC (167.2±4.6%), CTSL (180.5±0.3%), CTSV (169.0±2.3%), CTSX/Z/P (329.8±1.3%); MMP1 (1634.0±4.6%), MMP2 (119.6±2.0%), MMP7 (470.2±5.8%), MMP9 (291.8±2.0%) and uPA (217.1±6.9%) were found. However, ADAMTS13 (75.4±4.7%), CTSD (65.7±0.5%), KLK7 (70.7±7.2%) and PSEN1 (76.6±2.8%) levels were reduced.

23 proteases were differentially expressed in PD adenocarcinoma compared to healthy sample. CTSA (143.3±3.1%), CTSD (189.6±1.6%), CTSL (151.4±4.7%), CTSX/Z/P (282.9±1.9%), KLK7 (311.3±0.9%), KLK10 (569.9±1.4%), MMP9 (507.9±2.4%), MMP12 (172.0±3.1%), and uPA (214.1±3.8%) were clearly overexpressed. By contrast, family of ADAM proteases, ADAM8 (42.7±3.8%), ADAM9 (39.4±1.9%) and ADAMTS13 (50.9±8.8%), CTSB (53.5±6.0%), CTSE (38.1±9.6%), CTSS (86.4±6.0%), DPPIV/CD26 (53.8±3.2%), KLK3 (48.9±4.8%), MMP2 (58.0±3.5%), MMP3 (53.5±17.9%), MMP8 (45.7±12.7%), MMP13 (42.7±17.6%), PC9 (44.6±6.3%) and PSEN1 (38.3±0.7%) were greatly reduced.

Significant differences in expression patterns of ADAMTS1, KLK5, KLK11 and KLK13 were not found.

ADAMTS13 and PSEN1 levels were more expressed in mucosa of the healthy control than in adenocarcinoma samples. Otherwise, CTSX/Z/P expression increased with the differentiation of the tumour.

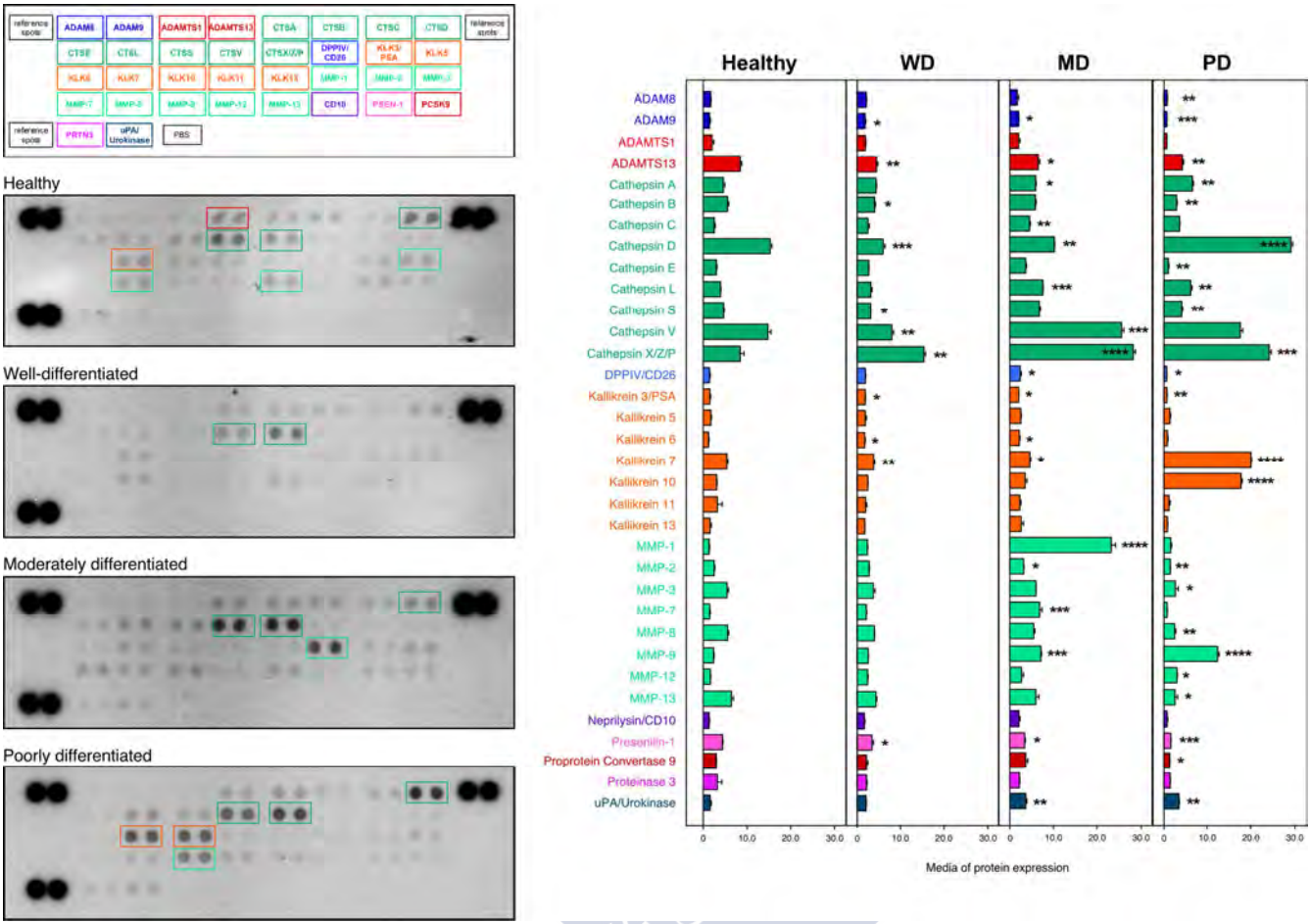

Figure 3.8. Differential expression of proteases in healthy stomach and gastric adenocarcinomas human samples. Out of the 34 proteases analysed in the array, 11 in WD, 18 in MD and 23 proteases in PD adenocarcinomas showed a different expression ($P < 0.05$) compared to healthy mucosa. ADAMTS13 and PSEN1 levels were more expressed in mucosa healthy controls than in all adenocarcinoma samples. CTSX/Z/P expression were higher as worse prognosis had the sample. 200 µg of tissue lysate was run on each array.

USC
UNIVERSIDADE
DE SANTIAGO
DE COMPOSTELA

CHAPTER 4: THE ROLE OF THE OBESTATIN/GPR39 SYSTEM IN HUMAN GASTRIC ADENOCARCINOMAS

Obestatin and the GPR39 receptor were reported to be involved in the control of mitogenesis of gastric cancer cell lines; however, the relationship between the obestatin/GPR39 system and gastric cancer progression remains unknown. In the present study, we determined the expression levels of the obestatin/GPR39 system in human gastric adenocarcinomas and explored their potential functional roles. Twenty-eight patients with gastric adenocarcinomas were retrospectively studied, and clinical data were obtained. The role of obestatin/GPR39 in gastric cancer progression was studied *in vitro* using the human gastric adenocarcinoma AGS cell line.[301]

OBESTATIN AND GPR39 ARE EXPRESSED IN AGS CELLS

As a model for this study, we selected the gastric adenocarcinoma AGS cell line. This cell line was derived from an untreated human adenocarcinoma of the stomach and retained the same cytological characteristics as the original malignant cells obtained from the patient.[302] As seen in Figure **4.1**, the expression of the obestatin/ GPR39 system was detected by immunocytochemistry. Intense and diffuse obestatin immunostaining was found in the cytoplasm **(Figure 4.1.1**), whereas GPR39 was detected in the perinuclear region (**Figure 4.1.3**). No immunostaining was found when obestatin or GPR39 antibodies were preadsorbed with homologous peptides (**Figure 4.1.2** and **4.1.4**, respectively).

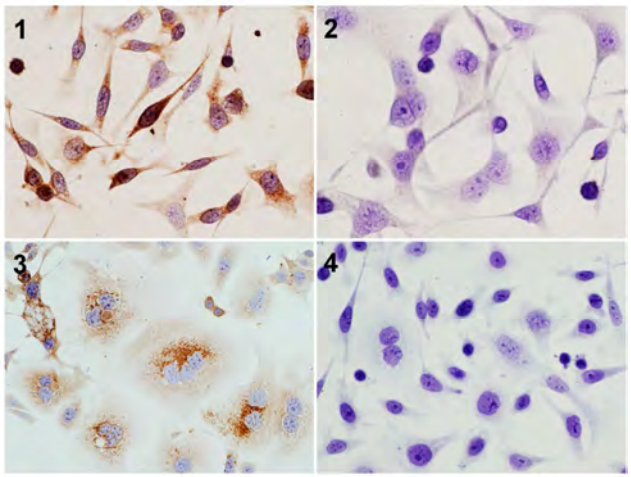

Figure 4.1. Obestatin and GPR39 are expressed in AGS cells. A) Immunocytochemical expression of obestatin and GPR39. 1) Obestatin immunoreactivity was intense and diffuse in the cytoplasm. 2) The preadsorption control [performed applying the primary antibody plus obestatin (10 nmol/mL per control peptide)] showed no immunoreactivity. 3) The expression of GPR39 presented a perinuclear location. 4) The preadsorption control [performed applying the primary antibody plus GPR39 control peptide (10 nmol/mL per control peptide)] showed no immunoreactivity. Objective magnification x20.

Moreover, an electron micrograph of obestatin expression showed a diffuse cytoplasmic pattern (**Figure 4.2.2**), while GPR39 was located in the mature face of the Golgi area, as well as a clear expression in the cell membrane, mainly located in the microvilli (**Figure 4.2.3** and **4.2.4**, respectively).

[301] Alén BO, Leal-López S, Alén MO*, et al*. The role of the obestatin/GPR39 system in human gastric adenocarcinomas. Oncotarget. 2016;7:5957-71.

[302] Barranco SC, Townsend CM Jr, Casartelli C*, et al*. Establishment and characterization of an in vitro model system for human adenocarcinoma of the stomach. Cancer Res. 1983;43:1703-9.

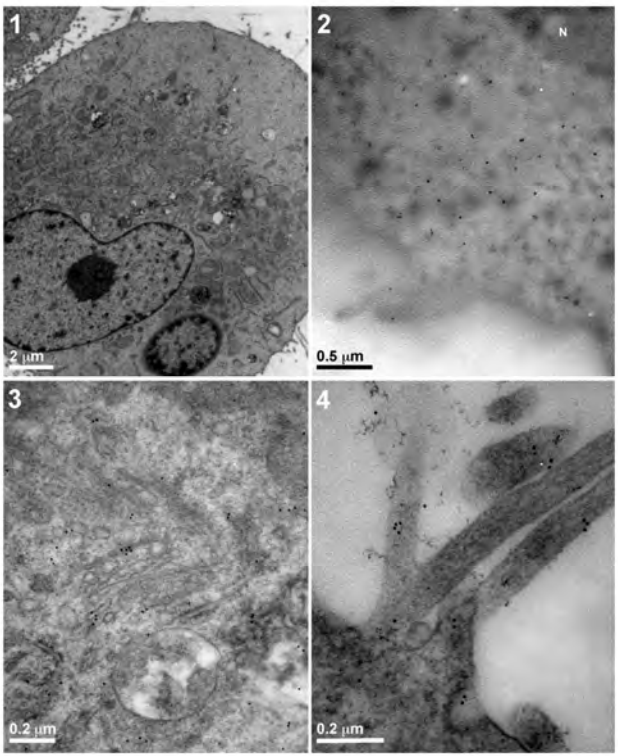

Figure 4.2. Electron micrograph of obestatin and GPR39 expression. 1) Morphology of the AGS cells in culture. 2) The expression of obestatin in the AGS cells showed a diffuse cytoplasmic pattern (gold particles). 3) The expression of GPR39 was located in the mature face of the Golgi area. 4) The expression of GPR39 was located in the cell membrane, mainly in the microvilli (gold particles).

OBESTATIN INDUCES PROLIFERATION IN AN AUTOCRINE/PARACRINE MANNER IN AGS CELLS

As **Figure 4.3** shows, obestatin (100 nM and 200 nM) exerted a mitogenic effect in the AGS cell line (162±1% and 181±2%, respectively) by means of BrdU incorporation. The neutralization of obestatin (100 nM) by anti-obestatin Ab preincubation diminished the BrdU incorporation to control levels. The autocrine/paracrine role of obestatin was tested by a combination of serum-free conditioned medium from AGS cells obtained at 24 and 48 h (CM24 and CM48, respectively) with neutralizing obestatin antibody.

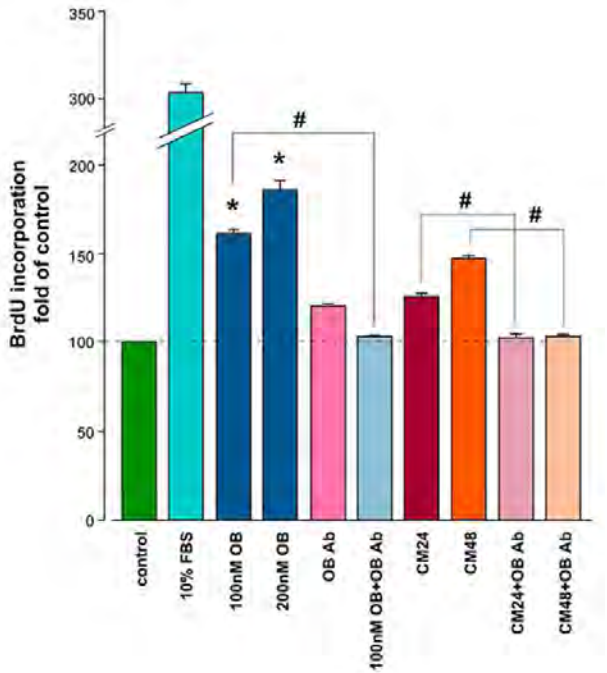

Figure 4.3. Mitogenic effect of obestatin in the AGS cells. AGS cells were treated with FBS (10%, v/v), OB (100 nM and 200 nM), OB-Ab (10 µg/mL), OB (100 nM) plus OB-Ab, CM24, CM48, CM24+OB-Ab and CM48+OB-Ab, and cell proliferation was evaluated after 48 h by means of BrdU incorporation. The data were expressed as a percentage of the basal proliferation of the untreated cells (Mean ± SEM). The asterisk (*) denotes $P<0.05$ when comparing the OB treated group with the control untreated group; the dagger (#) denotes $P<0.05$ when comparing the OB or CM plus OB Ab group with the OB or CM treated group.

The treatment of AGS cells with CM24 caused an increase in proliferation, which was completely abolished by CM24 + anti-obestatin Ab treatment. Similar results were obtained with the CM48 treatment, but with a higher impact. Likewise, the immunocytochemical analysis of the proliferation

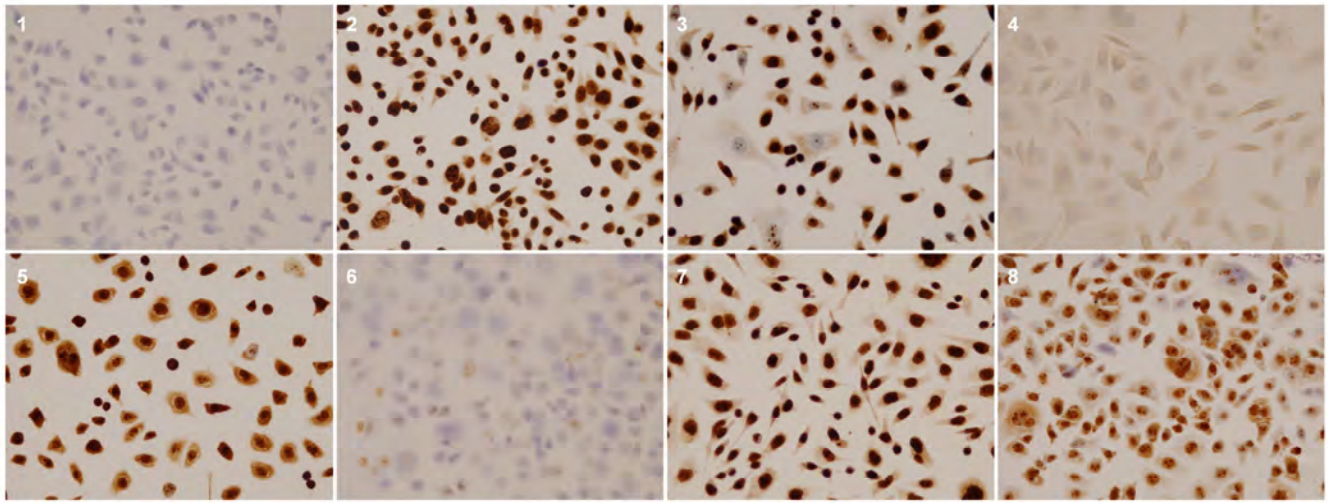

Figure 4.4. Immunocytochemical expression of Ki67 in AGS cells after 24 hour of proliferation. 1. Control without treatment. **2.** 10% FBS. **3.** 100nM OB. **4.** 100nM OB+OB-Ab (10 µg/mL). **5.** CM24. **6.** CM24+OB-Ab. **7.** CM48. **8.** CM48 +OB-Ab. Objective magnification x20.

marker Ki67[303] confirmed the proliferative activity of obestatin (**Figure 4.4**). The Ki67-immunopositive cells after obestatin treatment (100 nM, 24h; **Figure 4.4.3**) were similar to those obtained with FBS (**Figure 4.4.2**). Anti-obestatin Ab clearly reduced the Ki67 expression levels with respect to standard conditions (**Figure 4.4.4**). Furthermore, the presence of the anti-obestatin Ab reduced the Ki67 expression of AGS cells treated with CM24 (**Figure 4.4.6** and **4.4.5**, respectively), whereas Ab treatment partly decreased Ki67 expression in CM48-treated cells (**Figure 4.4.8** and **4.4.7**, respectively). This discrepancy with CM24 might be due to the numerous factors secreted by the cells, which were present in CM after 48 h.

OBESTATIN PROMOTES CELL MOBILITY AND INVASION *VIA* EMT AND CYTOSKELETON REMODELLING IN AGS CELLS

AGS cells are organized in clusters of polygon-shaped cells, few actin short stress fibres, and no lamellipodia with their cobblestone-like phenotype. These actin filaments in the form of stress fibres and the thin network formed at the edges could be depolymerized by the removal of serum, although the phenomenon was reversible when the cells were returned back to serum containing medium.[304] We then analysed the effect of obestatin on the morphology and cytoskeleton in serum-free medium to avoid interference (**Figure 4.5**). Under these conditions, obestatin treatment (200 nM, 24 h) promoted the dissociation of the cell clusters and induced cellular elongation with the formation of filopodia-like

[303] Schlüter C, Duchrow M, Wohlenberg C, *et al*. The cell proliferation-associated antigen of antibody Ki-67: a very large, ubiquitous nuclear protein with numerous repeated elements, representing a new kind of cell cycle-mantaining proteins. J Cell Biol. 1993;123:513-22.

[304] Palovuori R, Perttu A, Yan Y, *et al*. *Helicobacter pylori* induces formation of stress fibers and membrane ruffles in AGS cells by Rac activation. Biochem Biophys Res Commun. 2000;269:247-53.

structures (blue arrows) and lamellipodia-like structures (green arrows) typical of motile cells. Obestatin also induced strong actin polymerization including the development of stress fibres (pink arrows). Obestatin-treated cells presented the scattering/hummingbird-like phenotype previously reported in the case of *H. pylori* infection, mimicking an EMT.[305]

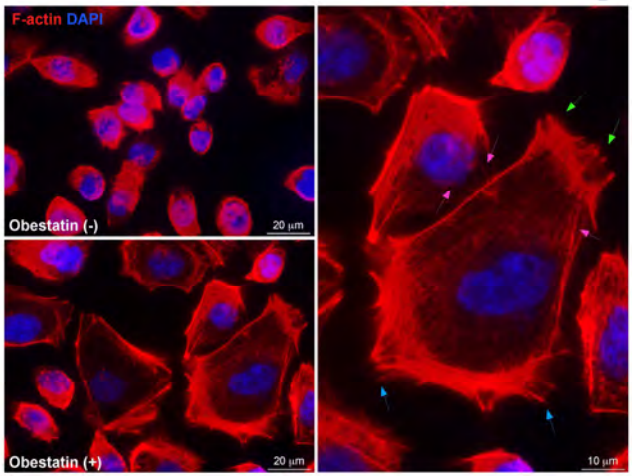

Figure 4.5. Effect of obestatin on the cytoskeleton reorganization in AGS cells. The AGS cells were stimulated with 200 nM OB for 24 h. Cells were stained with Phalloidin CruzFluor-594 (red) to visualize F-actin and DAPI (blue) to visualize the nucleus. Scale bar=20 µm. The image at the right represents a higher magnification view of the obestatin treated cells (scale bar=40 µm). Obestatin treatment induced cellular elongation with the formation of filopodia-like structures (blue arrows), lamellipodia-like structures (green arrows) and the development of stress fibres (pink arrows). Images are representative for at least three independent experiments.

We analysed whether obestatin was driving cell migration using a wound-healing assay. As shown in **Figure 4.6**, obestatin-treated cells exhibited a significant increase in their migration capability when compared with the control ($P < 0.05$, **Figure 4.6**).

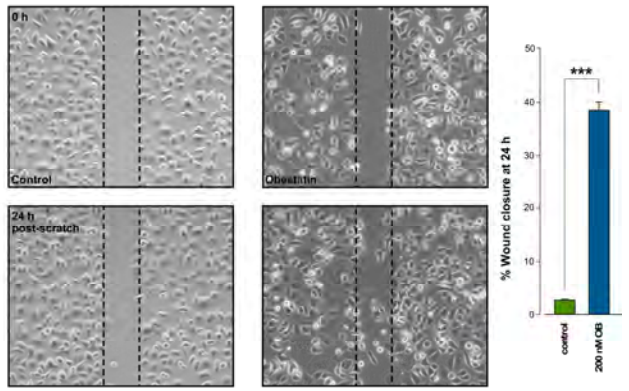

Figure 4.6. Migration of AGS cells promoted by obestatin. The AGS cells were treated or not with obestatin (200 nM). The wound was calculated by tracing along the border of the scratch using ImageJ64 analysis software and the following equation: %wound closure=[[wound area (0 h)-wound area (x h)]/ wound area (0 h)] x 100. The asterisk (***) denotes $P<0.001$ when comparing the treated with the untreated control group.

Additionally, the inverted version of the classical Boyden chamber invasion assay[222] (**Figure 4.7**), showed that the AGS cells were able to migrate through the membrane, mimicking basement membrane invasion and invade into the Matrigel as an extracellular matrix when obestatin was applied on top of the Matrigel as a chemoattractant (200 nM). The extent of cell invasion was quantified by measuring the fluorescence intensity at each confocal section every 5 µm from the membrane, and the differences between the untreated and treated cells were statistically significant ($P < 0.001$; **Figure 4.7 right panel**).

[305] Bessède E, Staedel C, Acuña-Amador LA, *et al*. *Helicobacter pylori* generates cells with cancer stem cell properties via epithelial-mesenchymal transition-like changes. Oncogene. 2014;33:4123-31.

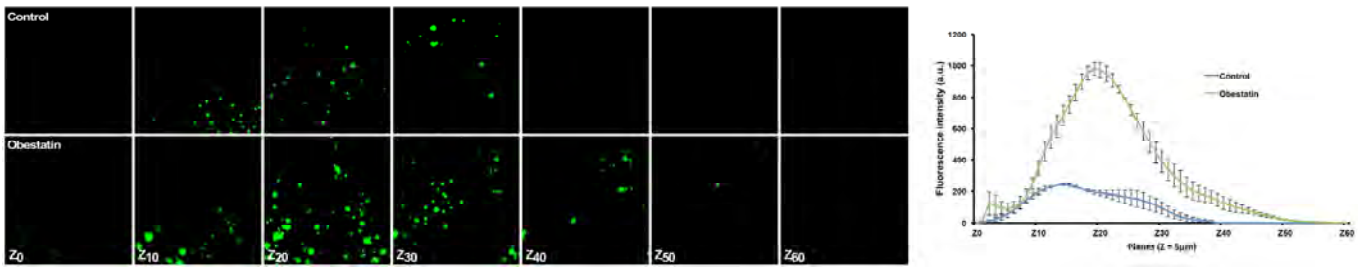

Figure 4.7. Obestatin promotes invasion in AGS cells. Sequential confocal microscopy sections scanned every 5 µm from the membrane to the top of the Matrigel in an inverted invasion assay. Obestatin (200 nM) was used as a chemoattractant. **Right panel.** Mean fluorescence intensity (a.u.) quantified at the indicated sequential confocal sections. Bars, SEM; *** *P*<0.001.

EMT is proposed to regulate the acquisition of migratory and invasive capability, which is a crucial mechanism in the initial steps in of metastatic progression.[306] Because obestatin increased migration and invasion, we assessed obestatin's influence on EMT by examining the expression of E-cadherin, β-catenin, vimentin, and N-cadherin (**Figure 4.8**). Obestatin treatment (200 nM) increased β-catenin (active form) and N-cadherin levels after 12 h (127±7% and 112±3%, respectively), whereas vimentin levels showed an intense augmentation along the tested period of time with a maximum at 24 h (158±19%). E-cadherin was not detected in the AGS cells, at least at the limits of immunoblot detection (data not shown). Indeed, this cell line harboured an E-cadherin mutation, leading to a truncated form of the protein that is not expressed.[307]

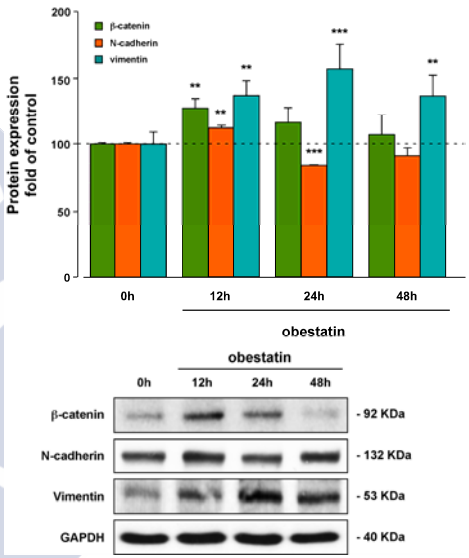

Figure 4.8. Immunoblot analysis of the EMT in AGS cells. The AGS cells were stimulated with obestatin (200 nM) for 12, 24, and 48 h and the blots were incubated with the corresponding antibodies to N-cadherin, β-catenin and vimentin. The protein expression was normalized relative to GAPDH. The data were expressed as mean±SEM obtained from intensity scans of six independent experiments. The asterisk (*, **, ***) denotes *P*<0.05, *P*<0.01 and *P*<0.001 when comparing the treated with the untreated control group.

[306] Wu WK, Cho CH, Lee CW, *et al*. Dysregulation of cellular signaling in gastric cancer. Cancer Lett. 2010;295:144-53.

[307] Oliveira MJ, Costa AM, Costa AC, *et al*. CagA associates with c-Met, E-cadherin, and p120-catenin in a multiproteic complex that suppresses *Helicobacter pylori*-induced cell-invasive phenotype. J Infect Dis. 2009;200:745-55.

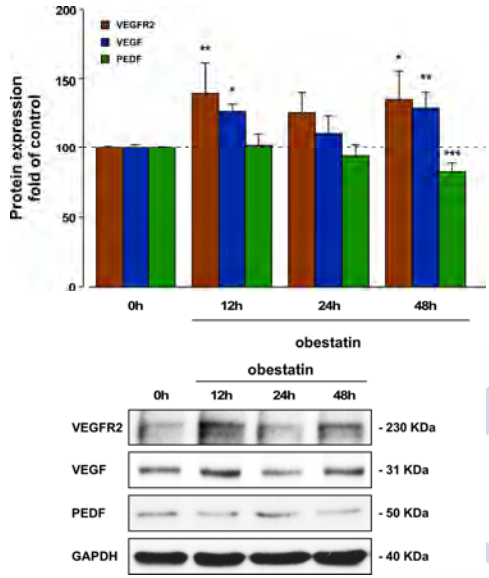

Figure 4.9. Immunoblot analysis of the pro-angiogenic activation of obestatin in AGS cells. The AGS cells were stimulated with obestatin (200 nM) for 12, 24, and 48 h and the blots were incubated with the corresponding antibodies to VEGF, VEGFR2 and PEDF. The protein expression was normalized relative to GAPDH. The data were expressed as mean±SEM obtained from intensity scans of six independent experiments. The asterisk (*, **, ***) denotes *P*<0.05, *P*<0.01 and *P*<0.001 when comparing the treated with the untreated control group.

Regarding the VEGF/VEGFR2 system, obestatin increased the VEGF and VEGFR2 levels at 12 h and 48 h (VEGF: 126±5% and 128±12%; VEGFR2: 140±21% and 134±20%, respectively; **Figure 4.9**), whereas it decreased the anti-angiogenic factor PEDF levels with a significant minimum at 48 h (72±7%).

OBESTATIN EXERTS ITS ACTIONS THROUGH THE GPR39 RECEPTOR IN AGS CELLS

First, the effect of acute GPR39 deficiency on obestatin signalling was determined by treatment of AGS cells with a GPR39 siRNA. Under these conditions, the constructs decreased GPR39 expression by 65±2% (**Figure 4.10**).

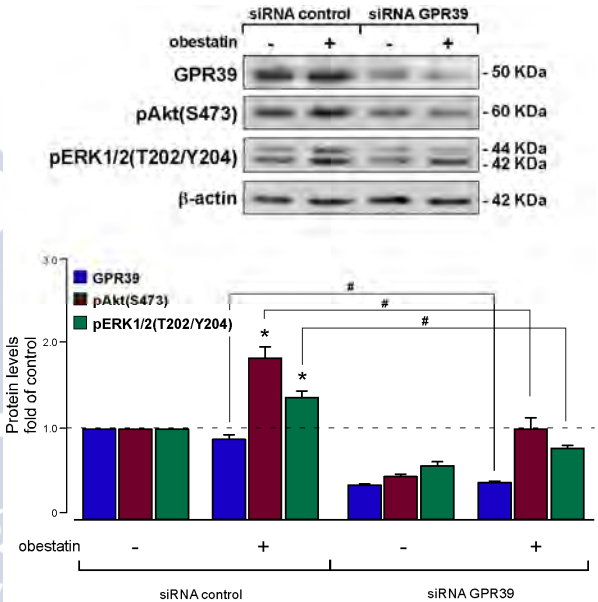

Figure 4.10. Effect of GPR39 knockdown by siRNA on obestatin-activated pAkt(S473) and pERK1/2(T202/Y204) in AGS cells. The AGS cells were transfected with GPR39 siRNA prior to obestatin treatment (200 nM, 10 min). GPR39 was expressed as a fold of its level to control siRNA-transfected cells (n=3). Activation of Akt [pAkt(S473)] and ERK1/2 [pERK1/2(T202/Y204)] was expressed relative to the control siRNA-transfected cells. Equal amounts of protein in each sample were used to assess the expression of GPR39 by western blotting. The level of proteins was expressed as fold change relative to the control siRNA-transfected cells (mean±SEM). The protein expression was normalized relative to actin. The data were expressed as mean±SEM obtained from intensity scans of independent experiments. The asterisk (*) denotes *P*<0.05 when comparing the treated control siRNA group with the control siRNA group; the dagger (#) denotes *P*<0.05 when comparing the GPR39 siRNA group with the control siRNA group.

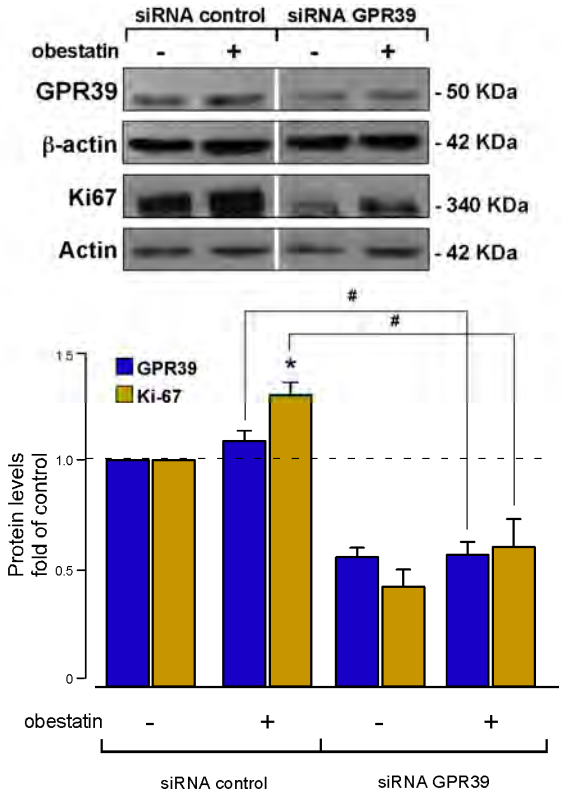

Figure 4.11. Effect of SiRNA depletion of GPR39 on obestatin-activated Ki67 expression in AGS cells. The AGS cells were transfected with GPR39 siRNA prior to obestatin treatment (200 nM, 24 h). Expression of Ki67 was denoted as a fold of the respective levels in control siRNA-transfected cells (n=3). Equal amounts of protein in each sample were used to assess the expression of GPR39 by western blotting. The level of proteins was expressed as fold change relative to the control siRNA-transfected cells (mean±SEM). The protein expression was normalized relative to actin. The data were expressed as mean±SEM obtained from intensity scans of independent experiments. The asterisk (*) denotes $P<0.05$ when comparing the treated control siRNA group with the control siRNA group; the dagger (#) denotes $P<0.05$ when comparing the GPR39 siRNA group with the control siRNA group.

In the presence of an si-control, the obestatin-activated Akt(S473) and ERK1/2(T202/Y204) phosphorylations were identical to the levels observed with the untransfected cells (data not shown). The silencing of GPR39 decreased subsequent pAkt(S473) and pERK1/2(T202/Y204) with respect to the control siRNA by 43±3% and 40±4% upon treatment of obestatin (200 nM, 10 min; **Figure 4.10**), respectively. Second, the effect of acute GPR39 deficiency on Ki67 expression was evaluated. Under these conditions, the constructs decreased GPR39 expression by 53±7% (**Figure 4.11**). The GPR39 knockdown decreased obestatin-induced Ki67 expression by 70±4% (**Figure 4.11**) with respect to si-control. Immunocytochemistry confirmed decreased levels of Ki67 in GPR39 knockdown cells compared with control cells (**Figure 4.12**).

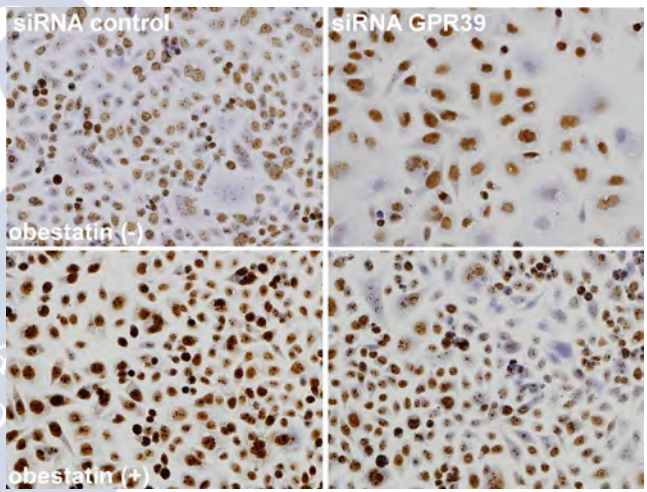

Figure 4.12. Effect of GPR39 knockdown by siRNA on the immunocytochemical expression of obestatin-activated Ki67 in AGS cells. The AGS cells were transfected with GPR39 siRNA prior to obestatin treatment (200 nM, 24 h). 1) siRNA control without treatment. 2) siRNA GPR39 without treatment. 3) siRNA control plus OB. 4) siRNA GPR39 plus OB. Objective magnification x20.

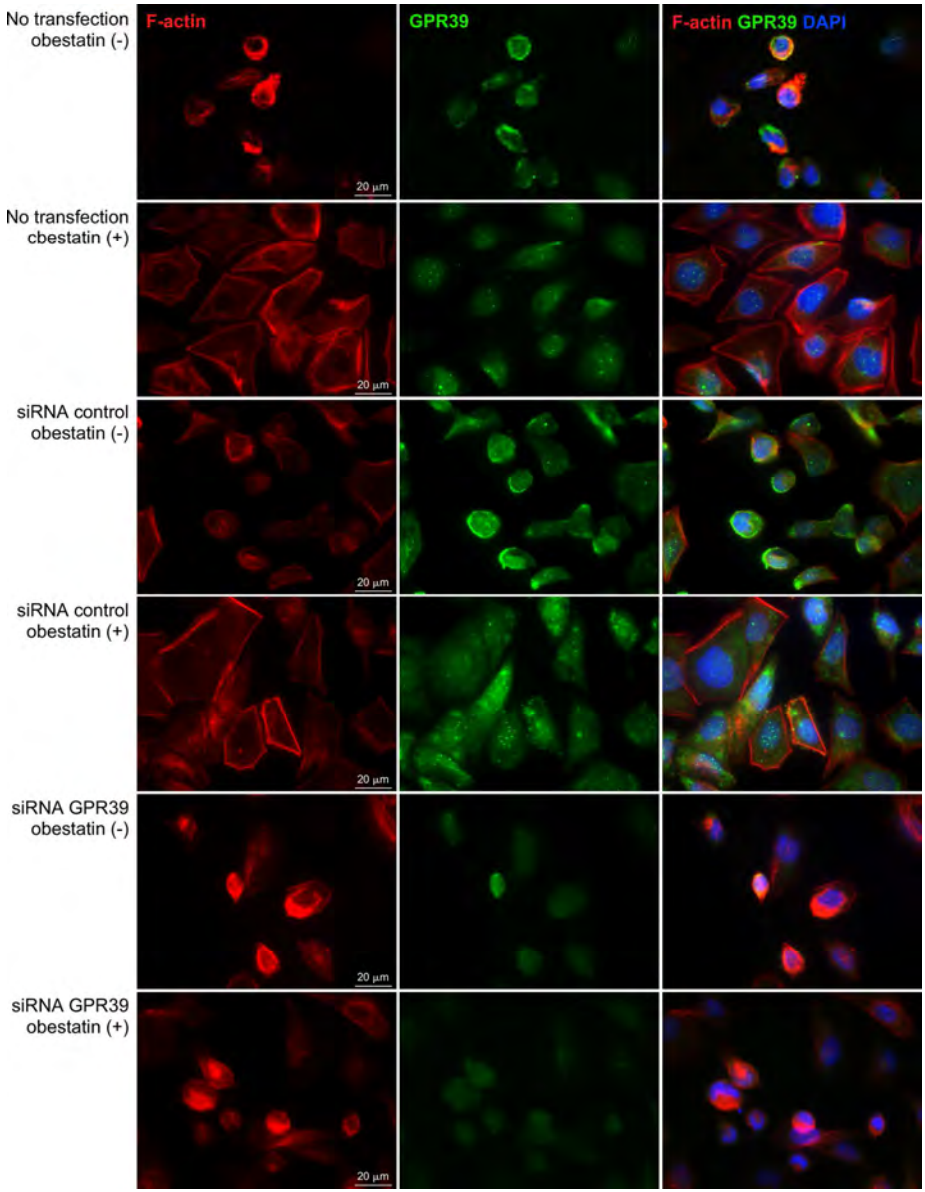

Figure 4.13. Effect of GPR39 knockdown by siRNA on the cytoskeleton reorganization in AGS cells. The AGS cells were transfected or not with GPR39 siRNA prior to obestatin treatment (200 nM, 24 h). Cells were stained with Phalloidin CruzFluor-594 (red) to visualize F-actin, anti-GPR39 antibody (green) to visualize the knockdown of the receptor and DAPI (blue) to visualize the nucleus. Objective magnification x63. Scale bar=20 µm. Images are representative for at least three independent experiments.

The above results implicated the obestatin/GPR39 system in EMT and cell motility, possibly by cytoskeletal modulation. Consistent with a role in actin polymerization, the GPR39 knockdown cells exhibited depolymerization and redistribution of the cellular F-actin, diminishing lamellipodia formation compared to the control cells after obestatin treatment (**Figure 4.13**). Taken together, these results suggest that the obestatin/GPR39 system induces cytoskeleton remodeling to facilitate AGS cell migration and invasion.

GPR39 AND OBESTATIN EXPRESSION IN HUMAN HEALTHY STOMACH TISSUE

As shown in **Figure 4.14**, no GPR39 expression was detected in the mucous cells of the gastric pits. Weak positivity was observed in parietal cells, whereas intense immunostaining was present in the chief cells located at the base of the oxyntic glands (**Figure 4.14.A** and **4.14.B**). Regarding obestatin expression, the obestatin-IR endocrine cells were localized from the neck to the base of the gastric glands in the oxyntic mucosa (**Figure 4.14.C** and **4.14.D**). These cells were small and roundish and showed typical morphology of closed-type endocrine cells, which were devoid of elongation contacting the lumen.[34]

GPR39, OBESTATIN AND Ki67 EXPRESSION IN HUMAN GASTRIC ADENOCARCINOMAS

The characteristics of the patient samples and the results obtained in the gastric adenocarcinomas studied are summarized in **Table 4.1**.

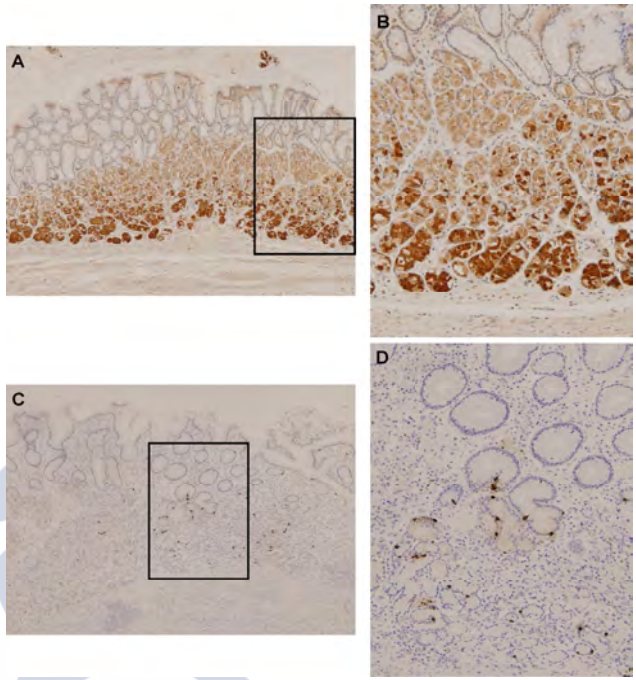

Figure 4.14. GPR39 and obestatin are expressed in human healthy stomach tissue. Immunohistochemical expression of GPR39 and obestatin in normal stomach. A) There was no GPR39 expression in the mucous cells of the gastric pits. A weak positivity was observed in parietal cells, whereas an intense immunostaining was present in the chief cells. Objective magnification x4. B) Higher magnification view (x10) of the GPR39 immunostaining in the chief cells. C) Obestatin immunoreactivity was only observed in neuroendocrine cells of oxyntic glands (x4). D) At higher magnification, obestatin producing cells were recognized as small round or spindle cells with brownish staining in the cytoplasm (x10).

Laurén classification	Age	Sex	Size (cm)	TNM staging	obestatin	GPR39	Ki67 (%)
Well differentiated							
Intestinal	72	F	3.0	pT4N2M1	NM-NC	2+, homogeneous	39
Intestinal	81	F	6.8	pT2bN1	0	1+ homogeneous	44
Intestinal	67	M	3.5	pT4N3M1	NM-NC	1+ heterogeneous	48
Intestinal	53	M	5.0	pT3N1	NM-NC	1+ heterogeneous	59
Intestinal	81	F	4.3	pT2	NM-NC	1+ heterogeneous	53
Intestinal	83	M	1.7	pT1N0	NM-NC	0 homogeneous	66
Intestinal	69	F	4.3	pT4	0	1+ homogeneous	37
Intestinal	76	M	4.3	pT3N1	NM-NC	2+, heterogeneous	37
Intestinal	81	M	7.5	pT3N3	NM-NC	2+	71
Moderately differentiated							
Intestinal	88	F	6.5	pT3	0	1+	53
Intestinal, with SRC	84	F	7.0	pT4N3M1	NM-NC	1+	79
Intestinal	68	F	6.8	pT4N3	0	2+ heterogeneous	72
Intestinal	53	F	2.0	pT4N1	0	1+	49
Intestinal	40	M	2.1	pT4	0	2+	69
Intestinal	72	M	7.5	pT4N3	NM-NC	2+	37
Intestinal	49	F	4.2	pT3N1	0	2+	93
Intestinal	82	F	7.5	pT4N3	0	2+, heterogeneous	81
Intestinal	61	M	5.1	pT4N2	NM-NC	2+	51
Intestinal	85	M	7.5	pT4N0	NM-NC	1+	68
Poorly differentiated							
Intestinal	76	M	7.0	pT3N3Mx	0	2+	21
Diffuse, with SRC	58	F	1.6	pT2Nx	NM-NC	2+, SRC negative	20
Mixed	67	M	5.7	pT3N3	NM-NC	2+	19
Mixed, with SRC (<50%)	80	F	7.5	pT3N0	NM-NC	3+	37
Diffuse	78	F	6.0	pT4N0	NM-NC	2+	23
Intestinal	85	M	6.5	pT2N1	NM-NC	3+	63
Mixed, with SRC	79	F	4.9	pT4N1	0	3+	31
Intestinal	64	M	4.5	pT4N2	0	3+	30
Diffuse, with SRC	62	F	2.3	pT2N1	0	2+, heterogeneous	47

Table 4.1. Summary of the characteristics and the obestatin, GPR39 and Ki67 immunostaining results of the gastric adenocarcinomas studied. NM-NC: Normal mucosa neuroendocrine cells; SRC: signet ring cells.

Figure 4.15 shows the results obtained for obestatin, GPR39, and Ki67 in the samples of human gastric adenocarcinomas, represented by a WD and a PD adenocarcinoma (**Figure 4.15.A** and **4.15.B**, respectively). In these samples, obestatin (**Figure 4.15.A.1** and **4.15.B.1**) was negative in all of the gastric adenocarcinomas studied (**Figure 4.15.A.3** and **4.15.B.3**), whereas intense staining was found in the neuroendocrine cells of the healthy gastric mucosa (**Figure 4.15.A.2** and **4.15.B.2**), although it was negative in the rest of the oxyntic mucosa. By contrast, GPR39 positivity was present in all of the tumours with varying intensity according to the classification of the samples. Lower expression was found in WD tumours (mostly 1+), and the highest expression was observed in the PD adenocarcinomas (2+/3+ or 3+, predominantly). The Golgi staining was more intense, in general, for the WD adenocarcinomas (**Figure 4.15.A.4** and **4.15.A.5**), was diminished for the MD and was not detectable in the majority of the analysed PD adenocarcinomas, although three of them presented high positivity in the Golgi area (**Figure 4.15.B.4** and **4.15.B.5**).

Ki67 immunohistochemistry using an MIB-1 antibody was used to evaluate the proliferative activities. Ki67 immunohistochemistry produced a mean Ki67 proliferative index (PI) of 50.4%±1.6 in the WD, 65.2%±1.9 in MD and 29.5%±1.8 in PD adenocarcinomas (**Figure 4.15.C**: WD/MD, ***P<0.001; MD/PD, *P<0.05; and WD/PD, *P<0.05). These results support previous data demonstrating that low Ki67 PI might lead to an unfavorable prognosis as it has been correlated to poorly differentiated histology, an advanced T stage, lymph node metastasis, and greater expression of EMT-related proteins.[308] Strong and enigmatic male dominance has been described in the incidence of gastric cancer with a male-to-female ratio of approximately 2:1, and these differences may be related to the protective effect of estrogens, especially for the intestinal-type adenocarcinomas.[309] Regarding Ki67 expression, we observed the following results for males: WD, 56.2%±6.2; MD, 56.2%±7.6; and PD: 33.3%±10.2. For female patients, the results were as follows: WD, 45.5%±3.4; MD, 71.2%±6.9; and PD, 31.6%±4.9, with statistically significant differences between WD/MD, and MD/PD (*P<0.05 and **P<0.01, respectively). However, the results for GPR39 expression correlated with the dedifferentiation of the tumour, with increased expression from WD (1.22 a.u.±0.2), MD (1.60 a.u.±0.2), to PD (2.44 a.u.±0.2) (**Figure 4.15.D**: WD/PD, **P<0.01; and MD/PD, **P<0.01; **Figure 4.15.D**). The expression levels organized by sex followed the same tendency, although the differences between the groups were statistically significant only in females (WD/PD, *P<0.05; and MD/PD, *P<0.05). These patterns of expression are summarized in **Figure 4.15.C** and **4.15.D**, and **Table 4.2** shows the correlations in these samples.

[308] Lee HE, Kim MA, Lee BL, et al. Low Ki-67 proliferation index is an indicator of poor prognosis in gastric cancer. J Surg Oncol. 2010;102:201-6.

[309] Chandanos E, Lagergren J. Oestrogen and the enigmatic male predominance of gastric cancer. Eur J Cancer. 2008;44:2397-403.

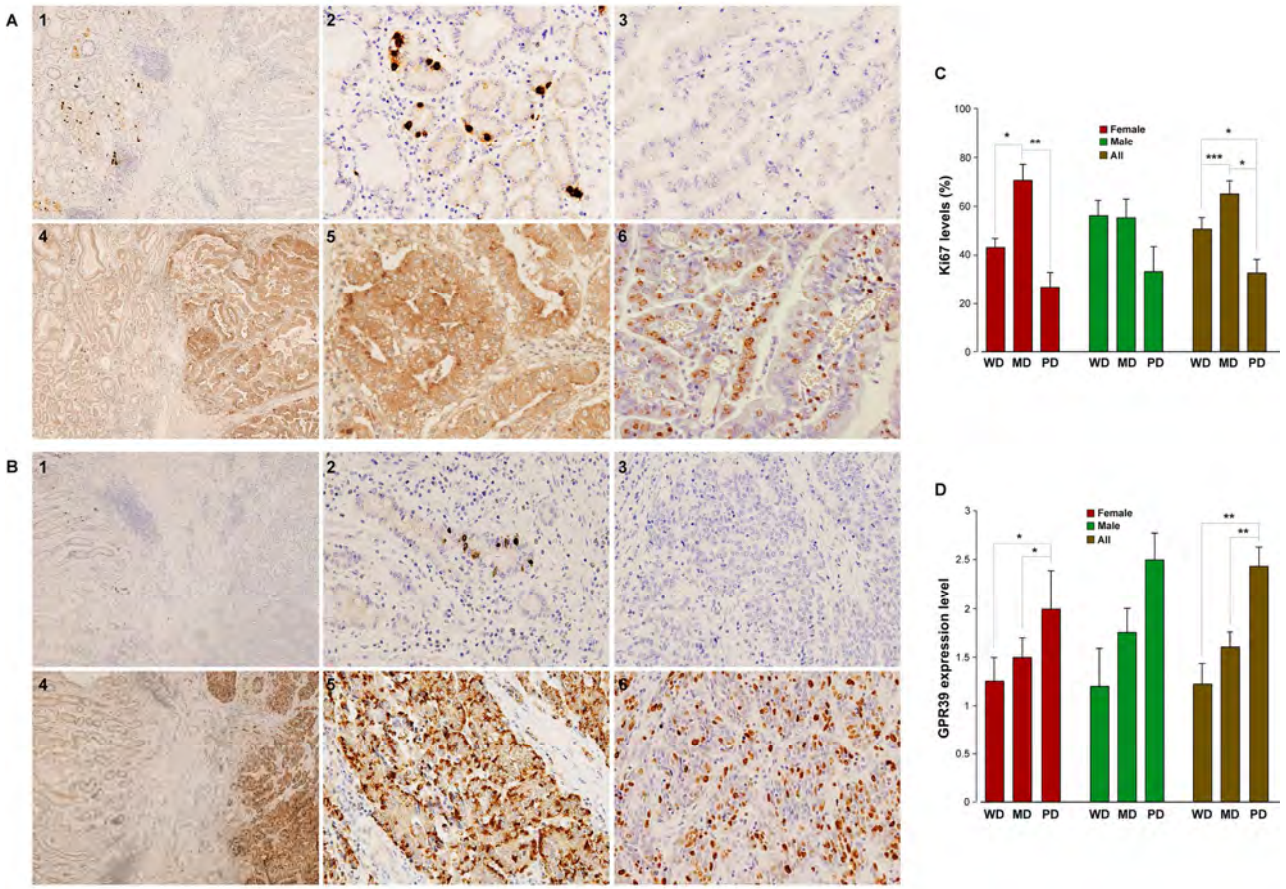

Figure 4.15. GPR39, obestatin and Ki67 expression in human gastric adenocarcinomas. A. Immunohistochemical expression of obestatin, GPR39, and Ki67 in a well differentiated gastric adenocarcinoma. 1) Obestatin expression is negative in all gastric adenocarcinomas studied. Positive expression of obestatin is only observed as an intense stain in neuroendocrine cells of gastric mucosa, being negative in mucous cells of the gastric pits and in the rest of the fundic glands. Objective magnification x4. 2) Higher magnification view of obestatin positivity in the healthy surround of the tumour (x20). 3) Obestatin expression is negative in the well-differentiated gastric adenocarcinoma (x20). 4) The intense expression of GPR39 is present in the tumour, whereas no immunostaining was found in the superficial areas of the mucosa (x4). 5) Higher magnification view of GPR39 positivity (x20). 6) Low Ki67 expression was found in this well-differentiated adenocarcinoma. **B. Immunohistochemical expression of obestatin and GPR39 in a poorly differentiated gastric adenocarcinoma.** 1) Obestatin expression is negative in all gastric adenocarcinomas studied. Positive expression of obestatin is only observed as an intense stain in neuroendocrine cells of gastric mucosa, being negative in mucous cells of the gastric pits and in the rest of the fundic glands (x4). 2) Higher magnification view of obestatin positivity in the healthy surround of the tumour (x20). 3) Obestatin is negative in the poorly differentiated gastric adenocarcinoma (x20). 4) The intense expression of GPR39 is present in the tumour, whereas no immunostaining was found in the superficial areas of the mucosa (x4). 5) Higher magnification view of GPR39 positivity (x20). 6) High Ki67 expression was found in this poorly differentiated adenocarcinoma. **C. Graphical representation of the Ki67 levels of expression in the studied gastric adenocarcinomas.** The asterisk (*, **, ***) denotes *P*<0.05, *P*<0.01 and *P*<0.001 when comparing groups. **D. Graphical representation of the GPR39 levels of expression in the studied gastric adenocarcinomas.** The asterisk (*, **, ***) denotes *P*<0.05, *P*<0.01 and *P*<0.001 respectively, when comparing groups.

	Age	Sex	Size	Differentiation	GPR39	Ki67 expression
Age	-	0.640	0.002**	0.797	0.682	0.823
Sex	0.09	-	0.812	0.651	0.902	0.780
Size	0.57	-0.05	-	0.477	0.217	0.633
Differentiation	-0.05	0.9	0.14	-	0.000***	0.049*
GPR39	-0.08	-0.02	0.24	0.66	-	0.182
Ki67 expression	-0.04	0.06	0.09	-0.37	-0.26	-

Table 4.2. Pearson Correlation of the data. Correlation coefficient (r) below and *P*-values above the diagonal. * means significant at the 0.05 level (2-tailed); ** means significant at the 0.01 level (2-tailed); and *** means significant at the 0.001 level (2-tailed). N = 28.

USC
UNIVERSIDADE
DE SANTIAGO
DE COMPOSTELA

CHAPTER 5: PEPSINOGEN I SECRETION: THE FUNCTION OF THE OBESTATIN/GPR39 SYSTEM IN HUMAN STOMACH

In previous chapters we described the expression of obestatin/GPR39 system in healthy human stomach as well as in human gastric adenocarcinomas. The positivity found for GPR39 in the chief cells of healthy stomach samples prompted us to investigate the relationship between the obestatin/GPR39 system and the secretion of pepsinogen in an *in vitro* model that endogenously expressed the three components of the study: obestatin, GPR39 and pepsinogen.

GPR39 receptor and pepsinogen PGI expression was determined in human stomach samples by immunohistochemistry. PGI secretion after exogenous administration of obestatin was determined by the haemoglobin method and by immunoblot in the gastric adenocarcinoma cell line AGS. The influence of the acute GPR39 deficiency on PGI secretion after obestatin treatment was determined using siRNA knockdown of GPR39.

GPR39 IS EXPRESSED IN THE CHIEF CELLS OF THE OXYNTIC MUCOSA OF THE HUMAN STOMACH

In chapter 4 it was reported the expression of the GPR39 receptor and obestatin in the healthy mucosa of the stomach and their implication in the development of gastric adenocarcinomas. Obestatin positive expression was found exclusively in the neuroendocrine cells localized from the neck to the base of the gastric glands in the oxyntic mucosa (**Figure 4.13.C**). Concerning the GPR39 expression, intense positivity was found in the chief cells of the oxyntic glands (**Figure 5.1.A**). GPR39 positivity was also detected in a few cells located between the neck and the base of the glands. These cells might be immature chief cells migrating towards the base of the oxyntic gland, namely, pre-chief cells or transitional cells. Indeed, it has been described that chief cells derive from an intermediate cell type, characterized by abundant mucinous vesicles in the neck of the gland, the mucous-neck cells, through a process of transdifferentiation.[310]

Regarding pepsinogen I, intense staining was observed in the chief cells of the oxyntic mucosa. The mentioned cells were filled with numerous large secretion granules showing specific labelling for pepsinogen I (**Figure 5.1.F**). This positivity was also found in mucous cells of the glandular necks (mucous neck cells) and in a few cells located at the boundaries between the neck and the base (**Figure 5.1.D**). **Figure 5.2** shows detailed zones of the neck region of the oxyntic glands. The serial sections (3 µm) utilized for the immunohistochemistal technique, showed that the mucous neck cells were pepsinogen I positive and GPR39 negative, and that the pre-chief cells were positive for both proteins (**Figure 5.2.C** and **5.2.F**).

To confirm this finding, we studied GPR39 and pepsinogen expression by immunofluorescence. As shown in **Figure 5.3**, the pre-chief cells immunoreactive for GPR39 (green) were also positive for pepsinogen I (red). In addition, a few mucous neck cells were found to be strongly immunolabelled for pepsinogen I but negative for GPR39 (**Figure 5.3.C**).

[310] Goldenring JR, Nam KT, Mills JC. The origin of pre-neoplastic metaplasia in the stomach: chief cells emerge from the Mist. Exp Cell Res. 2011;317:2759-64.

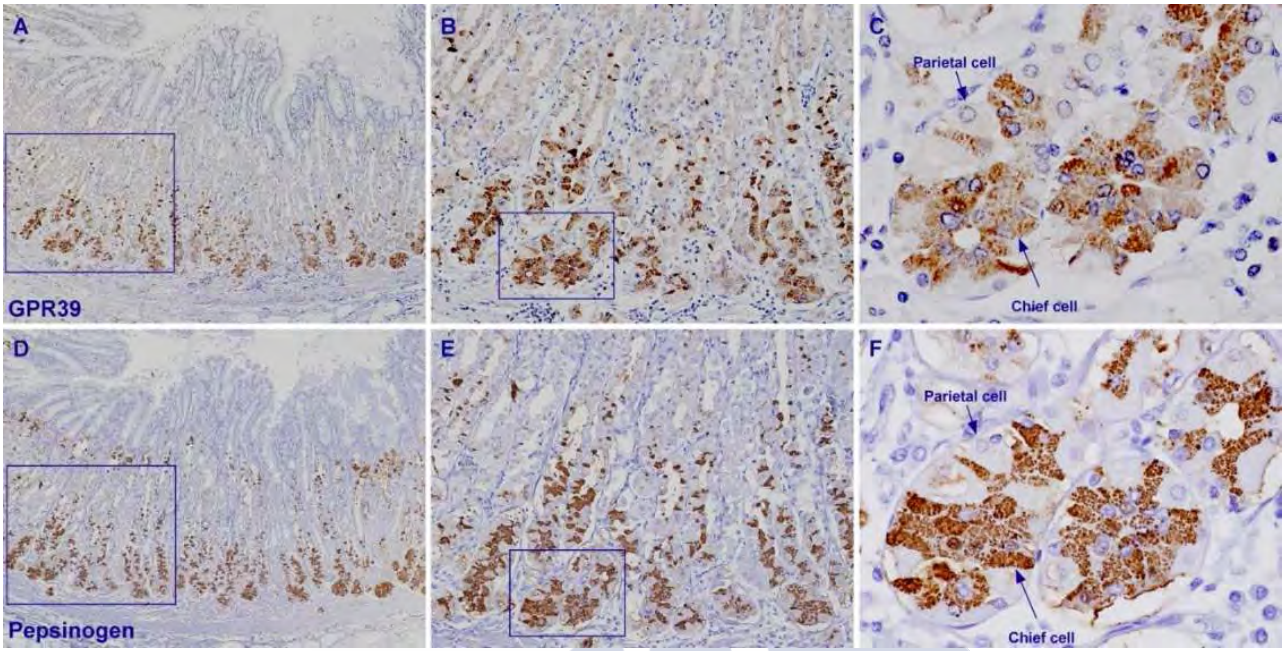

Figure 5.1. Immmunohistochemical expression of GPR39 and pepsinogen I in human healthy stomach. Expression at the base of the oxyntic gland. A. There was no GPR39 expression in the mucous cells or parietal cells of the gastric pits. An intense immunostaining was present in the chief cells situated at the base of the oxyntic glands. Objective magnification x4. **B.** Magnification view (x10) of the GPR39 intense immunostaining in the chief cells of the oxyntic glands. **C.** At higher magnification, GPR39 producing cells were clearly recognized with brownish staining in the cytoplasm. Parietal cells were negative for GPR39 (x40). **D.** Serial section (3 µm) of the same sample labelled for pepsinogen I. The intense PGI expression was observed mainly in the chief cells at the base of the oxyntic glands (x4), although few scattered cells were positive in the neck zone. **E.** Magnification view of the PGI positivity at the base of the oxyntic gland (x10). **F.** A higher magnification view shows that PGI expressing cells were filled with numerous secretion granules showing a specific labelling for PGI. Parietal cells were negative for PGI (x40).

Figure 5.3.D, **E** and **F**, show magnifications of the gastric glands sections (x20). At the lower region of the glands, pepsinogen I and GPR39 expression was found in the chief cells (**Figure 5.3.D**). The upper region shows a few cells positive for pepsinogen only, the mucous neck cells (**Figure 5.3.E**), whereas they were more abundant in the neck section (**Figure 5.3.F**). In the last region, GPR39 positivity was limited to some pepsinogen I positive cells morphologically intermediate and topographically interposed between mucous neck cells and chief cells, the pre-chief cells (**Figure 5.3.F**).[311] Taking into account the found location for GPR39, obestatin might regulate pepsinogen secretion in the chief cells, an important fact for the digestive process in the stomach.

[311] Cornaggia M, Capella C, Riva C, *et al*. Electron immunocytochemical localization of pepsinogen I (PgI) in chief cells, mucous-neck cells and transitional mucous-neck/chief cells of the human fundic mucosa. Histochemistry. 1986;85:5-11.

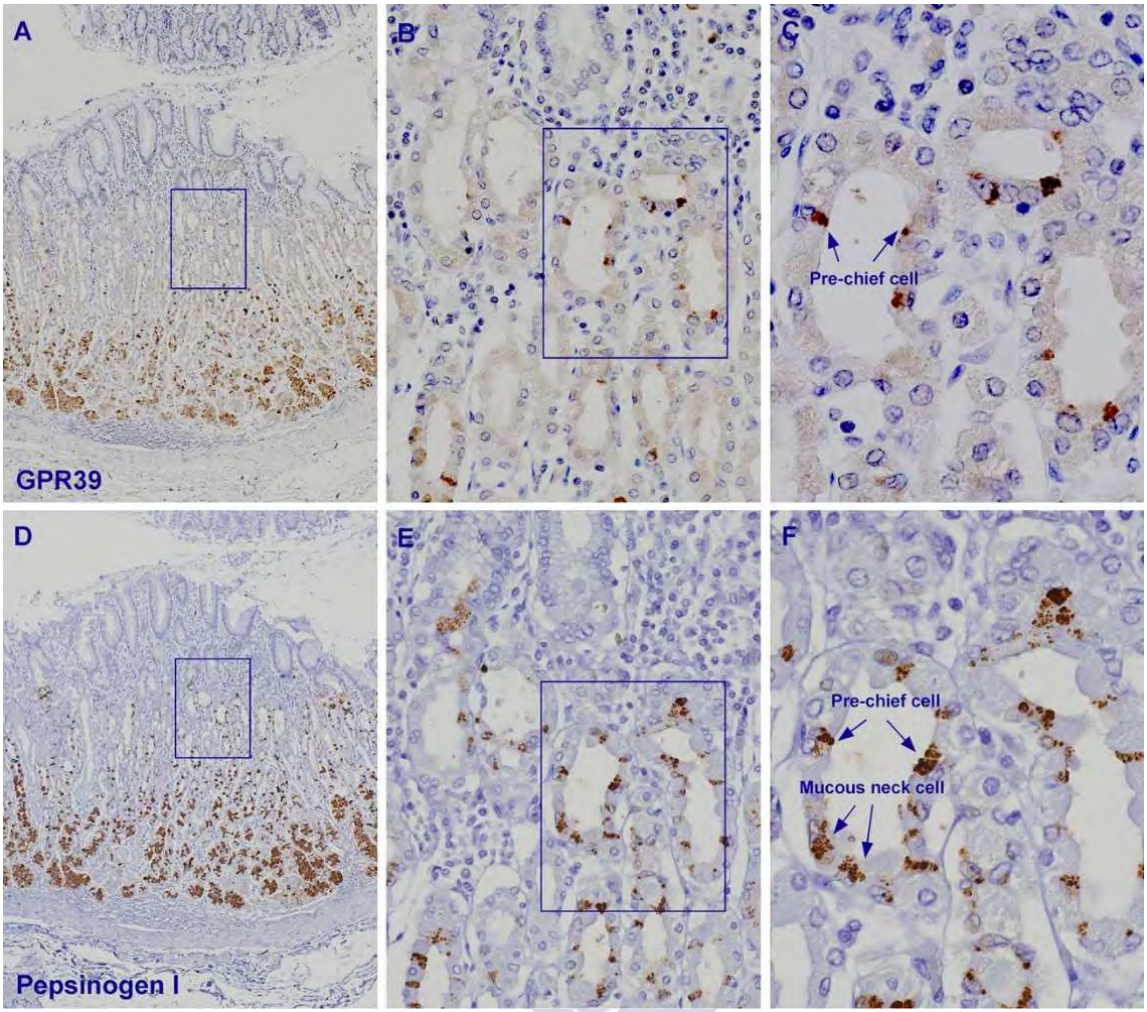

Figure 5.2. Immmunohistochemical expression of GPR39 and pepsinogen I in human healthy stomach. Expression at the neck of the oxyntic gland. A. General view of GPR39 expression in the oxyntic mucosa. Objective magnification x4. **B.** Magnification view (x10) of the GPR39 intense immunostaining in few cells of the neck section. **C.** At higher magnification, GPR39 producing cells were clearly recognized with brownish staining in the cytoplasm. These cells might be immature chief cells emerging to the base of the oxyntic gland (pre-zymogenic cells; x40). **D.** Serial section (3 µm) of the same sample labelled for pepsinogen I (x4). **E.** Magnification view of the PGI positivity at the neck zone (x10). **F.** A higher magnification view shows two cell types showing a specific labelling for PGI. The pre-zymogenic cells immunereactive for GPR39 were also positive for PGI. In addition, a few mucous neck cells were found to be strongly immunolabelled for PGI but negative for GPR39 (x40).

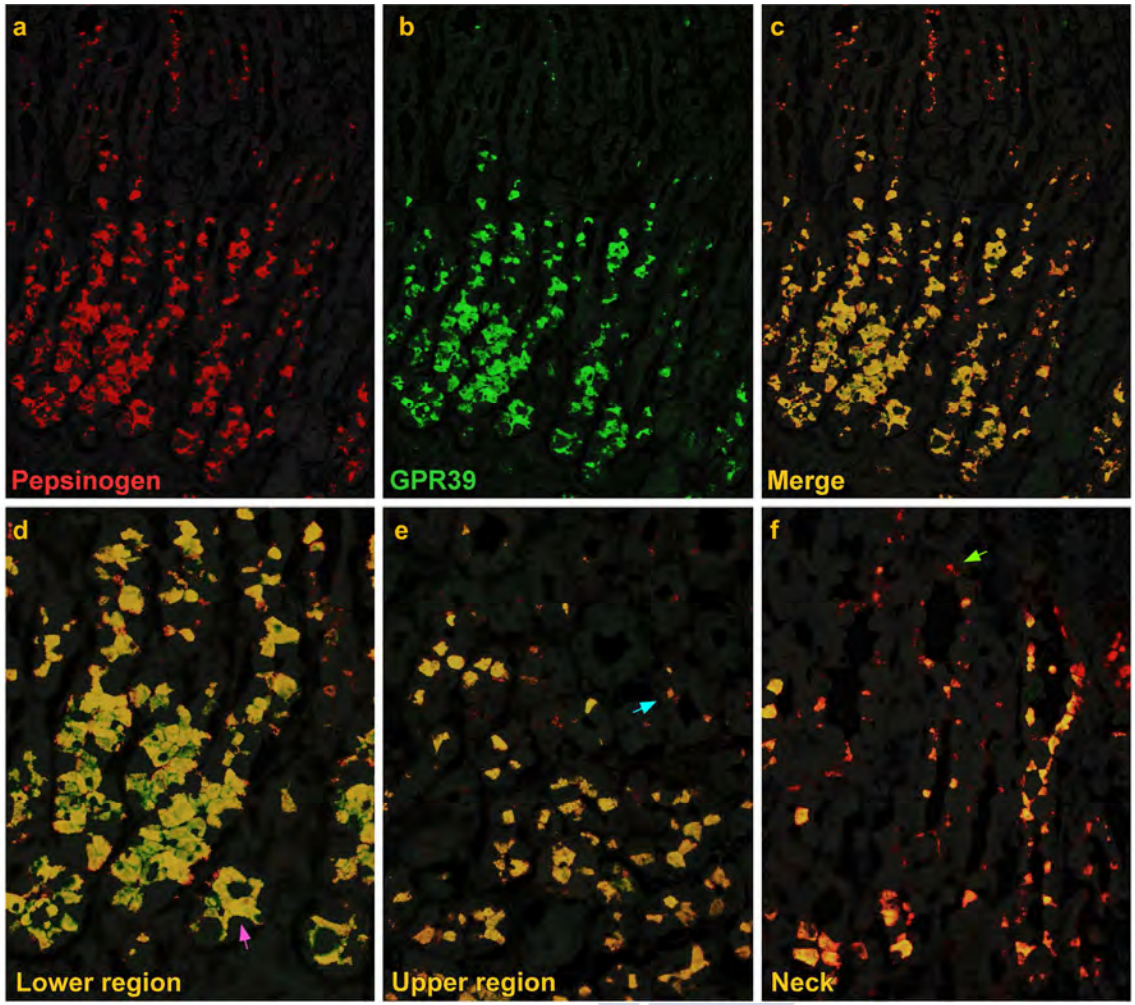

Figure 5.3. Immunofluorescence detection of GPR39 and pepsinogen I in human healthy stomach The figure shows the immunofluorescence detection of pepsinogen (red, **A**) GPR39 (green, **B**) in the same section of the gastric mucosa. Objective magnification 10x. Micrograph **C** (Merge) shows the colocalization of both proteins in the same cells mainly at the base of the oxyntic glands. **D.** At the lower region of the glands, pepsinogen I and GPR39 expression was found in the chief cells (pink arrow). **E.** The upper region shows a few cells positive for pepsinogen and GPR39, the pre-chief cells (blue arrow). **F.** The mucous neck cells were more abundant in the neck region (green arrow). **D-F.** Micrographs with objective magnification x20.

OBESTATIN STIMULATES PEPSINOGEN I SECRETION IN AGS CELLS

Previous works of our research group demonstrated that the obestatin/GPR39 system operates as an autocrine/paracrine signal in AGS cells.[301] Moreover, several groups described that the AGS cells were able to secrete pepsinogen I.[312,313] In this way, the AGS cell line[302] expressed the three components of the study: GPR39, obestatin and pepsinogen I, being a suitable model for our analysis. First, we performed a dose-response curve to evaluate the optimum dose of obestatin (200 nM, data not shown). The kinetic study of PGI secretion after obestatin treatment (200 nM) showed an augment in its secretion for all of the time tested, with a maximum at 40 min post stimulation (159±31% over control 98±16%; **Figure 5.4; upper panel**). This secretion was measured by using the haemoglobin method.[223] We corroborated this information by immunoblot at 40 min with similar results. Thus, obestatin treatment (200 nM) augmented pepsinogen secretion in a 43±6% over control measured by immunoblot (**Figure 5.4; bottom panel**).

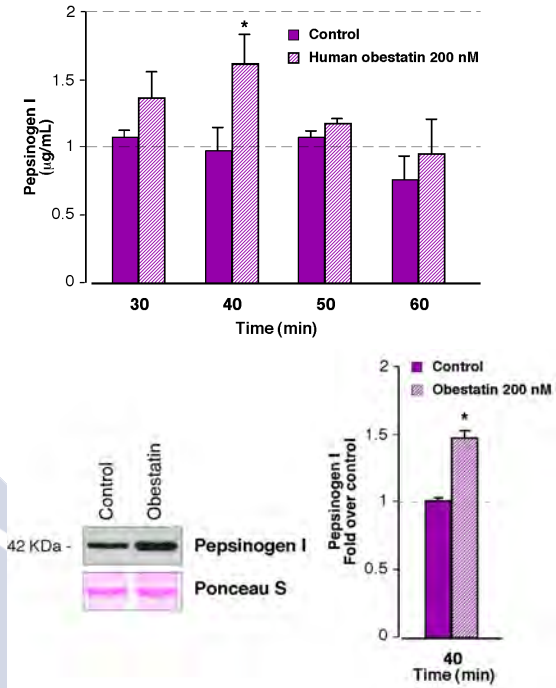

Figure 5.4. Obestatin stimulated pepsinogen I secretion in AGS cells. Upper panel) Kinetic study of PGI secretion after obestatin treatment (200 nM) at 30, 40, 50 and 60 min post stimulation. This secretion was measured by using the haemoglobin method. The data were expressed as mean±SEM obtained from 3 independent experiments. The asterisk (*) denotes P<0.05 when comparing groups. Bottom panel) Immunoblot detection of PGI in the secretome of AGS cells at 40 min after obestatin treatment (200 nM). Ponceau S staining (bottom panel) is shown to demonstrate total protein loading among lanes. The PGI expression was normalized relative to a band developed after Ponceau S treatment. The level of proteins was expressed as fold change relative to the control untreated cells. The data were expressed as mean±SEM obtained from intensity scans of 3 independent experiments. The asterisk (*) denotes P<0.05 when comparing groups.

[312] Basque JR, Chénard M, Chailler P, *et al*. Gastric cancer cell lines as models to study human digestive functions. J Cell Biochem. 2001;81:241-51.

[313] Chan EC, Chen KT, Lin YL. Vacuolating toxin from *Helicobacter pylori* activates cellular signaling and pepsinogen secretion in human gastric adenocarcinoma cells. FEBS Lett. 1996;399:127-30.

PEPSINOGEN SECRETION IS MEDIATED BY GPR39

To ascertain that the effect of obestatin on pepsinogen secretion described above was mediated by the GPR39 receptor, we tested the influence of the acute GPR39 deficiency by siRNA knockdown in AGS cells (**Figure 5.5**). Under these conditions, the constructs exhibited a decrease in the GPR39 expression by 83±4% in the cell lysate. Firstly, to check the efficiency of obestatin action in this cell line, we tested the effect on Akt phosphorylation at S473 [pAkt(S473)]. In the presence of a non-targeting control siRNA, the phosphorylation of human obestatin-activated Akt(S473) were similar to that observed without any transfection (data not shown). The silencing of the GPR39 subsequently decreased the levels of pAkt(S473) with respect to the control siRNA by 63±2% following treatment with obestatin (200 nM, 40 min). As happened for pAkt(S473), cells transfected with siRNA targeting GPR39 led to a significant decrease in obestatin-stimulated pepsinogen secretion respect to control siRNA measured in the secretome (81±4%).

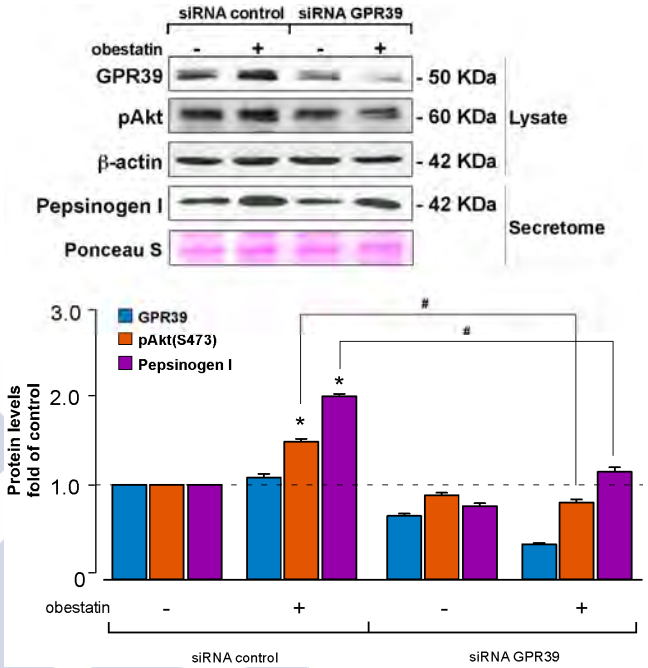

Figure 5.5. Effect of GPR39 knockdown by siRNA on obestatin-stimulated pepsinogen I secretion in AGS cells. The AGS cells were transfected with GPR39 siRNA prior to obestatin treatment (200 nM, 40 min). GPR39, pAkt(Ser473) were measured in the cell lysate. The protein expression was normalized relative to actin. Equal amounts of protein in each sample were used to assess the expression of GPR39 by western blotting. PGI was measured in the secretome of the cells. Ponceau S staining (bottom panel) is shown to demonstrate total protein loading among lanes. The PGI expression was normalized relative to a band developed after Ponceau S treatment. The level of proteins was expressed as fold change relative to the control siRNA-transfected cells. The data were expressed as mean±SEM obtained from intensity scans of 3 independent experiments. The asterisk (*) denotes $P<0.05$ when comparing the treated control siRNA group with the control siRNA group; the dagger (#) denotes $P<0.05$ when comparing the GPR39 siRNA group with the control siRNA group.

CHAPTER 6: OBESTATIN/GPR39 SYSTEM IN HUMAN CANCER LINES. EFFECTS ON PROLIFERATION AND INVASIVENESS

The obestatin proliferative effect and its signalling mechanisms had been already described for two gastric cancer cell lines: AGS and KATO III cells.[123,142] In AGS cells, obestatin also had an autocrine/paracrine role on proliferation and played a key role in the skeleton reorganization promoting invasion and migration of these cells, altering the expression of proteins involved in the EMT. Taken together, these data show an important implication of the obestatin/GPR39 system in the development of gastric tumours. GPR39 is a GPCR expressed in many tissues of the human body with specific physiological functions on them. Our recent data regarding obestatin and GPR39 in gastric cancer, prompted us to investigate the role of this system in the development of other cancers in human body.

OBESTATIN AND GPR39 ARE EXPRESSED IN CANCER CELL LINES

As a first approach, obestatin and GPR39 expression was invesigated in eight cancer cell lines (**Table 6.1**). As seen in **Figure 6.1**, the expression of the obestatin/GPR39 system was detected by immunocytochemistry in the cell lines of the study: HT-29, PANC-1, MCF7, BeWo, PC3, A431, A549 and SW872. All of the cell lines expressed the obestatin/GPR39 system at different levels of intensity and presented enhanced expression generally related to mitotic cells. No immunostaining was found when obestatin or GPR39 antibodies were preadsorbed with homologous peptides (data not shown).

Cell lines	Origin
HT-29[314]	Colorectal adenocarcinoma
PANC-1[315]	Pancreatic carcinoma
MCF7[316]	Breast adenocarcinoma
BeWo[317]	Choriocarcinoma
PC3[318]	Prostate adenocarcinoma
A431[319]	Epidermoid carcinoma
A549[320]	Lung carcinoma
SW872[321]	Liposarcoma
KATO III[322]	Gastric carcinoma

Table 6.1. Relation of the human cell lines used in this work.

[314] Fogh J, Trempe G. New human tumor cell lines. In Human Tumor Cells *in vitro*. Plenum Press, New York. 1975;115-59.

[315] Lieber M, Mazzetta JA, Nelson-Rees W, *et al*. Establishment of a continuous tumor-cell line (panc-1) from a human carcinoma of the exocrine pancreas. Int J Cancer. 1975;15:741-7.

[316] Soule HD, Vazguez J, Long A, et al. A human cell line from a pleural effusion derived from a breast carcinoma. J Natl Cancer Inst. 1973;51:1409-16.

[317] Pattillo RA, Gey GO. The establishment of a cell line of human hormone-synthesizing trophoblastic cells in vitro. Cancer Res. 1968;28:1231-6.

[318] Kaighn ME, Narayan KS, Ohnuki Y, *et al*. Establishment and characterization of a human prostatic carcinoma cell line (PC-3). Invest Urol. 1979;17:16-23.

[319] Giard DJ, Aaronson SA, Todaro GJ, *et al*. In vitro cultivation of human tumors: establishment of cell lines derived from a series of solid tumors. J Natl Cancer Inst. 1973;51:1417-23.

[320] Lieber M, Smith B, Szakal A, *et al*. 1976 A continuous tumor-cell line from a human lung carcinoma with properties of type II alveolar epithelial cells. Int J Cancer. 1976;15;17:62-70.

[321] Fogh J, Wright WC, Loveless JD. Absence of HeLa cell contamination in 169 cell lines derived from human tumors. J Natl Cancer Inst. 1977;58:209-14.

[322] Sekiguchi M, Sakakibara K, Fujii G. Establishment of cultured cell lines derived from a human gastric carcinoma. Jpn J Exp Med. 1978;48:61-8.

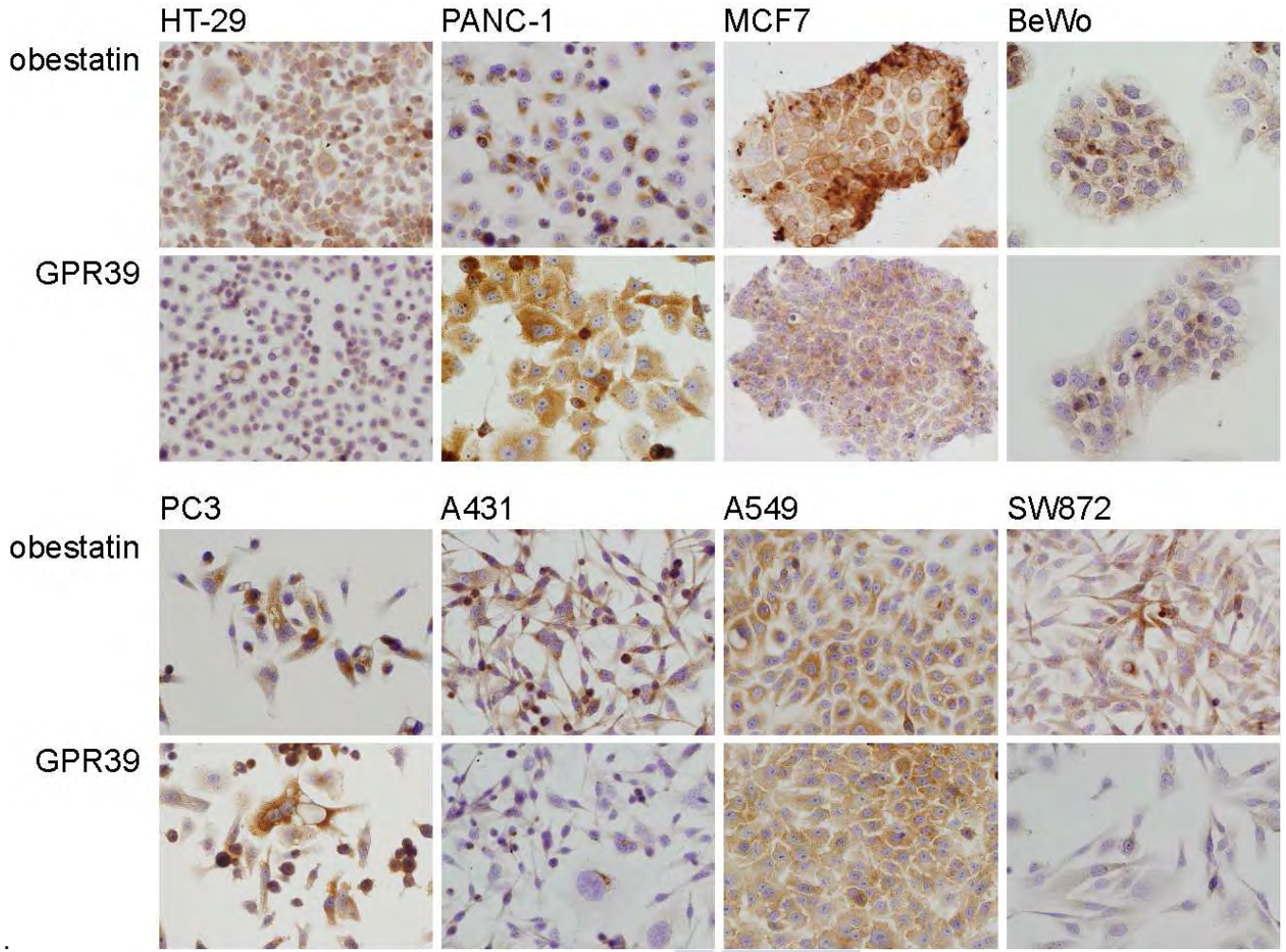

.

Figure 6.1. Immunocytochemical expression of obestatin and GPR39 in several human cancer cell lines. (See text below). Objective magnification x20.

HT-29. Intense and diffuse obestatin immunostaining was found in the cytoplasm, with an increased expression associated to mitosis. Intense GPR39 immunostaining but in a lesser extension than obestatin, also with increased pattern associated to mitosis.

PANC-1. Intense and localized perinuclear obestatin immunostaining was found, probably associated to Golgi, with increased expression associated to mitosis. Intense and diffuse GPR39 immunostaining was found in the cytoplasm.

MCF7. Intense and diffuse obestatin immunostaining was found in the cytoplasm. Intense and diffuse GPR39 immunostaining was found, but in a lesser extension than obestatin.

BeWo. Faint and diffuse obestatin immunostaining was found in the cytoplasm, with increased expression associated to mitosis. Faint and diffuse GPR39 immunostaining was found, also augmented in mitosis. Some cells appeared to exhibit Golgi staining.

PC3. Intense and diffuse obestatin immunostaining was found in the cytoplasm, although some cells presented perinuclear location, probably Golgi associated. Variable GPR39 staining was found, from faint to intense, always in a diffuse pattern.

A431. Intense and diffuse obestatin immunostaining was detected. Intensity augmented in mitosis. Intense GPR39 immunostaining was found with perinuclear location. Also increased expression associated to mitosis.

A549. From faint to intense diffuse obestatin immunostaining was found in the cytoplasm. Mitotic cells presented increased expression. Diffuse pattern for GPR39 was found in the cytoplasm with a few cells showing perinuclear location.

SW872. Intense and diffuse cytoplasmic obestatin expression was detected, also increased in mitotic cells. The cells presented diffuse cytoplasmic GPR39 expression. Some cells presented increased Golgi expression

OBESTATIN CAUSES CYTOSKELETON REORGANIZATION AND INCREASES PROLIFERATION IN KATO III CELL LINE

KATO III cell line was established from a signet ring cell carcinoma of the stomach, in which single cells diffusely infiltrate the surrounding tissues. They grow *in vitro* floating free and have cytological features of signet ring cells.[322] In our study, this cell line presented cytoplasmic immunoreactivity for obestatin and GPR39 (**Figure 6.2; upper panel**), difficult to locate due to the small size of the cell cytoplasm. Then, we analysed the effect of obestatin on the morphology and cytoskeleton in serum-free medium (**Figure 6.2; bottom panel**). Under these conditions, obestatin treatment (200 nM, 24 h) seriously affected the spherical morphology of these cells causing observable cytoskeleton reorganization. Obestatin induced cellular elongation with the formation of filopodia-like and/or lamellipodia-like structures typical of motile cells. In addition, obestatin treated cells presented GPR39 expression (green) located in the perinuclear region of the cytoplasm.

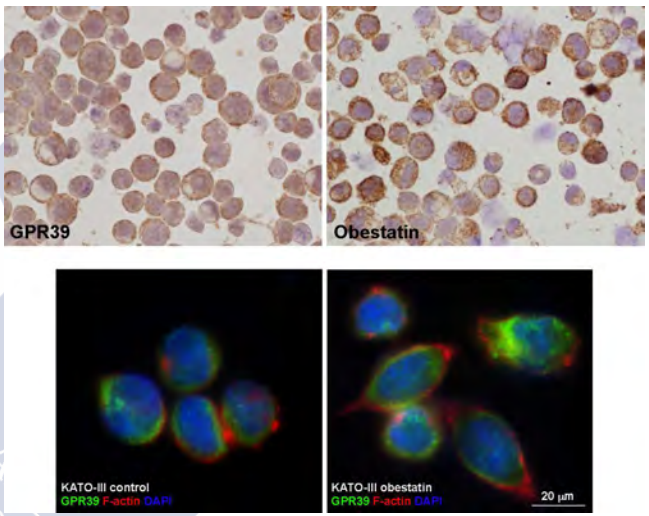

Figure 6.2. Upper panel. Immunocytochemical expression of obestatin and GPR39 in KATO III cells. Bottom panel. Obestatin effect in the cytoskeleton of KATO III cells. Cells were stimulated for 24 h with 100 nM OB. Cells were stained with rhodamine phalloidin (red) to visualize F-actin, anti-GPR39 antibody (green) to visualize the transfection of the receptor and DAPI (blue) to visualize the nucleus. Objective magnification x63. Scale bar=20 µm. Images are representative for at least three independent experiments.

Regarding proliferation of KATO III cells (**Figure 6.3; upper panel**), obestatin treated cells presented a significant increase in their proliferation compared to untreated cells (144.00±3.10%).

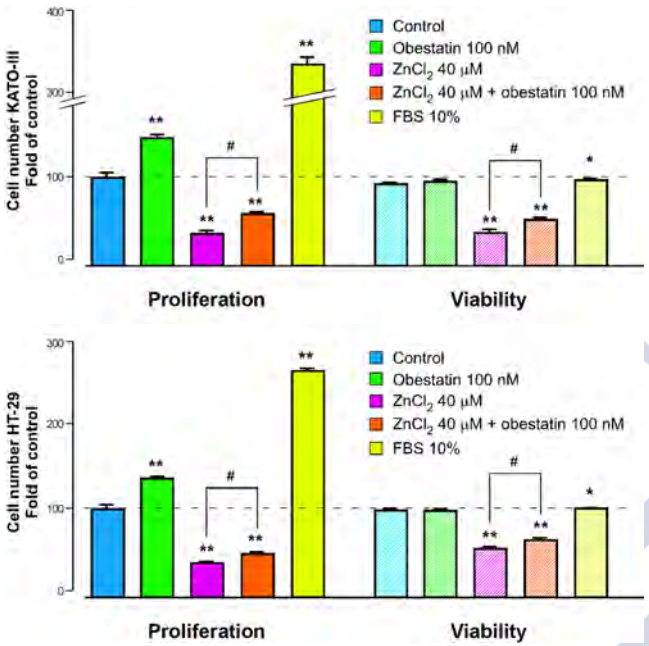

Figure 6.3. Upper panel. Mitogenic effect of obestatin in KATO III cells. Cells were treated with 100 nM obestatin, 40 µM $ZnCl_2$, 40 µM $ZnCl_2$ plus 100 nM obestatin, and 10% FBS. Cell proliferation was evaluated after the times indicated in Table 3. The data were expressed as a percentage of the basal proliferation of the untreated cells (Mean ± SEM). **Bottom panel. Mitogenic effect of obestatin in HT-29 cells.** Cells were treated with 100 nM obestatin, 40 µM $ZnCl_2$, 40 µM $ZnCl_2$ plus 100 nM obestatin, and 10% FBS. Cell proliferation was evaluated after the times indicated in Table 3. The data were expressed as a percentage of the basal proliferation of the untreated cells (Mean ± SEM).

As positive control, 10% FBS was used and KATO III proliferation increased to 336.00±8.20%. Due to the nature of KATO III cells, we quantified obestatin effect on proliferation by manual counting. To test whether the results were comparable to BrdU incorporation, we decided to perform the same experiments with the adherent HT-29 cell line. The results for HT-29 cell line (135.90±1.62%; **Figure 6.3; bottom panel**) were similar to those obtained by BrdU incorporation (140.00±3.02%; **Figure 6.4**).

Zn^{+2} has been described as a ligand for GPR39.[55] After bibliographic work, we selected the dose found in literature used to activate GPR39.[55] To test the effect of Zn^{+2} on proliferation, we treated the KATO III cells with 40 µM Zn^{+2}. The results were striking: KATO III cells were apoptotic after Zn^{+2} treatment (31.20±3.04%). However, the viable cells presented in the sample were able to proliferate significantly when they were co-treated with the obestatin plus Zn^{+2} cocktail (56.40±2.21%). These results correlated with the numbers of cell viability. The HT-29 cell line showed similar results regarding proliferation and apoptosis (**Figure 6.3; bottom panel**).

OBESTATIN STIMULATES PROLIFERATION OF CANCER CELL LINES *VIA* GPR39

After the verification of the obestatin/GPR39 system expression in the cell lines of the study, we next analysed the effect of exogenous administration of obestatin on cell proliferation by BrdU incorporation.

Cell line	OB	s.e.	*P* value	Sig.	PT	PDT
HT-29	140.00	3.02	0.0001	****	48	23
PANC-1	220.06	3.26	0.0002	***	96	52
MCF7	161.50	0.61	0.0038	**	72	38
BeWo	188.92	5.71	0.0001	****	96	40
PC3	132.63	5.48	0.0048	**	72	25
A431	127.00	7.27	0.0199	*	48	24
A549	139.74	4.65	0.0009	***	72	22
SW872	122.11	5.86	0.0068	**	72	65
KATO III[a]	144.00	3.10	0.0042	**	48	36

Table 6.2. Obestatin mitogenic effect on the cell lines of the study. The obestatin effect on proliferation was measured by BrdU incorporation, except for the non-adherent KATO III cell line, which was performed by manual counting. OB: obestatin, 100 nM. Sig: significance. PT: proliferation time (h). PDT: population double time (h). [a] Measured by manual counting.

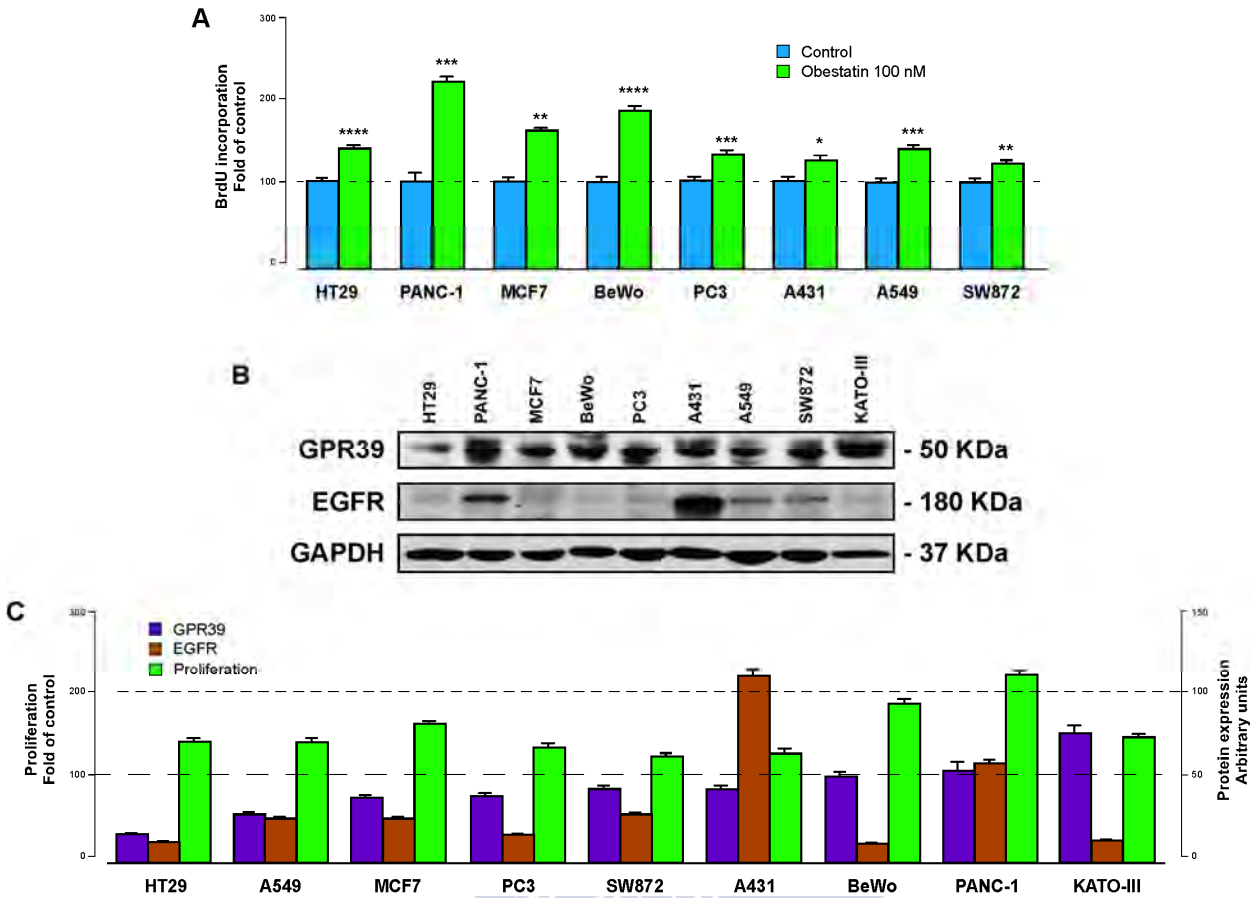

Figure 6.4. A. Mitogenic effect of obestatin in several cancer cell lines. Cells were treated with 100 nM obestatin and cell proliferation was evaluated after the corresponding times indicated in Table 3 by means of BrdU incorporation. The data were expressed as a percentage of the basal proliferation of the untreated cells (Mean ± SEM). **B. Immunoblot expression of GPR39 and EGFR in the cell lines of the study.** GPR39 expression was detectable in considerable amount in all the cell lines tested. EGFR expression was low in most of the cell lines except in A431 and PANC-1 cells. Protein expression was normalized by GAPDH. **C. Representation of the GPR39 and EGFR expression related to BrdU data normalized to PDT and ET.**

As Figure **6.4.A** shows, obestatin (100 nM) exerted a mitogenic effect in all of the tested cell lines. Obestatin maximum effect was observed in the PANC-1 cell line (220.06±3.26%). Nevertheless, the obestatin mitogenic effects were significant in all cell lines tested. Obestatin effect was less pronounced in the SW872 and the A431 cell lines (122.11±4.86% and 127.00±7.27%, respectively). **Table 6.2** summarizes the data obtained for the cell lines of the study. Our studies about the obestatin/GPR39 system described the existent crosstalk between GPR39 and EGFR.[142] To unveil the role of EGFR in our systems, GPR39 and EGFR immunoblot were performed. As **Figure 6.4.B** shows, GPR39 expression was detectable in considerable amount in all the cell lines tested; however, EGFR expression was low in most of the cell

lines. High expression was detected in A431[323] and PANC-1[324] cells, as previously described. BrdU data normalized to population doubling time (PDT) and to experimental time (ET) related to GPR39 and EGFR expression is represented in **Figure 6.4.C** Nevertheless, GPR39 crosstalk to RTKs is not only limited to EFGR. Obestatin activated RTKs screening involved other RTKs as was mentioned in Chapter 3.As mentioned above, the obestatin mitogenic effect was more pronounced for the PANC-1 cell line and in a much lesser extension in A431 cells. To ascertain whether obestatin effect was mediated by GPR39, we tested the effect of the GPR39 acute deficiency in PANC-1 cells (**Figure 6.5**) and the overexpression of the receptor in A431 cells (**Figure 6.6**). First, the effect of acute GPR39 deficiency on obestatin effects was determined by treatment of PANC-1 cells with a GPR39 siRNA. In the presence of a si-control, the proliferation of PANC-1 cells were similar to the levels observed with the untransfected cells (131.85±3.14% and 136.15±4.00%, respectively). The silencing of GPR39 decreased subsequent obestatin mitogenic effect with respect to the control siRNA (108.28±6.41%) upon treatment of obestatin (100 nM, 48 h; **Figure 6.5.A**), respectively. Second, the effect of acute GPR39 deficiency on cytoskeleton reorganization was evaluated (**Figure 6.5.B**). Obestatin treatment promoted the dissociation of the cell clusters and induced cellular elongation with the formation of filopodia/lamellipodia-like structures typical of motile cells in the untransfected cells and in the control siRNA cells.

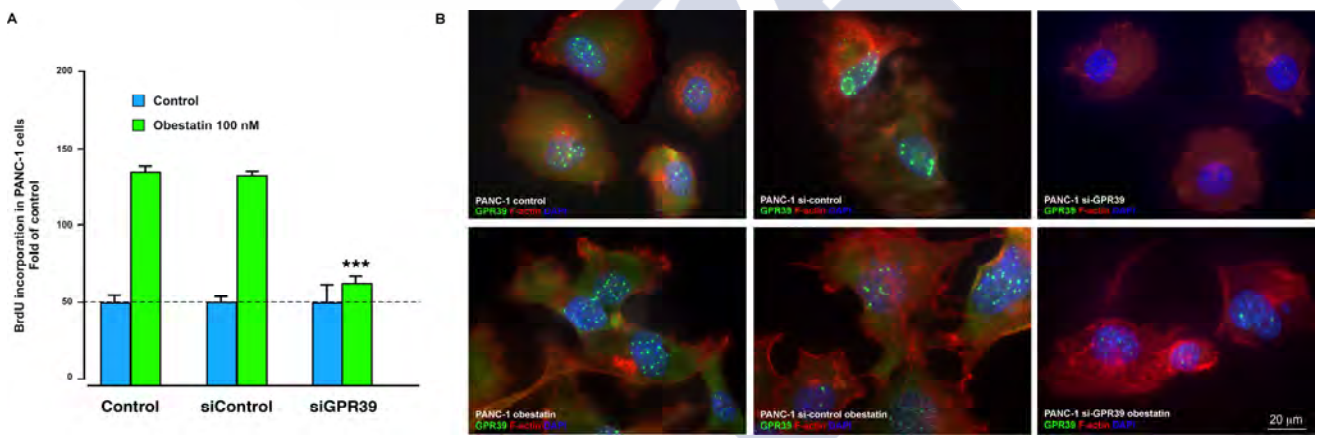

Figure 6.5. A. Mitogenic effect of obestatin in the PANC-1 cells. PANC-1 cells were treated with FBS (10%, v/v) (positive control, data not shown) and obestatin (100 nM; OB). Cell proliferation was evaluated after 48 h by means of BrdU incorporation. The data were expressed as a percentage of the basal proliferation of the untreated cells (Mean ± SEM). **B. Effect of GPR39 knockdown by siRNA on the cytoskeleton reorganization in PANC-1 cells.** The PANC-1 cells were transfected or not with GPR39 siRNA prior to obestatin treatment. Cells were stimulated for 24 h with 100 nM OB. Cells were stained with Phalloidin CruzFluor-594 (red) to visualize F-actin, anti-GPR39 antibody (green) to visualize the knockdown of the receptor and DAPI (blue) to visualize the nucleus. Objective magnification x63. Scale bar=20 µm. Images are representative for at least three independent experiments.

[323] King IC, Sartorelli AC. The relationship between epidermal growth factor receptors and the terminal differentiation of A431 carcinoma cells. Biochem Biophys Res Commun. 1986;140:837-43.

[324] Smith JJ, Derynck R, Korc M.Production of transforming growth factor alpha in human pancreatic cancer cells: evidence for a superagonist autocrine cycle. Proc Natl Acad Sci USA. 1987;84:7567-70.

Obestatin also induced strong actin polymerization including the development of stress fibres. The silencing of GPR39 caused the loss of the cytoskeleton reorganization promoted by obestatin. However, in the case of A431 cells (**Figure 6.6.A**), overexpression of GPR39 caused a significant augment in obestatin-promoted proliferation respect to the empty vector (+GFP), which is similar to untransfected cells (381.58±7.71%, 100.00±21.08, and 102.21±10.09, respectively). The impressive augment on BrdU incorporation after GPR39 overexpression might be due not only to the presence of GPR39, but to the large expression of EGFR present in this cell line.

Regarding the structural phenotype of obestatin-treated A431 cells, obestatin effect was more pronounced in GPR39 enriched cells and promoted a clear cellular elongation and the formation of lamellipodia-like structures. Obestatin also induced a stronger actin polymerization and the expression of stress fibres, enhancing an invasive phenotype (**Figure 6.6.C**). Consistent with a role in actin polymerization, the GPR39 knockdown PANC-1 cells exhibited depolymerisation and redistribution of the cellular F-actin, diminishing lamellipodia formation compared to the control cells after obestatin treatment (**Figure 6.5.B**). However, GPR39-overexpressing A431 cells, presented increased effect regarding cytoskeleton reorganization (**Figure 6.6.C**). Taken together, these results suggest that the obestatin/GPR39 system induces cytoskeleton remodelling to facilitate cell migration and invasion.

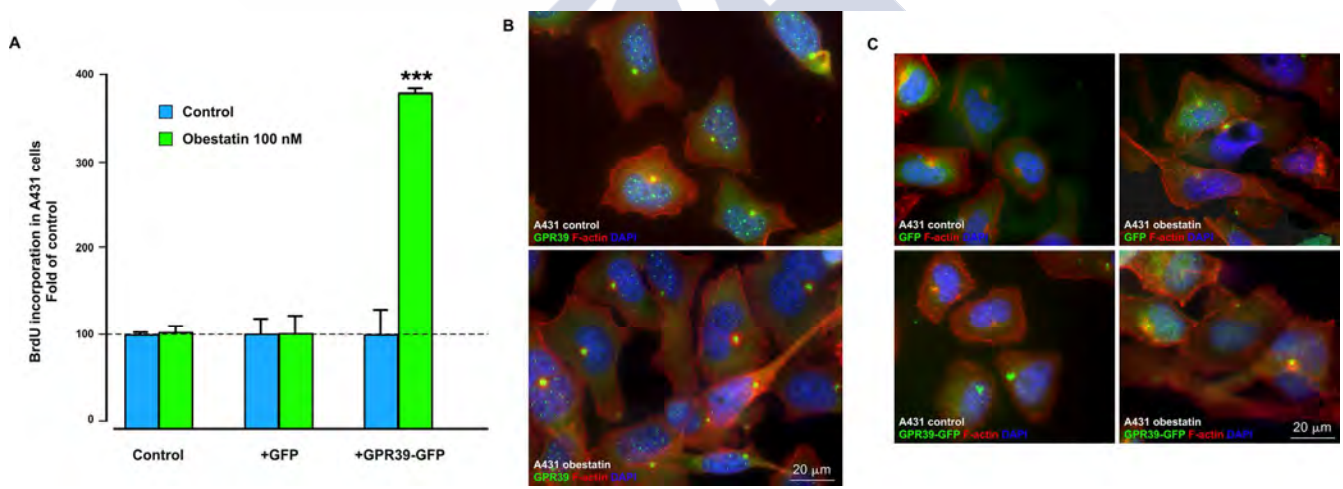

Figure 6.6. A. Mitogenic effect of obestatin in A431 cells. A431 cells were treated with FBS (10%, v/v) and obestatin (100 nM; OB). Cell proliferation was evaluated after 48 h by means of BrdU incorporation. The data were expressed as a percentage of the basal proliferation of the untreated cells (Mean ± SEM). **B/C. Effect of GPR39 overexpression on the cytoskeleton reorganization in A431 cells.** The A431 cells were transfected or not with GPR39 plasmid prior to obestatin treatment. Cells were stimulated for 24 h with 100 nM OB. Cells were stained with Phalloidin CruzFluor-594 (red) to visualize F-actin, anti-GPR39 antibody (green) to visualize the transfection of the receptor and DAPI (blue) to visualize the nucleus. Objective magnification x63. Scale bar=20 µm. Images are representative for at least three independent experiments.

USC
UNIVERSIDADE
DE SANTIAGO
DE COMPOSTELA

DISCUSSION

USC
UNIVERSIDADE
DE SANTIAGO
DE COMPOSTELA

CHAPTER 1

Classically, agonists of the GPCRs have been thought to display a linear efficacy in which activation of the receptor-related signalling network (e.g., G protein signalling, receptor phosphorylation, β-arrestin recruitment and internalization) is associated with the degree of the receptor activation, and this activation ranges from partial to full. Nonetheless, it is now recognized that β-arrestins initiate and determine the signals with different spatial and temporal patterns, thus resulting in singular cellular and pathophysiological consequences. This fact introduces a new concept that proposes the efficacy of G protein-coupled receptors as pluridimensional factors. This conclusion means that G protein-coupled receptors exhibit different active conformations that are able to trigger either the full range of receptor-associated activities or a subset of these activities. In this context, it appears that human obestatin (**1**) stabilizes the GPR39 conformations that are necessary for the complete signalling associated with the G protein and β-arrestin downstream pathways. This ligand action is clearly determined by amidation at the C-terminus of human obestatin (**1**), which was shown to be essential for signalling in all downstream pathways of the G protein- and β-arrestin-mediated signalling with the subsequent activation of ERK1/2 and Akt, respectively. As deduced from the structural studies, human non-amidated obestatin (**2**) does not possess the α-helical pattern of **1**, such as the α-helix formed between Ser20 and Leu23 and the α-helix formed from Gly8 to Lys11. Instead, a 3_{10} helix appears between Gly8 and Ser12. This structural change may be responsible for the negligible effect of **2** on the expression of Ki67, which is not comparable to that caused by human obestatin (**1**)**.** To date, Ki67 has not been unequivocally associated with either the G protein- or β-arrestin-mediated signalling. In fact, although Ki67 has been recognized as a relevant prognostic and predictive marker for proliferation, the exact intracellular regulation remains obscure. For **3**, the absence of the first five residues appears to be the key to the inability of this peptide to stabilize the GPR39 conformations associated with the activation of the G protein-dependent and β-arrestin-dependent signalling transductions. Furthermore, the impaired effect of peptide **3** on the expression of Ki67 compared with that induced by **1** reinforces the previous hypothesis. Regarding human (11-23)-obestatin (**4**), the loss of the first ten residues leads to a significant change in structure. This peptide presents the longer segment of an α-helix spanning from Tyr16 to Leu23. The biological data show that this ligand induces a selective coupling to only the β-arrestin portion of the GPR39 downstream signalling pathways. This evidence suggests that this peptide stabilizes a receptor conformation distinct from that induced by **1**. Interestingly, **4** exhibited a higher level of Ki67 expression than the other truncated obestatin analogues did. It is tempting to speculate that the structure of this ligand represents a key element needed for the stabilization of the GPR39 conformation coupled to β-arrestin signalling, thus controlling its interaction patterns and related functions. Finally, human (16-23)-obestatin (**5**) possesses a helical structure at its C-terminus. Nevertheless, its small size does not seem to be able to modulate the full range of GPR39 activities. Altogether, these results support the notion that more than one active conformation of GPR39 indeed exists and that the different ligands are able to stabilize a different subset of the available receptor conformations.

The behaviour of mouse obestatin (**6**) is also unique. This peptide is the same size as **1** and is also subject to amidation at its C-terminus. Moreover, **6** displays a characteristic pattern of helix sets: Gly8-Ser12, Ala14-Gln17, and His19-Ala22. Indeed, the first two helical regions are coincident with the 3_{10}-helix fragment present in **3**. However, the presence of this type of helix in **6** does not result in the activation of the human GPR39 receptor in ARPE-19 cells. In fact, mouse obestatin (**6**) did not activate either G protein-dependent or β-arrestin-dependent signal transduction over the time period studied. Additionally, this peptide failed to induce Ki67 expression, which is similar to the behaviour of human non-amidated obestatin (**2**). An inspection of the primary sequence indicated that the differences in primary structure between **1** and **6** are limited to only three amino acid residues, namely Val14Ala, Ser20Gly and Gln21Arg. The major dissimilarity is observed for Arg21, which can be positively charged. Spatially, this residue is located only two residues away from the neighbouring amidated Leu23. Thus, these structural differences may be responsible for the different bioactivities observed. Thus, in our biological model system, the activity of obestatin is species-specific.

In summary, a structure-activity relationship for obestatin has been derived by employing this peptide and several analogues as ligands for the seven-transmembrane receptor GPR39. The analysis of the data suggests that amidation at the C-terminus of human obestatin (**1**) is essential for this molecule to adopt an α-helix structure. This α-helix exists between Ser20 and Leu23 and from Gly8 to Lys11. The presence of this structure correlates with the stabilization of the GPR39 conformations that are necessary for the full range of receptor activities, e.g., G protein-dependent and β-arrestin-dependent signalling. Indeed, the change of this α-helix to a 3_{10} helix or the loss of this α-helical pattern can be correlated with the absence of complete activation, as observed for non-amidated obestatin (**2**). Additionally, GPR39 is able to adopt multiple active conformations, which are related to the activation of specific signalling mechanisms. In particular, human (11-23)-obestatin (**4**) is able to induce selective coupling to a portion of the downstream signalling pathways, e.g., β-arrestin-dependent signalling. This observation supports the idea that **4** stabilizes a receptor conformation different from that induced by human obestatin (**1**). Most likely, this activity is related to the presence of the α-helix segment from Tyr16 to Leu23. Because this peptide is present in the stomach, it might represent the first example of an endogenous biased ligand for GPR39. Finally, mouse (**6**) and human obestatin (**1**) exhibit clear conformational differences beyond their differences in primary structure. The mouse analogue adopts a distinct 3D structure, which cannot activate human GPR39. This evidence supports the existence of a species-specific activity. Overall, the data presented herein provide a new structural background, which could be useful for the development of particular ligands that are able to discernibly improve, diminish or inhibit specific aspects of the GPR39-associated signalling pathways.

CHAPTER 2

In cells, proteins interact specifically with receptors, co-factors, ligands and other peptides, generating a cellular environment difficult to replicate. Biomimetic approaches of structure determination have made very valuable contributions to undestanding the roles of many proteins. However, the accurate structural basis of their biological functions require observations in living cells. Its non-invasive character and its ability to provide data at atomic resolution make heteronuclear multi-dimensional NMR spectroscopy ideally suited for the task.[325] In this context, we have used NMR techniques to determine the solution structure of human obestatin (**1**) and the fragment peptides (6-23)-obestatin (**3**), (11-23)-obestatin (**4**), (16-23)-obestatin (**5**) and (1-10)-obestatin (**7**) in H_2O, PBS and HEK293 both wild type and transiently GPR39-transfected cells.

1H and 2D spectra data of obestatin truncates showed non-significant and very weak differences in their structure between samples. Significant CSPs effects in PBS solution might indicate a tendency to a α-helix organisation, for **3** and **7**. Nevertheless, NOE pattern appeared to reveal random coil conformations in all solutions with only strong sequential δNN(i, i+1) and δαN(i, i+1) NOEs. CSI analysis was employed due to the absence of extensive medium- and long-range NOE data and its application as a predictive approach for small proteins. In this sense, all truncates showed unstructured characteristics in H_2O, excluding **5** and **7**. These last peptides presented data consistent with some tendency to helicoidal structures in H_2O.

Regarding full-length obestatin samples, NMR data showed some noteworthy results. In H_2O and PBS solutions, our findings on CSPs changes, NOE pattern and CSI analysis pointed to a fairly high percentage of random coil conformations for this molecule. In the presence of wild type living cells, positive CSPs effects were found, which may imply a β-strand reorganization or a loss of helical structures in cells lacking receptor. Significantly, important CSPs changes were observed in Pro4 and His19 hydrogens when comparing WT:GPR39 resonances. Prolines hold a distinctive cyclic structure in its side chain that implies an exceptional conformational rigidity. This characteristic affects the rate of peptide bond formation between Pro and other amino acids and its behaviour as a structural disruptor of secondary structure elements such as α-helix and β-sheets. However, Pro is commonly found as the first residue of an α-helix and also in the edge strands of the β-sheets. Furthermore, peptide bonds to proline are able to populate both the *cis* and *trans* isomers.[326] The data observed for Pro4 in receptor-enriched cells might involve an *E*/*Z* obestatin isomerization. However, we did not found any SCE effect and/or double sets of signals for obestatin in the presence of HEK-GPR39 cells in the TOCSY spectrum that would indicate the presence of two conformers in equilibrium. Furthermore, the NOE pattern and the CSI analysis pointed to obestatin as an unstructured molecule, as well as happened for obestatin truncates. Nevertheless, considering the possibility of a conformational change in the Pro4 residues, the data observed for His19 and the only non-sequential NOE

[325] Sakakibara D, Sasaki A, Ikeya T, *et al*. Protein structure determination in living cells by in-cell NMR spectroscopy. Nature. 2009;458:102-5.

[326] Fischer G, Bang H, Mech C. Determination of enzymatic catalysis for the cis-trans-isomerization of peptide binding in proline-containing peptides. Biomed Biochim Acta. 1984;43:1101-11.

observed between Leu11 and Gly13, 3D structures of human obestatin were calculated. The data suggested that obestatin was only partially structured. The analysis of the bundle of the 6 structures obtained for the *E* configuration showed a possible helix structure between residues Ala3 and Phe5, which were overlapped. In the *Z* configuration, the bundle of the 6 structures presented an overlapping in the area from Phe1 to Lys10, which could form part of a helix conformation. Although these results are indicative of certain structuration in the molecule, a larger zone of obestatin appeared to be unstructured.

Peptides usually adopt several conformations in solution. Therefore, in most of the cases, the assessment of one single 3D structure is unrealistic and, indeed, NMR may easily generate virtual conformations, when ensemble averages are not properly taken into account. A good strategy to decrease conformational exchange is the use of low temperatures before the freezing point (0-8 °C). It has been speculated that these temperatures may induce the formation of structure that is similar to the conformation of the peptide in the receptor bound state.[42] Although in all the experiments described herein, the temperature was set at 5 °C, we could only infer a certain change in obestatin conformation when obestatin was placed in the presence of living cells. Although some extra signals were observed in the TOCSY spectra for the GPR39-enriched cells, these peaks could not be unambiguously assigned to a certain residue, in order to corroborate the existence of SCE effects in this system. However, when comparing both cell types, specific CSPs were observed for Pro4 and His19. These signals observed for Pro4 in the presence of GPR39, might be indicative of the possible proline *cis*/*trans* isomerization, which exclusively arose in the presence of the receptor and that, prior to bind to its receptor, obestatin (**1**) needs to adopt a specific conformation.

CHAPTER 3

Since obestatin discovering, many troublesome issues surrounded this small peptide. The first outstanding fact was its opposite function to ghrelin orexigenic action. The second, but not less critical, was its receptor, the GPR39. Obestatin did not have a good beginning. Very soon after Zhang's work was published, several groups discarded its actions regarding feeding.[56,127] Only one year later, Holst *et al* published their work regarding the GPR39 receptor: obestatin was not able to activate this receptor, but Zn^{+2} did.[55] However, all these results might be questionable. It was not until 2008 that De Spiegeleer's group demonstrated the quality of the obestatin peptides supplied by several companies concluding that these peptides were not suitable to obtain good and unquestionable results.[76] Regarding the obestatin binding assays to GPR39, the same group demonstrated in 2012 that iodinated obestatin was also a mixture of poly-iodinated peptides.[327] Indeed, already in 2008, Zhang mentioned this subject.[77] Along these years, we had some noteworthy results regarding obestatin structure and bioactivity, and demonstrated that obestatin biological effect is species-specific: mouse and human obestatin have different primary and secondary structures and, in consequence, different bioactivities.

GPCRs are regulated by phosphorylation and this process is a key event in determining the signalling properties of this receptor super-family. The process of stimulus-dependent receptor phosphorylation was mediated by both PKA[328] and G-protein-coupled receptor kinases (GRKs).[329,330] These different protein kinases, activated by distinct mechanisms, were able to phosphorylate different sites on the receptor and these varying GPCR "barcodes" resulted in different signalling outcomes, β-arrestin recruitment and internalization.

Having all this information in mind, our recent results regarding GPR39 phosphorylation and internalization were not a surprise. Although some groups proposed Zn^{+2} as the endogenous agonist of GPR39 due to its ability to activate inositol phosphate accumulation, amazingly, Zn^{+2} treatment diminished GPR39 basal phosphorylation. However, in our hands, obestatin was able to activate GPR39 phosphorylation above basal levels. This basal phosphorylation could represent a high constitutive activity for this receptor, mainly due to the critical importance of its C tail domain.

Receptor desensitization together with its internalization also represents an important physiological mechanism that modulates receptor response and acts as an information filter for intracellular signalling. Chartrel *et al* published in 2006 that obestatin did not promote GPR39 internalization and did not have effects in GPR39-transfected cells.[74] With regard to the internalization driven by obestatin, our results showed that its addition induced GPR39 internalization and endocytosis in receptor-enriched

[327] De Spiegeleer B, Van Dorpe S, Vergote V, *et al*. In vitro metabolic stability of iodinated obestatin peptides. Peptides. 2012;33:272-8.

[328] Benovic JL, Pike LJ, Cerione RA, *et al*. Phosphorylation of the mammalian beta-adrenergic receptor by cyclic AMP-dependent protein kinase. Regulation of the rate of receptor phosphorylation and dephosphorylation by agonist occupancy and effects on coupling of the receptor to the stimulatory guanine nucleotide regulatory protein. J Biol Chem. 1985;260:7094-101.

[329] Benovic JL, Mayor FJ, Somers RL, *et al*. Light-dependent phosphorylation of rhodopsin by beta-adrenergic receptor kinase. Nature. 1986;321:869-72.

[330] Bouzo-Lorenzo M, Santo-Zas I, Lodeiro M, *et al*. Distinct phosphorylation sites on the ghrelin receptor, GHSR1a, establish a code that determines the functions of ß-arrestins. Sci Rep. 2016;6:22495.

cells. The kinetic studies of GPR39 internalization showed that the obestatin-GPR39 complex was internalized in a time-dependent manner, showing a surface GPR39 loss over maximum at about 20 min on obestatin stimulation. Furthermore, the confocal microscopy results suggested the hypothesis that the complex might be being recycled by early endosomes and did not degradate in lysosomes. Additional studies are required to further investigate receptor internalization pathway.

We proposed a signalling mechanism for obestatin involving two routes triggered in parallel: the ERK1/2 and Akt signalling pathways (**Scheme 1**). Once obestatin receptor is activated, a signalling pathway is mediated by β-arrestin 1 involving the recruitment and activation of Src into a β-arrestin-scaffolded complex. Thus, Src functions as a switch that activates MMPs to initiate the proteolytic release of EGF-like ligands at the cell surface and then bind to EGFR. Ligand binding drives receptor dimerization, leading to activation of the intrinsic kinase and autophosphorylation of specific docking sites, among them for PI3K, and ending in the activation of Akt. Several studies have shown that Zn^{+2} induces EGFR phosphorylation through the extracellular release of EGF-like ligands that are mediated by MMPs. It might be possible that the stimulatory effects of Zn^{+2} on GPR39 signalling might be due to the activation of MMP-EGFR since obestatin requires EGFR transactivation and MMP activities.

It is widely demonstrated that the alteration in the expression of many members of the superfamily of RTKs is present in tumours and derived cell lines, and that these changes contribute to the development and progression of cancer.[147,148] In this chapter, our results showed that obestatin induced RTKs phosphorylation, which belonged mainly to the EGF, insulin, TrK, VEGF and ephrin receptor families. The four ErbB family members were significant activated by obestatin. All of them are important therapeutic targets and their downstream pathways regulate EMT, migration, and tumour invasion by FAK or Rho GTPases modulation and the increment of MMP9 activity.[331] Furthermore, receptor combinations produce synergies that have clear potential in cellular proliferation associated with tumour progression.[144] ErbB receptors form either homo- or hetero-dimers following ligand binding, and each dimer shows different affinity for ligands and different signalling properties.[154] In this way, cooperation of ErbB receptors in obestatin transduction pathway could be necessary to induce cell transformation.

The role of obestatin in glucose metabolism[70] and its ability to act throughout insulin receptor[71] have been already demonstrated. Insulin-like ligands bind to IGF1R and activate downstream signalling through IRSs to regulate cell proliferation *via* the Ras-Raf-MAPK pathway or survival and cell cycle progression *via* the PI3K/AKT/mTOR pathway.[239] Ras signalling pathways are also triggered by Trk receptors to the control of cell survival, proliferation, and differentiation.[244] Obestatin treatment displayed a notable activation of IGF1R, in line with the previous studies mentioned above and significantly up-regulated several Trks. All together, these data point to a strong interaction with signalling pathways proposed for the obestatin/GPR39 system.[123,142]

On the other hand, the results in both cell lines showed that obestatin could also be implied in metastatic processes. Eph and Tie receptors regulate several biological processes including angiogenesis, and vascular system development.[263,265] VEGFR family

[331]Appert-Collin A, Hubert P, Crémel G, *et al*. Role of ErbB receptors in cancer cell migration and invasion. Front Pharmacol. 2015;6:283.

plays a crucial role in pathological angiogenesis activating downstream signalling of the phospholipase (PLC)γ-PKC-MAPK pathway but not Ras pathway for cell proliferation.[332] Moreover, other obestatin-activated RTKs are implicated in Wnt signalling in tumour invasion[253] and regulate MMPs expression.[254]

In summary, the results obtained in both cell lines in response to obestatin corroborated the involvement of this peptide on proliferation, survival and cell differentiation; and diverse oncogenic processes like migration, invasion and angiogenesis. Its effect on glucose and insulin metabolism was also confirmed.[70] The differences in the phosphorylation patterns activated by obestatin in AGS and KATO III cells could be due to the morphological and/or molecular differences between both cell lines. The former has epithelial morphology;[302] however, the latter has spherical morphology[322] and is composed by two cell subtypes (floating and adherent).[333] For instance, the opposite effects observed for several RTKs, as the Axl and ephrin families could be due to these distinctive characteristics. Mer is involved in the regulation of the cytoskeletal dynamics,[334] and EphA6 and EphA7 are implied in cell adhesion and migration.[245] The fact that obestatin inhibited the activation of these receptors in the KATO III cells and stimulated their phosphorylation in AGS cells, might be associated to processes related to the epithelial-mesenquimal and the mesenquimal-epithelial transitions. Further investigations will be needed to clarify the precise role of obestatin in these processes.

MMPs have been reported as key regulators in the signalling pathway triggered by obestatin via the GPR39 receptor.[142] The protease expression profile obtained in response to obestatin in gastric cancer cells pointed to the involvement of other proteases in addition to MMPs. These proteases are all of them closely related to the pathology of cancer.

Comparing the results obtained in both cell lines, AGS and KATO III, obestatin had a more potent stimulatory effect in AGS cells. ADAMs family, CTSs, some KLKs and MMPs were the most overexpressed proteases in both cell lysates. ADAMs are a family of transmembrane and secreted metalloendopeptidases[335] and are characterized by a functional protease domain, which indicates that their biological function mainly depends on protein-protein interactions.[336] On the other hand, CTSs and KLKs are enzyme proteins with proteolytic activity differentially expressed in many human tumours and are potential cancer biomarkers. [290,337] These enzymes are involved in processes of plasticity, malignancy, tumour invasion and metastasis that carry on a poor prognosis of these pathologies. Additionally, MMPs are endopeptidases capable of degrading all kinds of extracellular matrix proteins, but also can process bioactive molecules. All MMPs were overexpressed by obestatin in both cell line lysates. In fact, MMP1, a protease that plays a major role in the invasion of gastric cancer,[285,286] was one of the most up-regulated proteins. MMPs are also thought to play a major role in cell behaviours such as cell proliferation, migration, differentiation, angiogenesis,

[332] Shibuya M. Tyrosine kinase receptor Flt/VEGFR family: its characterization related to angiogenesis and cancer. Genes Cancer. 2010;1:1119-23.

[333] Oda T, Kanai Y, Oyama T, *et a*l. E-cadherin gene mutations in human gastric carcinoma cell lines. Proc Natl Acad Sci USA. 1994;91:1858-62.

[334] Wang Y, Moncayo G, Morin PJ, *et al*. Mer receptor tyrosine kinase promotes invasion and survival in glioblastoma multiforme. Oncogene. 2013;32:872-82.

[335] Wolfsberg TG, Straight PD, Gerena RL. ADAM, a widely distributed and developmentally regulated gene family encoding membrane proteins with a disintegrin and metalloprotease domain. Dev Biol. 1995;169:378-83.

[336] Edwards DR, Handsley MM, Pennington CJ. The ADAM metalloproteinases. Mol Aspects Med. 2008;29:258-89.

[337] Diamandis EP, Yousef GM. Human tissue kallikreins: a family of new cancer biomarkers. Clin Chem. 2002;48:1198-205.

apoptosis and host defence[338] in addition to tumour invasion and metastasis.[155] However, obestatin was unable to stimulate the secretion of all of them in KATO III cells. The presence of two subpopulations and their ratio in KATO III cells could explain the different and, *a priori*, conflicting results compared to AGS cells. Finally, PSEN1 data were noticeable in AGS cells. Its expression was up-regulated, but obestatin treatment had inhibitory effects on its secretion. This result will need further investigations.

Summarizing, all proteases resulted overexpressed by obestatin, both in AGS and KATO III cells. These proteins are involved in degradation of extracellular matrix, as well as migration and invasion processes. Many of them have been considered as biomarkers of poor prognosis in numerous types of cancer, especially gastric cancer. These results on proteases and those mentioned above for RTKs, enhanced the role of obestatin in the oncogenic process.

The RTKs and MMPs array results from human gastric adenocarcinomas samples were heterogeneous. The wide range of functions of the different RTKs and proteinases families, varying according to the tissue or the process in which they are involved, makes difficult to establish the connection between cell lines and tissues. However, most of the up-regulated proteins observed in gastric adenocarcinomas are involved in oncogenic processes, many of them specifically in gastric cancer, which are in line with our previous results and the bibliography.

RTKs expression in human gastric adenocarcinoma tissue did not present any correlation with tumour differentiation or being compared to healthy tissue. Only the EphA1 and insulin receptor resulted more activated in worse-prognosis adenocarcinomas. By contrast, Axl was down-regulated in tumour tissues compared to the healthy sample. Surprisingly, the MD sample showed the highest differences with significant augments in the expression of more than half of the RTKs compared to the other samples.

PDGF receptors, c-Ret and ALK were highly activated in MD adenocarcinoma. PDGF family is correlated with cancer progression and metastasis of gastric carcinoma.[339] Furthermore, c-Ret is a molecular regulator in gastric inflammatory and cancer.[251] However, Tie1 was significantly down-regulated in MD and WD samples. EphA5 and EphA10 were more phosphorilated in adenocarcinomas of worse prognosis. EphA5 gene had significantly increased CpG methylation in gastric cancer *vs* non-metaplastic mucosa,[261] however, no EphA10 data was found for gastric cancer in the existing literature. In WD adenocarcinoma, the most activated receptor was the Wnt receptor, RYK. Regarding the VEGF family, only VEGFR2 in the WD and all of them in the MD sample were more activated, respect to healthy tissue. The overexpression of ErbB2 in gastric carcinomas and its status as one of the main stomach cancer biomarkers, has been confirmed by many studies;[236,237] nevertheless, our data were not conclusive.

Regarding proteases expression patterns, the adenocarcinomas presented significant variations compared to the healthy sample. PSEN1 and ADAMTS13 resulted more expressed in the healthy controls than in the adenocarcinoma samples. However, it has been recently published that PSEN1 is dramatically up-regulated in gastric cancer tissues

[338] Verma RP, Hansch C. Matrix metalloproteinases (MMPs): chemical-biological functions and (Q)SARs. Bioorg Med Chem. 2007;15:2223-68.

[339] Guo Y, Yin J, Zha L, *et al*. Clinicopathological significance of platelet-derived growth factor B, platelet-derived growth factor receptor-beta, and E-cadherin expression in gastric carcinoma. Contemp Oncol. 2013;17:150-5.

compared with their benign counterparts.[340] Meanwhile, ADAMTSs are related to anti-angiogenic capabilities,[341,342] and ADAMTS13 is involved in suppressing tumour cell invasion in some tumour as the gastric cancer.[343,344]

Concerning to the CTS family, CTS X/Z/P expression clearly increased with the dedifferentiation of the tumour. CTSA, CTSD and CTSL were found to be up-regulated and, CTSC, CTSE and CTSS down-regulated in the PD adenocarcinoma. CTSV, however, was found up-regulated in the MD sample. An association between *H. pylori* infection, a strong up-regulation of CTSX/Z/P and development of gastric cancer have shown.[345] Furthermore, it was reported that CTSL were significantly higher in gastric cancer[272] and CTSE was found in highest concentration in the surface of epithelial mucus-producing cells of the stomach.[278]

In the KLKs family, we observed a pronounced expression of KLK7 and KLK10 in the PD adenocarcinoma. It is already known that KLK7 facilitates tumour invasion and metastasis by degradation of extracellular matrix components and KLK10 is involved in carcinogenesis and is being used as a biomarker in this pathology.[346]

MMPs alterations in expression are mainly related to MMP1 and MMP9, being highly expressed in the MD and the PD samples, respectively. Both of them have special importance in gastric cancer.[347] Surprisingly, MMP2, 3, 7 and 8 were down-regulated in the PD sample compared to the healthy tissue. In the remaining proteases, differences in adenocarcinomas compared to control samples were also found for PC9 and uPA.

In this chapter, we found that obestatin is able to actively bind GPR39 and triggered signalling pathways involved in oncogenic processes in gastric cancer. In addition, the GPR39-RTK crosstalk is not only limited to the EGFR, but instead depends on the available RTKs present in the samples/tissues, and regulated the expression of proteases involved in processes and pathways already described for obestatin. All these data, together with the fact that human gastric adenocarcinomas expressed GPR39 allows us to hypothesize that the obestatin/GPR39 system might play a key role in the development and progression of gastric cancer.

[340] Li P, Lin X, Zhang JR, *et al*. The expression of presenilin 1 enhances carcinogenesis and metastasis in gastric cancer. Oncotarget. 2016;7:10650-62.

[341] Iruela-Arispe ML, Carpizo D, Luque A. ADAMTS1: a matrix metalloprotease with angioinhibitory properties. Ann N Y Acad Sci. 2003;995:183-90.

[342] Rodríguez-Manzaneque JC, Carpizo D, *et al*. Cleavage of syndecan-4 by ADAMTS1 provokes defects in adhesion. Int J Biochem Cell Biol. 2009;41:800-10.

[343] Oleksowicz L, Bhagwati N, DeLeon-Fernandez M. Deficient activity of von Willebrand's factor-cleaving protease in patients with disseminated malignancies. Cancer Res. 1999;59:2244-50.

[344] Koo BH, Oh D, Chung S, *et al*. Deficiency of von Willebrand factor-cleaving protease activity in the plasma of malignant patients. Thromb. Res. 2002;105:471-6.

[345] Teller A, Jechorek D, Hartig R, *et al*. Dysregulation of apoptotic signaling pathways by interaction of RPLP0 and cathepsin X/Z in gastric cancer. Pathol Res Pract. 2015;211:62-70.

[346] Liu XL, Wazer DE, Watanabe K, *et al*. Identification of a novel serine protease-like gene, the expression of which is down-regulated during breast cancer progression. Cancer Res. 1996;56:3371-9.

[347] Albo D, Shinohara T, Tuszynski GP. Up-regulation of matrix metalloproteinase 9 by thrombospondin 1 in gastric cancer. J Surg Res. 2002;108:51-60.

USC
UNIVERSIDADE
DE SANTIAGO
DE COMPOSTELA

CHAPTER 4

In this chapter, we determined the role of the obestatin/ GPR39 system in regulating motility, EMT, and invasion of adenocarcinoma cells. First, we found that obestatin promoted cell mobility and invasion by inducing EMT and cytoskeleton remodeling in AGS cells. Second, we showed that GPR39 was present in the chief cells located at the base of the oxyntic glands, while obestatin was identified in the neuroendocrine cells of the oxyntic glands. Third, the GPR39 pattern correlated with the dedifferentiation of gastric adenocarcinomas, and the obestatin expression was negative. We propose that the obestatin/GPR39 system displays an enhancer role in the development and progression of gastric adenocarcinoma.

The obestatin/GPR39 system has important regulatory roles in controlling proliferation and differentiation through a fine modulation of key players in these cellular pathways. Specifically, the obestatin/GPR39 system has been described to act as a pro-proliferative signal in gastric cancer cells, namely, KATO III and AGS.[123,142] For simplicity, and similar to the human gastric adenocarcinomas, we used the AGS cell line, which expresses the obestatin/GPR39 system and retains the characteristics of the parent tumour. In this study, our findings implicated an autocrine/paracrine regulation of cell proliferation, which activated Ki67 expression. Furthermore, this study shows that the obestatin/GPR39 system is a key regulator of EMT. This conclusion is based on the observation that obestatin induced a repertoire of biochemical (increased β-catenin, N-cadherin, and vimentin) and morphological (increased formation of lamellipodia) changes, that are characteristic of EMT. Thus, cytoskeleton reorganization induced by obestatin/ GPR39, shifting its epithelial phenotype to an invasive-like one, facilitated tumour migration, invasion, and metastasis. Recent studies have implicated mTORC1 and mTORC2 as key regulators of EMT.[348] Indeed, GPR39 activates mTOR signalling via the β-arrestin/MMP/EGFR/Akt pathway.[142] Additionally, obestatin was shown to increase the expression of VEGF and its receptor isoform VEGFR2 in these cells. Conversely, PEDF expression was down-regulated. Notably, the VEGF/VEGFR2 system is primarily responsible for both normal and tumour-related angiogenesis.[349] This finding implies that VEGF, which is produced by obestatin-stimulated cells, provides the needed vascularization of the developing tumour. This postulate is further supported by the down-regulation of the anti-angiogenic factor PEDF.[350]

In healthy human stomachs, positive expression of obestatin was observed in the neuroendocrine cells, while GPR39 expression was identified in the chief cells of the oxyntic glands. Therefore, the idea of an autocrine positive feedback of obestatin was ruled out; however, an endocrine mechanism by which obestatin accesses its own transmembrane receptor to optimally mediate receptor-ligand interactions is possible. Taking into account the GPR39 location, obestatin may regulate pepsinogen secretion in the chief cells, an important fact for the digestive process in the stomach.

[348] Gulhati P, Bowen KA, Liu J, *et al*. mTORC1 and mTORC2 regulate EMT, motility, and metastasis of colorectal cancer via RhoA and Rac1 signaling pathways. Cancer Res. 2011;71:3246-56.

[349] Veikkola T, Alitalo K. VEGFs, receptors and angiogenesis. Semin Cancer Biol. 1999;9:211-20.

[350] Zhang Y, Han J, Yang X, *et al*. Pigment epithelium-derived factor inhibits angiogenesis and growth of gastric carcinoma by down-regulation of VEGF. Oncol Rep. 2011;26:681-6.

A particularly interesting result is that chief cells expressed GPR39 together with the expression found in human adenocarcinomas. This fact might relate this cell type to the origin of the gastric adenocarcinoma. Indeed, the potential correlation between the chief cells and gastric cancer has been proposed.[351,310] These studies provided direct evidence by lineage tracing that under pathophysiological loss of acid-secreting parietal cells, the chief cell lineage can itself transdifferentiate into a mucous cell metaplasia, designated spasmolytic polypeptide expressing metaplasia, a precancerous lesion in stomach. Particularly in the presence of inflammation, this metaplastic lineage can regain proliferative capacity and, in humans, may also further differentiate into intestinal metaplasia. Thus, mature gastric chief cells have the ability to act as cryptic progenitors and reacquire proliferative capacity within the context of mucosal injury and inflammation

Of major clinical significance was the observation that the GPR39 expression found in gastric adenocarcinomas correlated with the dedifferentiation of the tumour. The histologic type is important for estimating tumour progression and the outcomes of patients with gastric carcinoma, as it represents an independent prognostic factor among the pathological variables of the tumour.[352] In that sense, the correlation found for GPR39 and the histologic type endorse the use of this receptor as a marker of tumour progression.

In conclusion, the present work addresses the role of the obestatin/GPR39 system in regulating motility, EMT, and invasion of gastric adenocarcinoma cells. More importantly, the levels of GPR39 expression in these tumours provide the rationale for including GPR39 as a prognostic marker of human gastric adenocarcinomas.

[351] Nam KT, Lee HJ, Sousa JF, *et al*. Mature chief cells are cryptic progenitors for metaplasia in the stomach. Gastroenterology. 2010;139:2028-37.

[352] Adachi Y, Yasuda K, Inomata M, *et al*. Pathology and prognosis of gastric carcinoma: well versus poorly differentiated type. Cancer. 2000;89:1418-24.

CHAPTER 5

Results from Chapter 5 offer three major findings related to the secretion of pepsinogen in response to obestatin. First, GPR39, the obestatin receptor was expressed intensely in the chief cells of the human stomach, which are the pepsinogen secretory cells. Second, exogenous obestatin increased pepsinogen release from an in vitro model: the AGS cells, being detectable at protein level in culture medium. Third, this stimulatory effect was mediated by the GPR39 receptor. Thus, obestatin has a functional role on chief cells, exerting a stimulatory action on pepsinogen secretion.

Obestatin and ghrelin are two peptides emerging from the same preproprotein, preproghrelin. Both are produced and secreted by the same cells in the oxyntic mucosa of the stomach, and were believed to possess opposing functions regarding feeding. Ghrelin orexigenic action is well established, but obestatin anorexigenic action was rapidly discarded. Among the multiple actions discovered for ghrelin, it has been described its acidic stimulatory effect in the parietal cells of the stomach. This influence of ghrelin on acid secretion is thought to be mediated via the release of histamine from ECL cells.[353] However, with the exception of our works on cancer cells of the stomach,[123,142,301] although numerous actions have been described for obestatin, none of them had a relationship with the main site of obestatin production, the stomach.

It is clear nowadays, that GPR39 receptor mediates obestatin actions in many cell lines and tissues. Our findings for GPR39 in the chief cells of the stomach, led us to propose a possible action for obestatin in healthy stomach, pepsinogen secretion. In fact, using an in vitro model of a cell line that endogenously expresses the GPR39 and secretes pepsinogen, we demonstrated that an exogenous administration of obestatin stimulates the pepsinogen release. This data proposes functionality for obestatin in the healthy stomach.

The signalling mechanisms underlying this novel action described for obestatin will be discussed. The regulatory mechanisms for pepsinogen secretion are not fully understood. As it was mentioned in the introduction, two main pathways are implicated in pepsinogen secretion. The first pathway implies the activation of adenylate cyclase (AC), with an increase in the cAMP and subsequent activation of PKA. The second one implies the activation of PLC, with the consequent hydrolysis of phosphatidylinositol 4,5-bisphosphate (PIP2), resulting in the formation of inositol trisphosphate (IP3) and diacylglycerol (DAG). IP3 and DAG increase calmodulin-dependent protein kinase II (CaMKII) activation and PKC, respectively. The first data regarding obestatin signalling, reported that this peptide stimulated cAMP production,[1] being a plausible mechanism for obestatin stimulatory effect on pepsinogen secretion. Considering the second pathway, it has been described that obestatin did not produce any intracellular calcium mobilization,[128] nor activated the typical calcium-dependent PKCs: PKCα, β and γ,[123] ruling out this possibility.

However, it has been reported that rat gastric chief cells are strongly stained to proteinase-activated receptor 2 (PAR2),[354] and that PAR2 triggers pepsinogen secretion in guinea pig gastric-isolated

[353] Sakurada T, Ro S, Onouchi T, *et al*. Comparison of the actions of acylated and desacylated ghrelin on acid secretion in the rat stomach. J Gastroenterol. 2010;45:1111-20.

[354] Kawao N, Sakaguchi Y, Tagome A, *et al*. Protease-activated receptor-2 (PAR-2) in the rat gastric mucosa: immunolocalization and facilitation of pepsin/pepsinogen secretion. Br J Pharmacol. 2002;135:1292-6.

chief cells,[355] leading to the hypothesis that PAR2 modulates pepsinogen secretion, although the signalling mechanisms remained to be investigated. PARs comprise a class A GPCR family, which activate complex intracellular signalling networks. These intricate mechanisms include interactions with other PARs, GPCRs, receptors tyrosine kinase and serine/threonine kinase (RTKs and receptor serine/threonine kinase RSTKs, respectively) and signal transducers at both the signalling and receptor trafficking level. Moreover, PARs differ from the usual GPCRs because they exhibit a unique mechanism of proteolytic activation.[356]

Obestatin exerts its actions through mechanisms that imply the activation of two main signalling routes activated in parallel via de GPR39 receptor: i) Gi-protein mediated ERK1/2 activation;[123] and ii) ß-arrestin 1-mediated Akt signalling pathway involving the EGFR cross-talk through the MMPs.[142] Data from chapter 3 gives support to the transactivation process triggered by obestatin. Analysis of protein arrays comprising 34 proteases showed that obestatin stimulated the secretion of diverse proteases, especially several human KLK-related peptidases. These KLKs could be involved in the activation of the PARs present in AGS cells, PAR2 among them, and might be an alternative via regulating the pepsinogen secretion stimulated by obestatin.

In summary, the system obestatin/GPR39 has a function in the chief cells of the human stomach, indicating a regulation of the secretion of pepsinogen. Nevertheless, the exact mechanisms involved in the obestatin stimulated pepsinogen secretion need further investigations.

[355] Fiorucci S, Distrutti E, Federici B, *et al*. PAR-2 modulates pepsinogen secretion from gastric-isolated chief cells. Am J Physiol Gastrointest Liver Physiol. 2003;285:G611-20.

[356] Gieseler F, Ungefroren H, Settmacher U, *et al*. Proteinase-activated receptors (PARs) - focus on receptor-receptor-interactions and their physiological and pathophysiological impact. Cell Commun Signal. 2013;11:86.

CHAPTER 6

As it has been mentioned before, the GPR39 is a GPCR ubiquitously expressed in the human body with specific functions regarding the location. For instance, GPR39 is expressed in the chief cells of the stomach, and exerts a role in pepsinogen secretion (see Chapter 5). However, in pathological conditions as cancer, this receptor becomes overexpressed and together with obestatin provokes stimulatory effects on regulating motility, EMT, and invasion of gastric adenocarcinoma cells (see Chapter 4).

In this chapter, obestatin effects were tested in nine human cancer cell lines that endogenously expressed both obestatin and the GPR39 receptor. Obestatin showed an enhancer effect in all of the cancer cell lines tested on proliferation, skeleton reorganization and invasiveness *via* the GPR39 receptor, demonstrating that its mitogenic and invasive potential is not only limited to the gastric adenocarcinoma cells;[301] therefore, the system might be an enhancer of cancer development in other tissues of the human body.

Regarding proliferation, obestatin most remarkable effect was observed in the PANC-1 cells. The effect on the rest of the cell lines tested was variable; being the less affected the SW872 and the A431 cell lines. These differences in the proliferation ratio could not only be due to GPR39 expression, but to the expression of diverse proteins that participate in the signalling mechanisms triggered by obestatin. Indeed, it has been established the GPR39-EGFR cross-talk in the signalling pathway of the obestatin/GPR39 system. EGFR is highly expressed in a variety of human tumours and is implicated in tumour development: activation of the EGFR signalling network results in tumour growth, inhibition of apoptosis, cell migration and invasion, cellular differentiation, and transformation. Moreover, the heterodimerization of EGFR with HER2 (ErbB2) induces a more potent activation of the EGFR than does EGFR homodimerization. When tumour cells overexpress both EGFR and HER2, they exhibit aggressive tumour cell growth, owing to the increased potential for EGFR/HER2 heterodimerization and signalling.[357] The results obtained in Chapter 3 supported this information. In fact, EGFR and ErbB2 resulted the most activated receptors after obestatin treatment. It has been also described that the rat tumour somatotroph cell line, GC, presented no proliferation upon obestatin treatment, possibly due to the low expression levels of EGFR.[128] All cell lines tested expressed reasonable quantities of GPR39: PANC-1, the highest, and A431 the lowest; conversely, EGFR expression was low, except for PANC-1 and A431 cells.[323,324] With these data in mind, GPR39 knockdown abolished obestatin proliferative capabilities in PANC-1 cells and, GPR39 overexpression caused a huge augment of the proliferation in the same conditions in A431 cells, together with effects on the cellular morphology of these cell lines, similarly as happened for the AGS cell line.

In summary, these results involved the obestatin/GPR39 system in the proliferation and cell motility, probably by cytoskeletal modulation to facilitate cell migration and invasion, of these human cancer cell lines. Moreover, obestatin proliferative action depends not only on GPR39, but also on the

[357] Hirsch FR, Varella-Garcia M, Cappuzzo F. Predictive value of EGFR and HER2 overexpression in advanced non-small-cell lung cancer. Oncogene. 2009;28:S32-7.

expression of key components of its signalling pathway: proteases and RTKs. However, the exact signalling mechanisms still need further investigations.

The KATO III cell line deserves special mention. This cell line harbours a point mutation in E-cadherin that generates two subtypes of cells in culture, floating and adherent, with different characteristics during the metastatic process.[358] Our results showed that obestatin treatment caused the conversion of floating spherical KATO III cells into adherent epithelial-like cells. This transformation might be related to the expression of the *nm23-H1* gen as changes in its expression are related to both populations in these cells; certainly, a diminution in its expression has been observed for the adherent culture. Additionally, *nm23-H1* is considered a metastasis-associated gene, and reductions in its expression have been significantly associated with aggressive behaviour in melanoma, breast, colon, and gastric carcinomas. Expression of nm23-H1 is inversely proportional to the metastasis of these carcinomas.[359] The relationship between the obestatin/GPR39 system and the expression of nm23 is an attractive field for future projects.

Several groups have designated Zn^{+2} as a ligand for GPR39[55] and some others considered that GPR39 is the Zn^{+2}-sensing receptor (ZnR). They reported that GPR39, activated by Zn^{+2}, has a role in promoting proliferation[81] and enhanced survival of colonocytes[82] and cancer prostate cells.[83] However, Zn^{+2} has also been described as an apoptotic agent in several human cancer cells: melanoma,[360] glioma,[361] bladder,[362] prostate,[363] and breast cancer cells.[364] Our results showed that Zn^{+2} treatment caused cell apoptosis and cell viability reduction in KATO III and HT-29 cells. Besides the mitogenic and survival increase induced by obestatin in these cells, obestatin counteracted Zn^{+2} effects. These discrepancies might be attributed to the fact that colonocytes and prostate cancer cells were short-term stimulated with Zn^{+2}, as well as this ion involvement in the EGFR signalling pathways. Treatment with Zn^{+2} triggers the activation of MAPK and PI3K/Akt signalling pathways through EGFR activation in several cell types.[147,148,149] These findings also suggest that there are specific marked differences to each cell type in the EGFR activation mechanism induced by Zn^{+2}.[148] These contradictory results added more questions to the intriguing relationship between Zn^{+2} and the GPR39 receptor. However, these data could imply Zn^{+2} in GPR39 signalling, probably due to the activation of the MMP-EGFR pathways, since obestatin needs EGFR transactivation and MMPs activity.

[358] Iizuka N, Tangoku A, Hazama S, *et al*. Nm23-H1 gene as a molecular switch between the free-floating and adherent states of gastric cancer cells. Cancer Lett. 2001;174:65-71.

[359] Tee YT, Chen GD, Lin LY, *et al*. Nm23-H1: a metastasis-associated gene. Taiwan J Obstet Gynecol. 2006;45:107-13.

[360] Provinciali M, Pierpaoli E, Bartozzi B, *et al*. Zinc induces apoptosis of human melanoma cells, increasing reactive oxygen species, p53 and FAS ligand. Anticancer Res. 2015;35:5309-16.

[361] Wang Y, Zhang S, Li SJ. Zn(2+) induces apoptosis in human highly metastatic SHG-44 glioma cells, through inhibiting activity of the voltage-gated proton channel Hv1. Biochem Biophys Res Commun. 2013;438:312-7.

[362] Hong SH, Choi YS, Cho HJ, *et al*. Induction of apoptosis of bladder cancer cells by zinc-citrate compound. Korean J Urol. 2012;53:800-6.

[363] Hong SH, Choi HJ, Lee JY, *et al*. Antiproliferative effects of zinc-citrate compound on hormone refractory prostate cancer. Chin J Cancer Res. 2012;24:124-9.

[364] Provinciali M, Donnini A, Argentati K, *et al*. Reactive oxygen species modulate Zn2+-induced apoptosis in cancer cells. Free Radical Bio Med. 2002;32:431-45.

CONCLUSIONS

USC
UNIVERSIDADE
DE SANTIAGO
DE COMPOSTELA

1. The structural features of human obestatin required for the interaction with its receptor comprises:

Amidation at the C-terminus, essential to adopt an α-helix structure and stabilize the GPR39 conformations necessary for the full range of receptor activities.

Human (11-23)-obestatin is able to induce selective coupling to the β-arrestin-dependent signalling, representing the first example of an endogenous biased ligand for GPR39.

Mouse and human obestatin exhibit clear conformational differences beyond their primary structure. This evidence supports the species-specific activity of obestatin.

Obestatin-GPR39 interaction might involve an *E*/*Z* isomerization of the peptide and the posibility that GPR39 could be acting as a prolyl *cis-trans* isomerase.

2. Regarding the activation/regulation mechanism of GPR39 receptor signalling triggered by obestatin:

Obestatin increases GPR39 phosphorylation and induces receptor endocytosis.

The RTKs and proteases expression profiles confirm the implication of EGFR and MMPs in the obestatin signalling pathway, and introduce other proteases and RTKs in the process of GPR39 transactivation.

3. The role of the obestatin/GPR39 system in human tissues includes:

The obestatin/GPR39 system regulates pepsinogen secretion.

This system also regulates proliferation, motility, EMT, and invasion of gastric cancer cells. More importantly, the GPR39 expression levels found in human gastric adenocarcinomas provide the rationale for including GPR39 as a prognostic marker of these tumours.

The ubiquitous expression of GPR39 and its cancer-associated overexpression, together with obestatin, provokes the proliferation and cell motillity of diverse human cancer cell lines. Moreover, these effects depend not only on GPR39, but also on the expression of key components of its signalling pathway, i.e. RTKs, proteases.

USC
UNIVERSIDADE
DE SANTIAGO
DE COMPOSTELA

RESUMO

USC
UNIVERSIDADE
DE SANTIAGO
DE COMPOSTELA

A obestatina é un péptido descuberto no 2005 mediante aproximacións bioinformáticas, que deriva da escisión post-traducional do xene da preproghrelina. Nun principio, foi identificada como un opoñente fisiolóxico á ghrelina na inxesta, non obstante, ao longo deste anos descartáronse as súas funcións anorexíxenas. A obestatina humana está formada por 23 aminoácidos cun residuo Leu terminal susceptible de ser amidado. Esta amidación terminal parece, ademais, ser fundamental para a súa funcionalidade. O estómago é o principal produtor desta hormona, así e todo, tamén pode atoparse no resto do tracto gastrointestinal (duodeno, xexuno, íleo), así como no páncreas, próstata, tiroides, hipófise, leite materno ou plasma. No momento do seu descubrimento, a obestatina foi descrita coma o ligando endóxeno do receptor orfo acoplado a proteínas G, GPR39, agora ben, unha serie de traballos posteriores non foron capaces de demostrar *binding* específico entre ligando e receptor, nin a activación de rutas transdutoras de sinais, polo que o feito de que o GPR39 sexa o receptor da obestatina púxose en dúbida. Un artigo publicado sobre a calidade dos péptidos utilizados, así como numerosos traballos subseguintes mostrando que a obestatina pode actuar especificamente a través deste receptor, apuntan claramente a que a obestatina si é capaz de unirse ao GPR39 e ser funcionalmente activa. A pesar da falta de reproducibilidade das accións biolóxicas da obestatina na inxesta, durante este período, describíronse numerosas funcións adicionais para este péptido. A obestatina ten efectos metabólicos e mioxénicos, actúa sobre o tecido adiposo, cardiovascular ou renal e ten funcións a niveis do sistema nervioso central. Con todo, unha das súas primeiras funcionalidades descubertas, e unha das máis importantes, son as capacidades mitoxénicas do péptido. O feito de que a obestatina regule a proliferación de células de cancro gástrico, unha das principais fontes desta hormona, suxire a implicación da mesma en diferentes procesos tales como a reparación de dano na mucosa gástrica, ou como combustible para a proliferación de células canceríxenas. Ademais, a obestatina únese ao grupo dos factores reguladores de MMPs, implicados en diferentes patoloxías humanas, tales como a inflamación ou o cancro. Parece bastante probable que a transactivación de EGFR por obestatina puidese ser un elemento chave polo que as MMPs regulan estes procesos. Tales mecanismos reflicten a importancia desta transactivación na sinalización intracelular da obestatina. Estes feitos levan a postular que o sistema obestatina/GPR39 ten un papel no desenvolvemento e progresión do cancro, especialmente do cancro gástrico. Tendo en conta estas calidades proliferativas é necesario un estudo máis exhaustivo destas capacidades, así como da relación existente entre a obestatina e o receptor GPR39, o cal axudará ao deseño futuro de novos fármacos relacionados con estas patoloxías.

Deste xeito, o principal obxectivo deste proxecto de tese foi o de establecer a relación entre a obestatina e o receptor GPR39 en eidos tanto sans como tumorais, dende o nivel estrutural ao tisular.

Este obxectivo dividiuse nos seguintes puntos:

Estudo dos requirimentos estruturais necesarios para a interacción da obestatina co seu receptor.

Determinar os mecanismos detallados de activación/regulación da transactivación GPR39/RTKs accionados por obestatina.

Análise e correlación do sistema obestatina/GPR39 no desenvolvemento e malignidade de tumores.

A procura de aplicacións terapéuticas para a obestatina implica, como primeiro paso, a determinación da súa estrutura 3D en solución e a

relación entre esa estrutura e a súa actividade biolóxica. Partindo desa base, empregamos unha combinación de dicroísmo circular, espectroscopía de resonancia magnética nuclear, e técnicas de modelización 3D para determinar a estrutura en solución da obestatina humana (**1**), a obestatina humana non amidada (**2**), os fragmentos humanos (6-23) (**3**), (11-23) (**4**), e (16-23) (**5**); e a obestatina de rato (**6**). Estes estudos foron realizados nunha solución micelar imitando a membrana plasmática (micelas de SDS). Os estudos de relación de actividade-estrutura foron efectuados avaliando as capacidades mitoxénicas *in vitro* destes péptidos na liña celular humana de epitelio pigmentario retiniano, ARPE-19, mediante a fosforilación de ERK1/2 e Akt, a expresión de Ki67, e a capacidade de proliferación celular mediante incorporación de BrdU. Os resultados obtidos concluíron que a amidación C-terminal da obestatina humana (**1**) era esencial para adoptar unha estrutura de α-hélice. Esta α-hélice atópase entre os residuos Gly8-Lys11 e Ser20-Leu23. A presenza desta estrutura enlázase coa estabilización conformacional do GPR39 necesaria para a gama completa de actividades do receptor. Isto implica que o GPR39 é capaz de adoptar múltiples conformacións activas, que están relacionadas coa activación de mecanismos de rutas de sinalización que rematan coa subsecuente activación de ERK1/2 e Akt. Observamos ademais, que o fragmento humano (11-23) (**4**) era capaz de inducir selectivamente a ruta de sinalización dependente de β-arrestinas. Este resultado podería implicar que **4** estabiliza unha conformación do receptor distinta da inducida pola obestatina humana (**1**) e esta actividade específica estaría relacionada coa presenza do segmento α-hélice entre os residuos Tyr16-Leu23. Este dato sobre o truncado (11-23) podería ademais, representar o primeiro exemplo dun ligando endóxeno parcial para o GPR39. Por último, os resultados amosaron que a obestatina de rato (**6**) e a obestatina humana (**1**) presentaban diferenzas conformacionais claras alén das súas diferenzas na estrutura primaria. O análogo murino adoptaba unha estrutura 3D distinta, que non era capaz de activar o receptor GPR39 humano. Esta evidencia apoiaría a existencia dunha actividade especie-específica para a obestatina humana.

Nas células, as proteínas interactúan especificamente con receptores, factores, co-ligandos e outros péptidos, xerando un entorno celular difícil de reproducir. Aproximacións biomiméticas na determinación estrutural como as micelas mencionadas anteriormente, proporcionan información moi valiosa sobre os distintos péptidos; agora ben, a base estrutural exacta das funcións biolóxicas dunha determinada proteína require observacións en células vivas. Dende o descubrimento da obestatina, diversos estudos intentaron determinar cales son os requisitos estruturais mínimos necesarios para a súa actividade biolóxica. Até o momento, non hai datos dispoñibles sobre a conformación bioactiva da obestatina cando interacciona co GPR39. Un estudo adecuado sobre a relación estrutura-actividade debe basearse no coñecemento da conformación exacta da obestatina cando se une ao receptor. O carácter non invasivo e a capacidade para proporcionar datos en resolución atómica fan á espectroscopía de RMN heteronuclear multidimensional axeitada para esta tarefa. Neste contexto, o seguinte obxectivo que nos plantexamos foi a determinación da conformación bioactiva da obestatina cando interactúa co seu receptor, GPR39, en condicións *quasi*-fisiolóxicas, en células vivas enriquecidas co receptor. Deste xeito, utilizamos técnicas de RMN para determinar a estrutura da obestatina humana (**1**) e os truncados humanos (6-23) (**3**), (11- 23) (**4**), (16-23) (**5**) e (1-10) (**7**) en H_2O, PBS e células HEK293 *wild type* e transfectadas transitoriamente co receptor GPR39. Os resultados

atopados nos truncados non mostraban diferenzas significativas na estrutura en células vivas. Ademais, semellaba que o equilibrio encontrábase desprazado cara conformacións desestruturadas en todos eles. Soamente os truncados **3** e **7** parecían presentar unha certa tendencia helicoidal en H_2O. En canto á obestatina completa, os datos de RMN amosaron resultados notables. Os cambios nos CSPs, o patrón NOE e a análise do CSI sinalaron que en H_2O e PBS a obestatina tendía a conformacións tipo *random coil*. En presenza de células vivas *wild type*, atopáronse CSP positivos que poderían implicar unha reorganización β pregada ou unha perda de estrutura helicoidal en células sen receptor. Sen embargo, en células tranfectadas co GPR39 observáronse diferencias moi significativas entre os CSPs dos residuos Pro4 e His19. Esta diferenza en Pro4 en presenza de células sen e con receptor podería implicar unha isomerización *E*/*Z* e o feito de que o GPR39 estaría actuando como unha prolil *cis*/*trans* isomerase. Pese a isto, non se atoparon efectos SCE e/ou conxuntos de dobres sinais para a obestatina en presenza de células HEK-GPR39 no espectro TOCSY, o que indicaría a presenza de dous confórmeros en equilibrio. Ademais, o patrón NOE e a análise do CSI sinalaron que a obestatina tendía a conformacións non estruturadas, así como acontecía para os diversos truncados. Aínda así, tendo en conta a posibilidade dun cambio conformacional no residuo Pro4 e os datos NOE observados, calculamos as estruturas 3D da obestatina humana en presenza de células vivas. Esta estrutura 3D indicaba que a obestatina podería estar parcialmente estruturada na zona N-terminal en ámbalas dúas conformacións *E* e *Z*, non obstante, a maior parte dos residuos parecen non estruturados. Atopamos sinais adicionais nos espectros TOCSY en presenza de células enriquecidas co GPR39 que non puideron ser asignados a un determinado residuo á fin de confirmar a existencia de efectos SCE neste sistema. Estes datos, xunto cos CSPs específicos atopados para Pro4 e His19 en células enriquecidas co receptor poderían indicar unha isomerización *cis*/*trans* da prolina, e que, antes de unirse ao seu receptor, a obestatina (**1**) adoptaría unha conformación específica.

Como se comentou anteriormente, a obestatina describiuse inicialmente coma o ligando endóxeno do GPR39. Non obstante, varios grupos cuestionaron este feito e incluso se propuxo o Zn^{+2} como agonista do GPR39, debido á súa capacidade de activar distintas vías de sinalización. En 2015, o grupo de Camiña usando experimentos de co-inmunoprecipitación demostraron *binding* específico entre a obestatina e o GPR39. Os nosos resultados relativos ao sistema tamén apoiaban este dato. A controversia xerada en canto ao modo de interacción, ou máis importante, se existe interacción entre a obestatina e o GPR39, levounos a investigar os primeiros pasos na vía sinalización do sistema, a fosforilación e a internalización do GPR39 mediada por obestatina. Os resultados amosaron que a obestatina aumentaba a fosforilación do GPR39 sobre o seu nivel basal. A elevada fosforilación basal podería representar unha alta actividade constitutiva do receptor, principalmente debido á importancia do seu dominio *C-tail*. Ademais, esta adición esóxena de obestatina, inducía a internalización e endocitose do GPR39 en células enriquecidas co receptor. Os estudos cinéticos de endocitose do GPR39 amosaron que o complexo obestatina-GPR39 era internalizado de forma dependente no tempo, mostrando unha perda máxima de expresión do GPR39 en superficie sobre os 20 min despois da estimulación con obestatina. Ademais, os resultados de microscopía confocal suxeriron a hipótese de que o complexo podería ser reciclado por endosomas temperáns e non degradado nos lisosomas. Non obstante, sería

necesario unha análise mais profunda para elucidar os sistemas exactos de internalización do receptor.

En células de cancro gástrico, xa se demostrara que a obestatina ao unirse a o GPR39 activaba dúas rutas en paralelo: i) a activación secuencial de Gi, PI3K, PKCε, Src e a posterior fosforilación de ERK1/2; e ii) unha vía dependente de β-arrestinas que activaba Akt e as súas dianas. Deste xeito, Src actuaba como un interruptor que activaba MMPs para iniciar a liberación proteolítica de ligandos EGF-*like* na superficie da célula, que se unirían posteriormente ao EGFR. Esta rede de sinalización engadía un novo compoñente nas vías de sinalización intracelular reguladas por obestatina. Esta transactivación de EGFR podería implicar un mecanismo fundamental polo cal as MMPs regularían estas patoloxías. En apoio a esta hipótese, numerosos estudos demostraron que os cambios na expresión e/ou mutacións en membros da familia de receptores tirosina quinase EGFR/ErbB están presentes en tumores e liñas celulares derivadas de estes tumores, e estas modificacións poden contribuír á progresión do cancro. Neste sentido, a obestatina engadiríase ao grupo de factores reguladores de MMPs, implicados en diversas enfermidades humanas, tales como enfermidades inflamatorias ou cancro. En resumo, MMPs e RTKs son pezas clave na patoloxía do cancro. Asumindo mediante traballos publicados anteriormente, que o sistema obestatina/GPR39 está implicado en procesos mitoxénicos en cancro gástrico, o seguinte obxectivo que planeamos foi o estudo detallado do mecanismo de activación/regulación da transactivación de GPR39 e receptores tirosina quinase desencadeada por obestatina. Ademais, tamén incluímos a identificación de distintas proteases activadas e o estudo das posibles repercusións no desenvolvemento do tumor. Como modelo escollemos as liñas celulares humanas de cancro gástrico KATO III e AGS. O nivel diferencial de fosforilación dos distintos RTKs e a expresión de proteases implicadas na vía de sinalización intracelular de obestatina foron estudadas mediante *arrays* de proteínas. Posteriormente, tamén estudamos estes perfís de activación/expresión de RTKs e proteases en catro mostras de tecido gástrico humano, unha mostra sa e tres adenocarcinomas con distinto grao de diferenciación. Os datos obtidos nas liñas celulares concluíron que a obestatina estimulaba a activación de diversos RTKs implicados en proliferación, supervivencia, diferenciación celular e diversos procesos oncoxénicos como a migración, a invasión e a anxioxénese. Os resultados tamén confirmaban o seu efecto sobre o metabolismo da glicosa e a insulina. En canto as proteases, a adición esóxena de obestatina aumentaba tanto a expresión como a secreción de proteases implicadas na degradación da matriz extracelular, así como en procesos de migración e invasión. Moitas delas, ademais, son consideradas biomarcadores de mala prognose en diversas patoloxías, entre elas, o cancro gástrico. Os perfís de expresión confirmaban tamén a implicación das MMPs na vía de sinalización obestatina e introducía outras proteases na transactivación de distintos RTKs mediada polo receptor GPR39. En resumo, os resultados que obtivemos sobre os mecanismos de sinalización do sistema amosaron que a obestatina era capaz de unirse activamente ao GPR39 e desencadear vías de sinalización implicadas en procesos oncoxénicos en cancro gástrico. Ademais, comprobamos que o *cross-talk* GPR39-RTK non se limitaba só ao EGFR, senón que dependía dos RTKs dispoñibles expresados nos distintos sistemas estudados; e que está colaboración regulaba a expresión de proteases implicadas en procesos e vías xa descritos para a obestatina. Todos estes datos, xunto co feito de que as mostras de adenocarcinoma gástrico humano expresasen

GPR39, permitiunos formular a hipótese de que o sistema obestatina/GPR39 podería desempeñar un papel clave no desenvolvemento e progresión do cancro gástrico.

Seguindo esta hipótese formulada, e dado o estado de coñecemento da relación entre o sistema obestatina/GPR39 e progresión do cancro gástrico, no seguinte paso quixemos determinar os niveis de expresión do sistema en adenocarcinomas gástricos humanos e elucidar o seu papel potencial funcional. Para isto, vinte e oito pacientes con adenocarcinoma gástrico foron estudados retrospectivamente, tendo en conta os seus datos clínicos. O papel do sistema obestatina/GPR39 na progresión do cancro gástrico, foi estudada *in vitro* mediante a liña celular de adenocarcinoma gástrico humano AGS. Os resultados que obtivemos amosaron unha regulación autócrina/parácrina do sistema na proliferación celular, activando tamén a expresión Ki67. Ademais, este estudo demostrou que o sistema obestatina/GPR39 podería ser un regulador clave da transición epitelio-mesénquima. Esta conclusión baséase na observación de que obestatina inducía unha serie de cambios bioquímicos (aumento da expresión de β-catenina, N-cadherina e vimentina) e morfolóxicos (aumento da formación de lamellipodia), que son característicos deste proceso. Deste xeito, a reorganización do citoesqueleto inducida polo sistema obestatina/GPR39, cambiando o fenotipo epitelial por outro pro-invasivo facilitaría a migración, invasión e metástase do tumor. Estes datos concordan con estudos recentes que implican aos complexos mTORC1 e mTORC2 como reguladores clave da transición epitelio-mesénquima, dado que o GPR39 activa a sinalización a través da ruta de mTOR, β-arrestina/MMP/EGFR/Akt. Os datos tamén amosaban que a obestatina aumentaba a expresión de VEGF e a isoforma do receptor VEGFR2 nas células AGS. Por outra banda, a expresión de PEDF víase diminuída. O sistema VEGF/VEGFR2 é o principal responsable dos procesos anxioxénicos en tecidos tanto sans como tumorais. Os datos observados suxiren que o VEGF, que é producido por células estimuladas con obestatina, ofrecería a necesaria vascularización do tumor en desenvolvemento. Esta premisa estaría apoiada pola regulación negativa do factor anti-anxioxénico PEDF. En canto ás mostras humanas de adenocarcinomas gástricos analizadas, puidemos comprobar que en mucosa sa, a obestatina soamente se expresaba nas células neuroendócrinas, mentres que a expresión de GPR39 se circunscribía ás células principais situadas no fondo das foveolas gástricas. Estes datos descartaban unha regulación autócrina da obestatina, apuntando a un mecanismo de tipo endócrino ligando-receptor para mediar as accións do sistema. O GPR39 tamén se expresaba de forma intensa e variable, na zona tumoral das mostras estudadas. Este resultado, xunto co feito de que se expresara tamén nas células principais da mucosa oxíntica, resulta particularmente interesante. Diversos estudos propuxeron unha correlación potencial entre as células principais e a orixe do cancro gástrico. En estados avanzados de gastrite crónica, unha perda de células parietais podería producir unha transdiferenciación de células principais xerando unha metaplasia de tipo SPEM, e posteriormente inclusive, unha metaplasia intestinal. Esta metaplasia sería un paso previo para unha posterior displasia e xeración dun cancro gástrico. Neste senso, de gran significado clínico resultaron os datos observados en canto á expresión GPR39 nos distintos adenocarcinomas. Canto peor era a prognose de tumor, maior expresión de GPR39 presentaba; é dicir, a expresión do receptor correlacionábase coa dediferenciación do tumor. Esta correspondencia entre o tipo histolóxico e a expresión de receptor apoiaría a inclusión do GPR39 como un marcador de progresión tumoral. En

conclusión, observamos que o sistema obestatina/GPR39 regulaba a motilidade, a transición epitelio-mesénquima, e a invasión en células humanas de cancro gástrico. Aínda máis, os niveis de expresión de GPR39 atopados neste tipo de tumores proporcionaron un fundamento lóxico para a inclusión do GPR39 como un marcador prognose en adenocarcinomas gástricos humanos.

A expresión atopada para o GPR39 en células principais da mucosa en mostras sas de estómago humano, levounos a investigar a posible relación existente entre o sistema obestatina/GPR39 e a secreción de pepsinóxeno I. A expresión do receptor e de pepsinóxeno foi determinada mediante técnicas inmunohistoquímicas. A secreción de pepsinóxeno I trala adición de obestatina foi determinada mediante distintos métodos nun modelo *in vitro* que expresaba endóxenamente os tres compoñentes do estudo: obestatina, GPR39 e pepsinóxeno; a liña de adenocarcinoma gástrico AGS. Os resultados atopados ofrecen tres conclusións importantes relacionadas coa secreción de pepsinóxeno I en resposta a obestatina. En primeiro lugar, o GPR39 presentaba unha expresión intensa nas células principais do estómago humano, que son as células secretoras de pepsinóxeno. O GPR39 colocalizaba con pepsinóxeno I nas células pre-zimoxénicas e células principais situadas entre o colo e a base das glándulas oxínticas. En segundo lugar, a obestatina esóxena aumentaba a secreción de pepsinóxeno I no noso modelo *in vitro*, as células AGS, que endóxenamente expresan GPR39. En terceiro lugar, este efecto estimulador estaba mediado polo receptor GPR39. Estes resultados propoñen funcionalidade para a obestatina en estómago san, xa que, a pesar das numerosas accións descritas para a obestatina, á excepción dos nosos traballos en cancro gástrico, ningún deles estaba relacionado co principal produtor do péptido. Agora ben, as vías de sinalización subxacentes a esta nova acción non están claras. Os mecanismos de regulación da secreción de pepsinóxeno non se coñecen totalmente. Dúas vías principais parece que están implicadas. A primeira vía activa AC, cun aumento de AMPc e a posterior activación de PKA. A segunda implica a activación de PLC, coa consecuente activación de CaMKII e PKC. A obestatina é capaz de aumentar a produción de AMPc, sendo esta vía un mecanismo plausible para este efecto secretor. Non obstante, está descrito que a obestatina non promove a mobilización de calcio intracelular, nin activa PKCs dependentes de calcio, descartando esta segunda vía como posible reguladora. PAR2 parece que tamén pode modular a secreción de pepsinóxeno. Os mecanismos de sinalización do sistema descritos anteriormente, amosaron que a obestatina estimulaba a secreción de KLKs. Estas KLKs poderían estar implicadas na activación de distintos receptores activados por proteinases presentes nas células AGS, PAR2 entre eles, e poderían ser unha alternativa, a través da cal se regularía a secreción de pepsinóxeno estimulada por obestatina. Non obstante, os mecanismos exactos de regulación do proceso precisarían investigacións máis detalladas.

Tendo en conta os datos obtidos relativos ao sistema obestatina/GPR39 en cancro gástrico xa mencionados na presente memoria, o último obxectivo que planeamos foi o estudo do papel deste sistema noutros tipos de cancro. Avaliamos os efectos da obestatina sobre a proliferación, capacidade de invasión e reorganización do citoesqueleto *via* GPR39 en nove liñas celulares cancerígenas humanas, para comprobar se o potencial mitoxénico e invasivo do sistema estaba restrinxido a células de adenocarcinoma gástrico. Os resultados amosaron que todas as liñas celulares expresaban endóxenamente tanto o ligando coma o receptor, e que esta expresión estaba asociade á mitose.

Asemade, a obestatina aumentaba a proliferación en todas elas. Observamos un máximo efecto nas células PANC-1 e menos pronunciado nas liñas SW872 e A431. Este efecto mitoxénico podería estar influenciado polo *cross-talk* existente entre GPR39 e EGFR e/ou outros RTKs dispoñibles nos distintos sistemas. Tendo en conta estes datos, silenciamos o receptor GPR39 en células PANC-1 e observamos que as capacidades proliferativas e pro-morfoxéncias da obestatina estaban claramente diminuídas. Polo contrario, a sobreexpresión do receptor causaba en células A431, que expresan gran cantidade de EGFR, un enorme aumento na proliferación, así como unha reestruturación do citoesqueleto de xeito semellante ao que se producía nas células AGS. Os datos obtidos na liña celular KATO III merecen unha mención especial. Observamos que o tratamento con obestatina causaba a conversión de células esféricas flotantes KATO III en células con morfoloxía epitelial de tipo adherente; inducindo a formación de estruturas tipo lamellipodio/filopodio e favorecendo un fenotipo invasivo. Esta transformación podería estar relacionada coa expresión do xene anti-metastásico *nm23-H1* e o seu efecto en ámbalas dúas poboacións celulares. En células KATO III e HT-29, así mesmo, a obestatina aumentaba a mitoxénese e a supervivencia celular. Nas dúas liñas celulares, a adición esóxena de Zn^{+2} actuaba como un promotor apoptótico reducindo a viabilidade. Este efecto era contrarrestado por obestatina. O Zn^{+2} foi descrito por algúns grupos como o agonista endóxeno do GPR39. O receptor, activado polo ión, aumentaba a proliferación e a supervivencia celular en distintas liñas celulares humanas. Sen embargo, as capacidades apoptóticas do Zn^{+2} tamén foron descritas en diferentes sistemas. Estes resultados, cos datos existentes sobre a implicación do ión na activación de EGFR, poderían suxerir que os efectos estimuladores do Zn^{+2} nas vías de sinalización mediadas polo GPR39, poderían ser debidos á activación de vías dependentes de MMP-EGFR; dado que a obestatina precisa da transactivación dos mesmos para exercer as súas funcións biolóxicas. En xeral, o conxunto de resultados implica ao sistema obestatina/GPR39 na proliferación e a motilidade celular, posiblemente mediante a modulación do citoesqueleto, para facilitar a migración e invasión celular en liñas celulares cancerígenas humanas. Ademais, a acción mitoxénica da obestatina dependería non só do GPR39, senón tamén da expresión de compoñentes clave na súa vía de sinalización: proteases e RTKs.

En resumo, as conclusións que se poden extraer da presente memoria son as seguintes. A amidación C-terminal da obestatina semella ser fundamental para a estrutura e a bioactividade. Asemade, esta actividade é especie-específica no caso da obestatina humana. O truncado (11-23) pode representar, á súa vez, o primeiro exemplo de ligando parcial endóxeno do GPR39. O receptor, así mesmo, podería estar actuando como unha prolil *cis*/*trans* isomerase e provocando a formación de conformacións bioactivas específicas da obestatina. Por outra banda, a obestatina aumenta a fosforilación e induce a internalización e endocitose do GPR39. A implicación de EGFR e MMPs na vía de sinalización da obestatina viuse claramente confirmada, introducindo outras proteases e RTKs no proceso de transactivación do GPR39. Dende o punto de vista funcional, observamos que o sistema obestatina/GPR39 pode ser un regulador clave da transición epitelio-mesénquima, facilitando así a migración, invasión e metástase en cancro gástrico. Neste senso, o GPR39 podería ser incluído como un marcador prognose deste tipo de tumores. Este efecto potenciador da obestatina sobre a proliferación, capacidade de invasión e reorganización do citoesqueleto tamén se observa en distintas liñas cancerígenas humanas. Por

último, a presenza de GPR39 nas células principais da mucosa oxíntica, así como o efecto estimulador da obestatina sobre a secreción de pepsinóxeno I proporcionaría a primeira función biolóxica coñecida do sistema en estómago san.

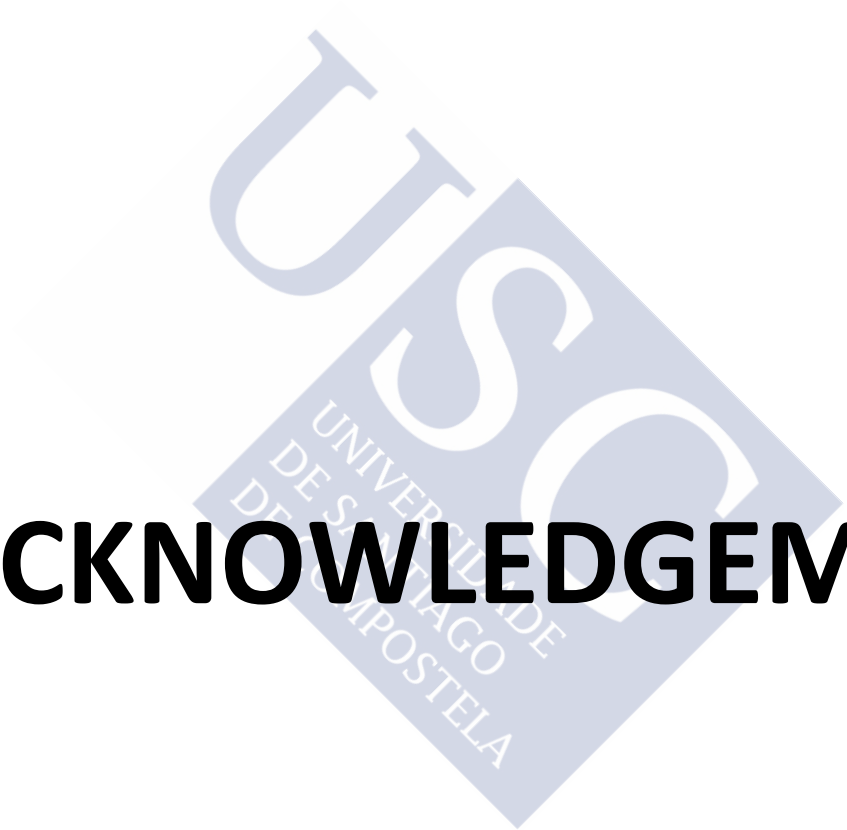

ACKNOWLEDGEMENTS

USC
UNIVERSIDADE
DE SANTIAGO
DE COMPOSTELA

Como punto e final a unha andaina de seis longos anos non hai mellor modo de pechar unha etapa que agradecendo a todas esas persoas que en maior ou menor medida a fixeron posible.

En primeiro lugar, quero agradecer aos meus tres directores de tese, á Dra. Yolanda Pazos, ao Dr. Felipe Casanueva e ao Dr. Tomás García-Caballero, a oportunidade que me brindaron ao depositar en min a confianza para levar a cabo este traballo. Ao Dr. Casanueva gustaríame agradecerlle especialmente o apoio e facilidades que sempre me ofreceu. A Tomás, a súa accesibilidade, consello, interese e axuda durante toda esta etapa. A Yola, non podo máis que darlle as grazas pola súa confianza, apoio e guía ao longo de todos estes anos. Sen a súa dedicación, paciencia e cariño esta tese non sería posible. Grazas por todas esas horas de traballo compartido e de alento nos malos momentos. Pola transmisión da ilusión e da recompensa do esforzo, e por compartir os éxitos e os fracasos.

Ao Dr. Manuel Martín Pastor e á Dra. Rosalía Gallego polo seu asesoramento, axuda, paciencia e amabilidade en numerosos pasos do camiño. Ao Dr. Jesús Jiménez Barbero e todo o seu equipo no CIC bioGUNE por recibirme e axudarme con tanto agarimo.

A Jesús, pola súa orientación e interese constantes, polo apoio e amabilidade no plano profesional e persoal.

A todos os compañeiros de Endocrino e do IDIS cos que pasei tantas horas de traballo e que sempre estiveron dispostos a botarme unha man cun sorriso. A Ángel, por ser un piar fundamental en todos estes anos. A Carlos, polas risas e bos momentos.

Aos meus "chicos" do labo 4-3, cos que compartín algúns dos momentos máis felices e máis tristes da miña vida e que fixeron destes anos un período inesquecible. A Gus, Jess, Lara, Saúl, Tania…. de todos e cada un levo recordos marabillosos. O traballo sempre é mais fácil se se comparte o día a día con xente coma vós. E Boli, a miña compañeira no camiño. Toda esta etapa tería sido moito máis difícil e menos importante sen ti. O mellor é saber que isto non remata despois de cruzar a meta.

Á miña familia e amigos que soportaron esta longa etapa predoutoral. A Ángel, polo seu sentido común e sabiduría, e ao meu anxiño pequecho por encherme de ledicia a vida.

A Maru, a miña pequena sis. Grazas por confiar en min sempre a cegas, polo primeiro impulso e polo apoio e ánimo que me axudou a chegar até aquí.

Aos meus pais. Nada do pouco ou moito do que conseguín ou conseguirei sería posible sen o seu amor e apoio infinitos.

A Pablo. Grazas por ser, por estar, por permanecer.

USC
UNIVERSIDADE
DE SANTIAGO
DE COMPOSTELA

BIBLIOGRAPHY

USC
UNIVERSIDADE
DE SANTIAGO
DE COMPOSTELA

1. Zhang JV, Ren PG, Avsian-Kretchmer O, *et al*. Obestatin, a peptide encoded by the ghrelin gene, opposes ghrelin's effects on food intake. Science. 2005;310:996-9.
2. Cummings DE, Overduin J. Gastrointestinal regulation of food intake. J Clin Invest. 2007;117:13-23.
3. Van der Lely AJ, Tschöp M, Heiman ML, *et al*. Biological, physiological, pathophysiological, and pharmacological aspects of ghrelin. Endocr Rev. 2004;25:426-57.
4. Kojima M, Hosoda H, Date Y, *et al*. Ghrelin is a growth-hormone-releasing peptide from stomach. Nature. 1999;402:656-60.
5. Kojima M, Hosoda H, Matsuo H, *et al*. Ghrelin: discovery of the natural endogenous ligand for the growth hormone secretagogue receptor. Trends Endocrinol Metab. 2001;12:118-22.
6. Horvath TL, Diano S, Sotonyi P, *et al*. Minireview: ghrelin and the regulation of energy balance: a hypothalamic perspective. Endocrinology. 2001;142:4163-9.
7. Inui A. Ghrelin: an orexigenic and somatotrophic signal from the stomach. Nat Rev Neurosci. 2001;2:551-60.
8. Yang J, Brown MS, Liang G, *et al*. Identification of the acyltransferase that octanoylates ghrelin, an appetite-stimulating peptide hormone. Cell. 2008;132:387-96.
9. Gutierrez JA, Solenberg PJ, Perkins DR, *et al*. Ghrelin octanoylation mediated by an orphan lipid transferase. Proc Natl Acad Sci USA. 2008;105:6320-5.
10. Korbonits M, Goldstone AP, Gueorguiev M, *et al*. Ghrelin: a hormone with multiple functions. Front Neuroendocrinol. 2004;25:27-68.
11. Bowers CY. Unnatural growth hormone-releasing peptide begets natural ghrelin. J Clin Endocrinol Metab. 2001;86:1464-9.
12. Baldanzi G, Filigheddu N, Cutrupi S, *et al*. Ghrelin and des-acyl ghrelin inhibit cell death in cardiomyocytes and endothelial cells through ERK1/2 and PI 3-kinase/AKT. J Cell Biol. 2002;159:1029-37.
13. Camina JP. Cell biology of the ghrelin receptor. J Neuroendocrinol. 2006;18:65-76.
14. McKee KK, Palyha OC, Feighner SD, *et al*. Molecular analysis of rat pituitary and hypothalamic growth hormone secretagogue receptors. Mol Endocrinol. 1997;11:415-23.
15. Kishimoto M, Okimura Y, Nakata H, *et al*. Cloning and characterization of the 50- flanking region of the human ghrelin gene. Biochem Biophys Res Commun. 2003;305:186-92.
16. Kanamoto N, Akamizu T, Tagami T, *et al*. Genomic structure and characterization of the 50-flanking region of the human ghrelin gene. Endocrinology. 2004;145:4144-53.
17. Jeffery PL, Duncan RP, Yeh AH, *et al*. Expression of the ghrelin axis in the mouse: an exon 4-deleted mouse proghrelin variant encodes a novel C terminal peptide. Endocrinology. 2005;146:432-40.
18. Hosoda H, Kojima M, Mizushima T, *et al*. Structural divergence of human ghrelin. Identification of multiple ghrelin-derived molecules produced by post-translational processing. J Biol Chem. 2003;278:64-70.
19. Yeh AH, Jeffery PL, Duncan RP, *et al*. Ghrelin and a novel preproghrelin isoform are highly expressed in prostate cancer and ghrelin activates mitogen-activated protein kinase in prostate cancer. Clinical Cancer Research. 2005;11:8295-03.
20. Gahete MD, Cordoba-Chacon J, Hergueta-Redondo M, *et al*. a A novel human ghrelin variant (In1-ghrelin) and ghrelin-O-acyltransferase are overexpressed in breast cancer: potential pathophysiological relevance. PLoS ONE. 2011;6:e23302.
21. Romero A, Kirchner H, Heppner K, *et al*. GOAT: the master switch for the ghrelin system? Eur J Endocrinol. 2010;163:1-8.
22. Gualillo O, Lago F, Casanueva FF, *et al*. One ancestor, several peptides post-translational modifications of preproghrelin generate several peptides with antithetical effects. Mol Cell Endocrinol. 2006;256:1-8.
23. Garg A. The ongoing saga of obestatin: is it a hormone? J Clin Endocrinol Metab. 2007;92:3396-8.
24. Zhu X, Cao Y, Voogd K, *et al*. On the processing of proghrelin to ghrelin. J Biol Chem. 2006;281:38867-70.
25. Ozawa A, Cai Y, Lindberg I. Production of bioactive peptides in an in vitro system. Anal Biochem. 2007;366:182-9.
26. Steiner DF. The proprotein convertases. Curr Opin Chem Biol. 1998;2:31-9.
27. Owen TC, Merkler, DJ. A new proposal for the mechanism of glycine hydroxylation as catalyzed by peptidylglycine alphahydroxylating monooxygenase (PHM). Med Hypoth. 2004;62:392-400.
28. Green BD, Irwin N, Flatt PR. Direct and indirect effects of obestatin peptides on food intake and the regulation of glucose homeostasis and insulin secretion in mice. Peptides. 2007;28:981-7.

29. Nagaraj S, Peddha MS, Manjappara UV. Fragments of obestatin as modulators of feed intake, circulating lipids, and stored fat. Biochem Biophys Res Commun. 2008;366:731-7.
30. Subasinghage AP, Green BD, Flatt PR, *et al*. Metabolic and structural properties of human obestatin (1-23) and two fragments peptides. Peptides. 2010;31:1697-705.
31. Vergote V, Van Dorpe S, Peremans K, *et al*. In vitro metabolic stability of obestatin: kinetics and identification of cleavage products. Peptides. 2008;29:1740-8.
32. Nagaraj S, Peddha MS, Manjappara UV. Fragment analogs as better mimics of obestatin. Regul Pept. 2009;158:143-8.
33. Furnes MW, Stenstrom B, Tømmerås K, *et al*. Feeding behavior in rats subjected to gastrectomy or gastric bypass surgery. Eur Surg Res. 2008;40:279-88.
34. Grönberg M, Tsolakis AV, Magnusson L, *et al*. Distribution of obestatin and ghrelin in human tissues: inmunoreactive cells in the gastrointestinal tract, pancreas, and mammary glands. J Histochem Cytochem. 2008;56:793-801.
35. Volante M, Rosas R, Ceppi P, *et al*. Obestatin in human neuroendocrine tissues and tumours: expression and effect on tumour growth. J Pathol. 2009;218:458-66.
36. Tsolakis AV, Grimelius L, Stridsberg M, *et al*. Obestatin/ghrelin cells in normal mucosa and endocrine tumours of the stomach. Eur J Endocrinol. 2009;160-941-9.
37. Choi E, Roland JT, Barlow BJ, *et al*. Cell lineage distribution atlas of the human stomach reveals heterogeneous gland populations in the gastric antrum. Gut. 2014;63:1711-20.
38. Dun SL, Brailoiu E, Yang J, *et al*. Distribution and biological activity of obestatin in the rat. J Endocrinol. 2006;191:481-9.
39. Chanoine JP, Wong AC, Barrios V. Obestatin, acylated and total ghrelin concentrations in the perinatal rat pancreas. Horm Res. 2006;66:81-8.
40. Scrima M, Campiglia P, Esposito C, *et al*. Obestatin conformational features: a strategy to unveil obestatin´s biological role? Biochem Biophys Res Commun. 2007;363:500-5.
41. Krishnarjuna B, Ganjiwale AD, Manjappara UV, *et al*. NMR Structure implications of enhanced efficacy of obestatin fragment analogs. Int J Pept Res Ther. 2011;17:259-70.
42. Martín-Pastor M, De Capua A, Álvarez CJ, *et al*. Interaction between ghrelin and the ghrelin receptor (GHS-R1a), a NMR study using living cells. Bioorg Med Chem. 2010;18:1583-90.
43. McKee KK , Tan CP, Palyha OC, *et al*. Cloning and characterization of two human G protein-coupled receptor genes (GPR38 and GPR39) related to the growth hormone secretagogue and neurotensin receptors. Genomics. 1997;46:426-34.
44. Kojima, M. Kangawa K. Ghrelin: structure and function. Physiol. Rev. 2005;85:495-522.
45. Zhang Y, Zhao H, Peng H, *et al*. Two alternatively spliced GPR39 transcripts in seabream: molecular cloning, genomic organization, and regulation of gene expression by metabolic signals. J Endocrinol. 2008;199:457-70.
46. Egerold KL, Holst B, Petersen PS, *et al*. GPR39 splice variants versus antisense gene LYPD1: expression and regulation in gastrointestinal tract, endocrine pancreas, liver, and white adipose tissue. Mol Endocrinol. 2007;21:1685-98.
47. Zhang JV, Li L, Huang Q, *et al*. Obestatin receptor in energy homeostasis and obesity pathogenesis. Prog Mol Biol Transl Sci. 2013;114:89-107.
48. Ishitobi Y, Akiyoshi J, Honda S, *et al*. Administration of antisense DNA for GPR39-1b causes anxiolytic-like responses and appetite loss in rats. Neurosci Res. 2012;72:257-62.
49. Yasuda S, Ishida J. GPR39-1b, the 5-transmembrane isoform of GPR39 interacts with neurotensin receptor NTSR1 and modifies its function. J Recept Signal Transduct Res. 2014;34:307-12.
50. Holst B, Holliday ND, Bach A, *et al*. Common structural basis for constitutive activity of the ghrelin receptor family. J Biol Chem. 2004;279:53806-17.
51. Holliday ND, Holst B, Rodionova EA, *et al*. Importance of constitutive activity and arrestin-independent mechanisms for intracellular trafficking of the ghrelin receptor. Mol Endocrinol. 2007;21:3100-12.
52. Depoortere I. GI functions of GPR39: novel biology. Curr Opin Pharmacol. 2012;12:647-52.
53. Moechars D, Depoortere I, Moreaux B, *et al*. Altered gastrointestinal and metabolic function in the GPR39-obestatin receptor-knockout mouse. Gastroenterology. 2006;131:1131-41.
54. Jackson VR, Nothacker HP, Civelli O. GPR39 receptor expression in the mouse brain. Neuroreport. 2006;17:813-6.
55. Holst B, Egerod KL, Schild E, *et al*. GPR39 signaling is stimulated by zinc ions but not by obestatin. Endocrinology. 2007;148:13-20.

56. Nogueiras R , Pfluger P, Tovar S, *et al*. Effects of obestatin on energy balance and growth hormone secretion in rodents. Endocrinology. 2007;148:21-6.
57. Zhao D, Pothoulakis C. Effects of NT on gastrointestinal motility and secretion, and role in intestinal inflammation. Peptides. 2006;27:2434-44.
58. Brighton PJ, Szekeres PG, Willars GB. Neuromedin U and its receptors: structure, function, and physiological roles. Pharmacol Rev. 2004;56:231-48.
59. De Smet B, Mitselos A, Depoortere I. Motilin and ghrelin as prokinetic drug targets. Pharmacol Ther. 2009;123:207-23.
60. Tremblay F, Perreault M, Klaman LD, *et al*. Normal food intake and body weight in mice lacking the G protein-coupled receptor GPR39. Endocrinology. 2007;148:501-6.
61. Verhulst PJ, Lintermans A, Janssen S, *et al*. GPR39, a receptor of the ghrelin receptor family, plays a role in the regulation of glucose homeostasis in a mouse model of early onset diet-induced obesity. J Neuroendocrinol. 2011;23:490-500.
62. Petersen PS, Jin C, Madsen AN, *et al*. Deficiency of the GPR39 receptor is associated with obesity and altered adipocyte metabolism. FASEB J. 2011;25:3803-14.
63. Tremblay F, Richard AM, Will S, *et al*. Disruption of G protein-coupled receptor 39 impairs insulin secretion in vivo. Endocrinology. 2009;150:2586-95.
64. Catalán V, Gómez-Ambrosi J, Rotellar F, *et al*. The obestatin receptor (GPR39) is expressed in human adipose tissue and is down-regulated in obesity-associated type 2 diabetes mellitus. Clin Endocrinol. 2007;66:598-601.
65. Egerold KL, Jin C, Petersen PS, *et al*. Beta-cell specific overexpression of GPR39 protects against streptozotocin-induced hyperglycemia. Int J Endocrinol. 2011;2011:401258.
66. Dittmer S, Sahin M, Pantlen A, *et al*. The constitutively active orphan G-protein-coupled receptor GPR39 protects from cell death by increasing secretion of pigment epithelium-derived growth factor. J Biol Chem. 2008;283:7074-81.
67. Sharir H, Zinger A, Nevo A, *et al*. Zinc released from injured cells is acting via the Zn2+-sensing receptor, ZnR, to trigger signaling leading to epithelial repair. J Biol Chem. 2010;285:26097-106.
68. Besser L, Chorin E, Sekler I, *et al*. Synaptically released zinc triggers metabotropic signaling via a zinc-sensing receptor in the hippocampus. J Neurosci. 2009;29:2890-901.
69. Chorin E, Vinograd O, Fleidervish I, *et al*. Upregulation of KCC2 activity by zinc-mediated neurotransmission via the mZnR/GPR39 receptor. J Neurosci. 2011;31:12916-26.
70. Gurriarán-Rodríguez U, Al-Massaddi O, Roca-Rivada A, *et al*. Obestatin as a regulator of adipocyte metabolism and adipogenesis. J Cell Mol Med. 2011;15:1927-40.
71. Gurriarán-Rodríguez U, Al-Massadi O, Crujeiras AB, *et al*. Preproghrelin expression is a key target for insulin action on adipogenesis. J Endocrinol. 2011;210:R1-7.
72. Gurriarán-Rodríguez U, Santos-Zas I, Al-Massadi O, *et al*. The obestatin/GPR39 system is up-regulated by muscle injury and functions as an autocrine regenerative system. J Biol Chem. 2012;287:38379-89.
73. Gurriarán-Rodríguez U, Santos-Zas I, González-Sánchez J, *et al*. Action of obestatin in skeletal muscle repair: stem cell expansion, muscle growth, and microenvironment remodeling. Mol Ther. 2015;23:1003-21.
74. Chartrel N, Alvear-Pérez R, Leprince J, *et al*. Comment on Obestatin, a peptide encoded by the ghrelin gene, opposes ghrelin's effects on food intake. Science. 2007;315:766.
75. Lauwers E, Landuyt B, Arckens L, *et al*. Obestatin does not activate orphan G protein-coupled receptor GPR39. Biochem Biophys Res Commun. 2006;351:21-5.
76. De Spiegeleer B, Vergote V, Pezeshki A, *et al*. Impurity profiling quality control testing of synthetic peptides using liquid chromatography-photodiode array-fluorescence and liquid chromatography-electrospray ionization-mass spectrometry: the obestatin case. Anal Biochem. 2008;376:229-34.
77. Zhang JV, Jahr H, Luo CW, *et al*. Obestatin induction of early-response gene expression in gastrointestinal and adipose tissues and the mediatory role of G protein-coupled receptor, GPR39. Mol endocrinol. 2008;22:1464-75
78. Pacheco-Pantoja EL, Ranganath LR, Gallagher JA, *et al*. Receptors and effects of gut hormones in three osteoblastic cell lines. BMC Physiol. 2011;11:12-52.
79. Fontenot E, DeVente JE, Seidel ER. Obestatin and ghrelin in obese and in pregnant women. Peptides. 2007;28:1937-44.
80. Cohen L, Asraf H, Sekler I, *et al*. Extracellular pH regulates zinc signaling via an Asp residue of the zinc-sensing receptor (ZnR/GPR39). J Biol Chem. 2008;287:33339-50.
81. Cohen L, Sekler I, Hershfinkel M. The zinc sensing receptor, ZnR/GPR39, controls proliferation and differentiation of colonocytes and thereby tight junction formation in the colon. Cell Death Dis. 2014;5:e1307.

82. Cohen L, Azriel-Tamir H, Arotsker N, *et al*. Zinc sensing receptor signaling, mediated by GPR39, reduces butyrate-induced cell death in HT29 colonocytes via upregulation of clusterin. PLoS One. 2012;7:e35482.
83. Asraf H, Salomon S, Nevo A, *et al*. The ZnR/GPR39 interacts with the CaSR to enhance signaling in prostate and salivary epithelia. J Cell Physiol. 2014;229:868-77.
84. Młyniec K, Budziszewska B, Reczyński W, *et al*. The role of the GPR39 receptor in zinc deficient-animal model of depression. Behav Brain Res. 2013;238:30-5.
85. Młyniec K, Budziszewska B, Holst B, *et al*. GPR39 (zinc receptor) knockout mice exhibit depression-like behavior and CREB/BDNF down-regulation in the hippocampus. Int J Neuropsychopharmacol. 2014;18:pii:pyu002.
86. Młyniec K, Doboszewska U, Szewczyk B, *et al*. The involvement of the GPR39-Zn(2+)-sensing receptor in the pathophysiology of depression. Studies in rodent models and suicide victims. Neuropharmacology. 2014;79:290-7.
87. Młyniec K, Singewald N, Holst B, *et al*. GPR39 Zn(2+)-sensing receptor: a new target in antidepressant development? J Affect Disord. 2015;174:89-100.
88. Nowak G. Zinc, future mono/adjunctive therapy for depression: Mechanisms of antidepressant action. Pharmacol Rep. 2015;67:659-62.
89. Popovics P, Stewart AJ. GPR39: a Zn(2+)-activated G protein-coupled receptor that regulates pancreatic, gastrointestinal and neuronal functions. Cell Mol Life Sci. 2011;68:85-95.
90. Michailov Y, Ickowicz D, Breitbart H. Zn2+-stimulation of sperm capacitation and of the acrosome reaction is mediated by EGFR activation. Dev Biol. 2014;396:246-55.
91. Granata R, Settanni F, Gallo D, *et al*. Obestatin promotes survival of pancreatic β-cells and human islets and induces expression of genes involved in the regulation of β-cell mass and function. Diabetes. 2008;57:967-79.
92. Favaro E, Granata R, Miceli I, *et al*. The ghrelin gene products and exendin-4 promote survival of human pancreatic islet endothelial cells in hyperglycaemic conditions, through phosphoinositide 3-kinase/Akt, extracellular signal-related kinase (ERK)1/2 and cAMP/protein kinase A (PKA) signalling pathways. Diabetologia. 2012;55:1058-70.
93. Unniappan S, Speck M, Kieffer TJ. Metabolic effects of chronic obestatin infusion in rats. Peptides. 2008;29:1354-61.
94. Granata R, Gallo D, Luque RM, *et al*. Obestatin regulates adipocyte function and protects against diet-induced insulin resistance and inflammation. FASEB J. 2012;26:3393-411.
95. Gargantini E, Grande C, Trovato L, *et al*. The role of obestatin in glucose and lipid metabolism. Horm Metab Res. 2013;45:1002-8.
96. Miegueu P, St Pierre D, Broglio F, *et al*. Effect of desacyl ghrelin, obestatin and related peptides on triglyceride storage, metabolism and GHSR signalling in 3T3-L1 adipocytes. J Cell Biochem. 2011;112:704-14.
97. Agnew A, Calderwood D, Chevallier OP, *et al*. Chronic treatment with a stable obestatin analog significantly alters plasma triglyceride levels but fails to influence food intake; fluid intake; body weight; or body composition in rats. Peptides. 2011;32:755-62.
98. Grala TM, Kay JK, Walker CG, *et al*. Expression analysis of key somatotropic axis and liporegulatory genes in ghrelin- and obestatin-infused dairy cows. Domest Anim Endocrinol. 2010;39:76-83.
99. Zhao CM, Furnes MW, Stenstrom B, *et al*. Characterization of obestatin- and ghrelinproducing cells in the gastrointestinal tract and pancreas of rats: an immunohistochemical and electron- microscopic study. Cell Tissue Res. 2008;331:575-87.
100. Walia P, Asadi A, Kieffer TJ, *et al*. Ontogeny of ghrelin, obestatin, preproghrelin, and prohormone convertases in rat pancreas and stomach. Pediatr Res. 2009;65:39-44.
101. Turk N, Dagistanli FK, Sacan O *et al*. Obestatin and insulin in pancreas of newborn diabetic rats treated with exogenous ghrelin. Acta Histochem. 2012;114:349-57.
102. Granata R, Volante M, Settanni F, *et al*. Unacylated ghrelin and obestatin increase islet cell mass and prevent diabetes in streptozotocin-treated newborn rats. J Mol Endocrinol. 2010;45:9-17.
103. Baragli A, Grande C, Gesmundo I, *et al*. Obestatin enhances in vitro generation of pancreatic islets through regulation of developmental pathways. PLoS One. 2013;8:e64374.
104. Gao XY, Kuang HY, Liu XM, *et al*. Decreased obestatin in plasma in metabolically obese, normal-weight men with normal glucose tolerance. Diab Res Clin Pract. 2008;79:e5-6.
105. Lippl F, Erdmann J, Lichter N, *et al*. Relation of plasma obestatin levels to BMI, gender, age and insulin. Horm Metab Res. 2008;40:806-12.

106. Li ZF, Guo ZF, Cao J, *et al*. Plasma ghrelin and obestatin levels are increased in spontaneously hypertensive rats. Peptides.2010;31:297-300.
107. Qader SS, Hakanson R, Rehfeld JF, *et al*. Proghrelin derived peptides influence the secretion of insulin, glucagon, pancreatic polypeptide and somatostatin: a study on isolated islets from mouse and rat pancreas. Regul Pept. 2008;146:230-7.
108. Ren AJ, Guo ZF, Wang YK, *et al*. Inhibitory effect of obestatin on glucose-induced insulin secretion in rats. Biochem Biophys Res Commun. 2008;369:969-72.
109. Egido EM, Hernandez R, Marco J, *et al*. Effect of obestatin on insulin, glucagon and somatostatin secretion in the perfused rat pancreas. Regul Pept. 2009;152:61-6.
110. Xin X, Ren AJ, Zheng X, *et al*. Disturbance of circulating ghrelin and obestatin in chronic heart failure patients especially in those with cachexia. Peptides. 2009;30:2281-5.
111. Ozbay Y, Aydin S, Dagli AF, *et al*. Obestatin is present in saliva: alterations in obestatin and ghrelin levels of saliva and serum in ischemic heart disease. BMB Rep. 2008;41:55-61.
112. Alloatti G, Arnoletti E, Bassino E, *et al*. Obestatin affords cardioprotection to the ischemic-reperfused isolated rat heart and inhibits apoptosis in cultures of similarly stressed cardiomyocytes. Am J Physiol Heart Circ Physiol. 2010;299:H470-81.
113. Iglesias MJ, Salgado A, Pineiro R, *et al*. Lack of effect of the ghrelin gene-derived peptide obestatin on cardiomyocyte viability and metabolism. J Endocrinol Invest. 2007;30:470-6.
114. Sazdova I, Ilieva B, Minkov I, *et al*. Obestatin as contractile mediator of excised frog heart. Cent. Eur J Biol. 2009;4:327-34.
115. Aragno M, Mastrocola R, Ghe C, *et al*. Obestatin-induced recovery of myocardial dysfunction in type 1 diabetic rats: underlying mechanisms. Cardiovasc Diabetol. 2012;11:129.
116. Li ZF, Guo ZF, Yang SG, *et al*. Circulating ghrelin and ghrelin to obestatin ratio are low in patients with untreated mild-to-moderate hypertension. Regul Pept. 2010;65:206-9.
117. Anderwald-Stadler M, Krebs M, Promintzer M, *et al*. Plasma obestatin is lower at fasting and not suppressed by insulin in insulin-resistant humans. Am J Physiol Endocrinol Metab. 2007;293:E1393-8.
118. Ren AJ, He Q, Shi JS, *et al*. Association of obestatin with blood pressure in the third trimesters of pregnancy. Peptides. 2009;30:1742-5.
119. Li ZF, Song SW, Qin,YW, *et al*. Bolus intravenous injection of obestatin does not change blood pressure level of spontaneously hypertensive rat. Peptides. 2009;30:1928-30.
120. Camiña JP, Campos JF, Caminos JE, *et al*. Obestatin-mediated proliferation of human retinal pigment epithelial cells: regulatory mechanisms. J Cell Phsiol. 2007;211:1-9.
121. Lago R, Gomez R, Dieguez C, *et al*. Unlike ghrelin, obestatin does not exert any relevant activity in chondrocytes. Ann Rheum Dis. 2007;66:1399-400.
122. Mészárosová M, Sitotkin AV, Grossmann R, *et al*. The effect of obestatin on porcine ovarian granulosa cells. Anim Reprod Sci. 2008;108:196-207.
123. Pazos Y, Álvarez CJ, Camiña JP, *et al*. Stimulation of extracellular signal-regulated kinases and proliferation in the human gastric cancer cells KATO-III by obestatin. Growth Factors. 2007;25:373-81.
124. Samson WK, White MM, Price C, *et al*. Obestatin acts in brain to inhibit thirst. Am J Physiol-Regul Integr Comp Physiol. 2007;292:R637-43.
125. Carlini VP, Schiöth HB, de Barioglio SR. Obestatin improves memory performance and causes anxiolytic effects in rats. Biochem Biophys Res Commun. 2007;352:907-12.
126. Szakács J, Csabafi K, Lipták N, *et al*. The effect of obestatin on anxiety-like behaviour in mice. Behav Brain Res. 2015;293:41-5.
127. Zizzari P, Longchamps R, Epelbaum J, *et al*. Obestatin partially affects ghrelin stimulation of food intake and growth hormone secretion in rodents. Endocrinology. 2007;148:1648-53.
128. Pazos Y, Alvarez CJ, Camiña JP, *et al*. Role of obestatin on growth hormone secretion: An in vitro approach. Biochem Biophys Res Commun. 2009;390:1377-81.
129. Szentirmai E, Krueger JM. Obestatin alters sleep in rats. Neurosci Lett. 2006;404:222-6.
130. Samson WK, Yosten GL, Chan JK, *et al*. Obestatin inhibits vasopressin secretion: evidence for a physiological role in the control of fluid homeostasis. J Endocrinol. 2008;196:559-64.
131. Lei Y, Liang Y, Chen Y, *et al*. Increased circulating obestatin in patients with chronic obstructive pulmonary disease. Multidiscip Respir Med. 2014;9:5.

132. Buscher AK, Buscher R, Hauffa BP, *et al*. Alterations in appetite regulating hormones influence protein-energy wasting in pediatric patients with chronic kidney disease. Pediatr Nephrol. 2010;25:2295-301.
133. Borges N, Moraes C, Barros AF, *et al*. Acyl-ghrelin and obestatin plasma levels in different stages of chronic kidney disease. J Ren Nutr. 2014;24:100-4.
134. Aygen B, Dogukan A, Dursun FE, *et al*. Ghrelin and obestatin levels in end-stage renal disease. J. Int. Med. Res. 2009;37:757-65.
135. Mafra D, Guebre-Egziabher F, Cleaud C, *et al*. Obestatin and ghrelin interplay in hemodialysis patients. Nutrition. 2010;26:1100-4.
136. Gao XY, Kuang HY, Liu XM, *et al*. Plasma obestatin levels in men with chronic atrophic gastritis. Peptides. 2008;29:1749-54.
137. Alexandridis E, Zisimopoulos A, Liratzopoulos N, *et al*. Obestatin/ghrelin ratio: a new activity index in inflammatory bowel diseases. Inflamm Bowel Dis. 2009;15:1557-61.
138. Gao XY, Kuang HY, Liu XM, *et al*. Circulating ghrelin/ obestatin ratio in subjects with Helicobacter pylori infection. Nutrition. 2009;25:506-11.
139. Monteleone P, Serritella C, Martiadis V, *et al*. Plasma obestatin, ghrelin, and ghrelin/obestatin ratio are increased in underweight patients with anorexia nervosa but not in symptomatic patients with bulimia nervosa. J Clin Endocrinol Metab. 2008;93:4418-21.
140. Germain N, Galusca B, Grouselle D, *et al*. Ghrelin and obestatin circadian levels differentiate bingeing-purging from restrictive anorexia nervosa. J Clin Endocrinol Metab. 2010;95:3057-62.
141. Sedlackova D, Kopeckova J, Papezova H, *et al*. Changes of plasma obestatin, ghrelin and NPY in anorexia and bulimia nervosa patients before and after a high-carbohydrate breakfast. Physiol Res. 2011;60:165-73.
142. Álvarez CJ, Lodeiro M, Theodoropoulou M, *et al*. Obestatin stimulates Akt signalling in gastric cancer cells through b-arrestin-mediated epidermal growth factor receptor transactivation. Endocr-Relat Cancer. 2009;16:599-611.
143. Manning BD, Cantley LC. Akt/PKB signalling: navigating downstream. Cell. 2007;129:1261-74.
144. Olayioye MA, Neve RM, Lane HA, *et al*. The ErbB signalling network: receptor heterodimerization in development and cancer. EMBO J. 2000;19:3159-67.
145. Wu W, Samet JM, Silbajoris R, *et al*. Heparin-binding epidermal growth factor cleavage mediates zinc-induced epidermal growth factor receptor phosphorylation. Am J Respir Cell Mol Biol. 2004;30:540-7.
146. Hwang JJ, Park MH, Choi SY, *et al*. Activation of the Trk signaling pathway by extracellular zinc. Role of metalloproteinases. J Biol Chem. 2005;280:11995-2001.
147. Wu W, Graves LM, Gill GN, *et al*. Src-dependent phosphorylation of the epidermal growth factor receptor on tyrosine 845 is required for zinc-induced Ras activation. J Biol Chem. 2002;277:24252-7.
148. Samet JM, Dewar BJ, Wu W, *et al*. Mechanisms of Zn(2+)-induced signal initiation through the epidermal growth factor receptor. Toxicol Appl Pharmacol. 2003;191:86-93.
149. Wu W, Silbajoris RA, Whang YE, *et al*. p38 and EGF receptor kinase-mediated activation of the phosphatidylinositol 3-kinase/Akt pathway is required for Zn2+-induced cyclooxygenase-2 expression. Am J Physiol Lung Cell Mol Physiol. 2005;289:L883-9.
150. Storjohann L, Holst B, Schwartz TW. Molecular mechanism of Zn2+ agonism in the extracellular domain of GPR39. FEBS Lett. 2008;582:2583-8.
151. Huovila AP, Turner AJ, Pelto-Huikko M, *et al*. Shedding light on ADAM metalloproteinases. Trends Biochem Sci. 2005;30:413-22.
152. Seals DF, Courtneidge SA. The ADAMs family of metalloproteases: multidomain proteins with multiple functions. Genes Dev. 2003;17:7-30.
153. Bhola NE, Grandis JR . Crosstalk between G-protein-coupled receptors and epidermal growth factor receptor in cancer. Front Biosci. 2008;13:1857-65.
154. Normanno N, De Luca A, Bianco C, *et al*. Epidermal growth factor receptor (EGFR) signalling in cancer. Gene. 2006;366:2-16.
155. Ohtsu H, Dempsey PJ, Eguchi S. ADAMs as mediators of EGF receptor transactivation by G-protein-coupled receptors. Am J Phys Cell Physiol. 2006;291:C1-10.
156. Markowska A, Ziolkowska A, Jaszczynska-Nowinka K, *et al*. Elevated blood plasma concentrations of active ghrelin and obestatin in benign ovarian neoplasms and ovarian cancers. Eur J Gynaecol Oncol. 2009;30:518-22.
157. Malendowicz W, Ziolkowska A, Szyszka M, *et al*. Elevated blood active ghrelin and unaltered total ghrelin and obestatin concentrations in prostate carcinoma. Urol Int. 2009;83,471-5.

158. Markowska A, Ziolkowska A, Nowinka K, *et al*. Elevated blood active ghrelin and normal total ghrelin and obestatin concentrations in uterine leiomyoma. Eur J Gynaecol Oncol. 2009;30:281-4.
159. Nurkalem C, Celik H, Dagli F, *et al*. Ghrelin and obestatin expression in serous ovarian tumours. Gynecol Endocrinol. 2012;28:941-4.
160. Gurgul E, Kasprzak A, Blaszczyk A, *et al*. Ghrelin and obestatin in thyroid gland - immunohistochemical expression in nodular goiter, papillary and medullary cancer. Folia Histochem Cytobiol. 2015;53:19-25.
161. Papotti M, Duregon E, Volante M. Ghrelin and tumors. Endocr Dev. 2013;25:122-34.
162. Seim I, Walpole C, Amorim L, *et al*. The expanding roles of the ghrelin-gene derived peptide obestatin in health and disease. Mol Cell Endocrinol. 2011;340:111-7.
163. Xie F, Liu H, Zhu YH, *et al*. Overexpression of GPR39 contributes to malignant development of human esophageal squamous cell carcinoma. BMC Cancer. 2011;11:86.
164. Bassilana F, Carlson A, DaSilva JA, *et al*. Target identification for a Hedgehog pathway inhibitor reveals the receptor GPR39. Nat Chem Biol. 2014;10:343-9.
165. Ruddon RW. Cancer biology. 4th ed. Oxford: Oxford University Press. 2007.
166. Statistics and outlook for stomach cancer. Cancer Research UK. 2014.
167. González CA, Sala N, Rokkas T. Gastric cancer: epidemiologic aspects. Helicobacter. 2013;18:34-8.
168. Keyama M, Higashi H. Helicobacter pylori CagA: a new paradigm for bacterial carcinogenesis. Cancer Sci. 2005;96:835-43.
169. Jakszyn P, González CA. Nitrosamine and related food intake and gastric and oesophageal cancer risk: A systematic review of the epidemiological evidence. World J Gastroenterol. 2006;12:4296-303.
170. Buckland G, Agudo A, Lujan L, *et al*. Adherence to a Mediterranean diet and risk of gastric adenocarcinoma within the European Prospective Investigation into Cancer and Nutrition (EPIC) cohort study. Am J Clin Nutr. 2009;91:381-90.
171. Trédaniel J, Boffetta P, Buiatti E, *et al*. Tobacco smoking and gastric cancer: Review and meta-analysis. Int J Cancer. 1997;72:565-73.
172. What Are The Risk Factors For Stomach Cancer? American Cancer Society. 2010.
173. Crew K, Neugut A. Epidemiology of gastric cancer. World Journal of Gastroenterol. 2006;12 354-62.
174. World Cancer Report 2014. World Health Organization. 2014.
175. Hereditary Diffuse Cancer. No Stomach for Cancer. 2014.
176. Gastric Cancer: Intestinal- and diffuse-type. International Cancer Genome Consortium. 2014.
177. Tseng CH, Tseng FH, Tseng T. Diabetes and gastric cancer: The potential links. World J Gastroenterol. 2014;20:1701-11.
178. Kim J, Cheong JH, Chen J, *et al*. Menetrier's Disease in Korea: Report of Two Cases and Review of Cases in a Gastric Cancer Prevalent Region. Yonsei Med J. 2004;45:555-60.
179. Tsukamoto T, Mizoshita T, Tatematsu M, *et al*. Gastric-and-intestinal mixed-type intestinal metaplasia: aberrant expression of transcription factors and stem cell intestinalization. Gastric Cancer. 2006;9:156-66.
180. IARC monographs on the evaluation of carcinogenic risks to humans. IARC. 2012:385-435.
181. Correa P. A human model of gastric carcinogenesis. Cancer Res. 1988;48:3554-60.
182. Blaser M, Parsonnet J. Parasitism by the 'slow' bacterium Helicobacter pylori leads to altered gastric homeostasis and neoplasia. J Clin Invest. 1994;94:4-8.
183. Jain RN, Brunkan CS, Chew CS, *et al*. Gene expression profiling of gastrin target genes in parietal cells. Physiol Genomics. 2006;24:124-32.
184. Li Q, Karam SM, Gordon JI. Diphtheria toxin-mediated ablation of parietal cells in the stomach of transgenic mice. J Biol Chem. 1996;271:3671-6.
185. Bredemeyer AJ, Geahlen JH, Weis VG, *et al*. The gastric epithelial progenitor cell niche and differentiation of the zymogenic (chief) cell lineage. Dev Biol. 2009;325:211-24.
186. El-Zimaity HMT, Ota H, Graham DY, *et al*. Patterns of gastric atrophy in intestinal type gastric carcinoma. Cancer. 2002;94:1428-36.
187. Filipe MI, Munoz N, Matko I, *et al*. Intestinal metaplasia types and the risk of gastric cancer: a cohort study in Slovenia. Int J Cancer. 1994;57:324-9.
188. Hattori T, Fujita S. Tritiated thymidine autotradiographic study on histogenesis and spreading of intestinal metaplasia in human stomach. Pathol Res Practice. 1979;164:224-37.

189. Schmidt PH, Lee JR, Joshi V, *et al*. Identification of a metaplastic cell lineage associated with human gastric adenocarcinoma. Lab Invest. 1999;79:639-46.
190. Yamaguchi H, Goldenring JR, Kaminishi M, *et al*. Association of spasmolytic polypeptide expressing metaplasia (SPEM) with carcinogen administration and oxyntic atrophy in rats. Lab Invest. 2002;82:1045-52.
191. Halldorsdottir AM, Sigurdardottir M, Jonasson JG, *et al*. Spasmolytic polypeptide expressing metaplasia (SPEM) associated with gastric cancer in Iceland. Dig Dis Sci. 2003;48:431-41.
192. Goldenring JR, Taek Nam K. Oxyntic atrophy, metaplasia and gastric cancer. Prog Mol Biol Transl Sci. 2010;96:117-31.
193. Ferlay J, Soerjomataram I, Dikshit R, *et al*. Cancer incidence and mortality worldwide: sources, methods and major patterns in GLOBOCAN 2012. Int J Cancer. 2015;136:E359-86.
194. Global battle against cancer won't be won with treatment alone. Effective prevention measures urgently needed to prevent cancer crisis. World Health Organization. 2014.
195. Orditura M, Galizia G, Sforza V, *et al*. Treatment of gastric cancer. World J Gastroenterol. 2014;20:1635-49.
196. Howson CP, Hiyama T, Wynder EL. The decline in gastric cancer: epidemiology of an unplanned triumph. Epidemiol Rev. 1986;8:1-27.
197. Malvezzi M, Bonifazi M, Bertuccio P, *et al*. An age-period-cohort analysis of gastric cancer mortality from 1950 to 2007 in Europe. Ann Epidemiol. 2010;20:898-905.
198. Bertuccio P, Chatenoud L, Levi F, *et al*. Recent patterns in gastric cancer: a global overview. Int J Cancer. 2009;125:666-73.
199. Parkin DM. The global health burden of infection-associated can¬cers in the year 2002. Int J Cancer. 2006;118:3030-44.
200. Jemal A, Center MM, DeSantis C, *et al*. Global patterns of cancer incidence and mortality rates and trends. Cancer Epidemiol Bio¬markers Prev. 2010;19:1893-907.
201. Aragonés N, Goicoa T, Pollán M, *et al*. Spatio-temporal trends in gastric cancer mortality in Spain: 1975-2008. Cancer Epidemiol. 2013;37:360-9.
202. Seoane-Mato D, Aragonés N, Ferreras E, *et al*. Trends in oral cavity, pharyngeal, oesophageal and gastric cancer mortality rates in Spain, 1952-2006: an age-period-cohort analysis. BMC Cancer. 2014;14:254.
203. Kumar V, Abbas AK, Aster JC. Pathologic Basis of Disease. 8th ed. Saunders Elsevier. 2010.
204. Laurén P. The two histological main types of gastric carcinoma: Diffuse and so-called intestinal-type carcinoma an attempt at a histo-clinical classification. Acta Pathol Microbiol Scand. 1965;64:31-49.
205. Leocata P, Ventura L, Giunta M, *et al*. Gastric carcinoma: a histopathological study of 705 cases. Ann Ital Chir. 1998;69:331-7.
206. The Cancer Genome Atlas Research Network. Comprehensive molecular characterization of gastric adenocarcinoma. Nature. 2014;513:202-9.
207. Edge SB, Byrd DR, Compton CC, *et al*. AJCC cancer staging manual. 7th ed. New York: Springer-Verlag. 2009.
208. Keller RLJ. The Computer Aided Resonance Assignment tutorial.2004. Goldau: CANTINA Verlag. Available: http://cara.nmr-software.org/portal/
209. Güntert P. Automated NMR structure calculation with CYANA. Methods Mol Biol. 2004;278:353-78.
210. Case DA, Cheatham TE 3rd, Darden T, *et al*. The Amber biomolecular simulation programs. J Comput Chem. 2005;26:1668-88.
211. Koradi R, Billeter M, Wüthrich K. MOLMOL: a program for display and analysis of macromolecular structures. J Mol Graph. 1996;14:51-4.
212. Laskowski RA, Rullmannn JA, MacArthur MW, *et al*. AQUA and PROCHECK-NMR: programs for checking the quality of protein structures solved by NMR. J Biomol NMR. 1996;8:477-86.
213. Kelly SM, Jess TJ, Price NC. How to study proteins by circular dichroism. Biochim Biophys Acta. 2005;1751:119-39.
214. Whitmore L, Wallace BA. DICHROWEB: an online server for protein secondary structure analyses from circular dichroism spectroscopic data. Nucleic Acids Res. 2004;32:W668-73.
215. Whitmore L, Wallace BA. Protein secondary structure analyses from circular dichroism spectroscopy: methods and reference databases. Biopolymers. 2008;89:392-400.
216. Greenfield NJ. Using circular dichroism spectra to estimate protein secondary structure. Nat Protoc. 2006;1:2876-90.
217. Rodríguez-Rigueiro T, Valladares-Ayerbes M, Haz-Conde M, *et al*. A novel procedure for protein extraction from formalin-fixed paraffin-embedded tissues. Proteomics. 2011;11:2555-9.

218. García-Caballero A, Gallego R, García-Caballero T, *et al*. Cellular and subcellular distribution of 7B2 in porcine Merkel cells. Anat Rec. 1997;248,:159-63.
219. Raghay K, Garcia-Caballero T, Bravo S, *et al*. Ghrelin localization in the medulla of rat and human adrenal gland and in pheochromocytomas. Histol Histopathol. 2008;23:57-65.
220. Gur S, Sikka SC, Abdel-Mageed AB, *et al*. Imatinib mesylate (Gleevec) induces human corpus cavernosum relaxation by inhibiting receptor tyrosine kinases (RTKs): identification of new RTK targets. Urology. 2013;82:745.
221. Kumar D, Moore R, Nash A, *et al*. Decidual GM-CSF is a critical common intermediate necessary for thrombin and TNF induced in-vitro fetal membrane weakening. Placenta. 2014;35:1049-56.
222. Muinelo-Romay L, Colas E, Barbazan J, *et al*. High-risk endometrial carcinoma profiling identifies TGF-β1 as a key factor in the initiation of tumor invasion. Mol Cancer Ther. 2011;10:1357-66.
223. Hersey SJ, Tang L, Pohl J, *et al*. Pepsinogen secretion in vitro. Methods Enzymol. 1990;192:124-39.
224. Méchin V, Damerval C, Zivy M. Total Protein Extraction with TCA-Acetone. Methods Mol Biol. 2007;355:1-8.
225. Alén BO, Nieto L, Gurriarán-Rodríguez U, *et al*. The NMR structure of human obestatin in membrane-like environments: insights into the structure-bioactivity relationship of obestatin. PLoS One. 2012;7:e45434.
226. Schwyzer R. In search of the "bio-active conformation" – is it induced by the target cell membrane? J Mol Recognit. 1995;8:3-8.
227. Berjanskii VM, Wishart DS. A simple method to predict protein flexibility using secondary chemical shifts. J Am Chem Soc. 2005;127:14970-1.
228. Whalen EJ, Rajagopal S, Lefkowitz RJ. Therapeutic potential of β-arrestin- and G-protein-biased agonists. Trends Mol Med. 2011;17:126-39.
229. Reiter E, Ahn S, Shukla AK, *et al*. Molecular mechanism of β-arrestin-biased agonism at seven-transmembrane receptors. Annu Rev Pharmacol Toxicol. 2012;52:179-97.
230. Yerushalmi R, Woods R, Ravdin PM, *et al*. Ki67 in breast cancer: prognostic and predictive potential. Lancet Oncol. 2010;11:174-83.
231. Gerdes J, Schwab U, Lemke H, *et al*. Production of a mouse monoclonal antibody reactive with a human nuclear antigen associated with cell proliferation. Int J Cancer. 1983;31:13-20.
232. Wishart DS, Sykes BD. Chemical shifts as a tool for structure determination. Methods Enzymol. 1994;239:363-92.
233. Celinski SA, Scholtz JM. Osmolyte effects on helix formation in peptides and the stability of coiled-coils. Protein Sci. 2002;11:2048-51.
234. Kopp R, Ruge M, Rothbauer E, *et al*. Impact of epidermal growth factor (EGF) radioreceptor analysis on long-term survival of gastric cancer patients. Anticancer Res. 2002;22:1161-7.
235. García I, Vizoso F, Martín A, *et al*. Clinical significance of the epidermal growth factor receptor and HER2 receptor in resectable gastric cancer. Ann Surg Oncol. 2003;10:234-41.
236. Yonemura Y, Ohoyama S, Kimura H, *et al*. The expression of proliferative-associated nuclear antigen p105 in gastric carcinoma. Cancer. 1991;67:2523-8.
237. Morishita A, Gong J, Masaki T. Targeting receptor tyrosine kinases in gastric cancer. World J Gastroenterol. 2014;20:4536-45.
238. Wang L, Yuan H, Li Y, *et al*. The role of HER3 in gastric cancer. Biomed Pharmacother. 2014;68:809-12.
239. Kashyap MK. Role of insulin-like growth factor-binding proteins in the pathophysiology and tumorigenesis of gastroesophageal cancers. Tumour Biol. 2015;36:8247-57.
240. Numata K, Oshima T, Sakamaki K, *et al*. Clinical significance of IGF1R gene expression in patients with Stage II/III gastric cancer who receive curative surgery and adjuvant chemotherapy with S-1. J Cancer Res Clin Oncol. 2016;142:415-22.
241. Ichikawa W, Terashima M, Ochiai A, *et al*. Impact of insulin-like growth factor-1 receptor and amphiregulin expression on survival in patients with stage II/III gastric cancer enrolled in the adjuvant chemotherapy trial of S-1 for Gastric Cancer. Gastric Cancer. 2016. [Epub ahead of print]
242. Li H, Xu L, Zhao L, *et al*. Insulin-like growth factor-I induces epithelial to mesenchymal transition via GSK-3β and ZEB2 in the BGC-823 gastric cancer cell line. Oncol Lett. 2015;9:143-148.
243. Du JJ, Dou KF, Peng SY, *et al*. Expression of NGF family and their receptors in gastric carcinoma: a cDNA microarray study. World J Gastroenterol. 2003;9:1431-4.
244. Kamiya A, Inokuchi M, Otsuki S, *et al*. Prognostic value of tropomyosin-related kinases A, B, and C in gastric cancer. Clin Transl Oncol. 2016;18:599-607.

245. Nakagawa M, Inokuchi M, Takagi Y, *et al*. Erythropoietin-producing hepatocellular A1 is an independent prognostic factor for gastric cancer. Ann Surg Oncol. 2015;22:2329-35.
246. Wang J, Dong Y, Wang X, *et al*. Expression of EphA1 in gastric carcinomas is associated with metastasis and survival. Oncol Rep. 2010;24:1577-84.
247. Song JH, Kim CJ, Cho YG, *et al*. Genetic and epigenetic analysis of the EPHB2 gene in gastric cancers. APMIS. 2007;115:164-8.
248. Davalos V, Dopeso H, Velho S, *et al*. High EPHB2 mutation rate in gastric but not endometrial tumors with microsatellite instability. Oncogene. 2007;26:308-11.
249. Yu G, Gao Y, Ni C, *et al*. Reduced expression of EphB2 is significantly associated with nodal metastasis in chinese patients with gastric cancer. J Cancer Res Clin Oncol. 2011;137:73-80.
250. Radomaska HS, Alberich-Jordá M, Will B, *et al*. Targeting CDK1 promotes FLT-3 activated acute myeloid leukemia differentiation through C/EBPα. J Clin Invest. 2012:122:2955-66.
251. Zhang F, Tang JM, Wang L, *et al*. Immunohistochemical detection of RET proto-oncogene product in tumoral and nontumoral mucosae of gastric cancer. Anal Quant Cytopathol Histpathol. 2014;36:128-36.
252. Murakumo Y, Jijiwa M, Asai N, *et al*. RET and neuroendocrine tumors. Pituitary. 2006;9:179-92.
253. Katoh M, Katoh M. Integrative genomic analyses of WNT11: transcriptional mechanisms based on canonical WNT signals and GATA transcription factors signaling. Int J Mol Med. 2009;24:247-51.
254. Fu HL, Valiathan RR, Arkwright R, *et al*. Discoidin domain receptors: unique teceptor tyrosine kinases in collagen-mediated signaling. J Biol Chem. 2013;288:7430-74.
255. Kurokawa Y, Matsuura N, Kawabata R, *et al*. Prognostic impact of major receptor tyrosine kinase expression in gastric cancer. Ann Surg Oncol. 2014;21:S584-90.
256. Moser C, Lang SA, Hackl C, *et al*. Oncogenic MST1R activity in pancreatic and gastric cancer represents a valid target of HSP90 inhibitors. Anticancer Res. 2012;32:427-37.
257. Song YA, Park YL, Kim KY, *et al*. RON is associated with tumor progression via the inhibition of apoptosis and cell cycle arrest in human gastric cancer. Pathol Int. 2012;62:127-36.
258. Lim J, Ryu JH, Kim EJ, *et al*. Inhibition of vascular endothelial growth factor receptor 3 reduces migration of gastric cancer cells. Cancer Invest. 2015;33:398-404.
259. Zhang X, Zheng Z, Shin YK, *et al*. Angiogenic factor thymidine phosphorylase associates with angiogenesis and lymphangiogenesis in the intestinal-type gastric cancer. Pathology. 2014;46:316-24.
260. Xi HQ, Wu XS, Wei B, *et al*. Aberrant expression of EphA3 in gastric carcinoma: correlation with tumor angiogenesis and survival. J Gastroenterol. 2012;47:785-94.
261. Sepulveda JL, Gutierrez-Pajares JL, Luna A, *et al*. High-definition CpG methylation of novel genes in gastric carcinogenesis identified by next-generation sequencing. Mod Pathol. 2016;29:182-93.
262. Konstantinova I, Nikolova G, Ohara-Imaizumi M, *et al*. EphA-ephrin-A-mediated beta cell communication regulates insulin secretion from pancreatic islets. Cell. 2007;129:359-70.
263. Nakayama T, Yoshizaki A, Kawahara N, *et al*. Expression of Tie-1 and 2 receptors, and angiopoietin-1, 2 and 4 in gastric carcinoma; immunohistochemical analyses and correlation with clinicopathological factors. Histopathology. 2004;44:232-9.
264. Lin WC, Li AF, Chi CW, *et al*. Tie-1 protein tyrosine kinase: a novel independent prognostic marker for gastric cancer. Clin Cancer Res. 1999;5:1745-51.
265. Wang J, Wu K, Zhang D, *et al*. Expressions and clinical significances of angiopoietin-1, -2 and Tie2 in human gastric cancer. Biochem Biophys Res Commun. 2005;337:386-93.
266. Seegar TC, Eller B, Tzvetkova-Robev D, *et al*. Tie1-Tie2 interactions mediate functional differences between angiopoietin ligands. Mol Cell. 2010;37:643-55.
267. Patan S. TIE1 and TIE2 receptor tyrosine kinases inversely regulate embryonic angiogenesis by the mechanism of intussusceptive microvascular growth. Microvasc Res. 1998;56:1-21.
268. Yuan HT, Venkatesha S, Chan B, *et al*. Activation of the orphan endothelial receptor Tie1 modifies Tie2-mediated intracellular signaling and cell survival. FASEB J. 2007;21:3171-83.
269. Gialeli C, Theocharis AD, Karamanos NK. Roles of matrix metalloproteinases in cancer progression and their pharmacological targeting. FEBS Journal. 2011;278:16-27.

270. Kim JM, Jeung HC, Rha SY, *et al*. The effect of disintegrin-metalloproteinase ADAM9 in gastric cancer progression. Mol Cancer Ther. 2014;13:3074-85.
271. Yang X, Sun HJ, Li ZR, *et al*. Gastric cancer-associated enhancement of von Willebrand factor is regulated by vascular endothelial growth factor and related to disease severity. BMC Cancer. 2015;15:80.
272. Russo A, Bazan V, Migliavacca M, *et al*. Prognostic significance of DNA ploidy, S-phase fraction, and tissue levels of aspartic, cysteine, and serine proteases in operable gastric carcinoma. Clin Cancer Res. 2000;6:178-84.
273. Liu Y, Xiao S, Shi Y, *et al*. Cathepsin B on invasion and metastasis of gastric carcinoma. Chin Med J. 1998;111:784-8.
274. Czyzewska J, Guzińska-Ustymowicz K, Kemona A, *et al*. The expression of matrix metalloproteinase 9 and cathepsin B in gastric carcinoma is associated with lymph node metastasis, but not with postoperative survival. Folia Histochem Cytobiol. 2008;46:57-64.
275. Dohchin A, Suzuki JI, Seki H, *et al*. Immunostained cathepsins B and L correlate with depth of invasion and different metastatic pathways in early stage gastric carcinoma. Cancer. 2000;89:482-7.
276. Santamaría I, Velasco G, Cazorla M, *et al*. Cathepsin L2, a novel human cysteine proteinase produced by breast and colorectal carcinomas. Cancer Res. 1998;58:1624-30.
277. Couvreur JM, Azuma T, Miller DA, *et al*. Assignment of cathepsin E (CTSE) to human chromosome region 1q31 by in situ hybridization and analysis of somatic cell hybrids. Cytogenet Cell Genet. 1990;53:137-9.
278. Azuma T, Pals G, Mohandas TK, *et al*. Human gastric cathepsin E. Predicted sequence, localization to chromosome 1, and sequence homology with other aspartic proteinases. J Biol Chem. 1989;264:16748-53.
279. Konno-Shimizu M, Yamamichi N, Inada K, *et al*. Cathepsin E is a marker of gastric differentiation and signet-ring cell carcinoma of stomach: a novel suggestion on gastric tumorigenesis. PLoS One. 2013;8:e56766.
280. Kim JJ, Kim JT, Yoon HR, *et al*. Upregulation and secretion of kallikrein-related peptidase 6 (KLK6) in gastric cancer.Tumor Biol. 2012;33:731-8.
281. Kolin DL, Sy K, Rotondo F, *et al*. Prognostic significance of human tissue kallikrein-related peptidases 6 and 10 in gastric cancer. Biol Chem. 2014;395:1087-93.
282. Konstantoudakis G, Florou D, Mavridis K, *et al*. Kallikrein-related peptidase 13 (KLK13) gene expressional status contributes significantly in the prognosis of primary gastric carcinomas. Clin Biochem. 2010;43:1205-11.
283. Florou D, Mavridis K, Scorilas A. The kallikrein-related peptidase 13 (KLK13) gene is substantially up-regulated after exposure of gastric cancer cells to antineoplastic agents. Tumour Biol. 2012;33:2069-78.
284. Holmberg C, Ghesquière B, Impens F, *et al*. Mapping proteolytic processing in the secretome of gastric cancer-associated myofibroblasts reveals activation of MMP-1, MMP-2, and MMP-3. J Proteome Res. 2013;12:3413-22.
285. Dedong H, Bin Z, Peisheng S, *et al*. The contribution of the genetic variations of the matrix metalloproteinase-1 gene to the genetic susceptibility of gastric cancer. Genet Test Mol Biomarkers. 2014;18:675-82.
286. Kim SJ, Shin JY, Lee KD, *et al*. Galectin-3 facilitates cell motility in gastric cancer by up-regulating protease-activated receptor-1 (PAR-1) and matrix metalloproteinase-1 (MMP-1). PLoS One. 2011;6:e25103.
287. Jiang H, Zhou Y, Liao Q, *et al*. Helicobacter pylori infection promotes the invasion and metastasis of gastric cancer through increasing the expression of matrix metalloproteinase-1 and matrix metalloproteinase-10. Exp Ther Med. 2014;8:769-74.
288. Chan YM, Jan YN. Roles for proteolysis and trafficking in notch maturation and signal transduction. Cell. 1998;94:423-6.
289. Zhang S, Zhang M, Cai F, *et al*. Biological function of presenilin and its role in AD pathogenesis. Transl Neurodegener. 2013;2:15.
290. Gocheva V, Joyce JA. Cysteine Cathepsins and the cutting edge of cancer invasión. Cell Cycle. 2007;6:60-4.
291. Balk SP, Ko YJ, Bubley GJ. Biology of prostate-specific antigen. J Clin Oncol. 2003;21:383-91.
292. Borgoño CA, Diamandis EP. The emerging roles of human tissue kallikreins in cancer. Nat Rev Cancer. 2004;4:876-90.
293. Mochizuki S, Okada Y. ADAMs in cancer cell proliferation and progression. Cancer Sci. 2007;98:621-8.
294. Tan Ide A, Ricciardelli C, Russell DL. The metalloproteinase ADAMTS1: a comprehensive review of its role in tumorigenic and metastatic pathways. Int J Cancer. 2013;133:2263-76.

295. Marr RA, Hafez DM. Amyloid-beta and Alzheimer's disease: the role of neprilysin-2 in amyloid-beta clearance. Front Aging Neurosci. 2014;6:187.
296. Maguer-Satta V, Besançon R, Bachelard-Cascales E. Concise review: neutral endopeptidase (CD10): a multifaceted environment actor in stem cells, physiological mechanisms, and cancer. Stem Cells. 2011;29:389-96.
297. Marimuthu A, Subbannayya Y, Sahasrabuddhe NA, *et al*. SILAC-based quantitative proteomic analysis of gastric cancer secretome. Proteomics Clin Appl. 2013;7:355-66.
298. Tang Z, Sheng H, Zheng X, *et al*. Upregulation of circulating cytokeratin 20, urokinase plasminogen activator and C-reactive protein is associated with poor prognosis in gastric cancer. Mol Clin Oncol. 2015;3:1213-20.
299. Khoi PN, Xia Y, Lian S, *et al*. Cadmium induces urokinase-type plasminogen activator receptor expression and the cell invasiveness of human gastric cancer cells via the ERK-1/2, NF-κB, and AP-1 signaling pathways. Int J Oncol. 2014;45:1760-8.
300. Pezzato E, Donà M, Sartor L, *et al*. Proteinase-3 directly activates MMP-2 and degrades gelatin and Matrigel; differential inhibition by (-) epigallocatechin-3-gallate. J Leukoc Biol. 2003;74:88-94.
301. Alén BO, Leal-López S, Alén MO, *et al*. The role of the obestatin/GPR39 system in human gastric adenocarcinomas. Oncotarget. 2016;7:5957-71.
302. Barranco SC, Townsend CM Jr, Casartelli C, *et al*. Establishment and characterization of an in vitro model system for human adenocarcinoma of the stomach. Cancer Res. 1983;43:1703-9.
303. Schlüter C, Duchrow M, Wohlenberg C, *et al*. The cell proliferation-associated antigen of antibody Ki-67: a very large, ubiquitous nuclear protein with numerous repeated elements, representing a new kind of cell cycle-mantaining proteins. J Cell Biol. 1993;123:513-22.
304. Palovuori R, Perttu A, Yan Y, *et al*. Helicobacter pylori induces formation of stress fibers and membrane ruffles in AGS cells by Rac activation. Biochem Biophys Res Commun. 2000;269:247-53.
305. Bessède E, Staedel C, Acuña-Amador LA, *et al*. Helicobacter pylori generates cells with cancer stem cell properties via epithelial-mesenchymal transition-like changes. Oncogene. 2014;33:4123-31.
306. Wu WK, Cho CH, Lee CW, *et al*. Dysregulation of cellular signaling in gastric cancer. Cancer Lett. 2010;295:144-53.
307. Oliveira MJ, Costa AM, Costa AC, *et al*. CagA associates with c-Met, E-cadherin, and p120-catenin in a multiproteic complex that suppresses Helicobacter pylori-induced cell-invasive phenotype. J Infect Dis. 2009;200:745-55.
308. Lee HE, Kim MA, Lee BL, *et al*. Low Ki-67 proliferation index is an indicator of poor prognosis in gastric cancer. J Surg Oncol. 2010;102:201-6.
309. Chandanos E, Lagergren J. Oestrogen and the enigmatic male predominance of gastric cancer. Eur J Cancer. 2008;44:2397-403.
310. Goldenring JR, Nam KT, Mills JC. The origin of pre-neoplastic metaplasia in the stomach: chief cells emerge from the Mist. Exp Cell Res. 2011;317:2759-64.
311. Cornaggia M, Capella C, Riva C, *et al*. Electron immunocytochemical localization of pepsinogen I (PgI) in chief cells, mucous-neck cells and transitional mucous-neck/chief cells of the human fundic mucosa. Histochemistry. 1986;85:5-11.
312. Basque JR, Chénard M, Chailler P, *et al*. Gastric cancer cell lines as models to study human digestive functions. J Cell Biochem. 2001;81:241-51.
313. Chan EC, Chen KT, Lin YL. Vacuolating toxin from Helicobacter pylori activates cellular signaling and pepsinogen secretion in human gastric adenocarcinoma cells. FEBS Lett. 1996;399:127-30.
314. Fogh J, Trempe G. New human tumor cell lines. In Human Tumor Cells in vitro. Plenum Press, New York. 1975;115-59.
315. Lieber M, Mazzetta JA, Nelson-Rees W, *et al*. Establishment of a continuous tumor-cell line (panc-1) from a human carcinoma of the exocrine pancreas. Int J Cancer. 1975;15:741-7.
316. Soule HD, Vazguez J, Long A, *et al*. A human cell line from a pleural effusion derived from a breast carcinoma. J Natl Cancer Inst. 1973;51:1409-16.
317. Pattillo RA, Gey GO. The establishment of a cell line of human hormone-synthesizing trophoblastic cells in vitro. Cancer Res. 1968;28:1231-6.
318. Kaighn ME, Narayan KS, Ohnuki Y, *et al*. Establishment and characterization of a human prostatic carcinoma cell line (PC-3). Invest Urol. 1979;17:16-23.
319. Giard DJ, Aaronson SA, Todaro GJ, *et al*. In vitro cultivation of human tumors: establishment of cell lines derived from a series of solid tumors. J Natl Cancer Inst. 1973;51:1417-23.

320. Lieber M, Smith B, Szakal A, *et al*. 1976 A continuous tumor-cell line from a human lung carcinoma with properties of type II alveolar epithelial cells. Int J Cancer. 1976;15;17:62-70.
321. Fogh J, Wright WC, Loveless JD. Absence of HeLa cell contamination in 169 cell lines derived from human tumors. J Natl Cancer Inst. 1977;58:209-14.
322. Sekiguchi M, Sakakibara K, Fujii G. Establishment of cultured cell lines derived from a human gastric carcinoma. Jpn J Exp Med. 1978;48:61-8.
323. King IC, Sartorelli AC. The relationship between epidermal growth factor receptors and the terminal differentiation of A431 carcinoma cells. Biochem Biophys Res Commun. 1986;140:837-43.
324. Smith JJ, Derynck R, Korc M.Production of transforming growth factor alpha in human pancreatic cancer cells: evidence for a superagonist autocrine cycle. Proc Natl Acad Sci USA. 1987;84:7567-70.
325. Sakakibara D, Sasaki A, Ikeya T, *et al*. Protein structure determination in living cells by in-cell NMR spectroscopy. Nature. 2009;458:102-5.
326. Fischer G, Bang H, Mech C. Determination of enzymatic catalysis for the cis-trans-isomerization of peptide binding in proline-containing peptides. Biomed Biochim Acta. 1984;43:1101-11.
327. De Spiegeleer B, Van Dorpe S, Vergote V, *et al*. In vitro metabolic stability of iodinated obestatin peptides. Peptides. 2012;33:272-8.
328. Benovic JL, Pike LJ, Cerione RA, *et al*. Phosphorylation of the mammalian beta-adrenergic receptor by cyclic AMP-dependent protein kinase. Regulation of the rate of receptor phosphorylation and dephosphorylation by agonist occupancy and effects on coupling of the receptor to the stimulatory guanine nucleotide regulatory protein. J Biol Chem. 1985;260:7094-101.
329. Benovic JL, Mayor FJ, Somers RL, *et al*. Light-dependent phosphorylation of rhodopsin by beta-adrenergic receptor kinase. Nature. 1986;321:869-72.
330. Bouzo-Lorenzo M, Santo-Zas I, Lodeiro M, *et al*. Distinct phosphorylation sites on the ghrelin receptor, GHSR1a, establish a code that determines the functions of ß-arrestins. Sci Rep. 2016;6:22495.
331. Appert-Collin A, Hubert P, Crémel G, *et al*. Role of ErbB receptors in cancer cell migration and invasion. Front Pharmacol. 2015;6:283.
332. Shibuya M. Tyrosine kinase receptor Flt/VEGFR family: its characterization related to angiogenesis and cancer. Genes Cancer. 2010;1:1119-23.
333. Oda T, Kanai Y, Oyama T, *et al*. E-cadherin gene mutations in human gastric carcinoma cell lines. Proc Natl Acad Sci USA. 1994;91:1858-62.
334. Wang Y, Moncayo G, Morin PJ, *et al*. Mer receptor tyrosine kinase promotes invasion and survival in glioblastoma multiforme. Oncogene. 2013;32:872-82.
335. Wolfsberg TG, Straight PD, Gerena RL. ADAM, a widely distributed and developmentally regulated gene family encoding membrane proteins with a disintegrin and metalloprotease domain. Dev Biol. 1995;169:378-83.
336. Edwards DR, Handsley MM, Pennington CJ. The ADAM metalloproteinases. Mol Aspects Med. 2008;29:258-89.
337. Diamandis EP, Yousef GM. Human tissue kallikreins: a family of new cancer biomarkers. Clin Chem. 2002;48:1198-205.
338. Verma RP, Hansch C. Matrix metalloproteinases (MMPs): chemical-biological functions and (Q)SARs. Bioorg Med Chem. 2007;15:2223-68.
339. Guo Y, Yin J, Zha L, *et al*. Clinicopathological significance of platelet-derived growth factor B, platelet-derived growth factor receptor-beta, and E-cadherin expression in gastric carcinoma. Contemp Oncol. 2013;17:150-5.
340. Li P, Lin X, Zhang JR, *et al*. The expression of presenilin 1 enhances carcinogenesis and metastasis in gastric cancer. Oncotarget. 2016;7:10650-62.
341. Iruela-Arispe ML, Carpizo D, Luque A. ADAMTS1: a matrix metalloprotease with angioinhibitory properties. Ann N Y Acad Sci. 2003;995:183-90.
342. Rodríguez-Manzaneque JC, Carpizo D, *et al*. Cleavage of syndecan-4 by ADAMTS1 provokes defects in adhesion. Int J Biochem Cell Biol. 2009;41:800-10.
343. Oleksowicz L, Bhagwati N, DeLeon-Fernandez M. Deficient activity of von Willebrand's factor-cleaving protease in patients with disseminated malignancies. Cancer Res. 1999;59:2244-50.
344. Koo BH, Oh D, Chung S, *et al*. Deficiency of von Willebrand factor-cleaving protease activity in the plasma of malignant patients. Thromb. Res. 2002;105:471-6.
345. Teller A, Jechorek D, Hartig R, *et al*. Dysregulation of apoptotic signaling pathways by interaction of RPLP0 and cathepsin X/Z in gastric cancer. Pathol Res Pract. 2015;211:62-70.

346. Liu XL, Wazer DE, Watanabe K, *et al*. Identification of a novel serine protease-like gene, the expression of which is down-regulated during breast cancer progression. Cancer Res. 1996;56:3371-9.
347. Albo D, Shinohara T, Tuszynski GP. Up-regulation of matrix metalloproteinase 9 by thrombospondin 1 in gastric cancer. J Surg Res. 2002;108:51-60.
348. Gulhati P, Bowen KA, Liu J, *et al*. mTORC1 and mTORC2 regulate EMT, motility, and metastasis of colorectal cancer via RhoA and Rac1 signaling pathways. Cancer Res. 2011;71:3246-56.
349. Veikkola T, Alitalo K. VEGFs, receptors and angiogenesis. Semin Cancer Biol. 1999;9:211-20.
350. Zhang Y, Han J, Yang X, *et al*. Pigment epithelium-derived factor inhibits angiogenesis and growth of gastric carcinoma by down-regulation of VEGF. Oncol Rep. 2011;26:681-6.
351. Nam KT, Lee HJ, Sousa JF, *et al*. Mature chief cells are cryptic progenitors for metaplasia in the stomach. Gastroenterology. 2010;139:2028-37.
352. Adachi Y, Yasuda K, Inomata M, *et al*. Pathology and prognosis of gastric carcinoma: well versus poorly differentiated type. Cancer. 2000;89:1418-24.
353. Sakurada T, Ro S, Onouchi T, *et al*. Comparison of the actions of acylated and desacylated ghrelin on acid secretion in the rat stomach. J Gastroenterol. 2010;45:1111-20.
354. Kawao N, Sakaguchi Y, Tagome A, *et al*. Protease-activated receptor-2 (PAR-2) in the rat gastric mucosa: immunolocalization and facilitation of pepsin/pepsinogen secretion. Br J Pharmacol. 2002;135:1292-6.
355. Fiorucci S, Distrutti E, Federici B, *et al*. PAR-2 modulates pepsinogen secretion from gastric-isolated chief cells. Am J Physiol Gastrointest Liver Physiol. 2003;285:G611-20.
356. Gieseler F, Ungefroren H, Settmacher U, *et al*. Proteinase-activated receptors (PARs) - focus on receptor-receptor-interactions and their physiological and pathophysiological impact. Cell Commun Signal. 2013;11:86.
357. Hirsch FR, Varella-Garcia M, Cappuzzo F. Predictive value of EGFR and HER2 overexpression in advanced non-small-cell lung cancer. Oncogene. 2009;28:S32-7.
358. Iizuka N, Tangoku A, Hazama S, *et al*. Nm23-H1 gene as a molecular switch between the free-floating and adherent states of gastric cancer cells. Cancer Lett. 2001;174:65-71.
359. Tee YT, Chen GD, Lin LY, *et al*. Nm23-H1: a metastasis-associated gene. Taiwan J Obstet Gynecol. 2006;45:107-13.
360. Provinciali M, Pierpaoli E, Bartozzi B, *et al*. Zinc induces apoptosis of human melanoma cells, increasing reactive oxygen species, p53 and FAS ligand. Anticancer Res. 2015;35:5309-16.
361. Wang Y, Zhang S, Li SJ. Zn(2+) induces apoptosis in human highly metastatic SHG-44 glioma cells, through inhibiting activity of the voltage-gated proton channel Hv1. Biochem Biophys Res Commun. 2013;438:312-7.
362. Hong SH, Choi YS, Cho HJ, *et al*. Induction of apoptosis of bladder cancer cells by zinc-citrate compound. Korean J Urol. 2012;53:800-6.
363. Hong SH, Choi HJ, Lee JY, *et al*. Antiproliferative effects of zinc-citrate compound on hormone refractory prostate cancer. Chin J Cancer Res. 2012;24:124-9.
364. Provinciali M, Donnini A, Argentati K, *et al*. Reactive oxygen species modulate Zn2+-induced apoptosis in cancer cells. Free Radical Bio Med. 2002;32:431-45.

SUPPLEMENTARY MATERIAL

USC
UNIVERSIDADE
DE SANTIAGO
DE COMPOSTELA

CHAPTER 1

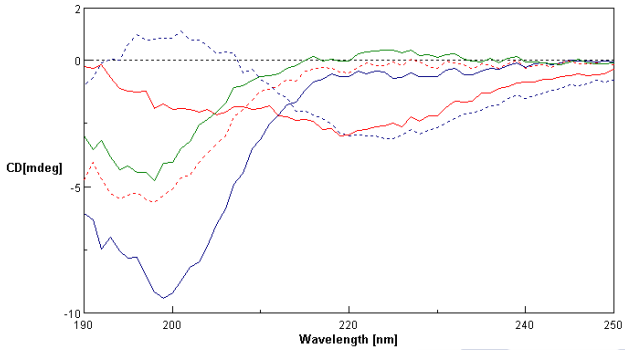

Figure S1.1. Far-UV CD spectra of the peptides in 25 mM PBS under identical conditions. The concentration was 40 µM in all samples. Color code: solid blue, human obestatin (**1**); dotted blue, non-amidated obestatin (**2**); solid red, human (6-23)-obestatin (**3**); dotted red, (11-23)-obestatin (**4**); and solid green, (16-23)-obestatin (**5**).

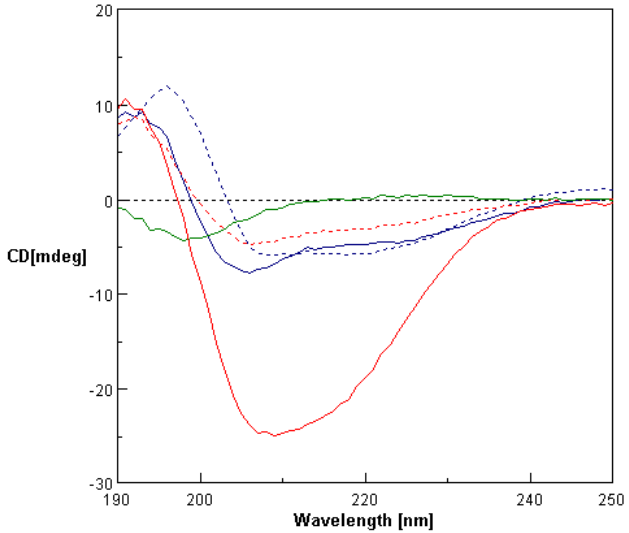

Figure S1.2. Far-UV CD spectra of the peptides in 2.8 mM SDS under identical conditions. The concentration was 40 µM in all samples. Color code: solid blue, human obestatin (**1**); dotted blue, non-amidated obestatin (**2**); solid red, human (6-23)-obestatin (**3**); dotted red, (11-23)-obestatin (**4**); and solid green, (16-23)-obestatin (**5**).

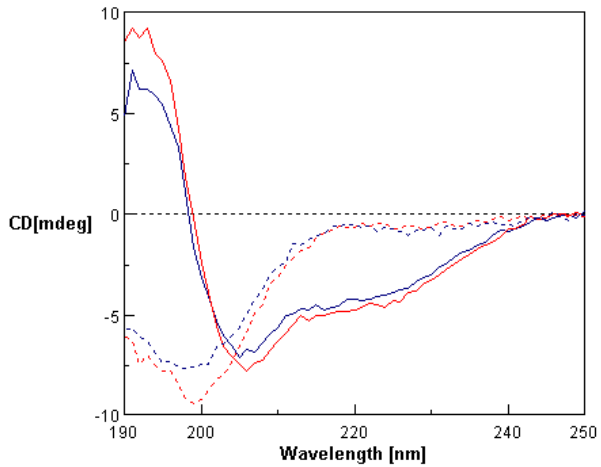

Figure S1.3. Far-UV CD spectra of human obestatin (**1**) and mouse obestatin (**6**) in 25 mM PBS or 2.8 mM SDS under identical conditions. The concentration was 40 µM in all samples. Color code: solid red, human obestatin (**1**) in SDS; dotted red, human obestatin (**1**) in PBS; solid blue, mouse obestatin (**6**) in SDS; and dotted blue, mouse obestatin (**6**) in PBS.

Sample	Environment	Method/ref	% Secondary structure content				NRMSD
			Helical	Strand	Turns	Unordered	
Human obestatin (1)	PBS	K2d	7	50	-	43	0,590
		CONTINLL/4	10,4	29,9	24,5	35,2	0,151
		CONTINLL/7	6,4	21,0	15,0	57,6	0,130
	SDS	K2d	13	31	-	56	0,210
		CONTINLL/4	22,7	26,2	21,9	29,1	0,071
		CONTINLL/7	21,2	19,8	15,4	43,5	0,071
Human non amidated-obestatin (2)	PBS	K2d	5	48	-	48	1,143
		CONTINLL/4	13,7	35,8	23,3	31,7	0,459
		CONTINLL/7	7,7	30,1	17,6	44,5	0,459
	SDS	K2d	28	23	-	49	0,327
		CONTINLL/4	24,3	28,5	18,2	29,0	0,096
		CONTINLL/7	24,3	28,4	18,3	28,9	0,096
Human (6-23)-obestatin (3)	PBS	K2d	7	50	-	43	0,575
		CONTINLL/4	9,6	31,7	23,4	35,2	0,095
		CONTINLL/7	5,4	22,5	13,5	58,6	0,118
	SDS	K2d	91	1	-	8	0,367
		CONTINLL/4	40,8	4,8	23,0	31,4	0,145
		CONTINLL/7	43,7	5,0	25,4	25,9	0,145
Human (11-23)-obestatin (4)	PBS	K2d	7	50	-	43	0,742
		CONTINLL/4	10,1	31,2	24,4	34,4	0,127
		CONTINLL/7	6,1	22,3	14,8	56,8	0,131
	SDS	K2d	17	29	-	54	0,214
		CONTINLL/4	23,4	27,4	21,4	27,8	0,082
		CONTINLL/7	22,8	24,6	18,6	34,0	0,082
Human (16-23)-obestatin (5)	PBS	K2d	7	49	-	44	0,783
		CONTINLL/4	8,8	31,1	24,3	35,8	0,134
		CONTINLL/7	4,6	21,9	14,2	59,3	0,151
	SDS	K2d	6	47	-	46	0,713
		CONTINLL/4	7,2	33,5	23,5	35,7	0,219
		CONTINLL/7	3,4	24,9	14,3	57,3	0,314
Mouse obestatin (6)	PBS	K2d	7	51	-	42	0,833
		CONTINLL/4	10,2	31,3	24,4	34,1	0,140
		CONTINLL/7	10,7	22,8	15,4	54,6	0,225
	SDS	K2d	11	33	-	55	0,287
		CONTINLL/4	20,0	27,6	22,5	29,8	0,142
		CONTINLL/7	18,5	21,3	16,0	44,2	0,142

Table S1.1. Quantification of obestatins secondary structure by CD. The following table describes the quantification of the CD spectra in two different environments. The quantification was performed using the DICHROWEB server and the data were fit using K2d and CONTINLL. The latter was paired with two different data sets for data ranging from 190 to 240 nm. The NRMSD refers to the quality of the curve fitting based on the reference data sets.

Residue	HN	Hα	Hβ	Hγ	Hδ	others
PHE 1		4.187	Hβ2/Hβ3		7.186	
ASN 2	8.149	4.699	Hβ2/Hβ3 2.564/2.463			Hδ21/Hδ22 7.425/6.747
ALA 3	8.152	4.192	1.172			
PRO 4		4.338	Hβ2/Hβ3 2.014/1.770	Hγ2/Hγ3 1.864/1.590	Hδ2/Hδ3 3.240/3.609	
PHE 5	7.126	4.581	Hβ2/Hβ3 3.134/2.941	7.036		Hε 7.106
ASP 6	8.341	4.592	Hβ2/Hβ3 2.736/2.478			
VAL 7	8.012	3.908	2.091	0.899		
GLY 8	8.341	Hα2/Hα3 3.858/3.789				
ILE 9	7.465	3.978	1.767	0.810	0.770	Hγ12/Hγ13 1.402/1.099
LYS 10	7.915	4.256	1.752	1.358	1.577	2.855
LEU 11	8.002	4.256	Hβ2/Hβ3 1.656/1.567	1.357	Hδ1/Hδ2 0.820/0.770	
SER 12	8.334	4.266	Hβ2/Hβ3 3.915/3.858			
GLY 13	8.192	3.952				
VAL 14	7.554	3.858	2.053	Hγ1/Hγ2 0.926/0.829		
GLN 15	8.331	4.266	1.955	2.212		Hε21/Hε22 7.295/6.648
TYR 16	7.923	4.241	Hβ2/Hβ3 2.912/2.867		6.922	H□ 6.694
GLN 17	8.142	3.958	1.905	2.234		Hε21/Hε22 7.325/6.697
GLN 18	7.913	4.022	1.870	2.210		Hε21/Hε22 7.286/6.692
HIS 19	8.022	4.612	Hβ2/Hβ3 3.251/3.029		Hδ2 7.324	Hε1 8.575
SER 20	8.012	4.158	Hβ2/Hβ3 3.796/3.627			
GLN 21	8.182	4.168	Hβ2/Hβ3	2.287		Hε21/Hε22 7.385/6.688
ALA 22	7.923	4.166	1.318			
LEU 23	7.684	4.167	1.605	1.487	Hδ1/Hδ2 0.829/0.779	
NHE	NH_1/NH_2 7.206/6.827					

Table S1.2. ^{1}H chemical shifts (ppm) for human obestatin (**1**) in SDS-d_{25} micelles at 298K.

Residue	HN	Hα	Hβ	Hγ	Hδ	others
PHE 1		4.217	Hβ2/Hβ3 3.141/3.095		7.219	Hε 7.129
ASN 2	8.155	4.727	Hβ2/Hβ3 2.599/2.491			Hε21/Hε22 7.441/6.765
ALA 3	8.158	4.221	1.210			
PRO 4		4.376	Hβ2/Hβ3 2.032/1.795	Hγ2/Hγ3 1.893/1.610	Hδ2/Hδ3 3.635/3.271	
PHE 5	7.126	4.625	Hβ2/Hβ3 3.169/2.977		7.077	Hε 7.160 Hζ 7.063
ASP 6	8.352	4.635	Hβ2/Hβ3 2.767/2.508			
VAL 7	8.030	3.926	2.126	0.934		
GLY 8	8.371	Hα2/Hα3 3.874/3.817				
ILE 9	7.515	3.993	1.806	Hγ2 0.934	Hδ1 0.842	Hγ12/Hγ13 1.439/1.123
LYS 10	7.928	4.271	1.792	1.398	1.602	Hε 2.893
LEU 11	8.031	4.263	1.594	1.687	Hδ1/Hδ2 0.858/0.804	
SER 12	7.978	4.271	Hβ2/Hβ3 3.931/3.879			
GLY 13	8.160	Hα2/Hα3 4.017/3.929				
VAL 14	7.551	3.923	2.101	Hγ1/Hγ2 0.959/0.872		
GLN 15	8.291	4.287	1.958	Hγ 2.223		Hε21/Hε22 7.322/6.667
TYR 16	7.903	4.322	Hβ2/Hβ3 2.930/2.896		6.960	Hε 6.725
GLN 17	8.065	4.039	Hβ2/Hβ3 1.958/1.881	2.228		Hε21/Hε22 7.323/6.725
GLN 18	7.981	4.057	Hβ2/Hβ3 1.962/1.883	2.256		Hε21/Hε22 7.335/6.702
HIS 19	8.155	4.579	Hβ2/Hβ3 3.251/3.098		Hδ2 7.297	
SER 20	8.025	4.288	Hβ2/Hβ3 3.782/3.694			
GLN 21	8.176	4.261	Hβ2/Hβ3 2.056/1.891	2.293		Hε21/Hε22 7.432/6.672
ALA 22	8.079	4.253	1.297			
LEU 23	7.689	4.085	1.495		Hδ1/Hδ2	

Table S1.3. ^{1}H chemical shifts (ppm) for human non amidated obestatin (**2**) in SDS-d_{25} micelles at 298K.

Residue	HN	Hα	Hβ	Hγ	Hδ	others
ASP 6	8.341	4.595	Hβ2/Hβ3 2.736/2.478			
VAL 7	8.012	3.908	2.093	0.897		
GLY 8	8.341	3.862				
ILE 9	7.465	3.978	1.767	0.887	0.797	Hγ12/Hγ13 1.402/1.096
LYS 10	7.915	4.256	1.752	1.358	1.582	2.856
LEU 11	8.002	4.252	1.649		0.799	
SER 12	8.334	4.266	Hβ2/Hβ3 3.915/3.856			
GLY 13	8.192	3.952				
VAL 14	7.554	3.860	2.050	Hγ1/Hγ2 0.926/0.822		
GLN 15	8.331	4.266	1.955	Hγ 2.212		Hε21/Hε22 7.296/6.648
TYR 16	7.923	4.240	2.890		6.922	Hε 6.694
GLN 17	8.144	3.958	Hβ2/Hβ3 1.925/1.878	2.234		Hε21/Hε22 7.320/6.697
GLN 18	7.913	4.022	1.870	2.210		Hε21/Hε22 7.325/6.692
HIS 19	8.022	4.255	Hβ2/Hβ3 3.251/3.029		Hδ2 7.324	Hε1 8.531
SER 20	8.012	4.158	Hβ2/Hβ3 3.775/3.627			
GLN 21	8.182	4.171	Hβ2/Hβ3 2.049/1.933	2.287		Hε21/Hε22 7.385/6.674
ALA 22	7.923	4.166	1.325			
LEU 23	7.684	4.177	1.605	1.488	0.808	
NHE	NH_1/NH_2 7.211/6.827					

Table S1.4. ^{1}H chemical shifts (ppm) for human (6-23)-obestatin (**3**) in SDS-d_{25} micelles at 298K.

Residue	HN	Hα	Hβ	Hγ	Hδ	others
LEU 11		3.954	1.645	1.575	0.782	
SER 12	8.611	4.357	3.751			
GLY 13	8.260	Hα3/Hα2 3.954/3.816				
VAL 14	7.586	3.733	1.874	Hγ1/Hγ2 0.757/0.706		
GLN 15	8.266	4.100	1.872	Hγ2/Hγ3 2.151/2.108		Hε21/Hε22 7.149/6.502
TYR 16	7.851	4.064	2.794		6.785	Hε 6.572
GLN 17	8.048	3.764	1.837	2.185		Hε21/Hε22 7.185/6.570
GLN 18	7.765	3.890	1.734	2.088		Hε21/Hε22 7.094/6.566
HIS 19	7.797	4.530	Hβ2/Hβ3 3.139/2.879		Hδ2 7.264	Hε1 8.488
SER 20	7.839	3.977	Hβ2/Hβ3 3.614/3.432			
GLN 21	7.998	4.042	Hβ2/Hβ3 1.931/1.823	2.178		Hε21/Hε22 7.254/6.554
ALA 22	7.748	4.048	1.224			
LEU 23	7.503	4.054	1.501	1.388	Hδ1/Hδ2 0.724/0.678	
NHE	NH_1/NH_2 7.064/6.696					

Table S1.5. ^{1}H chemical shifts (ppm) for human (11-23)-obestatin (**4**) in SDS-d_{25} micelles at 298K.

Residue	HN	Hα	Hβ	Hγ	Hδ	others
TYR 16		4.094	Hβ2/Hβ3 2.944/2.878		6.907	Hε 6.603
GLN 17		4.105	Hβ2/Hβ3 1.756/1.672	2.007		Hε21/Hε22 7.236/6.576
GLN 18	8.043	4.018	Hβ2/Hβ3 1.824/1.770	2.175		Hε21/Hε22 7.241/6.553
HIS 19	8.351	4.526	Hβ2/Hβ3 3.158/3.007		Hδ2 7.193	
SER 20	8.053	4.191	Hβ2/Hβ3 3.670/3.728	4.566		
GLN 21	8.176	4.116	Hβ2/Hβ3 1.942/1.833	2.168		Hε21/Hε22 7.258/6.544
ALA 22	7.916	4.067	1.191			
LEU 23	7.635	4.083	1.497	1.375	Hδ1/Hδ2 0.736/0.683	
NHE	NH_1/NH_2 7.109/6.672					

Table S1.6. ^{1}H chemical shifts (ppm) for human (16-23)-obestatin (**5**) in SDS-d_{25} micelles at 298K.

Residue	HN	Hα	Hβ	Hγ	Hδ	others
PHE 1		4.188	Hβ2/Hβ3 3.101/3.064		7.190	Hε 7.101
ASN 2	8.140	4.690	Hβ2/Hβ3 2.567/2.463			Hδ21/Hδ22 7.424/6.746
ALA 3	8.141	4.189	1.177			
PRO 4		4.340	Hβ2/Hβ3 2.003/1.758	Hγ2/Hγ3 1.856/1.584	Hδ2/Hδ3 3.248/3.602	
PHE 5	7.105	4.585	Hβ2/Hβ3 3.140/2.942		7.045	Hε 7.135
ASP 6	8.320	4.615	Hβ2/Hβ3 2.732/2.482			
VAL 7	7.991	3.915	2.095	0.898		
GLY 8	8.330	Hα2/Hα3 3.837/3.801				
ILE 9	7.474	3.978	1.766		0.808	Hγ12/Hγ13 1.396/1.093
LYS 10	7.913	4.246	1.751	1.361	1.585	Hε 2.865 Hζ 7.175
LEU 11	7.928	4.250	1.646	1.322	Hδ1/Hδ2 0.819/0.778	
SER 12	8.006	4.281	Hβ2/Hβ3 3.897/3.825	7.921		
GLY 13	8.211	3.916				
ALA 14	7.773	4.136	1.301			
GLN 15	8.221	4.176	1.909	2.143		Hε21/Hε22 7.299/6.656
TYR 16	7.818	4.350	Hβ2/Hβ3 2.950/2.886		6.956	Hε 6.689
GLN 17	7.942	4.060	Hβ2/Hβ3 1.948/1.825	2.192		Hε21/Hε22 7.314/6.678
GLN 18	7.852	4.067	Hβ2/Hβ3 1.933/1.830	2.196		Hε21/Hε22 7.303/6.686
HIS 19	8.111	4.584	Hβ2/Hβ3 3.099/3.260		Hδ2 7.304	Hε1 8.530
GLY 20	8.191	3.814				
ARG 21	7.961	4.226	Hβ2/Hβ3 1.803/1.706	1.565	3.083	Hε 7.056 HH1/HH2 6.701/6.382
ALA 22	8.086	4.226	1.286			
LEU 23	7.807	4.176	1.609	1.444	Hδ1/Hδ2 0.829/0.779	
NHE	NH_1/NH_2 7.245/6.796					

Table S1.7. ^{1}H chemical shifts (ppm) for mouse obestatin (**6**) in SDS-d_{25} micelles at 298K.

USC
UNIVERSIDADE
DE SANTIAGO
DE COMPOSTELA

CHAPTER 2

Residue	HN	Hα	Hβ	Hγ	Hδ	others
TYR 16	8.25	4.01	2.84			
GLN 17	8.58	4.13	Hβ/Hβ2 1.55/1.64	1.95		
GLN 18	8.64	4.03	Hβ1/Hβ2 1.61/1.70	2.02		
HIS 19	8.77	4.59	Hβ1/Hβ2 2.93/3.02			
SER 20	8.51	4.25	3.63			
GLN 21	8.63	4.14	Hβ1/Hβ2 1.64/1.78	2.05		
ALA 22	8.42	4.11	0.99			
LEU 23	8.26	4.10	1.28	1.22	Hδ1/Hδ2 0.46/0.50	

Table S2.1. ^{1}H chemical shifts (ppm) for human (16-23)-obestatin (**5**) in H_2O at 298K.

Residue	HN	Hα	Hβ	Hγ	Hδ	others
TYR 16		4.21	2.84			
GLN 17		4.36	Hβ1/Hβ2 1.91/1.99	2.28		
GLN 18	8.58	4.27	Hβ1/Hβ2 1.97/2.05	2.34		
HIS 19						
SER 20	8.43		3.87			
GLN 21	8.58	4.37	Hβ1/Hβ2 2.00/2.14	2.39		
ALA 22	8.36	4.33	0.99			
LEU 23	8.22	4.33	1.68	1.61	Hδ1/Hδ2 0.94/1.04	

Table S2.2. ^{1}H chemical shifts (ppm) for human (16-23)-obestatin (**5**) in PBS at 298K.

Residue	HN	Hα	Hβ	Hγ	Hδ	others
TYR 16		4.19	3.12			
GLN 17		4.30	1.94	2.3		
GLN 18		4.22	Hβ1/Hβ2 2.01/2.08	2.39		
HIS 19		4.71	3.19			
SER 20		4.42	3.89			
GLN 21		4.33	Hβ1/Hβ2 2.03/2.17	2.43		
ALA 22		4.30	1.43			
LEU 23		4.29	1.72	1.61	Hδ1/Hδ2 0.92/0.97	

Table S2.3. ^{1}H chemical shifts (ppm) for human (16-23)-obestatin (**5**) in HEK293-WT cells at 298K.

Residue	HN	Hα	Hβ	Hγ	Hδ	others
TYR 16		4.18	3.09			
GLN 17		4.30	1.92	2.25		
GLN 18	8.70	4.22	Hβ1/Hβ2 1.98/2.13	2.34		
HIS 19	8.74	4.71	Hβ1/Hβ2 3.15/3.23			
SER 20	8.55	4.42	3.86			
GLN 21	8.69	4.33	Hβ1/Hβ2 1.99/2.12	2.38		
ALA 22	8.47	4.29	1.38			
LEU 23	8.37	4.29	1.67	1.58	Hδ1/Hδ2 0.90/0.94	

Table S2.4. ^{1}H chemical shifts (ppm) for human (16-23)-obestatin (**5**) in HEK293-GPR39 cells at 298K.

	PBS-H_2O					WT-PBS					GPR39-WT				
Residue	**HN**	**Hα**	**Hβ**	**Hγ**	**Hδ**	**HN**	**Hα**	**Hβ**	**Hγ**	**Hδ**	**HN**	**Hα**	**Hβ**	**Hγ**	**Hδ**
TYR 16		0.2	0				-0.02	0.02				-0.01	0		
GLN 17		0.23	Hβ1/Hβ2 0.36/0.35	0.33			-0.06	-0.01	0.02			0	0	0.05	
GLN 18	-0.06	0.24	Hβ1/Hβ2 0.36/0.35	0.32			-0.05	Hβ1/Hβ2 0.04/0.03	0.05			0	Hβ1/Hβ2 -0.03/0.05	0.05	
HIS 19												0	0		
SER 20	-0.08		0.24					0.02				0	-0.03		
GLN 21	-0.05	0.23	Hβ1/Hβ2 0.36/0.36	0.34			-0.04	Hβ1/Hβ2 0.03/0.03	0.04			0	Hβ1/Hβ2 -0.04/-0.05	0.05	
ALA 22	-0.06	0.22	0.40				-0.03	0.04				-0.01	-0.05		
LEU 23	-0.04	0.23	0.40	0.39	Hδ1/Hδ2 0.48/0.54		-0.04	0.04	0	Hδ1/Hδ2 -0.02/-0.07		0	-0.05	-0.03	Hδ1/Hδ2 -0.03/-0.03

Table S2.5. CSPs between (16-23)-obestatin (**5**) spectra. δ ≥ 0,1 ppm were considered significant differences and were marked in red.

Residue	CSI H_2O	CSI PBS	CSI WT	CSI GPR39
TYR 16	-1	-1	-1	-1
GLN 17	-1	0	0	0
GLN 18	-1	0	-1	-1
HIS 19	0		0	0
SER 20	-1		0	0
GLN 21	-1	0	0	0
ALA 22	-1	0	0	0
LEU 23	0	+1	+1	+1

Table S2.6. Secondary structure prediction of (16-23)-obestatin (**5**) using CSI.

Residue	HN	Hα	Hβ	Hγ	Hδ	others
LEU 11		4.08	1.69		0.93	
SER 12	8.76		3.89			
GLY 13	8.55	4.02				
VAL 14	8.07	4.06	2.00	Hγ1/Hγ2 0.84/0.90		
GLN 15	8.51	4.29	Hβ1/Hβ2 1.91/2.20	2.27		
TYR 16	8.17	4.55	Hβ1/Hβ2 2.92/3.06			
GLN 17	8.21	4.27	Hβ1/Hβ2 1.92/2.02	2.30		
GLN 18	8.38	4.23	Hβ1/Hβ2 1.96/2.03	2.34		
HIS 19	8.59	4.75	Hβ1/Hβ2 3.19/3.30			
SER 20	8.40	4.44	3.87			
GLN 21	8.54	4.34	Hβ1/Hβ2 2.00/2.13	2.39		
ALA 22	8.34	4.31	1.38			
LEU 23	8.19	4.30	1.67	1.60	Hδ1/Hδ2 0.87/0.93	

Table S2.7. ^{1}H chemical shifts (ppm) for human (11-23)-obestatin (**4**) in H_2O at 298K.

Residue	HN	Hα	Hβ	Hγ	Hδ	others
LEU 11		4.05	1.68		0.92	
SER 12		4.57	3.89			
GLY 13	8.54	4.01				
VAL 14	8.04	4.06	2.01	Hγ1/Hγ2 0.84/0.90		
GLN 15	8.49	4.29	Hβ1/Hβ2 1.91/2.18	2.27		
TYR 16	8.16	4.55	Hβ1/Hβ2 2.92/3.05			
GLN 17	8.21	4.26	Hβ1/Hβ2 1.92/2.02	2.28		
GLN 18	8.37	4.23	Hβ1/Hβ2 1.94/2.03	2.31		
HIS 19						
SER 20		4.41	3.88			
GLN 21	8.50	4.33	Hβ1/Hβ2 1.99/2.13	2.38		
ALA 22	8.28	4.30	1.38			
LEU 23	8.15	4.29	1.66	1.60	0.90	

Table S2.8. ^{1}H chemical shifts (ppm) for human (11-23)-obestatin (**4**) in PBS at 298K.

Residue	HN	Hα	Hß	Hν	Hδ	others
LEU 11		4.09	1.70		0.95	
SER 12		4.59	3.91			
GLY 13						
VAL 14		4.06	2.02	Hγ1/Hγ2 0.86/0.92		
GLN 15		4.31	Hβ1/Hβ2 1.94/2.20	2.29		
TYR 16		4.55	Hβ1/Hβ2 2.94/3.07			
GLN 17		4.27	Hβ1/Hβ2 1.93/2.03	2.30		
GLN 18		4.23	Hβ1/Hβ2 1.97/2.06	2.35		
HIS 19		4.72	3.17			
SER 20		4.43	3.86			
GLN 21		4.35	Hβ1/Hβ2 2.01/2.15	2.39		
ALA 22		4.32	1.40			
LEU 23		4.31	Hβ1/Hβ2 1.59/1.69		0.92	

Table S2.9. ^{1}H chemical shifts (ppm) for human (11-23)-obestatin (**4**) in HEK293-WT cells at 298K.

Residue	HN	Hα	Hß	Hν	Hδ	others
LEU 11		4.07	Hβ1/Hβ2 1.69/1.75		0.94	
SER 12		4.57	3.90			
GLY 13	8.700	4.01				
VAL 14	8.23	4.04	2.01	Hγ1/Hγ2 0.84/0.91		
GLN 15	8.65	4.29	Hβ1/Hβ2 1.98/2.18	2.27		
TYR 16	8.34	4.53	Hβ1/Hβ2 2.93/3.04			
GLN 17	8.32	4.25	Hβ1/Hβ2 1.91/2.02	2.28		
GLN 18	8.52	4.21	Hβ1/Hβ2 1.96/2.05	2.33		
HIS 19	8.62	4.70	Hβ1/Hβ2 3.15/3.24			
SER 20		4.43	3.87			
GLN 21		4.35	Hβ1/Hβ2 2.00/2.13	2.38		
ALA 22		4.32	1.39			
LEU 23		4.31	Hβ1/Hβ2 1.59/1.67			

Table S2.10. ^{1}H chemical shifts (ppm) for human (11-23)-obestatin (**4**) in HEK293-GPR39 cells at 298K.

	PBS-H_2O					WT-PBS					GPR39-WT				
Residue	**HN**	**Hα**	**Hβ**	**Hγ**	**Hδ**	**HN**	**Hα**	**Hβ**	**Hγ**	**Hδ**	**HN**	**Hα**	**Hβ**	**Hγ**	**Hδ**
LEU 11		-0.03	-0.01		-0.01		0.04	0.02		0.03		-0.02	0.02		-0.01
SER 12			0				0.04	0.02				-0.02	-0.01		
GLY 13	-0.01	-0.01					0.02	0.02							
VAL 14	-0.03	0	0.01	0				0.01	Hγ1/Hγ2 0.02/0.02			-0.02	-0.01	Hγ1/Hγ2 -0.02/-0.01	
GLN 15	-0.02	0	Hβ1/Hβ2 0/-0.02	0			0.02	Hβ1/Hβ2 0.02/0.02	0.02			-0.02	Hβ1/Hβ2 -0.02/-0.02	-0.02	
TYR 16	-0.01	0	Hβ1/Hβ2 0/-0.01				0	Hβ1/Hβ2 0.02/0.02				-0.02	Hβ1/Hβ2 -0.01/-0.03		
GLN 17	0	-0.01	0	-0.02			0.01	Hβ1/Hβ2 0.01/0.01	0.02			-0.02	Hβ1/Hβ2 -0.02/-0.01	-0.02	
GLN 18	-0.01	0	Hβ1/Hβ2 -0.02/0	-0.03			0	Hβ1/Hβ2 0.03/0.03	0.01			-0.02	Hβ1/Hβ2 -0.01/-0.01	-0.02	
HIS 19												-0.02	0.02		
SER 20		0.03	0.01				0.02	-0.02				-0.01	0.01		
GLN 21	-0.04	-0.01	Hβ1/Hβ2 -0.01/0				0.02	Hβ1/Hβ2 0.02/0.02	0.03			-0.02	Hβ1/Hβ2 -0.01/-0.02	-0.03	
ALA 22	-0.06	-0.01	0	-0.01			0.02	0.02				-0.03	-0.01		
LEU 23	-0.04	-0.01	-0.01	0	0		0.02	-0.02		0.02		-0.02	Hβ1/Hβ2 0/-0.02		

Table S2.11. CSPs between (11-23)-obestatin (**4**) spectra. δ ≥ 0,1 ppm were considered significant differences and were marked in red.

Residue	CSI H_2O	CSI PBS	CSI WT	CSI GPR39
LEU 11	0	-1	0	-1
SER 12		0	0	0
GLY 13	0	0		0
VAL 14	+1	+1	+1	0
GLN 15	0	0	0	0
TYR 16	0	0	0	0
GLN 17	0	-1	0	-1
GLN 18	-1	-1	-1	-1
HIS 19	+1		0	0
SER 20	0	0	0	0
GLN 21	0	0	0	0
ALA 22	0	0	0	0
LEU 23	+1	+1	+1	+1

Table S2.12. Secondary structure prediction of (11-23)-obestatin (**4**) using CSI.

Residue	HN	Hα	Hβ	Hγ	Hδ	others
PHE 1	8.47	4.41	Hβ1/Hβ2 2.77/2.90			
ASN 2	8.72	4.53	Hβ1/Hβ2 2.31/2.44			
ALA 3	8.38	4.29	0.94			
PRO 4		4.16	Hβ1/Hβ2 1.66/1.90	1.47	Hδ1/Hδ2 3.40/3.54	
PHE 5	8.15	4.41	2.81			
ASP 6	8.35	4.47	Hβ1/Hβ2 2.38/2.54			
VAL 7	8.02	3.86	1.78	0.53		
GLY 8	8.46	3.71				
ILE 9	7.93	3.97	1.51	Hγ1/Hγ2 1.06/0.77	Hδ1/Hδ2 0.43/0.50	
LYS 10	8.30	4.08	1.50	1.04	Hδ1/Hδ2 1.39/2.70	Hε 7.51

Table S2.13. ^{1}H chemical shifts (ppm) for human (1-10)-obestatin (**7**) in H_2O at 298K.

Residue	HN	Hα	Hβ	Hγ	Hδ	others
PHE 1	8.33	4.62	Hβ1/Hβ2 3.05/3.24			
ASN 2	8.31	4.63	Hβ1/Hβ2 2.55/2.65			
ALA 3	8.37	4.51	1.35			
PRO 4		4.36	Hβ1/Hβ2 2.01/2.24	1.84	Hδ1/Hδ2 3.66/3.78	
PHE 5	8.06	4.61	Hβ1/Hβ2 3.10/3.13			
ASP 6	8.19	4.63	Hβ1/Hβ2 2.58/2.66			
VAL 7	8.04	4.14	2.19	0.98		
GLY 8	8.47	3.96				
ILE 9	7.92	4.19	1.89	Hγ1/Hγ2 1.19/1.84	0.93	
LYS 10	7.96	4.21	Hβ1/Hβ2 1.72/1.83	1.40	1.65	

Table S2.14. ^{1}H chemical shifts (ppm) for human (1-10)-obestatin (**7**) in PBS at 298K.

Residue	HN	Hα	Hβ	Hγ	Hδ	others
PHE 1	8.47	4.61	Hβ1/Hβ2 3.03/3.24			
ASN 2	8.43	4.62	Hβ1/Hβ2 2.54/2.66			
ALA 3	8.55	4.50	1.37			
PRO 4		4.36	Hβ1/Hβ2 2.02/2.25	1.84	Hδ1/Hδ2 3.67/3.80	
PHE 5	8.26	4.59	3.10			
ASP 6	8.30	4.62	Hβ1/Hβ2 2.55/2.67			
VAL 7	8.18	4.13	2.19	0.98		
GLY 8	8.58	3.94				
ILE 9	8.06	4.19	1.89	1.18	0.92	
LYS 10	8.12	4.19	Hβ1/Hβ2 1.72/1.83	0.95	1.40	

Table S2.15. ^{1}H chemical shifts (ppm) for human (1-10)-obestatin (**7**) in HEK293-WT cells at 298K.

Residue	HN	Hα	Hβ	Hγ	Hδ	others
PHE 1	8.47	4.61	Hβ1/Hβ2 3.03/3.24			
ASN 2	8.43	4.63	Hβ1/Hβ2 2.54/2.66			
ALA 3	8.55	4.50	1.37			
PRO 4		4.36	Hβ1/Hβ2 2.02/2.25	1.84	Hδ1/Hδ2 3.67/3.80	
PHE 5	8.26	4.59	3.10			
ASP 6	8.30	4.62	Hβ1/Hβ2 2.56/2.67			
VAL 7	8.18	4.13	2.20	0.98		
GLY 8	8.57	3.94				
ILE 9	8.06	4.19	1.89	1.18	0.93	
LYS 10	8.12	4.19	Hβ1/Hβ2 1.72/1.83	0.96	1.41	

Table S2.16. ^{1}H chemical shifts (ppm) for human (1-10)-obestatin (**7**) in HEK293-GPR39 cells at 298K.

	PBS-H_2O					WT-PBS					GPR39-WT				
Residue	**HN**	**Hα**	**Hβ**	**Hγ**	**Hδ**	**HN**	**Hα**	**Hβ**	**Hγ**	**Hδ**	**HN**	**Hα**	**Hβ**	**Hγ**	**Hδ**
PHE 1	-0.14	0.21	Hβ1/Hβ2 0.28/0.34			0.14	-0.01	Hβ1/Hβ2 -0.02/0			0	0	0		
ASN 2	0.41	0.10	Hβ1/Hβ2 0.24/0.21			0.12	-0.01	Hβ1/Hβ2 -0.01/0.01			0	0.01	0		
ALA 3	-0.01	0.22	0.41			0.18	-0.01	0.02			0	0	0		
PRO 4		0.20	Hβ1/Hβ2 0.35/0.34	0.37	Hδ1/Hδ2 0.26/0.24			Hβ1/Hβ2 0.01/0.01	0	Hδ1/Hδ2 0.01/0.02		0	0	0	0
PHE 5	-0.09	0.20	0.29			0.20	-0.02	-0.01			0	0	0		
ASP 6	-0.16	0.16	Hβ1/Hβ2 0.20/0.12			0.11	-0.01	Hβ1/Hβ2 -0.03/0.01			0	0	Hβ1/Hβ2 0.01/0		
VAL 7	0.02	0.28	0.41	0.45		0.14	-0.01	0	0		0	0	0.01	0	
GLY 8	0.01	0.25				0.11	-0.02				-0.01	0			
ILE 9	-0.01	0.22	0.38	0.13	0.05	0.14	0	0	-0.01	-0.01	0	0	0	0	0.01
LYS 10	-0.34	0.13	0.22	0.36	0.26	0.16	-0.02	0	-0.45	-0.25	0	0	0	0.01	0.01

Table S2.17. CSPs between (1-10)-obestatin (**7**) spectra. δ ≥ 0,1 ppm were considered significant differences and were marked in red.

Residue	**CSI H_2O**	**CSI PBS**	**CSI WT**	**CSI GPR39**
PHE 1	-1	0	0	0
ASN 2	-1	-1	-1	-1
ALA 3	0	+1	+1	+1
PRO 4	-1	0	0	0
PHE 5	-1	0	0	0
ASP 6	-1	-1	-1	-1
VAL 7	0	+1	+1	+1
GLY 8	-1	0	0	0
ILE 9	0	+1	+1	+1
LYS 10	-1	-1	-1	-1

Table S2.18. Secondary structure prediction of (1-10)-obestatin (**7**) using CSI.

Residue	HN	Hα	Hβ	Hγ	Hδ	others
ASP 6		4.35	Hβ1/Hβ2 2.76/2.87			
VAL 7	8.65	4.21	2.14	0.98		
GLY 8	8.48	3.94				
ILE 9	8.02	4.18	1.84	Hγ1/Hγ2 1.17/1.45	0.89	
LYS 10	8.44	4.37	Hβ1/Hβ2 1.74/1.81	Hγ1/Hγ2 1.37/1.45	1.67	Hε 7.53
LEU 11	8.36	4.40	Hβ2/Hβ3 1.54/1.62	1.42	Hδ1/Hδ2 0.85/0.91	
SER 12	8.34	4.48	3.89			
GLY 13	8.46	4.03				
VAL 14	8.02	4.06	2.03	Hγ1/Hγ2 0.85/0.91		
GLN 15	8.50	4.30	Hβ1/Hβ2 1.98/2.19	Hγ1/Hγ2 1.92/2.27		
TYR 16	8.16	4.55	Hβ1/Hβ2 2.93/3.06			
GLN 17	8.20	3.27	Hβ1/Hβ2 1.93/2.03	2.31		
GLN 18	8.37	4.24	Hβ1/Hβ2 1.96/2.04	2.35		
HIS 19	8.60	4.76	Hβ1/Hβ2 3.21/3.31			
SER 20	8.41	4.45	Hβ1/Hβ2 3.86/3.90			
GLN 21	8.54	4.35	Hβ1/Hβ2 2.00/2.13	2.39		
ALA 22	8.34	4.32	1.39			
LEU 23	8.19	4.31	1.67	1.60	Hδ1/Hδ2 0.88/0.94	

Table S2.19. ^{1}H chemical shifts (ppm) for (6-23)-obestatin (**3**) in H_2O at 298.

Residue	HN	Hα	Hβ	Hγ	Hδ	others
ASP 6	7.82	4.41	Hβ1/Hβ2 2.87/3.12			
VAL 7		4.21	2.16	0.99		
GLY 8	8.49	3.97				
ILE 9	7.99	4.19	1.84	Hγ1/Hγ2 1.18/1.47	0.90	
LYS 10	8.45	4.40	Hβ1/Hβ2 1.75/1.86	1.45		
LEU 11	8.51	4.43	1.68	1.41	Hδ1/Hδ2 0.89/0.95	
SER 12	7.88	4.27	3.86			
GLY 13						
VAL 14	7.87	4.10	1.99	Hγ1/Hγ2 0.81/0.90		
GLN 15						
TYR 16	8.12	4.49	Hβ1/Hβ2 3.09/3.25			
GLN 17						
GLN 18						
HIS 19	8.24	4.50	Hβ1/Hβ2 3.10/3.26			
SER 20	8.24	4.30	3.89			
GLN 21						
ALA 22	8.34	4.33	1.40			
LEU 23	8.29	4.32	1.69	1.61	0.93	

Table S2.20. ^{1}H chemical shifts (ppm) for human (6-23)-obestatin (**3**) in PBS at 298K.

.

Residue	HN	Hα	Hβ	Hγ	Hδ	others
ASP 6		4.29	Hβ1/Hβ2 2.71/2.84			
VAL 7	8.77	4.20	2.15	0.99		
GLY 8	8.65	3.93				
ILE 9	8.21	4.16	1.84	1.19	0.90	
LYS 10	8.62	4.35	1.78	1.45	1.67	
LEU 11	8.57	4.40	1.64	1.53	0.90	
SER 12	8.51	4.47	3.89			
GLY 13	8.62	4.02				
VAL 14	8.19	4.03	2.03	Hγ1/Hγ2 0.85/0.93		
GLN 15	8.67	4.30	Hβ1/Hβ2 1.97/2.19	2.28		
TYR 16	8.37	4.53	Hβ1/Hβ2 2.93/3.05			
GLN 17	8.34	4.25	Hβ1/Hβ2 1.93/2.02	2.30		
GLN 18	8.55	4.22	1.97	2.34		
HIS 19	8.63	4.70	Hβ1/Hβ2 3.16/3.23			
SER 20	8.55	4.41	3.88			
GLN 21	8.68	4.33	Hβ1/Hβ2 2.00/2.14	2.40		
ALA 22	8.47	4.29	1.40			
LEU 23	8.38	4.29	1.69	1.58	0.93	

Table S2.21. ^{1}H chemical shifts (ppm) for human (6-23)-obestatin (**3**) in HEK293-WT cells at 298K.

Residue	HN	Hα	Hβ	Hγ	Hδ	others
ASP 6		4.31	Hβ1/Hβ2 2.71/2.83			
VAL 7	8.75	4.20	2.15	0.98		
GLY 8	8.62	3.94				
ILE 9	8.17	4.16	1.84	1.18	0.89	
LYS 10	8.59	4.35	1.78	1.40	1.45	
LEU 11	8.53	4.40	1.63	1.53	0.90	
SER 12	8.49	4.47	3.89			
GLY 13	8.59	4.01				
VAL 14	8.15	4.03	2.02	Hγ1/Hγ2 0.84/0.92		
GLN 15	8.65	4.30	Hβ1/Hβ2 1.96/2.19	2.29		
TYR 16	8.33	4.53	Hβ1/Hβ2 2.93/3.05			
GLN 17	8.32	4.25	Hβ1/Hβ2 1.92/2.03	2.30		
GLN 18	8.51	4.22	1.95	2.33		
HIS 19	8.63	4.71	Hβ1/Hβ2 3.16/3.25			
SER 20	8.52	4.42	3.88			
GLN 21	8.67	4.33	Hβ1/Hβ2 2.00/2.3	2.42		
ALA 22	8.45	4.30	1.40			
LEU 23	8.34	4.30	1.68	1.58	0.92	

Table S2.22. ^{1}H chemical shifts (ppm) for human (6-23)-obestatin (**3**) in HEK293-GPR39 cells at 298K.

	PBS-H_2O					WT-PBS					GPR39-WT				
Residue	**HN**	**Hα**	**Hβ**	**Hγ**	**Hδ**	**HN**	**Hα**	**Hβ**	**Hγ**	**Hδ**	**HN**	**Hα**	**Hβ**	**Hγ**	**Hδ**
ASP 6		0.06	Hβ1/Hβ2 0.11/0.25				-0.12	Hβ1/Hβ2 -0.16/-0.28				0.02	Hβ1/Hβ2 0/-0.01		
VAL 7		0	0.02	0.01			-0.01	-0.01	0		-0.02	0	0	-0.01	
GLY 8	0.01	0.03				0.16	-0.04				-0.03	0.01			
ILE 9	-0.03	0.01	0	Hγ1/Hγ2 0.01/0.02	0.01	0.22	-0.03	0	0.01	0	-0.04	0	0	-0.01	-0.01
LYS 10	0.01	0.03	Hβ1/Hβ2 0.01/0.05	0.04		0.17	-0.05	Hβ1/Hβ2 0.03/-0.19	0		-0.03	0	0	-0.05	-0.22
LEU 11	0.15	0.03	0.10	-0.01	Hδ1/Hδ2 0.04/0.04	0.06	-0.03	-0.04	0.12	-0.02	-0.04	0	-0.01	0	0
SER 12	-0.46	-0.21	-0.03			0.63	0.20	0.03			-0.02	0	0		
GLY 13											-0.03	0			
VAL 14	-0.15	0.04	-0.04	Hγ1/Hγ2 -0.04/-0.01		0.32	-0.07	0.04	Hγ1/Hγ2 0.04/0.03	-	-0.04	0	-0.01	-0.01	
GLN 15											-0.02	0	Hβ1/Hβ2 -0.01/0	0.01	
TYR 16	-0.04	-0.06	Hβ1/Hβ2 0.16/0.19			0.25	0.04	Hβ1/Hβ2 -0.16/-0.20			-0.04	0	0		
GLN 17											-0.02	0	Hβ1/Hβ2 -0.01/0.01	0	
GLN 18											-0.04	0	-0.02	-0.01	
HIS 19	-0.36	-0.26	Hβ1/Hβ2 -0.11/-0.05			0.39	0.20	Hβ1/Hβ2 0.06/-0.03			0	0.01	Hβ1/Hβ2 0/0.02		
SER 20	-0.17	-0.15	0.01			0.31	0.11	-0.01			-0.03	0.01	0		
GLN 21											-0.01	0	Hβ1/Hβ2 0/-0.01	0.02	
ALA 22	0	0.01	0.01			0.13	-0.04	0			-0.02	0.01	0		
LEU 23	0.10	0.01	0.02	0.01	0.02	0.09	-0.03	0	-0.03	0	-0.04	0.01	-0.01	0	-0.01

Table S2.23. CSPs between (6-23)-obestatin (**3**) spectra. δ ≥ 0,1 ppm were considered significant differences and were marked in red.

Residue	CSI H_2O	CSI PBS	CSI WT	CSI GPR39
ASP 6	-1	-1	-1	-1
VAL 7	+1	+1	+1	+1
GLY 8	0	0	0	0
ILE 9	+1	+1	+1	+1
LYS 10	0	0	0	0
LEU 11	+1	+1	+1	+1
SER 12	0	-1	0	0
GLY 13	0		0	0
VAL 14	+1	+1	0	0
GLN 15	0		0	0
TYR 16	0	0	0	0
GLN 17	0		-1	-1
GLN 18	-1		-1	-1
HIS 19	+1	-1	0	0
SER 20	0	-1	0	0
GLN 21	0		0	0
ALA 22	0	0	0	0
LEU 23	+1	+1	+1	+1

Table S2.24. Secondary structure prediction of (6-23)-obestatin (**3**) using CSI.

Residue	HN	Hα	Hβ	Hγ	Hδ	others
PHE 1						
ASN 2	8.65	4.71	Hβ1/Hβ2 2.62/2.75			
ALA 3	8.36	4.50	1.35			
PRO 4		4.36	Hβ1/Hβ2 2.00/2.24	1.83	Hδ1/Hδ2 3.65/3.77	
PHE 5	8.10	4.59	3.09			
ASP 6	8.23	4.62	Hβ1/Hβ2 2.61/2.72			
VAL 7	8.02	4.09	2.16	0.96		
GLY 8	8.43	3.93				
ILE 9	7.86	4.14	1.84	1.16	0.88	
LYS 10	8.35	4.33	Hβ1/Hβ2 1.75/1.82	1.43	1.65	
LEU 11	8.29	4.39	1.62	1.54	Hδ1/Hδ2 0.84/0.90	
SER 12	8.29	4.46	3.89			
GLY 13	8.43	4.03				
VAL 14	7.99	4.04	2.03	Hγ1/Hγ2 0.86/0.91		
GLN 15	8.48	4.28	Hβ1/Hβ2 1.93/2.18	2.26		
TYR 16	8.14	4.54	Hβ1Hβ2 2.92/3.06			
GLN 17	8.18	4.26	Hβ1/Hβ2 1.93/2.03	2.30		
GLN 18	8.36	4.23	Hβ1/Hβ2 1.94/2.04	2.34		
HIS 19	8.58	4.74	Hβ1/Hβ2 3.21/3.29			
SER 20	8.40	4.43	3.88			
GLN 21	8.53	4.34	Hβ1/Hβ2 2/2.12	2.39		
ALA 22	8.33	4.30	1.38			
LEU 23	8.18	4.30	Hβ1/Hβ2 1.60/1.67	1.60	0.92	

Table S2.25. ^{1}H chemical shifts (ppm) for human obestatin (**1**) in H_2O at 298K.

Residue	HN	Hα	Hβ	Hγ	Hδ	others
PHE 1						
ASN 2						
ALA 3	8.35	4.51	1.34			
PRO 4			Hβ1/Hβ2 2.01/2.24	1.84	Hδ1/Hδ2 3.65/3.77	
PHE 5	8.08	4.59	3.10			
ASP 6	8.19	4.61	Hβ1/Hβ2 2.57/2.67			
VAL 7	8.04	4.11	2.19	0.97		
GLY 8	8.46	3.93				
ILE 9	7.86	4.14	1.85	1.17	0.88	
LYS 10	8.35	4.34	1.77	1.45		Hε 3.22
LEU 11	8.29	4.39	1.64	1.54	0.86	
SER 12	8.29	4.47	3.89			
GLY 13	8.45	4.03				
VAL 14	7.98	4.06	2.03	Hγ1/Hγ2 0.86/0.91		
GLN 15	8.48	4.29	Hβ1/Hβ2 1.93/2.19	2.27		
TYR 16	8.16	4.55	Hβ1Hβ2 2.92/3.07			
GLN 17	8.21	4.26	Hβ1/Hβ2 1.93/2.04	2.30		
GLN 18	8.37	4.23	Hβ1/Hβ2 1.94/2.04	2.32		
HIS 19						
SER 20						
GLN 21	8.51	4.34	Hβ1/Hβ2 2.02/2.13	2.39		
ALA 22	8.29	4.30	1.39			
LEU 23	8.15	4.30	1.68	1.60	0.90	

Table S2.26. ^{1}H chemical shifts (ppm) for human obestatin (**1**) in PBS at 298K.

Residue	HN	Hα	Hβ	Hγ	Hδ	others
PHE 1						
ASN 2						
ALA 3	8.55	4.50	1.37			
PRO 4		4.37	Hβ1/Hβ2 2.15/2.43	2.56	3.78	
PHE 5	8.29	4.58	3.09			
ASP 6	8.30	4.60	Hβ1/Hβ2 2.55/2.66			
VAL 7	8.19	4.10	2.20	0.98		
GLY 8	8.57	4.01				
ILE 9	8.01	4.13	1.85	1.18	0.89	
LYS 10	8.51	4.34	1.77	1.40		
LEU 11	8.47	4.39	1.64	1.52	0.84	
SER 12	8.44	4.46	3.88			
GLY 13	8.57	3.93				
VAL 14	8.13	4.04	2.04	Hγ1/Hγ2 0.84/0.92		
GLN 15	8.63	4.29	Hβ1/Hβ2 1.95/2.19	2.29		
TYR 16	8.32	4.53	Hβ1Hβ2 2.92/3.04			
GLN 17	8.31	4.25	Hβ1/Hβ2 1.92/2.03	2.30		
GLN 18	8.51	4.22	Hβ1/Hβ2 1.96/2.05	2.33		
HIS 19	8.61	4.59	2.96			
SER 20		4.40	3.87			
GLN 21		4.33	Hβ1/Hβ2 2.00/2.12	2.40		
ALA 22	8.43	4.29	1.39			
LEU 23	8.33	4.29	1.68	1.58	0.89	

Table S2.27. ^{1}H chemical shifts (ppm) for human obestatin (**1**) in HEK293-WT cells at 298K.

Residue	HN	Hα	Hβ	Hγ	Hδ	others
PHE 1						
ASN 2						
ALA 3	8.55	4.50	1.36			
PRO 4		4.37	Hβ1/Hβ2 1.84/2.02	2.25	Hδ1/Hδ2 3.68/3.80	
PHE 5	8.29	4.58	3.09			
ASP 6	8.30	4.61	Hβ1/Hβ2 2.56/2.66			
VAL 7	8.20	4.11	2.20	0.98		
GLY 8	8.57	3.93				
ILE 9	8.00	4.13	1.85	1.17	0.89	
LYS 10	8.52	4.34	1.77	Hγ1/Hγ2 1.39/1.46	1.65	
LEU 11	8.47	4.40	1.64	1.53	0.90	
SER 12	8.45	4.47	3.89			
GLY 13	8.58	4.00				
VAL 14	8.13	4.04	2.03	Hγ1/Hγ2 0.85/0.92		
GLN 15	8.63	4.29	Hβ1/Hβ2 1.96/2.19	2.28		
TYR 16	8.32	4.53	Hβ1Hβ2 2.92/3.05			
GLN 17	8.31	4.25	Hβ1/Hβ2 1.93/2.02	2.30		
GLN 18	8.51	4.22	Hβ1/Hβ2 1.96/2.01	2.33		
HIS 19	8.58	4.69	Hβ1/Hβ2 3.14/3.22			
SER 20	8.47	4.41	3.87			
GLN 21	8.64	4.33	Hβ1/Hβ2 2.00/2.13	2.40		
ALA 22	8.43	4.29	1.39			
LEU 23	8.33	4.29	1.68	1.58	0.93	

Table S2.28. ^{1}H chemical shifts (ppm) for human obestatin (**1**) in HEK293-GPR39 cells at 298K.

	PBS-H_2O					WT-PBS					GPR39-WT				
Residue	**HN**	**Hα**	**Hβ**	**Hγ**	**Hδ**	**HN**	**Hα**	**Hβ**	**Hγ**	**Hδ**	**HN**	**Hα**	**Hβ**	**Hγ**	**Hδ**
PHE 1															
ASN 2															
ALA 3	-0.01	0.01	-0.01			0.20	-0.01	0.03			0	0	-0.01		
PRO 4			Hβ1/Hβ2 0.01/0	0.01	0			-0.18				0	Hβ1/Hβ2 -0.31/-0.41	-0.31	-0.04
PHE 5	-0.02	0	0.01			0.21	-0.01	-0.01			0	0	0		
ASP 6	-0.04	-0.01	Hβ1/Hβ2 -0.04/-0.05			0.11	-0.01	Hβ1/Hβ2 -0.02/-0.01			0	0.01	Hβ1/Hβ2 0.01/0		
VAL 7	0.02	0.02	0.03	0.01		0.15	-0.01	0.01	0.01		0.01	0.01	0	0	
GLY 8	0.03	0				0.11	0.08				0	-0.08			
ILE 9	0	0	0.01	0.01	0	0.15	-0.01	0	0.01	0.01	-0.01	0	0	-0.01	0
LYS 10	0	0.01	-0.02	0.02		0.16	0	0	-0.05		0.01	0	0	0.03	
LEU 11	0	0	0.02	0	-0.01	0.18	0	0	-0.02	-0.02	0	0.01	0	0.01	0.06
SER 12	0	0.01	0			0.15	0.01	-0.01			0.01	0.01	0.01		
GLY 13	0.02	0				0.12	-0.10				0.01	0.07			
VAL 14	-0.01	0.02	0	0		0.15	-0.02	0.01	Hγ1/Hγ2 -0.02/0.01		0	0	-0.01	0.01	
GLN 15	0	0.01	Hβ1/Hβ2 0/0.01	0.01		0.15	0	Hβ1/Hβ2 0.02/0	0.02		0	0	Hβ1/Hβ2 0.01/0	-0.01	
TYR 16	0.02	0.01	Hβ1/Hβ2 0/0.01			0.16	-0.02	Hβ1/Hβ2 0/-0.03			0	0	Hβ1/Hβ2 0/0.01		
GLN 17	0.03	0	Hβ1/Hβ2 0/0.01	0		0.10	-0.01	Hβ1/Hβ2 -0.01/-0.01	0		0	0	Hβ1/Hβ2 0.01/-0.01	0	
GLN 18	0.01	0.01	Hβ1/Hβ2 0.02/0	-0.02		0.14	-0.02	Hβ1/Hβ2 0/0.01	0.01		0	0	Hβ1/Hβ2 0/-0.04	0	
HIS 19											-0.03	0.10	0.18		
SER 20												0.01	0		
GLN 21	-0.02	0	Hβ1/Hβ2 0.02/0.01	0			-0.01	Hβ1/Hβ2 -0.02/-0.01	0.01			0	Hβ1/Hβ2 0/0.01	0	
ALA 22	-0.04	0	0.01			0.14	-0.01	0			0	0	0		
LEU 23	-0.03	0	0.05	0	-0.02	0.18	-0.01	0	-0.02	-0.01	0	0	0	0	0.04

Table S2.29. CSPs between obestatin (**1**) spectra. δ ≥ 0,1 ppm were considered significant differences and were marked in red.

Residue	CSI H_2O	CSI PBS	CSI WT	CSI GPR39
PHE 1				
ASN 2	0			
ALA 3	+1	+1	+1	+1
PRO 4	0		0	0
PHE 5	0	0	0	0
ASP 6	-1	-1	-1	-1
VAL 7	+1	+1	+1	+1
GLY 8	0	0	0	0
ILE 9	+1	+1	+1	+1
LYS 10	0	0	0	0
LEU 11	+1	+1	+1	+1
SER 12	0	0	0	0
GLY 13	0	0	0	0
VAL 14	0	+1	0	0
GLN 15	0	0	0	0
TYR 16	0	0	0	0
GLN 17	-1	-1	-1	-1
GLN 18	-1	-1	-1	-1
HIS 19	+1		0	0
SER 20	0		0	0
GLN 21	0	0	0	0
ALA 22	0	0	0	0
LEU 23	+1	+1	+1	+1

Table S2.30. Secondary structure prediction of obestatin (**1**) using CSI.

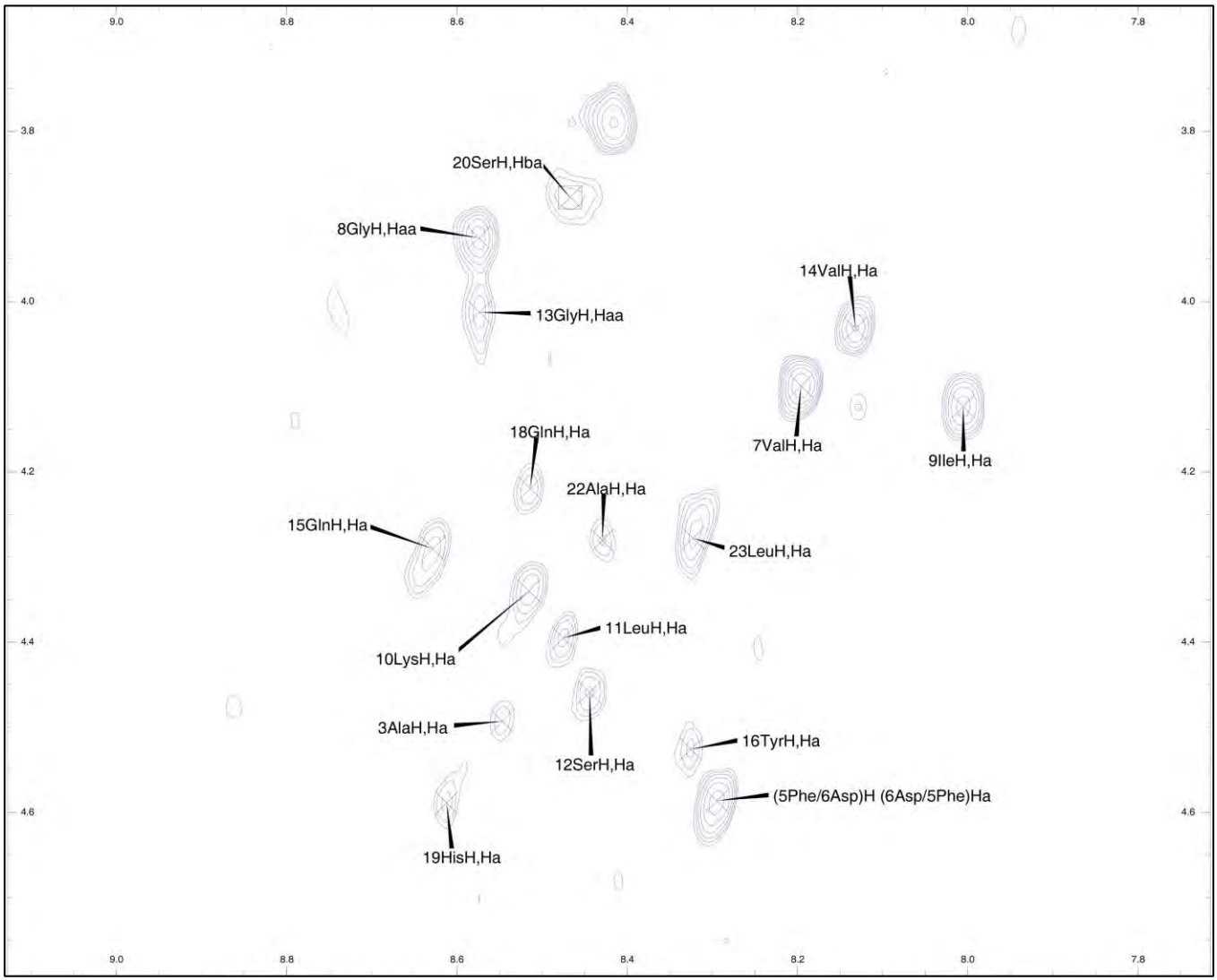

Figure S2.1. Amide region of 2D TOCSY spectra for human obestatin (**1**) in HEK293-WT cells.

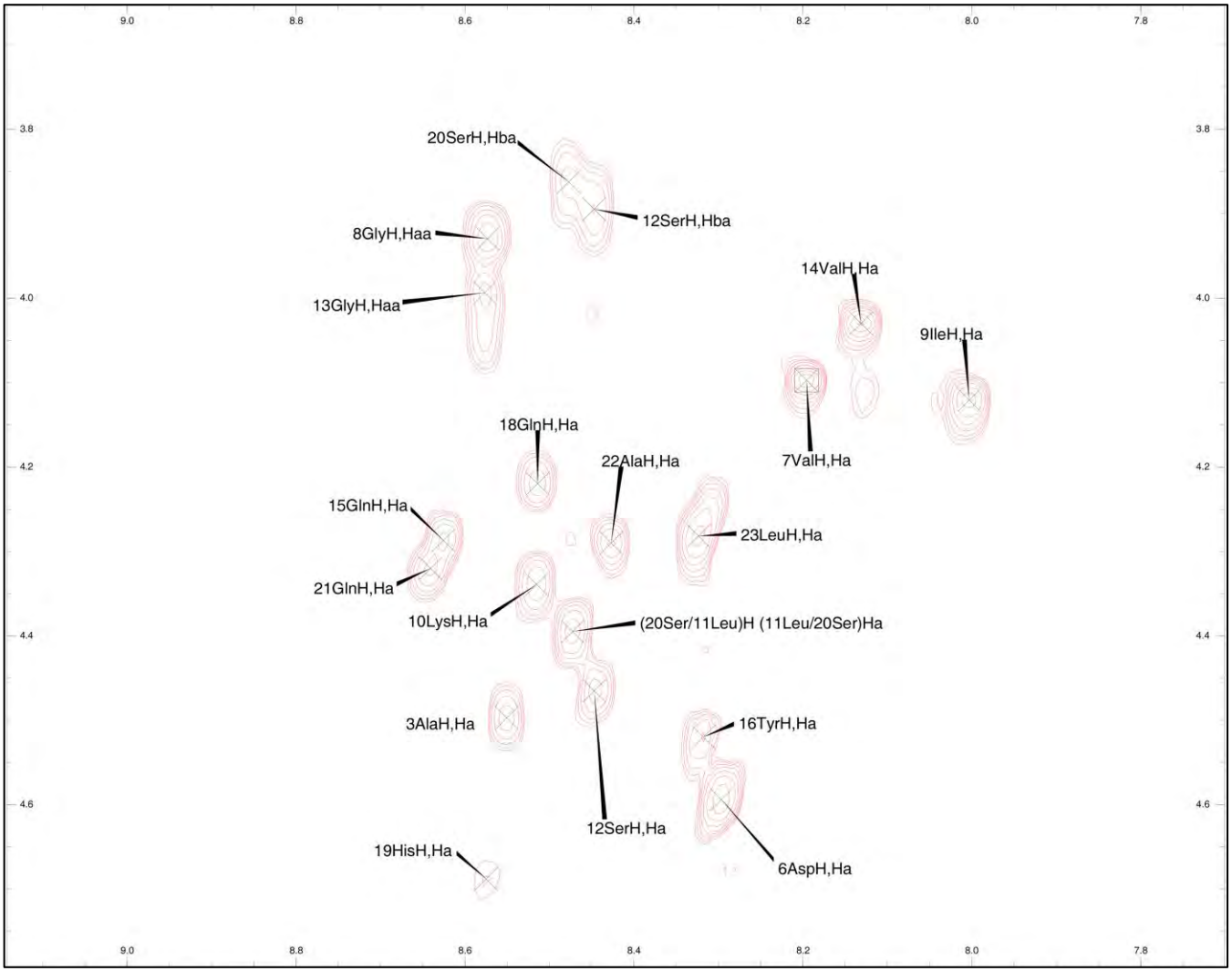

Figure S2.2. Amide region of 2D TOCSY spectra for human obestatin (**1**) in HEK293-GPR39 cells.

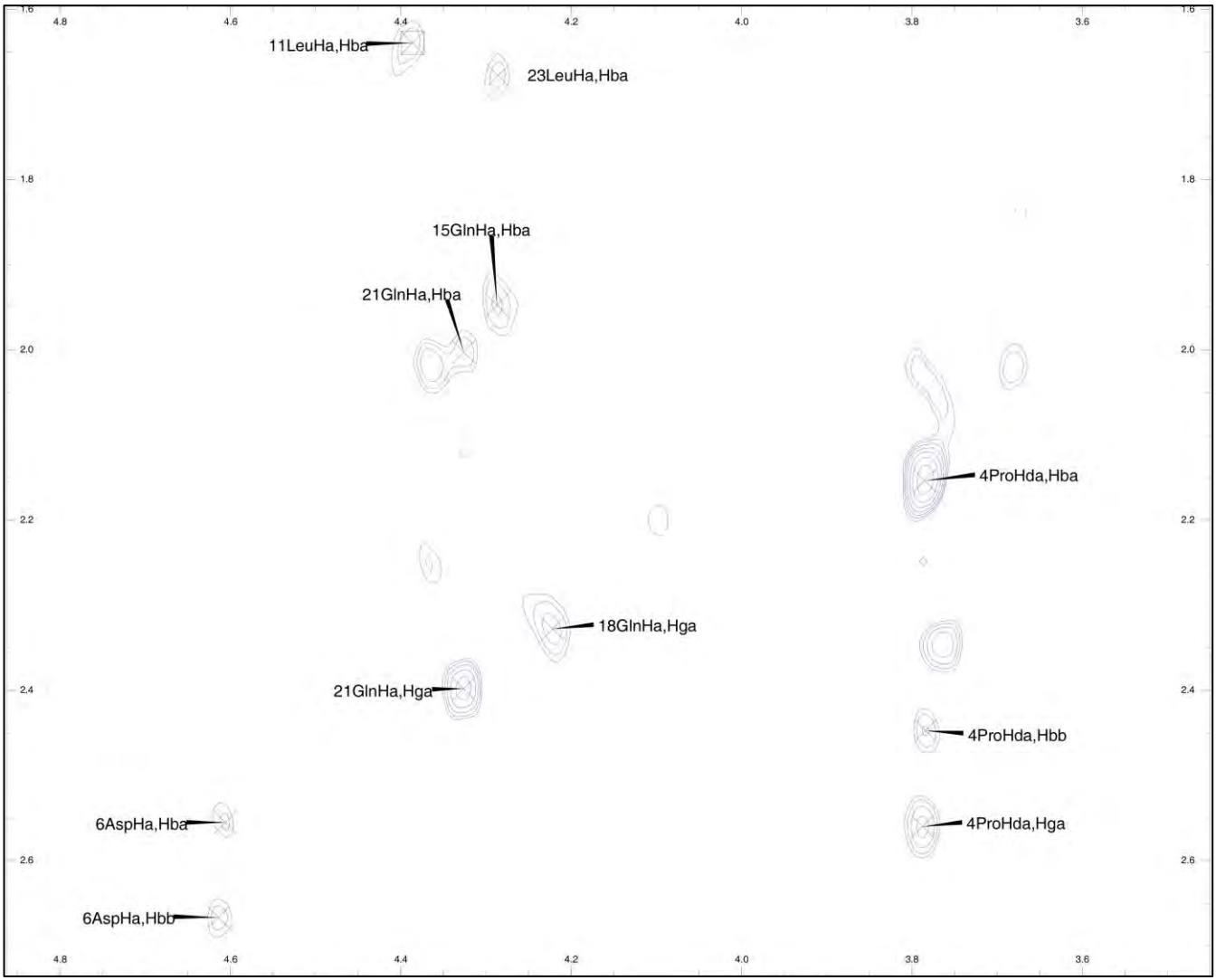

Figure S2.3. Alpha region of 2D TOCSY spectra for human obestatin (**1**) in HEK293-WT cells.

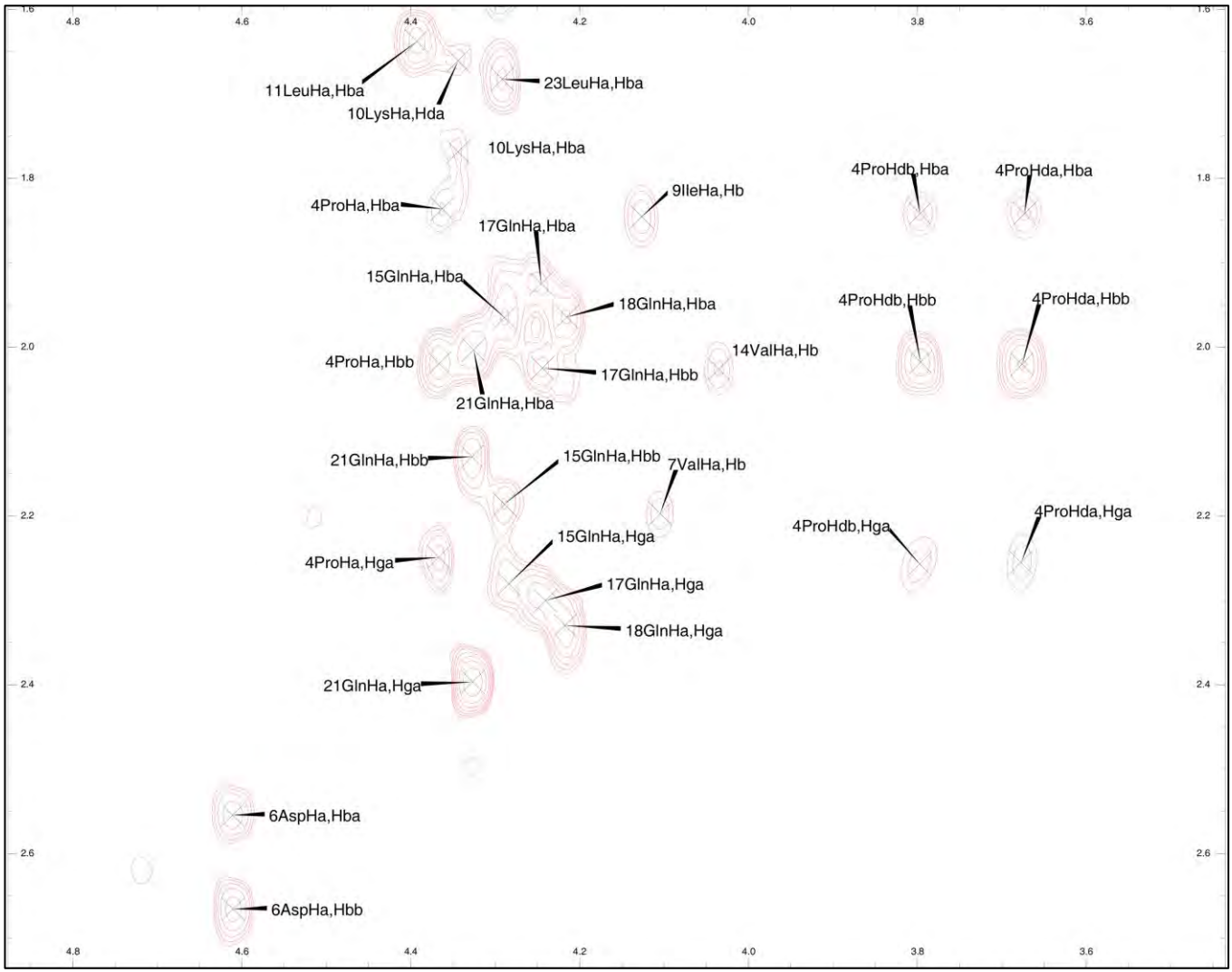

Figure S2.4. Alpha region of 2D TOCSY spectra for human obestatin (**1**) in HEK293-GPR39 cells.

USC
UNIVERSIDADE
DE SANTIAGO
DE COMPOSTELA